LEABHARLANN CHOLÁISTE NA TRÍONÓIDE, BAILE ÁTHA CLIATH | TRINITY COLLEGE LIBRARY DUBLIN
Ollscoil Átha Cliath | The University of Dublin

Terms and Conditions of Use of Digitised Theses from Trinity College Library Dublin

Copyright statement

All material supplied by Trinity College Library is protected by copyright (under the Copyright and Related Rights Act, 2000 as amended) and other relevant Intellectual Property Rights. By accessing and using a Digitised Thesis from Trinity College Library you acknowledge that all Intellectual Property Rights in any Works supplied are the sole and exclusive property of the copyright and/or other IPR holder. Specific copyright holders may not be explicitly identified. Use of materials from other sources within a thesis should not be construed as a claim over them.

A non-exclusive, non-transferable licence is hereby granted to those using or reproducing, in whole or in part, the material for valid purposes, providing the copyright owners are acknowledged using the normal conventions. Where specific permission to use material is required, this is identified and such permission must be sought from the copyright holder or agency cited.

Liability statement

By using a Digitised Thesis, I accept that Trinity College Dublin bears no legal responsibility for the accuracy, legality or comprehensiveness of materials contained within the thesis, and that Trinity College Dublin accepts no liability for indirect, consequential, or incidental, damages or losses arising from use of the thesis for whatever reason. Information located in a thesis may be subject to specific use constraints, details of which may not be explicitly described. It is the responsibility of potential and actual users to be aware of such constraints and to abide by them. By making use of material from a digitised thesis, you accept these copyright and disclaimer provisions. Where it is brought to the attention of Trinity College Library that there may be a breach of copyright or other restraint, it is the policy to withdraw or take down access to a thesis while the issue is being resolved.

Access Agreement

By using a Digitised Thesis from Trinity College Library you are bound by the following Terms & Conditions. Please read them carefully.

I have read and I understand the following statement: All material supplied via a Digitised Thesis from Trinity College Library is protected by copyright and other intellectual property rights, and duplication or sale of all or part of any of a thesis is not permitted, except that material may be duplicated by you for your research use or for educational purposes in electronic or print form providing the copyright owners are acknowledged using the normal conventions. You must obtain permission for any other use. Electronic or print copies may not be offered, whether for sale or otherwise to anyone. This copy has been supplied on the understanding that it is copyright material and that no quotation from the thesis may be published without proper acknowledgement.

The immunomodulatory effects of NOD1 activation

2014

Patrick Joseph Kelly

B.A. (Mod.) Molecular Medicine

A thesis submitted to

Trinity College Dublin

as completion of the degree of Doctor of Philosophy

Supervisor: Prof Kingston Mills

Immune Regulation Research Group

School of Biochemistry and Immunology

Trinity College Dublin

TRINITY COLLEGE
5 JAN 2015
LIBRARY DUBLIN

Thesis 10439

DECLARATION OF AUTHORSHIP

I declare that this thesis has not been submitted as an exercise for a degree at this or any other university and it is entirely my own work.

I agree to deposit this thesis in the University's open access institutional repository or allow the library to do so on my behalf, subject to Irish Copyright Legislation and Trinity College Library conditions of use and acknowledgement.

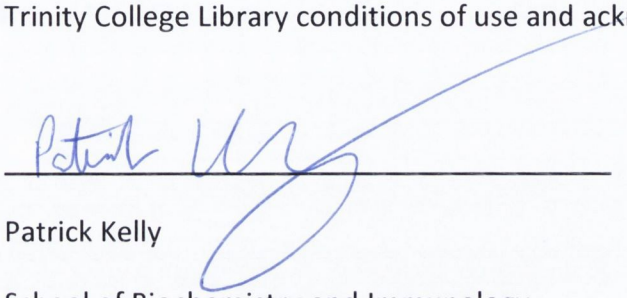

Patrick Kelly

School of Biochemistry and Immunology,

University of Dublin, Trinity College

ABSTRACT

NOD1 and NOD2 are cytosolic pathogen recognition receptors (PRRs) which detect peptidoglycan derivatives and contribute to the host defence during bacterial infection. Transgenic mice lacking NOD1 or NOD2 are susceptible to a variety of bacterial infections. Although other PRRs, such as TLRs, are more potent activators of the innate immune response, NOD1 and NOD2 have been shown to have a significant role in potentiating innate and adaptive immune responses. In addition, there is a growing consensus that NOD1 and NOD2 can synergistically enhance TLR-mediated responses. In contrast, NOD2 has also been implicated as a suppressor of pathogenic inflammation in the gut. Evidence from genetic polymorphism analysis has shown that loss of function mutations in the NOD2 gene increase the risk of acquiring Crohn's disease. While no consensus has been reached on the mechanisms behind the NOD2-mediated protection, there is evidence that NOD2 is involved in the production of IL-10, an important suppressor of inflammation in the gut. NOD1 and NOD2 share the same signalling pathways, but thus far there has been no evidence to suggest that NOD1 has similar anti-inflammatory functions. NOD1 polymorphisms have been linked with the inflammatory disorders asthma and atopic eczema but the involvement of NOD1 in the pathogenesis of these diseases is still unclear. This study identified novel mechanisms by which NOD1 modulates the innate immune system and also showed that a NOD1 agonist can attenuate inflammation in a mouse model of autoimmunity. Administration of the NOD1 agonist TriDAP attenuated experimental autoimmune encephalomyelitis (EAE) when administered at the induction phase of disease. This was associated with a suppression of IFN-γ and IL-17 production by autoantigen-specific T cells in the central nervous system and peripheral lymph nodes during acute disease. NOD1 activation was shown to induce the production of the immunosuppressive cytokine IL-10 by peritoneal macrophages in a p38-dependent manner. In vivo NOD1 activation induced an IL-10-mediated expansion of immunosuppressive macrophages in the peritoneal cavity. Macrophages from mice treated with the NOD1 agonist underwent M2 activation in an IL-4-dependent manner. Moreover, these M2 macrophages expressed the anti-inflammatory mediators of tissue repair, IL-10, relm-α and arginase. In contrast with macrophages from LPS-treated mice, macrophages isolated from NOD1 agonist-treated mice attenuated EAE when transferred into sick mice. The findings of this study suggest NOD1 mediates anti-inflammatory responses by inducing the production of IL-10 and IL-4, which expand a population of immunosuppressive M2-like macrophages. These results provide new evidence of a role for NOD1 in immune homeostasis and immune regulation.

ACKNOWLEDGEMENTS

First and foremost I would like to thank my supervisor Kingston for his guidance during my studentship. His experience and judgement have been indispendible during the writing of this thesis and his knowledge and support have been essential in my education as a researcher. The occasional rugby ticket was also much appreciated, although when he found out my family supports Munster that benefit was swiftly retracted!

To my first teacher in the lab Sarah, whose guidance and know-how has made me into the scientist I am today! The results found on these pages would not be the same without her help.

To all the post-docs/P.I.s who have come and gone, Aisling, Caroline, Padraig R, Padraig D, Lisa, Neil, Kevin, Jean, Rowan, Pat, Jim, Sarah J, Jan, Heather, Miezko and Mathilde thanks for all the support during the last four years. It's a credit to all of you that I've had such a wealth of knowledge to tap into and that no silly question goes unanswered!

Thanks to Catherine for cooking the books and for the occasional gossip! Special thanks to Vivienne who made the trains run on time even when you forgot to buy a rail ticket, there was no train supposed to run that day and you had set fire to all the trains... I'm fairly sure she was a wizard. Thanks to Orla who has admirably stepped into the breach and may not have realised how much hassle it is to take care of so many helpless scientists! Thanks to Barry, FACS guru and friend.

To the PhD students who have gone before, Karen, Michelle, Stephen and Cheryl, thanks for making it seem so easy! To the fellow PhD ~~slaves~~ students, Ania M, Anna, Aideen, Alicja, Aoife, Lydia and Sarah, thanks for making the work environment so much fun and accesible. You make long days an awful lot shorter!

To Shane, fellow Tolkien-nerd and conveyor of Teenage Mutant Ninja Turtles-related reassurance. To Graham, ever since I met you for the second time ever and we waxed lyrical about our respective break-ups I've known I have a friend I can confide in! Thanks for all the support. To Ania S, for making me realise that I'm not the only pessimist in science and that everything works out in the end! To Conor, who has shown me that you can "waste" an awful lot of time being a nerd and still be the most knowledgeable person in the room. Conor, we'll always have that Valentine's week away from our girlfriends in

Worchester and New York with karaoke, hot-tubs and Simpson's quotes... I've said too much... To my PhD buddy Lara, thanks for making the last four years so much fun and for remaining such a good friend even though you cheated and wrote up a year early! You pushed me to be better at work and play and taught me NEVER to drink Diet Coke.

To my friends from college: the girls Lou and Sinéad, and the ladies Laura and Jessie. You have all been a great support to my mental health and my appreciation of copious amounts of wine! Thanks to the lads from school, Ronan, Niall and the Daves, for preventing me from becoming a complete hermit during the writing of the thesis. Special mention goes to the trip to Silverstone, a mental anguish so harsh I wasn't sure I'd be able to continue with my PhD. Luckily the lads have cleared my post-traumatic stress by mentioning it at every opportunity and suggesting we go back...

To my Mam and Dad for the faith and support that have been given so freely over my lifetime and especially during this PhD. I'll never be able to thank you enough for the chance you've given me. To Damien and Thomas, it helps having siblings that are also my best friends, thanks for all the support.

To Sharee, I'll never regret doing this PhD as it brought you back into my life. You make me a better person (not to mention researcher!!) than I could ever have thought possible. You took care of me so well when I was writing that I'm pretty sure I have to give you a footrub every day for eternity... Thank you!

PUBLICATIONS

Sweeney CM, Lonergan R, Basdeo SA, Kinsella K, Dungan LS, Higgins SC, **Kelly PJ,** Costelloe L, Tubridy N, Mills KH, Fletcher JM. 2011.

IL-27 mediates the response to IFN-β therapy in multiple sclerosis patients by inhibiting Th17 cells. *Brain Behavioural Immunology* 25(6):1170-81.

ABBREVIATIONS

AP-1	Activator protein 1
APC	Antigen presentation cell
BMDC	Bone marrow-derived dendritic cells
BMM	Bone marrow-derived macrophages
CARD	Caspase recruitment domain
CD	Cluster of differentiation
CFA	Complete Freund's Adjuvant
CNS	Central nervous system
CpG	Cytosine-guanine dinucleotide
CPM	Counts per minute
CTL	Cytotoxic T-cell
CTV	Cell trace violet
DAMP	Danger-associated molecular patterns
DAP	Diaminopimelic acid
DC	Dendritic cells
DMSO	Dimethyl sulfoxide
DNA	Deoxyribonucleic acid
EAE	Experimental autoimmune encephalomyelitis
EB/AO	Ethidium bromide/Acridine orange
EBI3	Epstein barr virus induced 3
ELISA	Enzyme-linked immunoabsorbent assay
ERK	Extracellular signal-regulated kinase
FACS	Fluorescent-activated cell sorting
FCS	Foetal calf serum
FMO	Fluorescence minus one

FoxP3	Forkhead box P3
GA	Glatiramer acetate
GM-CSF	Granulocyte-macrophage colony stimulating factor
IAP	Inhibitor of apoptosis protein
IBD	Inflammatory bowel disease
IFN	Interferon
IkB	Inhibitor of kB
IL	Interleukin
IRF	Interferon regulatory factor
iT-reg	Inducible T-reg
LN	Lymph node
LPM	Large peritoneal macrophage
LPS	Lipopolysaccharide
LRR	Leucine rich repeats
MACS	Magnetic activated cell sorting
MAL	MyD88-adaptor-like
MAPK	Mitogen-activated protein kinase
M-CSF	Macrophage colony stimulating factor
MDP	Muramyl dipeptide
MDSC	Myeloid-derived suppressor cells
MHC	Major histocompatibility complex
MIP-1	Macrophage inflammatory protein-1
MMP	Matrix metalloprotease
MOG	Myelin oligodendrocyte glycoprotein
MRC1	Mannose receptor
MS	Multiple sclerosis
Mtb	*Mycobacterium tuberculosis*

MyD88	Myeloid differentiation primary response gene 88
MΦ	Macrophage
NFkB	Nuclear factor kappa B
NK	Natural killer
NLR	NOD Like receptors
NO	Nitric oxide
NOD	Nucleotide-binding oligomerisation domain
NOS	Nitric oxide synthase
nT-reg	Natural T-reg
OVA	Ovalbumin
PAMP	Pathogen-associated molecular patterns
PBS	Phospho-buffered saline
PCR	Polymerase chain reaction
PD-L2	Programmed death ligand 2
PEC	Peritoneal exudate cells
PGN	Peptidoglycan
PLP	Proteolipid protein
PMA	Phorbol myristate acetate
PML	Progressive multifocal leukoencephalopathy
PPMS	Primary progressive MS
PRR	Pathogen recognition receptor
PT	Pertussis toxin
RANTES	Regulated on activation normal T cell expressed and secreted
Relm-α	Resistin-like molecule-α
RIP2	Receptor-interacting protein-2
RNA	Ribonucleic acid
ROR	Retinoic acid receptor-related orphan receptor

RRMS	Relapsing remitting MS
s/n	Supernatant
S1P	Sphingosine-1-phosphate
SIP	Standard isotonic percoll
SOCS	Suppressor of cytokine signalling
SPM	Small peritoneal macrophage
SPMS	Secondary-progressive MS
STAT	Signal transducer and activator of transcription
TAM	Tumour-associated macrophages
Tbet	T box expressed in T-cells
TCR	T-cell receptor
TGF	Transforming growth factor
Th	T helper
TIR	Toll/interleukin-1 receptor
TLR	Toll-like receptor
TNF	Tumour necrosis factor
T-reg	T-regulatory
TSLP	Thymic stromal lymphopoietin
VLA-4	Very late antigen-4

TABLE OF CONTENTS

DECLARATION OF AUTHORSHIP i

ABSTRACT iii

ACKNOWLEDGEMENTS iv

PUBLICATIONS vi

ABBREVIATIONS vii

TABLE OF CONTENTS xi

CHAPTER 1: General introduction 1

1.1 The immune system 1

1.2 The innate immune system 1

1.2.1 Pathogen recognition receptors 2

1.2.1.1 Toll-like receptors 3

Table 1.1 Examples of TLR ligands 4

1.3 The adaptive immune system 4

1.3.1 Antigen presentation 5

1.3.2 T-cells 6

1.3.2.1 Th1 and Th2 cells 6

1.3.2.2 Th17 cells 8

1.3.2.3 γδ T-cells 9

1.3.2.4 Regulatory T-cells 10

Fig 1.1 The differentiation of T-helper subsets. 12

1.4 IL-10 13

1.5 Mononuclear phagocytes 15

Fig 1.2 The mononuclear-phagocyte system. 16

1.5.1 Monocytes 17

1.5.2 Dendritic cells 17

1.5.3 Macrophages 18

1.6 Macrophage activation 19

1.6.1 Classical/M1 activation of macrophages 19

1.6.2 Alternative/M2 activation of macrophages 19

1.6.3 Regulatory macrophages 20

Table 1.2 The expression of macrophage markers and their function 22

Fig 1.3 The activation states of macrophages. 23
1.7 Colony stimulating factors and macrophage activation 24
1.8 The balance of M1/M2 activation and disease 25
1.8.1 The role of macrophage activation during cancer 26
1.8.2 The role of macrophage activation during chronic bacterial infection 27
1.8.3 The role of macrophage activation in autoimmunity and inflammatory disease 28
1.9 Nod-like receptors 30
Table 1.3 Examples of NLR agonists 30
1.9.1 NOD1 and NOD2 signalling 31
NOD1 and NOD2 and infection. 33
1.9.3 NOD1 and NOD2 and inflammatory disease 34
1.10 Multiple sclerosis 36
1.11 Experimental autoimmune encephalomyelitis 39
1.12 Aim of study 42

CHAPTER 2: Materials and methods 43
2.1 Materials 43
Table 2.1.1Recombinant murine cytokines 46
Table 2.1.2 Small molecule inhibitors 46
Table 2.1.3 Real-time PCR primers 46
Table 2.1.4 PRR ligands 47
Table 2.1.5 Antigens 48
Table 2.1.6 NA/LE Antibodies 48
Table 2.1.7 ELISA antibodies, standards and blocking solutions. 48
Table 2.1.8 Fluor-conjugated FACS antibodies 49
Table 2.1.9 Biotin-antibody cocktails used for the purification of cells by negative magnetic selection 50
Table 2.1.9 Reagents for restimulation of cells for intracellular staining 50
2.2 Mice 50
2.3 Methods 51
2.3.1 General protocols for cell culture 51
2.3.1.1 Preparation of a single cell suspension 51
2.3.1.2 Red blood cell lysis 51
2.3.1.3 Cell counting 51
2.3.2 Cell culture 51

2.3.2.1 Generation of bone marrow derived dendritic cells 52
2.3.2.2 Generation of bone marrow derived macrophages 52
2.3.3 Intraperitoneal injections 53
2.3.3.1 The isolation of peritoneal cells by peritoneal lavage 53
Table 2.3.1 Panel of fluor-conjugated antibodies used for analysing the PEC 53
2.3.4 Subcutaneous injections 54
2.3.5 Footpad injections 54
2.3.5.1 In vivo stimulation of γδ T-cells 54
Table 2.3.2 Panel of fluor-conjugated antibodies for the analysis of γδ T-cells ex vivo .. 54
2.3.6 Protocols associated with EAE 55
2.3.6.1 Actively induced EAE 55
2.3.6.1.2 Passively induced EAE 55
2.3.6.2 Mononuclear cell isolation from the central nervous system 56
Table 2.2.3 The panel of fluor-conjugated antibodies used for analysing mononuclear brain cells ex vivo 56
2.3.6.3 The transfer of peritoneal macrophages into mice with EAE 57
2.3.6.4 Immunisation of mice with MOG and CFA for the isolation of antigen-specific T-cells 57
2.3.7 Cell Purification 58
2.3.7.1 Purification of $CD4^+$ or $CD3^+$ T-cells using negative magnetic selection 58
Fig 2.2.1 Sample purities for $CD3^+$ T-cells (A) and $CD4^+$ T-cells (B) sorted by negative magnetic selection 59
2.3.7.2 Purification of naive T-cells by FACS 60
Table 2.2.4 The panel of fluor-conjugated antibodies used for sorting naive T-cells 60
Fig 2.2.2 The gating strategy for sorting naive T-cells by FACS 60
2.3.7.3 Purification of peritoneal macrophages by FACS 61
Table 2.2.5 Panel of fluor-conjugated antibodies used for sorting peritoneal macrophages 61
2.3.7.4 Purification of peritoneal neutrophils 62
Fig 2.2.3 Sample purities for neutrophils purified by continuous Percoll gradient 62
2.3.7.5 Depletion of innate cells from the PEC by FACS 62
Table 2.2.6 Panel of fluor-conjugated antibodies used for depleting DC and eosinophils by FACS 63
Table 2.2.7 Panel of fluor-conjugated antibodies used for depleting peritoneal macrophages and neutrophils by FACS 63
Fig 2.2.4 The gating strategy used to deplete (A) neutrophils, (B) macrophages, (C) DC and (D) eosinophils from the total PEC 64

2.3.8 In vitro cell stimulations 65
2.3.8.1 Stimulation of BMDC with TLR agonists and TriDAP 65
2.3.8.2 Stimulation of BMM with TriDAP or LPS 65
2.3.8.3 Stimulation of PEC in vitro with TriDAP or LPS 65
2.3.8.4 Stimulation of peritoneal neutrophils 66
2.3.8.5 Stimulation of depleted PEC 66
2.3.9 T-cell stimulations 66
2.3.9.1 In vitro stimulation of $CD4^+$ T-cell 66
2.3.9.2 Stimulation of $CD4^+$ T-cells in the presence of TriDAP 66
2.3.9.3 Stimulation of $CD4^+$ T-cells in the presence of supernatant from PEC 67
Table 2.2.8 Panel of fluor-conjugated antibodies used for the FACS analysis of $CD4^+$ T-cells stimulated in the presence of supernatant from treated PEC 67
2.3.10 T-cell and APC co-cultures 68
2.3.10.1 Antigen presentation assay with stimulated BMDC and $CD4^+$ T-cells 68
2.3.10.2 Antigen-specific restimulation of cells from mice with EAE 68
2.3.10.3 Co-culture of *M. tuberculosis* stimulated BMDC and purified T-cells 68
2.3.10.4 Co-culture of LPM with OVA-specific $CD4^+$ T-cells 69
Table 2.2.9 Panel of fluor-conjugated antibodies used for the co-culture of LPM and OVA-specific $CD4^+$ T-cells 69
2.3.11 FACS Analysis 70
2.3.11.1 The discrimination of live and dead cells 70
2.3.11.2 Surface marker staining 70
2.3.11.3 Intra-nuclear staining 70
2.3.11.4 Stimulation of cells for intracellular cytokine staining 71
2.3.11.4.1 Intracellular staining 71
2.3.11.4.2 Intracellular staining of YM1 71
2.3.11.4.3 Intracellular staining of relm-α 72
Table 2.2.10 Panel of fluor-conjugated antibodies used for the staining of YM1 an relm-α in peritoneal macrophages 72
2.3.11.4 Acquisition and analysis of FACS data 72
2.3.12 Measurement of cell proliferation 73
2.3.12.1 Labelling of cells with CTV 73
2.3.12.2 The measurement of proliferation by the incorporation of [^{3}H] thymidine 73
2.3.13 Enzyme linked immunosorbent assay (ELISA) 74
2.3.14 Gene expression assays using real-time PCR 75
2.3.14.1 RNA isolation 75

2.3.14.2 Reverse transcription PCR 75
2.3.14.3 Real-time PCR 75

CHAPTER 3: The effect of the NOD1 agonist TriDAP on the clinical symptoms of EAE 77

3.1 Introduction 77
3.2 Results 81
3.2.1 The effect of the NOD1 agonist TriDAP on antigen-specific immune responses in vivo and the clinical course of EAE 81
3.2.2 The effect of TriDAP on cytokine production by T-cells from MOG-immunized mice 82
3.2.3 The effect of TriDAP on the ability of DC to present antigen to antigen-specific T-cells. 83
3.2.4 The effect of TriDAP on the ability of DC to respond to *M. tuberculosis* 84
3.2.5 The effect of TriDAP on IL-1β and IL-23-mediated IL-17 production in vivo. 86
3.3 Discussion 87

CHAPTER 4: The effect of the NOD1 agonist TriDAP on the production of cytokines by innate immune cells 99

4.1 Introduction 99
4.2 Results 101
4.2.1 The effect of TriDAP on TLR-stimulated cytokine production by BMDC 101
4.2.2 The effect of TriDAP on cytokine production by BMM 102
4.2.3 The effect of TriDAP on cytokine production by peritoneal exudate cells 103
4.2.4 The effect of p38 MAPK and phosphoinositide-3 kinase inhibitors on TriDAP-mediated cytokine production by PEC 104
4.2.5 The role of different innate cells in TriDAP-mediated IL-10 and IL-6 production 105
4.2.6 The effect of TriDAP on cytokine production by peritoneal macrophages. 106
4.2.7 The effect of TriDAP on peritoneal neutrophils 107
4.2.8 The effect of supernatant from TriDAP treated PEC on the polarisation of $CD4^+$ T-cells 107
4.3 Discussion 111

CHAPTER 5: The effect of the NOD1 agonist TriDAP on the expansion and activation of macrophages in vivo 131

5.1 Introduction 131
Fig 5.1.1 The maintenance of LPM and SPM, two distinct peritoneal macrophage subsets. 134
5.2 Results 135
5.2.1 The characterisation of the innate immune cells from peritoneal cavity of naive mice 135

5.2.2 The characterisation of the peritoneal cavity 16 h after the injection of TriDAP or LPS 136

5.2.3 The characterisation of the peritoneal cavity 4 days after the injection of TriDAP or LPS 138

5.2.4 The characterisation of surface proteins expressed by LPM and SPM 139

5.2.5 Injection of TriDAP induces the proliferation of LPM and SPM. 141

5.2.6 The expression of the M2 markers relm-α and YM1 by LPM and SPM. 143

5.2.7 The effect of TriDAP on the expression of M2 and M1 associated mRNA 144

5.2.8 The role of IL-4 in the TriDAP-induced expansion and M2 activation of LPM 146

5.2.9 The role of IL-10 in the TriDAP-induced expansion and M2 activation of LPM 150

5.2.10 The effect of TriDAP on the population of Treg cells in the peritoneal cavity 153

5.2.11 The effect of TriDAP on the ability of LPM to present antigen 153

5.2.12 The effect of macrophage transfer on the clinical symptoms of EAE. 154

5.2.13 TriDAP-mediated M2 activation suppresses the development of pathogenic T-cells 157

5.2.14 Gating strategies for sorting macrophages by FACS 159

Fig 5.2.1 Gating strategy for sorting LPM by FACS 159

Fig 5.2.2 Gating strategy for sorting total macrophages by FACS 159

5.3 Discussion 161

Fig 5.3.1 The possible mechanism for the TriDAP and LPS-mediated expansion of LPM and SPM. 168

CHAPTER 6 General discussion 205

CHAPTER 7: Bibliography 213

Chapter 1:

General introduction

CHAPTER 1: General introduction

1.1 The immune system

Millions of years of evolution have allowed living organisms to interact with each other and the environment around them. The host has developed specific mechanisms of defense to cope with invading pathogenic organisms, the innate and adaptive immune system.

The immune system consists of a number of different cell types, including white blood cells or leukocytes, which originate from a common pluripotent cell within the bone marrow [1]. The pluripotent stem cells develop into leukocytes via two distinct pathways. The lymphoid pathway gives rise to T-cells, B-cells and NK-cells while the myeloid pathway gives rise to mononuclear and polymorphonuclear leukocytes. These two lineages make up the majority of immune cells.

Innate immunity is the first line of defence against pathogens and uses innate immune cells and molecules to respond quickly and specifically to infection. The adaptive immune system is slower but confers long lasting immunity. After initial infection, the adaptive immune response generates memory T-cells and B-cells which allow the host to respond to reinfection quickly and efficiently. Both aspects of the immune system interact with one another, with the innate priming the adaptive. This recognition, response and memory form the basis of the immune system.

1.2 The innate immune system

The simplest way the host prevents infection is by forming a barrier of epithelial cells at mucosal surfaces, such as the skin, gut and airways, to deny access to internal tissues. In addition to physically blocking the entrance of pathogens, epithelial cells produce anti-microbial proteins called defensins [2]. Upon interaction with microbes, epithelial cells produce immune mediators that modulate the innate immune system. Innate effector cells include macrophages and neutrophils, which are recruited to the site of infection to carry out their function. These are phagocytic cells that engulf an invading organism into a compartment called the phagosome. This compartment can acidify and kill the organism. Other compartments within phagocytic cells, called lysosomes, release peptides, enzymes and nitric oxide (NO), which are lethal to microbes [1].

Innate immune cells also have the ability to initiate the inflammatory response by secreting pro-inflammatory cytokines and lipid-based inflammatory mediators. Inflammation is characterised by heat, swelling, pain and redness, which are reflections of changes to the local blood vessels. The blood vessels increase in diameter leading to reduced blood flow. The vessel walls also become more permeable and express cell adhesion molecules, which bind passing immune cells. Proteins called chemokines are secreted to attract immune cells to the site of infection. In short, inflammation allows the efficient access of immune effector cells to the site of infection and is a vital feature of the innate immune system.

The induction of the inflammatory response is initiated by the interaction of innate immune cells, such as epithelial cells, macrophages and DC, with invading organisms. This is facilitated by proteins called pathogen recognition receptors (PRRs), which recognise repetitive structures, called pathogen associated molecular patterns (PAMPs), that are unique to microorganisms [3]. PAMPs are part of unique and essential microbial structures, such as bacterial cell wall components peptidoglycan (PGN) and lipopolysaccharide (LPS). PRRs confer a certain amount of specificity to the innate immune system, while also facilitating the expression of immune response genes, which induce the production of effector proteins, such as cytokines and chemokines [4]. In addition to PAMPs, there is growing evidence that innate immune cells can recognise "self"-molecules that are released during tissue damage. These so called danger associated molecular patterns (DAMPs) are hypothesised to discern commensal microbial growth from pathogenic infection [5].

1.2.1 Pathogen recognition receptors

PRRs are proteins which detect PAMPs or DAMPs inside and outside the cell. They are split into several families including the Toll-like receptors (TLRs) and Nod-like receptors (NLRs). Upon binding of a PAMP to a PRR, the signalling domain of the receptor interacts with other adaptor signalling proteins, which in turn activate transcription factors, such as NFkB [6]. These transcription factors induce the transcription of immune response genes that are essential for the functions of innate immune cells.

After activation, an innate immune cell produces a range of mediators including acute phase proteins, chemokines, cytokines and co-stimulatory molecules. Depending on which PRR is activated, a different set of genes are transcribed, and therefore a different cytokine or chemokine milieu is generated, which enables a specific response to a variety of infections. The production of cytokines, the expression of co-stimulatory molecules and the presentation of antigenic peptides on the surface of innate immune cells are essential for the propagation of the adaptive immune response [3].

1.2.1.1 Toll-like receptors

TLRs were the first family of PRRs to be described. They are homologues of Drosphilia Toll and are heavily conserved across many species. TLRs are transmembrane proteins that recognise a variety of PAMPs including components of bacterial cell wall, DNA and RNA (Table 1.1). Ten human and twelve murine TLRs have been described to date; these are all located on the plasma membrane except for TLR3, TLR7, TLR8 and TLR9, which are located intracellularly [7].

LPS is a classic example of a microbial PAMP; LPS is a lipid-carbohydrate complex found in the outer membrane of Gram-negative bacteria and is recognised by TLR4. TLR4 is one of the best characterised PRR and was the subject of Nobel Prize winning research by Hoffman and Beutler [8, 9]. The activation of innate immune cells in response to TLR ligation is mediated by adaptor proteins that initiate complex signalling pathways. MyD88 is an adaptor protein which is recruited to an activated TLR via a conserved TIR domain and is used by all TLRs except TLR3. Activation of the MyD88 pathway leads to the production of inflammatory cytokines, such as TNF-α, via the transcription factor NFkB [10]. In addition to NFkB activation, the MyD88 signalling pathway also induces the phosphorylation of mitogen-activated protein kinases (MAPKs) p38 and ERK, which in turn mediate the activation of the transcription factor AP-1 [11]. This plays a role in producing cytokines such as IL-10 and IL-23 in response to TLR activation [12, 13]. Different adaptor molecules such as MAL and TRAM can induce MyD88-independent signalling pathways, which result in the production of different sets of cytokines. TLR4 uses the adaptor protein TRAM to produce the cytokines called the type 1 interferons (IFNs) via a set of transcription factors called the interferon regulatory factors (IRFs) [14,

15]. The differences between the TLR signalling pathways allow the innate immune system to prime the adaptive immune system in a specific way, depending on which TLR is activated.

Table 1.1 Examples of TLR ligands

TLR	TLR2	TLR3	TLR4	TLR5	TLR7	TLR9
PAMP	PGN	dsRNA	LPS	Flagellin	ssRNA	CpG DNA

1.3 The adaptive immune system

The adaptive immune response is unique in its ability to generate immunological memory. Once exposed to an invading organism, the adaptive immune system generates memory cells, which respond quicker and more efficiently to reinfection. This sophisticated system has developed specificity by recognising microbial peptides called antigens. The cells of the adaptive immune system are called lymphocytes. When fully mature, lymphocytes enter the circulation or reside in the peripheral lymphoid organs such as the spleen or lymph nodes. Here they survey antigen presenting cells and can become activated. There are two types; B-cells and T-cells. B-cells produce proteins called antibodies which bind to pathogens, neutralising them and improving the efficiency of their phagocytosis [1]. B-cells recognise antigen by direct binding of antibody-pathogen complexes. T-cells have a range of functions including the killing of infected cells and the production of cytokines [1]. T-cells depend on presentation of antigen by cells of the innate immune system. The recognition of a specific antigen depends on the ability of the adaptive immune system to generate a lymphocyte with the corresponding antigen receptor [16].

Lymphocytes must respond to a diverse range of antigens and therefore the immune system must generate lymphocytes that express a diverse range of antigen receptors. This is achieved by somatic gene rearrangements and mutations [1]. Different parts of the variable region of the antigen receptor are encoded by sets of genes. One gene from each set is randomly chosen to form the antigen receptor during maturation of lymphocytes, giving a unique antigen receptor to each lymphocyte. After a lymphocyte encounters its

corresponding antigen it starts to divide to produce identical progeny in a process known as clonal expansion [16]. These antigen-specific lymphocytes become effector cells, which will actively help to fight infection, or long lasting memory cells, which will respond faster to restimulation with the same antigen.

1.3.1 Antigen presentation

Presentation of a microbial peptide by antigen presenting cells (APC) of the innate immune system is a vital step in the activation of antigen specific T-cells. Peptides from microbes, when presented to a T-cell, will evoke either new clonal expansion or, if that microbe has been encountered before, a secondary memory response to that organism. Phagocytic cells of the innate immune system, such as macrophages and DCs, can act as APC by processing microbial proteins and presenting them on their surface in protein complexes called major histocompatibility complex (MHC) class I or class II molecules.

MHC class I molecules normally present peptides which are processed in the cytosol, perhaps from a virus or intracellular bacteria, but occasionally MHC class I molecules can present peptides that have been taken from the exogenous environment [1]. The MHC class I-antigen complex is then moved to the surface of the cell where it can interact with $CD8^+$ cytotoxic T-cells [16]. Peptides which form complexes with MHC class II molecules are processed within endocytic vesicles and originate from extracellular pathogens. The MHC class II-antigen complex is then moved to the surface of the cell where it can interact with $CD4^+$ T-cells [16].

T-cells contain a corresponding antigen receptor called the T-cell receptor (TCR), which binds directly to the MHC-antigen complex. The T-cell proteins CD4 and CD8 are co-receptors, which facilitate the binding of the MHC-antigen complex with the TCR. However, the presentation of the antigen alone is not sufficient for clonal expansion of T-cells. In fact if the specific TCR-MHC interaction takes place in the absence of co-stimulatory molecule interactions, the T-cell becomes anergic [1, 5]. This prevents T-cells from responding to self-antigens that are presented in the absence of infection, which can lead to autoimmunity.

During infection, PAMPs induce APCs to express co-stimulatory molecules such as CD80/CD86. These molecules bind to CD28 on T-cells and prevent anergy while promoting survival of the T-cell [1]. In addition to co-stimulatory molecules, APCs can produce co-inhibitory molecules, such as PD-L2, that actively inhibit clonal expansion [17]. Activated innate immune cells also release cytokines which further differentiate T-cells into specific subtypes. These three signals; antigen presentation, co-stimulation and cytokine secretion, are required for competent activation of T-cells and highlight the importance of priming the innate immune system to achieve an efficient adaptive immune response [1, 5, 16].

1.3.2 T-cells

T-cells begin their development in the bone marrow as lymphoid progenitor cells, which then migrate to the thymus to undergo positive and negative selection. This process allows immature T-cells to interact with many different self-MHC molecules via their unique TCR. Cells that recognise self-MHC molecules survive while those that interact strongly with self-MHC molecules are eliminated to prevent autoimmunity [1]. These mature T-cells then migrate to the peripheral lymph organs where they can become activated via APCs such as DC. The activated T-cells then migrate to the site of infection to carry out their function. Most T-cells express TCRs containing αβ subunits, but a smaller subset of T-cells express a TCR containing the subunits γδ. T-cells are further catergorised by the co-receptors CD4 or CD8. $CD8^+$ Cytotoxic lymphocytes (CTLs) are responsible for the direct killing of abnormal or infected cells [16]. $CD4^+$ T-cells are called T helper cells (Th cells) and help regulate immune responses by producing specific cytokines [16]. $CD4^+$ Th cells are further subdivided on the basis of which cytokines they produce (Fig 1.1).

1.3.2.1 Th1 and Th2 cells

$CD4^+$ effector T-cells were initially divided into two subtypes based on the cytokines they produce, with each subtype specialising in a particular form of defence. Mosmann et al first described two different subsets in 1986, Th1 and Th2 cells [18]. Th1 cells promote cell-mediated immunity against intracellular pathogens by secreting IFN-γ and TNF-α (Fig

1.1). IFN-γ-producing Th1 cells are important for inducing the classical (M1) activation of macrophages [19] and enhancing their anti-bacterial function. In addition, these cytokines can activate natural killer (NK) cells that mediate the killing of infected cells [1]. In turn NK cells can promote Th1 polarisation by producing IFN-γ themselves, which upregulates the expression of IL-12R on the surface of T-cell, therefore making them more susceptible to Th1 polarisation. NK cells also produce IL-12, which directly induces Th1 polarisation.

Th2 cells mediate humoral immunity against extracellular bacteria and parasites by secreting IL-4, IL-13, IL-5 and IL-10 (Fig 1.1). IL-4 and IL-13 are responsible for the expansion of B-cells and antibody isotope class switching [1]. In addition, IL-4 and IL-13 mediates parasite pinocytosis and tissue repair by inducing the alternative (M2) activation of macrophages [19]. IL-5 is responsible for the chemotaxis and differentiation of eosinophils, which are involved in mediating immune responses against extracellular pathogens and allergens [1]. The polarisation of either of these Th cell subsets is mediated by the signalling of specific cytokines, which activate transcription factors that are exclusive to each subset.

IL-12 is also known as IL-12p70 and is formed by the production of two subunits, IL-12p40 and IL-12p35. IL-12 is produced by innate immune cells, such as M1 macrophages or DC, in response to PAMPs, and it induces the polarisation of naive T-cells into Th1 cells [20] (Fig 1.1). IL-27 is a cytokine made up of two subunits, IL-27p28 and EBI3 [21]. IL-27 increases the expression of the IL-12 receptor (IL-12Rβ2) on the surface of T-cells, thereby enhancing IL-12-mediated Th1 polarisation [22]. The Tbox transcription factor (T-bet) is expressed by Th1 cells in response to IL-12 and enhances the expression of the IFN-γ and IL-12Rβ2 genes [23]. Furthermore, T-bet deficient mice have defective Th1 cell differentiation and enhanced Th2 responses [24] (Fig 1.1).

IL-4 or IL-13 induces the polarisation of Th2 cells, forming a positive feedback loop resulting in additional IL-4/IL-13 production and Th2 differentiation [25] (Fig 1.1). The transcription factor GATA3 is upregulated in response to IL-4. GATA3 mediates the expression of genes essential for Th2 differentiation and simultaneously inhibits the production of IFN-γ [26] (Fig 1.1). The initial production of IL-4 in response to extracellular pathogens is thought to come from basophils and innate lymphoid cells, though the exact mechanism behind pathogen recognition is unclear [27]. Tissue damage has also been

shown to be important in the development of Th2 cells; damaged epithelial cells can produce mediators, such as TSLP and IL-33, which promote Th2 differentiation indirectly [28, 29]. In addition, DC can promote Th2 polarisation by the induction of the co-stimulatory molecule OX40L [30].

The activation of these two Th cell subtypes is reciprocal; IFN-γ inhibits the induction of Th2 cells and IL-4 inhibits the induction of Th1 cells [31] (Fig 1.1).In addition, the expression of T-bet and GATA3 are mutually exclusive; the deletion of either transcription factor leads to the automatic upregulation of the other [26, 32].

1.3.2.2 Th17 cells

Recently a T-cell population, distinct from the classical Th1 and Th2 subtypes, has been discovered and characterised by its ability to produce the cytokine IL-17A [33]. These are designated Th17 cells and are abundant at the mucosa, where they mediate inflammation in response to pathogens [34]. In addition to producing IL-17A, Th17 cells also produce IL-17F, IL-21, granulocyte-macrophage colony stimulating factor (GM-CSF) and IL-22 (Fig 1.1). IL-17RA binds both IL-17A and IL-17F and is ubiquitously expressed, hence, IL-17A/F mediate their effects via a wide range of cell types [34]. IL-17A (also known as IL-17) induces the production of pro-inflammatory cytokines such as IL-6, TNF-α, IL-1β, granulocyte-CSF (G-CSF) and GM-CSF and is critical for recruiting neutrophils to the site of inflammation [34]. Mice deficient in IL-17RA have profound neutropenia,a failure to recruit neutrophils. This results in a compromised resistance to mucosal infection, as neutrophils are essential for the engulfment and clearance of micro-organisms [35]. In addition the Th17 cell has been implicated as the pathogenic cell type in a range of experimental autoimmune models, such as EAE and psoriasis [36, 37]. Moreover, recent studies have shown that an IL-17RA blocking antibody or IL-17A neutralising antibody is a promising therapy for psoriasis [38].

IL-23 has been shown to be essential in the differentiation and/or expansion of Th17 cells (Fig 1.1); mice deficient for IL-23p19, a subunit of mature IL-23, fail to generate Th17 cells [39]. The receptor for IL-23 (IL-23R) is not expressed by naive T-cells, indicating that IL-23 is involved in the expansion of Th17 cells but not their initial differentiation [40]. IL-1β has

also been implicated in the expansion of Th17 cells; mice deficient in the receptor for IL-1β (IL-1RI) have reduced antigen-specific Th17 responses and are resistant to EAE [41].

Further studies demonstrated that Th17 differentiation is dependent on the production of IL-6 and TGF-β [42] (Fig 1.1). IL-6 was shown to induce the expression of the Th17-specific transcription factor RORγt by initiating the production of IL-21 by naive T-cells; the production of IL-21 works as an autocrine feedback loop that propagates RORγt expression [43, 44]. Das et al argued that TGF-β does not directly induce Th17 polarisation but inhibits the expression of STAT4 and GATA3, therefore blocking the differentiation of Th1 and Th2 cells respectively. [45].

The differentiation of Th17 cells was originally shown to be sensitive to inhibition by both Th2 and Th1 cytokines [46], however, new findings have shed light on more complex patterns of regulation (Fig 1.1). IL-4 has been shown to be a potent suppressor of initial Th17 polarisation by blocking the STAT3 transcription factor from binding to the *Il17a* gene, however, the sensitivity of Th17 cells to IL-4-mediated suppression wanes if the cells undergo prolonged stimulation by TGF-β, IL-6 and IL-23 [47]. IFN-γ, IL-12 and IL-27 all inhibit the differentiation of Th17 cells in vitro and in vivo [48-50] (Fig 1.1). However, it has been shown that a subset of functionally potent Th17 cells can produce IL-17 and IFN-γ concomitantly, or switch off IL-17 entirely to become IFN-γ-producing "ex Th17" cells [51]. The plasticity of Th17 cells is increasingly being recognised as more studies implicate "ex-Th17" cells in the pathogenesis of autoimmunity [52, 53].

1.3.2.3 γδ T-cells

A subset of T-cells are characterised by the expression of an alternative TCR consisting of γ and δ chains. γδ T-cells can recognise antigen independent of MHC presentation [54]. In addition, γδ T-cells can respond rapidly to PRR ligation or pro-inflammatory cytokines even in the absence of TCR stimulation [55, 56], hence, these cells have been classified as part of both the innate and adaptive immune systems. Subsets of resident γδ T-cells are found at mucosal sites, such as the gut and lungs, and are thought to be vital for early immune responses [57]. Bonnevile et al suggest that the primary function of γδ T-cells is to recognise danger signals associated with tissue damage and infection, rather than playing a role in the antigen specific immune response [58].

Certain subsets of γδ T-cells can produce IL-17 in response to infection or pro-inflammatory cytokines (Fig 1.1). They form part of the initial phase of immune defence by secreting IL-17 days earlier than conventional Th17 adaptive responses [59]. The early production of IL-17 by γδ T-cells has been shown to be critical in restraining bacterial and fungal infection at the mucosa [60, 61]. IL-17 production by γδ T-cells mediates protection by inducing neutrophil recruitment. Furthermore, studies have shown that mice deficient in functional γδ T-cells are susceptible to bacterial infection [62, 63]. The rapid production of IL-17 is thought to be dependent on the constitutive expression of the IL23R on the surface of resting γδ T-cells. Conventional αβ T-cells are refractory to IL-23 stimulation until differentiated into Th17 cells, however, γδ T-cells respond to IL-23 in the absence of other signals [55]. IL-1β has also been shown to enhance the IL-23-mediated production of IL-17 by γδ T-cells and mice deficient in IL-1R1, the receptor that IL-1β binds to, are resistant to the induction of EAE [41].

γδ T-cells can also regulate conventional αβ T-cells via the secretion of polarising cytokines. IL-21 and IL-17 secretion by γδ T-cells has been shown to drive conventional Th17 cell responses (Fig 1.1) [55]. Sutton et al have reported that γδ T-cells play a role in driving the pathogenesis of autoimmune disease, as mice deficient in γδ T-cells develop attenuated EAE as a result of a compromised expansion of pathogenic Th17 cells [55].

1.3.2.4 Regulatory T-cells

As well as effector T-cells that mediate immune defence against infection, there are regulatory T-cells (Treg) that regulate effector cells to prevent execessive inflammation and autoimmunity [64]. Treg cells are broadly subdivided by their origin and cell markers into two subsets, naturally-occurring Treg (nTreg) cells and inducible Treg (iTreg) cells. nTreg cells are generated in the thymus in a similar fashion to conventional naive T-cells and are responsible for the suppression of self-reactive T-cells during steady state homeostasis [65]. Sakaguchi et al identified CD25 (IL-2Rα) as an effective marker for Treg cells and demonstrated that depletion of T-reg cells in conventional mice or the transfer of $CD25^-$ T-cells into athymic nude mice leads to spontaneous autoimmunity [64]. The transcription factor forkhead box P3 (FoxP3) is now known to maintain Treg cells following the discovery that FoxP3 deficiency is the cause of spontaneous autoimmunity

in scurfy mice [66]. FoxP3 controls the expression of Treg-associated genes, such as CD25, CTLA4 and glucocorticoid-induced TNF receptor (GITR), while simultaneously inhibiting the expression of GATA3, T-bet and RORγt [67].

In addition to nTreg cells, naive $CD4^+$ and $CD8^+$ T-cells can differentiate into functional iTreg cells in the periphery in a process known as peripheral conversion [68, 69]. Peripheral conversion can be induced in response to suboptimal antigen stimulation or the presence of the right cytokine milieu. A population of functionally suppressive iTreg cells can be generated in a number of ways, hence, the populations of "iTreg cells" described thus far are highly heterogeneous. TGF-β has been described as a key factor in the conversion of naive $CD4^+CD25^-$ T-cells into functionally suppressive $CD4^+CD25^+FoxP3^+$ iTreg cells (Fig 1.1) [70]. IL-10 can also induce the differentiation of naive T-cells into IL-10-producing iTreg cells, also known as Tr1 cells [71]. Tr1 cells do not express FoxP3 but are functionally suppressive during autoimmune disease [72, 73]. iT-regs mediate the suppression of immune responses by producing IL-10 and TGF-β, which inhibit the activation of effector T-cells as well as inducing the differentiation of new iTreg cells (Fig 1.1) [71].

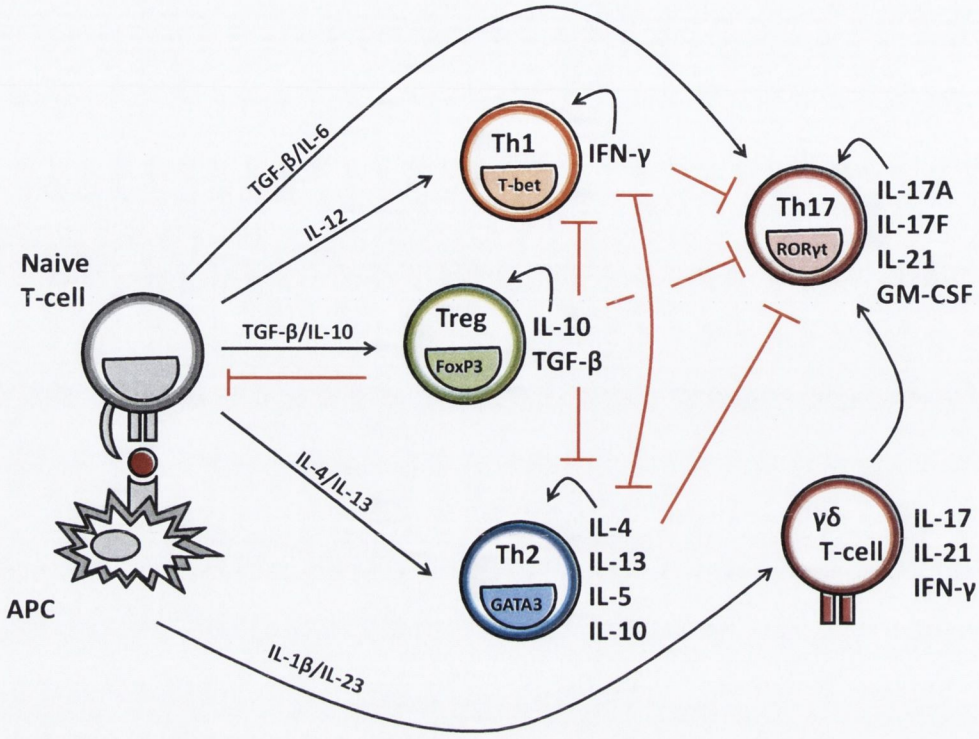

Fig 1.1 The differentiation of T-helper subsets. Naive T helper cells can be activated by an APC, such as a DC or macrophage, by the presentation of antigen via MHC-II. To become fully activated a naive T-cell must also interact with co-stimulatory molecules present on activated APCs. A naive T-cell can be polarised into Th1, Th2 or Th17 subsets depending on the cytokines present in the microenvironment. These subsets are characterised by the transcription factors and cytokines they produce. Cytokines produced by the particular subset promote the polarisation of that subset and also inhibit the polarisation of other Th subsets. Naive T-cells may also become Treg cells that actively inhibit T-cell activation. γδ T-cells are thought to be activated by cytokines in the absence of TCR stimulation and contribute to the polarisation of Th cells by producing cytokines themselves.

1.4 IL-10

IL-10 was first characterised by Mossman et al in 1989 as a cytokine secreted by Th2 clones. It was initially called cytokine synthesis inhibitory factor because of the inhibitory effect it had on the production of IFN-γ [74]. IL-10 is now known to be an anti-inflammatory cytokine that can suppress a variety of pro-inflammatory cytokines and is produced by a variety of innate and adaptive immune cells. IL-10 binds to a receptor with two chains, IL-10R1 and IL-10R2 [75]. The presence of both of the receptor chains is required for IL-10 signalling. This was confirmed by Spencer et al who showed that splenocytes are refractory to IL-10 stimulation in the absence of one or the other of the receptors [76]. IL-10R2 is ubiquitously expressed and IL-10R1 is mainly expressed on leukocytes. As a result, IL-10 can suppress most cells of the innate and adaptive immune system. IL-10 is produced by a variety of leukocytes including innate immune cells (DC, macrophages, neutrophils, eosinophils etc) and adaptive immune cells ($CD4^+$ and $CD8^+$ T-cells) [77].

IL-10 inhibits the production of cytokines, the expression of CD80, CD86 and MHC-II, and the secretion of chemokines by APC such as macrophages and DC [78, 79]. In addition, IL-10 can also make cells refractory to signalling from cytokines. IL-10-treated T-cells respond less readily to stimulation with IFN-γ or IL-4 [79]. As a result, IL-10 limits the activation of immune responses and prevents collateral tissue damage caused by excessive inflammation. The importance of IL-10 in mediating immune homeostasis is confirmed by the observation of spontaneous colitis in IL-10-deficient mice [80]. IL-10 is also important for restraining inflammation during a microbial infection; the lethality of pathogenic infections increases in the absence of IL-10 due to excessive TNF-α, IL-12, and IFN-γ production [81, 82]. IL-10 is important for restraining pathogenic immune responses but it can also inhibit the efficient clearance of infection. IL-10-deficient mice develop enhanced Th1 responses that are more capable of clearing bacterial and fungal infections [83, 84]. The role of IL-10 in Th2 immunity is more complicated. IL-10 production by macrophages can promote Th2 differentiation [85], however, the symptoms of experimental asthma and allergy, which are mediated by Th2 responses, are exacerbated in IL-10 deficient mice [86]. In contrast to its suppressive effects on effector Th cell subsets, IL-10 can act on Treg cells to maintain the expression of FoxP3 [87]. This function

allows IL-10 to potentiate an immunosuppressive T-cell response, in addition to mediating immunosuppression directly.

IL-10 mediates its function by activating the STAT3 transcription factor [88]. IL-10 also activates STAT1 and STAT5, but STAT3 activation is the only one necessary for the suppressive effects of IL-10. Deletion of STAT3 completely abrogates the ability of macrophages and neutrophils to respond to IL-10 [89]. STAT3 induces the expression of suppressor of cytokine signalling (SOCS) proteins SOCS1 and SOCS3. These proteins block the signalling pathways of IL-10, IFN-γ and IL-4, therefore rendering cells unresponsive to stimulation by these cytokines [90-92]. IL-10 has also been shown to stabilise the expression of IkB-α, therefore preventing the function of NFkB [93].

Myeloid cells produce IL-10 in response to different TLR agonists, including LPS, CpG and PGN [94]. TLR2 agonists are especially potent inducers of IL-10, and there is some evidence that NOD2 may participate in enhancing TLR2-mediated IL-10 production by activating RIP2 [95]. TLR agonists promote IL-10 production by the activation of the MAPKs, ERK and p38. Knocking out both ERK and p38 completely abrogates IL-10 production by myeloid cells, but signalling can still be maintained if one or the other is functional [94]. Both of these MAPKs activate the transcription factor AP-1, which mediates the transcription of the IL-10 gene. IL-10 production by Th2 cells is mediated by the activation of the main Th2 transcription factors GATA3 and STAT6 in response to IL-4. In addition, the production of IL-10 by Th2 cells requires the activation of ERK, which is thought to be activated by a high antigen dose via the TCR receptor [96]. In contrast to myeloid cells, T-cells do not require p38 activation for the production of IL-10 [96]. Other cytokines can disrupt or enhance the production of IL-10 by modulating different steps in the associated signalling cascade. IL-27 can promote the production of IL-10 from Th cells by enhancing the activation of ERK [97]. IFN-γ inhibits the production of IL-10 by inducing the release of glycogen synthase kinase, which directly inhibits AP-1 activation [98].

1.5 Mononuclear phagocytes

Mononuclear phagocytes are innate myeloid cells that are derived from a common progenitor in the bone marrow (Fig 1.2). They consist of monocytes, macrophages and DC. Their functions are varied, including the phagocytosis of pathogens and cellular debris, antigen presentation, cytokine production, and immune homeostasis [1, 99]. During steady state, macrophages and DC reside in the tissue and function as sentinels by scavenging debris and processing antigen [100-102]. There is strong evidence that resident populations of macrophages and DC are derived prenatally from bone marrow precursors and maintain themselves in the tissue by self-proliferation during the life span of the host [103, 104] (Fig 1.2). During infection or tissue injury these resident cells mediate the recruitment of monocytes, which differentiate into new macrophages/DC and mediate immune responses and bacterial clearance [102] (Fig 1.2).

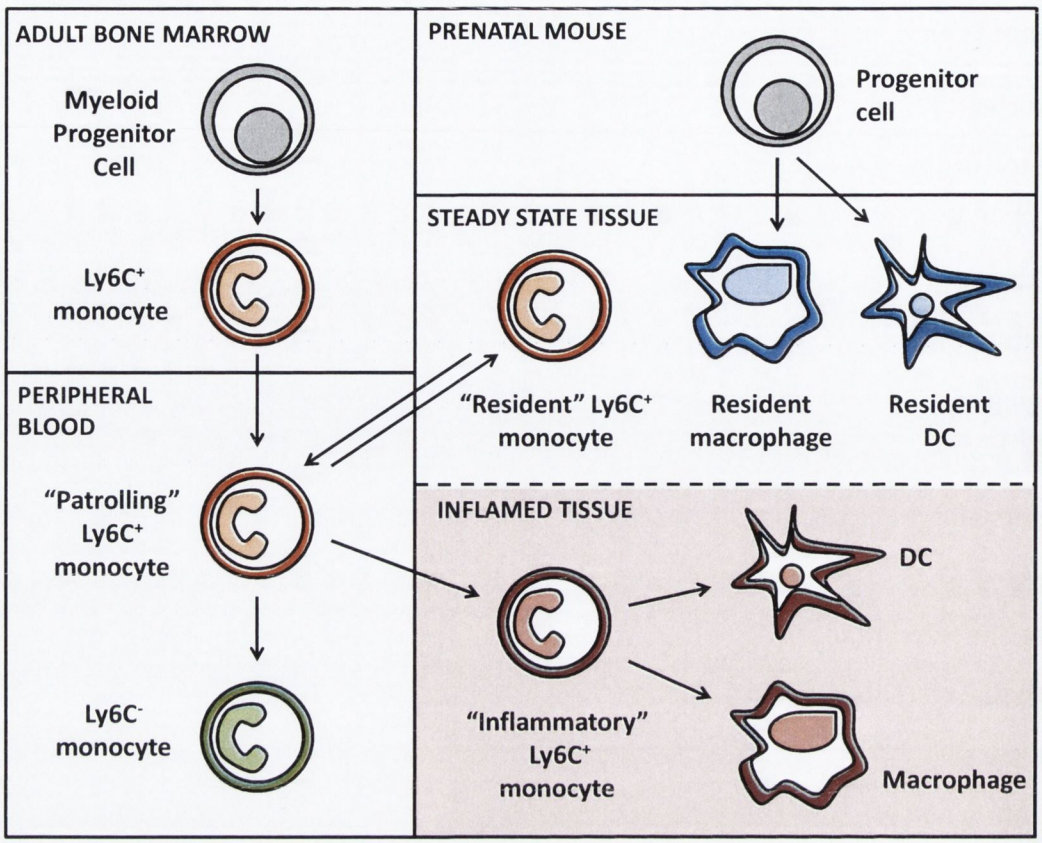

Fig 1.2 The mononuclear-phagocyte system. Tissue resident macrophages and DC are developed from progenitor cells in the pre-natal mouse and are self-sustained throughout adult life. Resident DC and macrophages provide a sentinel function in tissues and react to infection and tissue injury. $Ly6C^+$ monocytes are derived from myeloid progenitors in the bone marrow and patrol the peripheral blood. During the steady state, $Ly6C^+$ monocytes infiltrate in and out of tissue and provide similar functions to resident phagocytes. In the absence of inflammation they do not differentiate into macrophages or DC. $Ly6C^+$ monocytes differentiate into $Ly6C^-$ monocytes, which patrol the peripheral blood and are important for the detection of vascular injury. $Ly6C^+$ monocytes infiltrate inflamed tissue during infection or injury and differentiate into effector DC/macrophages under the influence of secreted stimuli such as GM-CSF, M-CSF, IL-10 and IFN-γ.

1.5.1 Monocytes

Monocytes are innate myeloid cells that mature from bone marrow progenitor cells and circulate the peripheral blood, constituting approximately 5-10 % of blood leukocytes in mammals. These cells are progenitors of specialised myeloid cells, including macrophages and DC. The monocyte population in the blood is heterogenous and thought to be reflective of the variety of specialised cells into which they differentiate [102]. Seminal studies by Van Furth et al described the infiltration of blood monocytes into inflamed tissues and observed their differentiation into macrophages or DC [105, 106]. These infiltrating monocytes were further defined as a specific population of $Ly6C^+$ cells that could easily differentiate into DC and macrophages in vitro and in vivo [99]. $Ly6C^-$ monocytes are thought to monitor the vascular system, mediate the removal of damaged endothelial cells and recruit neutrophils to sites of damage or infection [107].

Recent work by Jakubzick et al described a population of $Ly6C^+$ monocytes that, under steady state conditions, enter into tissue and do not differentiate. These monocytes function similar to DC by monitoring the tissue and acquiring antigen but do not fully mature [108]. This novel discovery underpins the existence of a functional population of tissue resident monocytes which, in the absence of inflammation, do not contribute to renewal of DC or macrophages. However, under inflammatory stimulus, such as thioglycolate or bacterial infection, infiltrating monocytes fully differentiate into specialised myeloid cells and carry out specific immune-related functions [100, 109].

1.5.2 Dendritic cells

DC are professional APCs which bridge the gap between the innate and adaptive immune systems. They were first defined by Steinman et al in 1973 as an effective APC that was characteristically and functionally different from macrophages [101, 110-113]. DC are identifiable by surface expression of the integrins CD11b, a common marker for all myeloid-derived cells, and CD11c on their surface [114]. There are several subtypes of DC; myeloid DC, which are the conventional and more populous subtype, and plasmacytoid DC. Myeloid DC respond well to extracellular infection by expressing high levels of TLR2 and TLR4 on their surface. They present antigen efficiently, making them effective at activating naive T-cells. Plasmacytoid DC are a rarer subtype that respond more readily to

viral infections by expressing high amounts of TLR7 and TLR9 [115, 116]. In addition, plasmacytoid DC can be differentiated from their more common myeloid counterparts by the lower expression of CD11b. In response to activation, plasmacytoid DC produce large amounts of type 1 IFNs that mediate immune responses to viral infection [117].

Myeloid DC are formed from myeloid progenitor cells that traffic from the bone marrow to "seed" tissue with DC-precursors (Fig 1.2). Upon arrival in the tissue monocytes differentiate into DC under the influence of flt3-L [118, 119]. Here they act as sentinels by continuously examining a variety of antigen. DC can also differentiate from blood monocytes in response to LPS, however, the exact mechanisms behind this are unclear [120] (Fig 1.2). DC are highly effective at phagocytosis of particulates, which allows them to effectively patrol the tissue for antigen. When activated via PAMPs, fully mature DC become highly efficient at presenting antigen to the T-cells of the adaptive immune system. For example, immature DC express low amounts of MHC class II and co-stimulatory molecules on their surface but are constantly capturing and processing antigen [121]. However, by expressing high concentrations of TLRs and NLRs, DC become activated by PAMPs and consequently express higher amounts of MHC class II and co-stimulatory molecules [122]. Subsequently, the mature DC migrate to peripheral lymphoid organs where they can present antigen to naive T-cells [123]. DC also help the polarisation of T-cells into their various subtypes by producing polarising cytokines, including IL-1β, IL-23, IL-12 and IL-27, in response to activation by PAMPs [124, 125].

1.5.3 Macrophages

Macrophages are an essential component of innate immunity. Similar to DC, they originate from a myeloid-precursor located in the bone marrow (Fig 1.2). There are several different types of tissue-specific resident macrophages that have distinct functions, such as microglia, osteoclasts and alveolar macrophages. Macrophages patrol tissue and phagocytose foreign materials such as microbes, dead cells and other debris. In addition, they function as first responders during infection or injury by detecting PAMPs and DAMPs via various PRRs. Macrophages directly kill pathogens by encasing them in phagolysosomes, structures containing microbicidal enzymes and free radicals. During the steady state, tissue-resident macrophages are anti-inflammatory, by default, to protect against indiscriminate inflammation. For example, the gut maintains macrophages in an

anti-inflammatory state by the production of IL-10, to ensure that commensal microbes do not propagate indiscriminate inflammation [126]. If IL-10 is absent, macrophages cause gut inflammation by reacting indiscriminately to commensal bacteria [127]. During infection or injury the population of tissue resident macrophages is deemed too small to mediate a return to normal homeostasis, therefore, additional inflammatory monocytes are recruited, which differentiate into effector macrophages (Fig 1.2). These macrophages undergo classical (M1) or alternative (M2) activation depending on the cues from the microenvironment. This plasticity allows macrophages to fulfil a variety of roles depending on the situation.

1.6 Macrophage activation

1.6.1 Classical/M1 activation of macrophages

During an inflammatory response, resting macrophages are converted into potent anti-microbial cells with an enhanced ability to phagocytose and produce NO [128] (Table 1.2; Fig 1.3). This is called classical or M1 activation and occurs primarily during bacterial and viral infection. Classical/M1 activation is initiated by the detection of PAMPs, such as LPS, and is enhanced by IFN-γ. M1 macrophages produce high concentrations of pro-inflammatory cytokines, such as IL-6, TNF-α and IL-1β [129, 130]. The classical/M1 activation of macrophages increases the expression of MHC-II and CD86, hence, mediating efficient activation of Th cells [130, 131]. M1 macrophages are also characterised by their production of large amounts of IL-12 [130], which amplifies the production of IFN-γ by Th1 cells, creating a positive feedback loop that further activates macrophages.

1.6.2 Alternative/M2 activation of macrophages

IFN-γ is produced by Th1 cells, which are reciprocally regulated by IL-4 and IL-13-producing Th2 cells. IL-4 was initially thought to inhibit M1 activation in parallel with Th1 inhibition; incubation of macrophages with IL-4 was shown to inhibit pro-inflammatory cytokine production and the production of NO [132]. Further investigation revealed that rather than inactivating macrophages, IL-4 was mediating an exclusive activation state in macrophages (Fig 1.3) [133]. IL-13, another Th2 cytokine, was shown to have a similar

effect [130]. This "alternative" or M2 activation state is characterised by the upregulation of arginase and mediators of tissue repair (Table 1.2) [129, 130, 134]. In addition IL-4/IL-13 activated macrophages produce low concentrations of IL-12 and high concentrations of IL-10 to prevent Th1 polarisation and M1 activation (Table 1.2; Fig 1.3). M2 macrophages have evolved in conjunction with Th2 cells, which are essential in the defense against extracellular microbes and protozoa such as *Trypanasoma cruzi* and *Schistosoma mansoni* [135, 136]. To this end IL-4 and IL-13 induces the expression of the mannose receptor (MRC1) on the surface of M2 macrophages, which mediates a form of pinocytosis that is efficient at engulfing the relatively large protozoa [137]. Extracellular bacteria and parasitic infections cause large amounts of collateral damage to invaded tissues, and M2 macrophages have evolved to mediate tissue repair and suppress excess inflammation by producing YM1, relm-α and IL-10 [129, 134] (Table 1.2; Fig 1.3).

IL-4 is produced by a myriad of innate immune cells including basophils, mast cells and innate lymphoid cells in response to tissue injury and parasite recognition [27]. The production of IL-4 is then amplified by Th2 cells in response to innate IL-4 production, propagating M2 activation. This suggests that M2 macrophage activation is dependent on complex cellular interaction and not by direct recognition of pathogens by macrophages. IL-4 production by macrophages has been observed in certain circumstances [138, 139], indicating that macrophages may have the potential to induce alternative activation in an autocrine manner.

1.6.3 Regulatory macrophages

In addition to these two effector activation states, macrophages can become regulatory cells, which actively suppress immune responses and resolve inflammation. These cells produce many of the characteristic markers of M2 macrophages and are therefore characterised as "M2-like" (Table 1.2). IL-4/IL-13-dependent, alternatively activated macrophages are classified M2a, and regulatory "M2 like" macrophages are categorised as M2b and M2c (Fig 1.3) [129].

M2b macrophages are characterised by a high production of IL-10 and a low production of IL-12 [129]. In contrast to M2a macrophages, M2b macrophages produce high levels of TNF-α, IL-6 and IL-1β but can still suppress LPS-mediated inflammation, which is indicative

of an anti-inflammatory function [140]. In addition M2b macrophages can induce the polarisation of Th2 cells via the secretion of IL-10, preventing the activation of M1 macrophages by IFN-γ [85]. The activation of M2b macrophages has been shown to be dependent on the binding of immune complexes by the scavenger receptor, FcγR, followed by stimulation by TLR agonists [130, 141].

M2c macrophages are induced by high concentrations of IL-10 or glucocorticoids and are thought to be involved in tissue repair and immunosuppression [109, 126, 142, 143]. They produce IL-10 and TGF-β, both of which are involved in suppressing inflammatory responses. Hayashi et al described that IL-10-producing macrophages were essential in the prevention of experimental colitis [126]. They are often observed during chronic bacterial infections when IL-10 is used to subvert the immune system; chronic infection of *Mycobacterium tuberculosis* induces M2c activation via autocrine IL-10 production [143]. IL-10 is also produced by macrophages under M1 activating conditions; LPS can directly induce IL-10 production during M1 activation [144]. IL-10 can suppress M1 activation directly via the suppression of IFN-γ producing Th1 cells. This suggests that IL-10 is important for switching off M1 activation and turning on M2 activation.

These categories are an oversimplification of a dynamic process; macrophages are plastic and constantly respond to signalling cues in the microenvironment. In reality macrophages are merely effectors of a particular inflammatory response, fine tuning the balance between type 1 inflammation, type 2 inflammation and resolution.

Table 1.2 The expression of macrophage markers and their function

Type	Gene	Protein	Function
M1	Nos2	iNOS	Production of NO, pathogen killing, pyrogenic
	Il12b	IL-12p40	Th1 polarisation
	Il1b	IL-1β	Pyrogenic, Th17 polarisation
	Tnf	TNF-α	Pyrogenic
M2a	Arg1	Arginase	Arginine catabolism, T-cell suppression, tissue repair
	Retnla	Relm-α	Tissue repair, T-cell suppression
	Chi3l3	YM1	Tissue repair and growth factor
	Il10	IL-10	Th1 and myeloid cell suppression, Th2 polarisation
	Tgfb	TGF-β	T-reg polarisation, tissue repair, growth factor
	Mrc1	MRC1	Parasite pinocytosis
	Pdcd1lg2	PD-L2	T-cell suppression
M2b	Il10	IL-10	Th1 and myeloid cell suppression, Th2 polarisation
	Tnf	TNF-α	Pyrogenic
	Il1b	IL-1β	Pyrogenic, Th17 polarisation
	Il6	IL-6	Pyrogenic, Th17 polarisation
M2c	Il10	IL-10	Th1 and myeloid cell suppression, Th2 polarisation
	Tgfb	TGF-β	T-reg polarisation, tissue repair, growth factor
	Mrc1	MRC1	Parasite pinocytosis

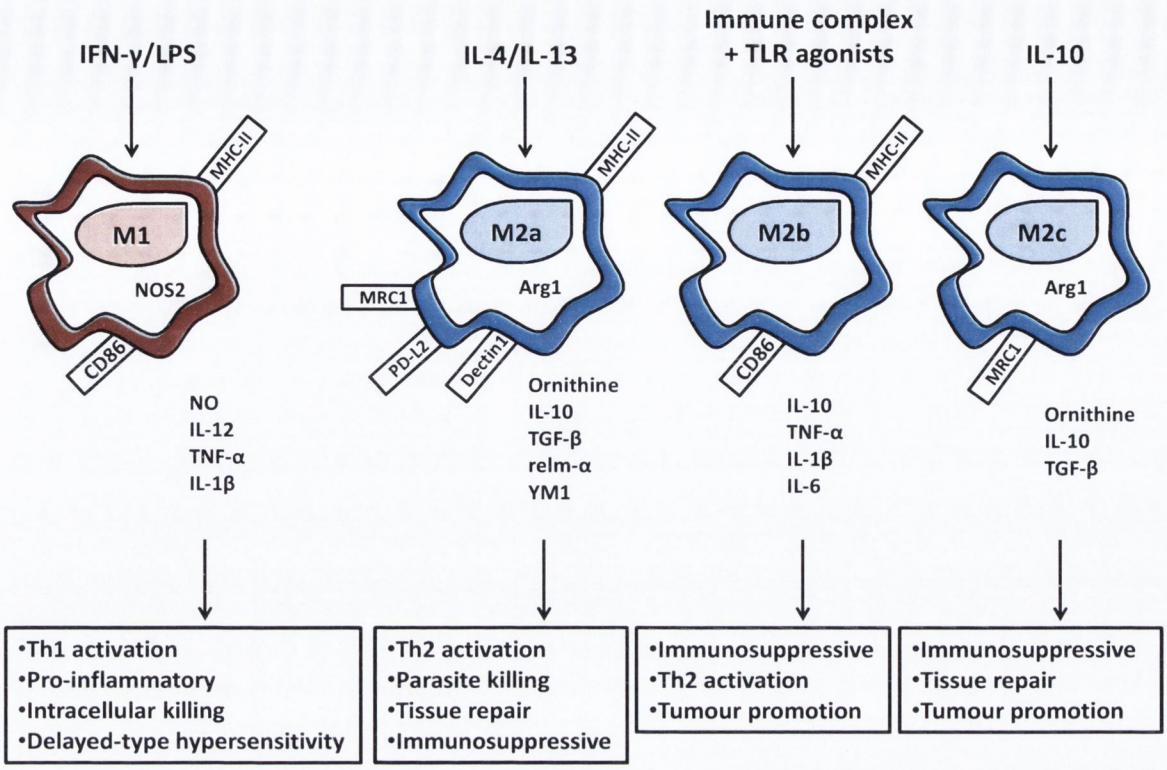

Fig 1.3 The activation states of macrophages. Macrophages can function under a number of different activation states. Classical/M1 activation is caused during infection by the detection of LPS by the macrophage via TLR4. IFN-γ production by cell-mediated immune responses enhances this activation state. M1 activation induces the production of NO, pro-inflammatory cytokines and co-stimulatory molecules, and the enhancement of pathogen killing and phagocytosis. Alternative/M2 activation (M2a) is caused by IL-4 and IL-13 in response to parasitic infection. M2a activation switches off NO production in favour of arginase-mediated ornithine production, induces the production of anti-inflammatory cytokines and tissue repair mediators, and enhances MRC2-mediated pinocytosis of parasites. "M2-like" activation results in two subsets, M2b and M2c. M2b activation is induced by the binding of immune complexes to the FcγR and the stimulation of the macrophage with TLR agonists. M2b activation causes the production of both pro- and anti-inflammatory cytokines but maintains an anti-inflammatory function. M2c activation is induced by IL-10 and causes the production of anti-inflammatory cytokines. M2c activation also mediates tissue repair by the arginase-mediated production of ornithine.

1.7 Colony stimulating factors and macrophage activation

Granulocyte/macrophage colony-stimulating factor (GM-CSF) and macrophage colony-stimulating factor (M-CSF) were first defined by their ability to differentiate bone marrow precursor cells into fully mature myeloid cells. GM-CSF induces the differentiation of granulocyte and DC-like macrophage populations and M-CSF induces the differentiation of macrophage populations [145]. GM-CSF and M-CSF also have a role in modulating the immune response as they have the ability to affect fully mature myeloid cells. [146].

The general function of GM-CSF and M-CSF is to give survival and proliferation signals to populations of granulocytes, DC, monocytes and macrophages [146, 147]. They also provide differentiation signals to bone marrow precursors and GM-CSF and M-CSF are commonly used in vitro to generate DC-like and macrophage-like populations, respectively. GM-CSF derived cells are commonly known as bone marrow derived DC (BMDC) and have strong antigen presentation capabilities and DC-like morphology. M-CSF derived cells are known as bone marrow derived macrophages (BMM) and have strong phagocytic capabilities and macrophage-like morphology [148]. These two types of CSF-derived myeloid cell produce different cytokine profiles in response to LPS stimulation. BMDM produce large amounts of TNF-α, IL-6, IL-23 and IL-12, whereas BMM produce large amounts of IL-10. This has lead to the proposal of qualifying BMDM and BMM as M1-like and M2-like macrophages, respectively [149].

M-CSF is expressed during normal homeostasis by a variety of cells, including epithelial cells, stromal cells and macrophages [147] and is detected readily in vivo in the absence of a stimulus. GM-CSF is produced by a similar repertoire of cells but requires a stimulus such as LPS [147]. This data, coupled with the qualification of BMM as M2-like macrophages, has lead to the hypothesis that M-CSF maintains resident M2 macrophages during the steady state. This is reinforced by the fact that the generation of resident macrophages, such as osteoclasts, is compromised in M-CSF-deficient mice [150, 151]. Contrastingly, GM-CSF-deficient mice show no depletion of the myeloid compartment, except that the differentiation of alveolar macrophages is compromised [152]. M-CSF can interfere with the GM-CSF-mediated generation of BMM culture, indicating that M-CSF may have a suppressive effect on the functions of GM-CSF [149].

These observations have lead to the hypothesis of "M-CSF resistance". This suggests that during normal homeostasis, M-CSF maintains a population of anti-inflammatory M2-like resident macrophages. These macrophages respond to LPS by producing IL-10, which helps to maintain immune homeostasis and tissue integrity. This "M-CSF resistance" is overcome in the case of pathogenic infection by the presence of GM-CSF, as well as the production of known M1-inducers, IFN-γ and LPS.

1.8 The balance of M1/M2 activation and disease

M2-like macrophages are known to have role in maintaining homeostasis during the steady state, but they also play an important role in returning tissue to normal homeostasis after infection. During the initial inflammatory response to infection, production of GM-CSF overcomes the homeostatic M-CSF signals and allows IFN-γ and LPS to initiate the M1 activation of macrophages. M1 macrophages then clear the site of inflammation of any pathogens by phagocytosis and the release of pro-inflammatory mediators. However, the activation of M1 macrophages impairs tissue repair by maintaining inflammation and producing metallo-matrix proteases (MMPs) [153]. Unregulated inflammation can lead to tissue damage and eventually organ failure, therefore, it is essential that M1 activation be restricted.

During tissue repair an M2-activating environment is created via the production of cytokines such as IL-4, IL-10 and TGF-β [154-156]. In addition, it is possible that ubiquitously expressed M-CSF can play a part in suppressing M1 macrophage activation and inducing M2 activation [149]. M2 macrophages have been shown to stimulate the growth of epithelial cells and fibroblasts by producing platelet-derived growth factor (PDGF) and TGF-β [154]. In tandem with promoting growth and repair of tissue, TGF-β promotes the conversion of naive T-cells into iTregs, which suppresses excess inflammation. Similarly, relm-α, IL-10 and arginase have all been shown to contribute to the suppression of inflammation and promotion of tissue repair [157-160].

This balance between M2 and M1 activation is important for the maintenance of normal homeostasis, however, when the balance shifts one way or the other the normal functions of the host are compromised. An example of this is the role of excessive M2 activation in pathogenic fibrosis, such as idiopathic pulmonary fibrosis and hepatic fibrosis

[154]. M2 macrophages mediate pathogenesis by driving the production of PDGF and TGF-β, therefore inducing the excessive proliferation of fibroblasts [161]. However, M2 associated proteins arginase, relm-α and IL-10 are all involved in suppressing fibrosis, indicating that the balance between homeostasis and pathogenesis is extremely complex [157, 159, 162].

The study of macrophages in disorders such as fibrosis has helped to define the general functions of M1 and M2 macrophages. It has also helped to highlight the inherent plasticity of macrophages and how different stimuli in the microenvironment can induce switches in macrophage phenotype to the benefit or detriment of the host. This is especially relevant in the case of cancer, chronic bacterial infection and autoimmunity, where macrophage polarisation can play an important part in pathogenesis or amelioration of disease.

1.8.1 The role of macrophage activation during cancer

The potential of M2 macrophages for activating cellular growth and suppressing inflammation has been characterised best in cancer. Tumour associated macrophages (TAMs) and myeloid-derived suppressor cells (MDSCs) express many of the characteristic markers of M2 macrophages, including TGF-β, IL-10, relm-α and YM1 [163]. The phenotype of these macrophages is dependent on signals in the microenvironment and tumours actively subvert macrophage activation by producing M2 polarising cytokines, such as IL-10 and TGF-β. Progressive tumour growth is closely linked to the abundance of growth factors and angiogenesis, therefore, it is not surprising that the presence of M2-like macrophages, which help to create a proliferative environment, correlates strongly with tumour growth and negative outcomes [164, 165]. In addition to providing growth signals, M2 macrophages inhibit anti-tumour immune responses by the production of immunosuppressive mediators such as relm-α and IL-10 [163].

TAMs also promote the differentiation of Treg cells by producing IL-10 and TGF-β, therefore restraining immune responses directed at tumour killing [166]. Conversely, M1 macrophages inhibit tumour growth by promoting a pro-inflammatory environment and inducing anti-tumour Th1 cell responses [163]. The balance of macrophage activation can be shifted towards an M1 phenotype by the addition of IL-12 or IFN-γ, resulting in the

inhibition of tumor growth [167, 168]. Furthermore, the depletion of M2 macrophages significantly enhances the generation of anti-tumour M1 macrophages [169], indicating that reciprocal regulation of M1 versus M2 macrophages occurs during tumour growth. The understanding of pro- versus anti-tumour macrophage responses opens up opportunities for therapies based on shifting the balance of M1 versus M2 macrophages during cancer. Clinical trials are ongoing to monitor the efficacy of blocking TAMs from trafficking to the tumour, but results are unclear thus far [170].

1.8.2 The role of macrophage activation during chronic bacterial infection

The primary role of M1 macrophages is to combat bacterial infection. Common bacterial PAMPs induce the production of IL-12 from innate immune cells, enhancing the production of IFN-γ from Th1 cells. In addition, NK cells produce IFN-γ in response to recognition of infected cells. IFN-γ, in combination with LPS, activates M1 macrophages, which clear bacterial infection. M2 macrophages are essential for immune defense against parasitic infection and extracellular bacteria but are not effective at mediating clearance of intracellular bacterial infections. Furthermore, the production of TGF-β, IL-10 and arginase suppress the production of IFN-γ and M1 macrophage activation [171-173], and thus, inhibits cell-mediated immunity. Therefore the balance of M1 versus M2 activation is important for the efficient clearance of bacterial infection. Certain bacterial infections subvert the immune system and encourage chronic infection by shifting the balance of macrophage activation.

Mycobacterial infections are a good example of a bacterial infection preventing clearance by modulating the activation of macrophages. El Kasmi et al have shown that *M. tuberculosis* and *M. bovis* both induced the production of arginase by macrophages, indicating M2 activation. They showed that arginase production inhibited the expression of iNOS, reducing anti-microbial responses. Furthermore, they showed that inhibition of arginase during *M. tuberculosis* infection enhanced bacterial clearance. They observed a similar improvement in parasitic clearance when arginase was inhibited during *T. gondii* infection [171]. Schreiber et al have shown that *M. tuberculosis* can induce M2 activation via macrophage-derived IL-10. Furthermore, they observed that IL-10 inhibited the IFN-γ-mediated killing of bacteria via the upregulation of arginase [143]. Importantly they

observed that IL-10 did not compromise IFN-γ production by Th1 cells but significantly increased arginase expression in favour of iNOS expression. This suggests that the inhibition of bacterial clearance is dependent on the switch from M1 to M2 macrophage activation. Similarly, Tumitan et al showed that chronic infection by *Yersinia psuedotuberculosis* or *Y. enterocolitica* in susceptible mice was associated with the activation of IL-10-, arginase- and TGF-β-producing M2 macrophages. Conversely, M1 macrophages that produced NO, TNF-α and IL-12 were present in mouse strains resistant to *Yersinia* infection [174, 175].

IL-10-producing macrophages are a recurring feature of chronic bacterial infections. *Coxiella burnetii* is an intracellular bacteria that causes Q fever and sometimes persists as a chronic bacterial infection. *C. burnetti* infected macrophages produce large amounts of IL-10, TGF-β and arginase, which is indicative of M2 macrophages. Ghigo et al showed that these macrophages were responsible for impaired bacterial killing during chronic infection with *C. burnetti* [176]. Interestingly, Meghari et al showed that IL-10 was the essential cytokine that reduced the ratio of pathogen-killing M1 macrophages in favour of the M2 macrophages during chronic *C. burnetti* infection [177]. IL-10 has a similar function during chronic *Brucella abortus* infection; neutralisation of IL-10 was sufficient to restore bactericidal M1 phenotypes in mice strains susceptible to *B. abortus* infection [178].Taken together these studies implicate M2 activation and IL-10 production as important mechanisms that can be exploited by bacteria to subvert the immune system leading to chronic infection.

1.8.3 The role of macrophage activation in autoimmunity and inflammatory disease

The immune system is designed to discriminate self from non-self to prevent indiscriminate immune responses to tissues of the host. When homeostasis of the immune system breaks down, molecules or cells of the host immune system can become pathogenic and attack the cells and tissue of the body in a process called autoimmunity. Macrophages have been implicated as potential autoimmune effector cells in a number of autoimmune diseases including multiple sclerosis, rheumatoid arthritis and Crohn's disease.

Crohn's disease is a chronic inflammatory bowel disease caused by irregular immune responses to the contents of the gut, however, the pathogenesis of the disease is poorly understood. Pro-inflammatory M1 macrophages have a controversial role in inflammation associated with Crohn's. M1-associated cytokines IL-23, TNF-α and IL-12 have all been implicated as important mediators of pathogenic inflammation during experimental colitis [179], moreover, increased amounts of TNF-α and IL-23-producing M1 macrophages are observed in the intestine of Crohn's patients [180]. In contrast, Smith et al argue that M1-associated TNF-α is depressed in Crohn's patients [181]. They hypothesised that dysfunction of M1 macrophages reduces bacterial clearance, which propagates chronic pathogenic inflammation. M2 macrophages may also play a role in preventing colitis; myeloid-derived IL-10 has been shown to be necessary to maintain homeostasis by differentiating iTreg cells in the gut [87].

M1 macrophages produce many cytokines that that have been implicated in the generation of experimental autoimmune diseases. IL-1β and IL-23 have been shown to be essential for the generation of pathogenic Th17 cells during EAE and are produced by M1 macrophages in response to LPS and IFN-γ [36, 41]. In addition, M1 macrophages infiltrate the brain during relapses in relapsing-recurring EAE. Mikita et al have shown that arginase-expressing M2 macrophages are present in the CNS during remission, moreover, studies have shown that the transfer of M2 macrophages ameliorates the symptoms of EAE [182, 183]. More recently, Liu et al have shown that amelioration of disease using a Rho-kinase inhibitor was dependent on the induction of M2 macrophages in the spinal cords of mice with EAE [184]. Although the mechanism of attenuation is unclear, M2 macrophages are thought to inhibit pathogenic microglia, NO-producing M1 macrophages and Th17 cells, therefore reducing neuronal damage.

These studies highlight the importance in maintaining balanced macrophage activation during normal immune responses. Broadly speaking M2 macrophages are capable of preventing excessive damage during autoimmune responses or excessive inflammation. This suggests that activation of M2 macrophage activation has therapeutic potential for autoimmune and/or inflammatory disorders.

1.9 Nod-like receptors

NLRs are a family of PRRs that specialise in detecting intracellular PAMPs such as PGN or DAMPs such as ATP (Table 1.3). They recognise and bind their ligands using leucine rich repeats (LRR) and recruit adaptor proteins using conserved domains such as the caspase recruitment domain (CARD). These conserved domains also divide the receptors into different NLR subfamilies.

The NALP subfamily contain pyrin domains and are important for the formation of the protein complex called the inflammasome. The inflammasome regulates caspase-1, which in turn processes the cytokines IL-1β and IL-18 [185]. The CARD-containing subfamily consists of the proteins NOD1 and NOD2, which recognise degraded peptidoglycan. NOD1 detects L-Ala-γ-d-Glu-*m*-diaminopimelic acid (DAP) containing peptidoglycan [186, 187], which is characteristic of most Gram-negative bacteria and some Gram-positive bacteria such as *Listeria monocytogenes.* NOD2 detects muramyl dipeptide (MDP) [188, 189] which is found in both Gram negative and Gram positive bacteria. Similar to the TLRs, NLRs are another link between the detection of pathogens, the activation of innate immune cells and consequently the activation of the adaptive immune system.

Table 1.3 Examples of NLR agonists

NLR	Conserved Domain	PAMP/DAMP
NOD1	**CARD**	**DAP**
NOD2	**CARD**	**MDP**
NAIP	**BIR**	**Flagella**
NLRP1	**Pyrin**	**Anthrax lethal toxin, MDP**
NLRP3	**Pyrin**	**ATP, Nigericin, Viral RNA, Amyloid-β, MDP**

1.9.1 NOD1 and NOD2 signalling

NOD1 and NOD2 sense degraded PGN and are important in detecting and responding to bacteria. NOD1 is expressed in most cell types including myeloid immune cells, lymphoid immune cells and epithelial cells [190]. The expression of NOD2 is more restricted but is still widely expressed across a variety of cell types including macrophages, DC, epithelial cells and keratinocytes [191-193]. Both receptors are found within the cytosol, therefore, agonists must gain entry to the cytosol before binding to their receptors. Although MDP has been shown to enter the cytosol of intestinal epithelial cells directly via the transporter SLC15A1 [194], both NOD1/2 agonists have been shown to enter the cytosol of macrophages and epithelial cells by clathrin and dynamin-mediated endocytosis [195]. After endocytosis NOD1/2 agonists are internalised into the cytosol in a pH-dependent fashion by endosomal transporters, including SLC15A4 [195, 196]. NOD1 and NOD2 move to intracellular membranes upon PGN recognition, which is thought to increase the efficiency of activation after the endocytosis of agonists [197, 198]. NOD1 agonists enter the endosomal pathway at different rates depending on the additional structures attached to the NOD1-binding DAP motif; for example, TriDAP contains two peptides attached to the DAP motif and enters the endosome more readily than ie-DAP, which contains only one peptide [196]. The endocytosis of MDP can be improved by the addition of lipophilic moieties [196]. The variability of potency between different agonists is primarily dependent on their ease of endocytosis, however, small differences in receptor activation have also been dependent on the other structures, such as additional peptides [196]. The reason for the difference in rate of endocytosis is unclear but may depend on interactions between the attached peptides and any cell surface proteins. Although endocytosis is an efficient mechanism for the entrance of NOD1/2 agonists, it is not necessary for the activation of NOD1 and NOD2. Lee et al observed that the disruption of the cell membrane by detergents allowed potent NOD1/2-dependent NFkB activation even in the absence of endosomal trafficking [196]. This allows NOD1 and NOD2 to be activated by agonists that gain entrance into the cytosol by means other than endocytosis, including bacterial invasion and type IV secretion systems.

NOD1 and NOD2 bind their ligands via a LRR, which induces the oligomerisation of the receptors via their conserved NACHT domains [187, 199]. This forms scaffolding upon which adaptor proteins bind. Receptor-interacting protein 2 (RIP2) is an adaptor protein

that interacts with both NOD1 and NOD2 via CARD-CARD interactions [200, 201]. RIP2 has a kinase domain that recruits the E3 ubiquitin ligases, inhibitor-of-apoptosis protein (IAP) and pellino3. The recruited IAP and pellino3 attach polyubiquitin chains to RIP2, attracting other signalling proteins [200, 202]. The adaptor protein TAB binds to the ubiquitin chains and recruits the TAB-associated kinase TAK. TAK then mediates the activation of the IKK complex, degradation of the NFkB inhibitor IkBα, and allows the transcription factor NFkB to translocate to the nucleus. In addition, RIP2 can directly interact with NEMO, and promotes its activation by ubiquitination. The activation of NEMO results in the degradation of IkBα and the translocation of NFkB [200]. TAK can also phosphorylate the MAPKs, p38, ERK and JNK [190, 203]. In addition, NOD1 and NOD2 have been shown to activate the MAPKs, in a RIP2 independent manner, via direct interaction with the protein CARD9 [190]. Activation of the MAPKs results in the activation of the transcription factor AP1 [204]. As well as the activation of the NFkB and MAPK pathways, ligation of NOD1 has been shown to bind TRAF3 via RIP2. TRAF3 mediates the activation of interferon regulatory factor 7 (IRF7) transcription factor, and thus, the production of the cytokine IFN-β [205].

In response to the activation of multiple transcription factors, NOD1 and NOD2 induce the production of pro-inflammatory cytokines and chemokines, such as IL-6, IL-1β and TNF-α, from a range of immune cells, such as epithelial cells, macrophages and DC [206, 207]. In addition, administration of NOD agonists can induce the chemotaxis of innate immune cells in vivo via the production of chemokines, MIP-1 and RANTES [208]. Epithelial cells express both NOD1 and NOD2 and produce anti-microbial peptides and pro-inflammatory cytokines in response to NOD1/2 agonists [209, 210]. Although NOD1, NOD2 and the TLRs activate overlapping transcription factors, current evidence suggests that NOD1 and NOD2 are not as effective as the TLRs at inducing cytokine production by innate immune cells, and hence, NOD agonists would appear to be redundant to the other, more potent, TLR agonists. However, multiple studies have agreed that NOD1 and NOD2 agonists can synergise with TLR agonists to promote the production of cytokines [211]. This would suggest that the function of NOD agonists may be to modulate TLR responses, rather than initiate an immune response in their own right.

As well as having an effect on innate immune cells, NOD1 and NOD2 also have a significant effect on the initiation of the adaptive immune response. As early as the 1970s

it has been reported that PGN components have adjuvant activity [212, 213]. Administration of NOD1 or NOD2 agonists alone promote RIP2-dependent Th2 responses in vivo, which are mediated by TSLP production by stromal cells [214, 215]. The use of RIP2-deficient mice has revealed a role for NOD1 agonists in polarising other subsets of T helper cells, including Th1 and Th17 cells, when administered in conjunction with TLR stimulation [201]. Further studies have shown NOD2 is essential for the efficient Th1 responses during *T. gondii* infection, while both NOD1 and NOD2 are involved in Th17 responses during *Citrobacter rodentium* infection [216, 217]. These infection studies provide further support for the hypothesis that NOD-mediated Th1 and Th17 responses are only induced in the presence of TLR agonists.

NOD1 and NOD2 and infection.

As functional PRRs, NOD1 and NOD2 play an important role in mounting an effective immune response to bacterial infection. The generation of mice that are deficient in either NOD1 ($NOD1^{-/-}$), NOD2 ($NOD2^{-/-}$) or both NOD1 and NOD2 ($NOD1^{-/-}NOD2^{-/-}$) have allowed scientists to investigate the importance of these receptors in a variety of infection models. $NOD1^{-/-}$mice have increased susceptibility to infection with certain bacteria, such as *Helicobacter pylori* [218], *Listeria monocytogenes* [219] and *Pseudomonas aeruginosa* [219]. The increased bacterial load in $NOD1^{-/-}$ mice was associated with defective immune responses, including impaired chemokine, cytokine and NO production. NOD2 has been implicated in bacterial sensing at the mucosal sites in the host; $NOD2^{-/-}$ mice are more susceptible to *Staphlococcus aureus* infection of the skin [209], *E. coli* infection of the lungs [220] and *L. monocytogenes* infection of the intestinal tract [221]. In addition to defending against bacterial infection, NOD1 and NOD2 are also required for an efficient immune response to the protozoa *T. cruzi* [222] and *T. gondi* [216], respectively.

The role of NOD1 and NOD2 in response to infection often overlaps due to their shared signalling pathways; NOD1 and NOD2 are both involved in the clearance of pulmonary *Legionella pnemophilia* infections and are important for early Th17 responses during *C. rondentium* infection of the gut. There is now consensus that NOD1 and NOD2, due to their modest ability to activate immune cells, contribute to innate immunity by

modulating the activation of the more potent TLRs. However, there is a growing literature to suggest that NOD1 may provide a "back-up" mechanism for the activation of immune responses in intestinal cells that lack TLR activation. NOD1 has shown to be vital for the detection of enteric bacteria, such as *E. coli* and *Camplyobacter jejuni,* which avoid TLR-activation [223, 224].

NOD1 and NOD2 are cytosolic receptors, therefore, the importance of NOD1 and NOD2 in bacterial infection is often associated with the presence of bacterial virulence factors that allow efficient entry of microbial components into the cytosol. *H. pylori* has been shown to activate NOD1 by injecting PGN directly into the cytosol via a type IV secretion system and *S. aureus* induces NOD2 activation after PGN enters the cytosol via the pore-forming α-toxin [209, 218].

1.9.3 NOD1 and NOD2 and inflammatory disease

Crohn's disease is an inflammatory disorder of the gut that is thought to be driven by inappropriate immune responses to the contents of the intestine. The pathogenesis of the disease is unclear but there is evidence that both environmental and genetic factors play a role. Evidence from genetic polymorphism analysis has shown that a mutation in the CARD15 gene, which impairs NOD2 signalling, is a risk factor for Crohn's disease [225, 226]. This implies that NOD2 activation may suppress pathogenic inflammation in the gut, however, the mechanism of NOD2-mediated protection is unclear. The mutation causes a change near the LRR domain of the receptor and reduces the capacity of MDP to bind to NOD2 and induce NFkB activation [227]. Monocytes from patients who exhibit the mutation have impaired IL-1β, TNF-α, IL-6 and IL-8 production [227-229], indicating an impairment of bacterial recognition by phagocytes with defective NOD2. The idea that a fully functional NOD2 would protect against Crohn's disease seems counter intuitive given that these cytokines are important pro-inflammatory mediators, however, there is a hypothesis that Crohn's disease -associated inflammation is enhanced due to impaired bacterial clearance. Pro-inflammatory mediators are required to clear acute infection in the gut; failure to clear the initial microbial challenge could result in the chronic inflammation observed in Crohn's disease patients. Consistent with this theory, tissue

samples from Crohn's disease patients have exacerbated NFkB responses, which may be indicative of a heightened immune response to an increased bacterial load [230].

This hypothesis is reinforced by the discovery of impaired defensin production by gut Paneth cells from CARD15 mutants in response to MDP [231, 232]. Defensin production by Paneth cells is important for the maintenance of mucosal barriers, therefore, the decrease in defensin production in CARD15 mutants creates a plausible link between defective NOD2 function, compromised barrier function and excessive gut inflammation. In fact, CARD15 mutant mice were more susceptible to infection by *L. monocytogenes* when challenged orally, however, intraperitoneal infection was cleared as effectively as WT mice [221]. The lack of mucosal immunity was associated with a decrease in defensin production, and implies that NOD2 mutations compromise gut barrier functions, hence, CARD15 mutants fail to clear bacterial infection and have a higher propensity to acquire Crohn's disease.

One study has argued against this hypothesis; Maeda et al developed mice with a knock-in of the CARD15 mutation which had enhanced NFkB activation and IL-1β in response to NOD2 activation [233]. They argued that the CARD15 mutation associated with elevated risk of Crohn's disease is a gain of function mutation and allows increased activation of NOD2 and therefore a higher propensity for gut inflammation. In contrast, Kim et al have developed another CARD15 mutation knock-in mouse that shows loss of function NOD2 responses [228]. Similar to human monocytes from patients carrying CARD15 mutations, they showed that monocytes from mice expressing the mutant CARD15 gene produced less TNF-α and IL-6 in response to MDP and bacterial infection. The differences between the two models are unclear and only serve to question the validity of knock in mutation studies.

Some studies argue that NOD2 plays a role in regulating immune responses in the gut. In this case the loss of a functional NOD2 receptor releases the "brake" on pro-inflammatory responses and allows the propagation of pathogenic inflammation. IL-10 is essential for gut homeostasis; spontaneous colitis occurs in IL-10-deficient mice [80]. Monocytes from patients with the CARD15 mutation have impaired IL-10 production in response to TLR2 ligands [234]. Jamontt et al showed recently that NOD2 signalling can promote colitis in IL-10-deficient mice. IL-10-deficient macrophages were hyperresponsive to NOD2

activation and produced increased amounts of IL-6, TNF-α and IL-12 in comparison with their WT counterparts [235]. These studies imply that NOD2 mediates anti-inflammatory responses during bacterial infection and that loss of this signal may potentiate pathogenic inflammation. Similarly, Watanabe et al showed that administration of MDP could inhibit TLR2-mediated IL-12 production by DC, which reduced their capability of generating Th1 cells. They also showed that NOD2-deficient DC produced higher concentrations of IL-12 and promoted enhanced Th1 responses when cultured with naive T-cells [125]. This hypothesis has been reinforced by the efficacy of neutralising IL-12 on ameliorating the symptoms of Crohn's disease [236]. Furthermore, Watanabe et al showed that administration of MDP attenuated experimental colitis and was associated with a decrease in TLR-mediated pro-inflammatory cytokine production.

NOD1 polymorphisms have been linked to an increased risk of developing asthma and atopic eczema [237, 238]. These studies are observational and thus far no mechanistic studies have been carried out on NOD1 polymorphisms. A recent paper by Chun et al showed that NOD1 agonists could exacerbate experimental allergic asthma [239]. The exacerbation was associated with the NOD1-mediated activation of eosinophils via interaction with airway epithelial cells. This study implicates bacterial recognition via NOD1 in the pathogenesis of asthma, but it remains to be seen whether or not this study sheds any light on the mechanisms behind the correlation of asthma risk and NOD1 polymorphisms. As NOD1 and NOD2 share similar signalling pathways, several studies have tried to link NOD1 polymorphisms with the risk of inflammatory bowel disease but have had mixed results [240-243]. Nevertheless, there may still be potential in searching for a similar anti-inflammatory role for NOD1 during bacterial infection or chronic inflammation.

1.10 Multiple sclerosis

MS is an inflammatory disease of the central nervous system (CNS) that causes physical and mental disability. The reduction in cognitive function is a result of neurological damage caused by autoimmune responses [244]. The autoimmune response specifically targets the myelin sheath, which covers nerve cells and is essential for efficient neurotransmission. The resulting inflammation subsequently damages the nerve cells,

exacerbating the neurological decline [245]. The CNS tissue of MS patients has plaques of demyelination in the brain, spinal cord and optic nerves. These plaques are associated with large cellular infiltrates, consisting of $CD4^+$ and $CD8^+$ T-cells, B-cells and monocytes. Macrophages containing myelin debris are also found in the plaques [246]. While the central role of inflammation in MS pathology is clear, the mechanisms that lead to the initiation of the autoimmune response are poorly defined. The disease is the leading cause of non-traumatic neurological disability in young people and usually presents between the ages of 20-40. Although the disease is not life shortening, the quality of life of patients is severely affected.

The location and presentation of plaques is heterogeneous and, consequently, symptoms present themselves in a myriad of ways. Common symptoms include reduction of motor capability, loss of visual acuity and memory impairment. MS can be catergorised as either relapsing-remitting (RRMS) or primary progressive (PPMS). The most common form (85-90% of patients) is RRMS, which is characterised by episodes of acute symptoms followed by recovery [246]. This form of disease is progressive if untreated; each episode causes more severe impairment and lasting symptoms, however, this varies from patient to patient. The attacks are thought to be caused by infiltrating myelin-reactive T-cells, which cause inflammation and oedema [246]. Approximately 40% of RRMS patients develop secondary progressive disease (SPMS), characterised by a steady decline in cognitive function and memory without any period of remission [247]. The consensus view is that SPMS pathology is initiated by a neurodegenerative process, which does not rely on the acute episodic immune invasions. This hypothesis suggests that early immunosuppressive therapy may prevent the progression of RRMS to SPMS. PPMS is a much rarer form (10-15% of patients), characterised by ongoing neurological decline, without remission, starting from the onset of disease. This disease is refractory to any type of immunotherapy [248] indicating that PPMS and RRMS may be very different diseases.

The aetiology of MS disease is unclear but many studies have focused on the role of an auto-antigen, which is targeted by self-reactive T-cells of the immune system. T-cells from MS patients react with a number of myelin antigens and genetic studies have shown correlations between MHC-related genes and disease [246]. This data highlights the role of T-cells in the pathogenesis of disease. This is reinforced by the observation that epitope spreading occurs in EAE, the mouse model for multiple sclerosis, and antigen

specific T-cells isolated from mice with EAE can reproduce disease upon transfer into naive mice.

Genetic influences also play a substantial role in pathogenesis. There is a high prevalence of disease in people of Northern European descent, which has migrated to countries with indigenous populations of low disease prevalence, such as the in the Maori of New Zealand [249]. The concordance rate among monozygotic twins is 25-30%, while the prevalence between dizygotic twins and non-twin siblings is 3-5% and 0.1-0.4%, respectively [249]. While the genetic influence is high, 70% of monozygotic twins show no concordance, which suggests environmental factors play a large part in pathogenesis.

The correlation between infection and pathogenesis of MS has been extensively studied but no clear association has been found [250, 251]. The hypothesis suggests that infection with particular microbes in genetically susceptible individuals may cause MS and that latent infection or remerging infection may explain the periodic acute relapses associated with RRMS. Infectious agents may expose novel antigens through tissue damage and cause self-recognition during an active immune response. Others suggest that infectious agents may carry antigen similar to host antigens and cause self-reaction via molecular mimicry. Epstein Barr virus is one of the infectious agents currently undergoing investigation as close to 100% of MS patients have evidence of exposure to the virus, in comparison with 90% for healthy controls [252].

The current therapies for MS were all based on a knowledge of the role of CNS inflammation in disease pathology. Due to the lack of knowledge on the precipitating cause of MS, no prophylactic therapy is currently used. Immunosuppressive corticosteroids are used to treat acute attacks with the aim of improving cognitive function by suppressing CNS inflammation [249]. Occasionally corticosteroids have no effect on the acute attack and loss of cognitive function can persist. IFN-β is used as a firstline therapy for RRMS. Although the mechanism of action was unclear, IFN-β is now known to induce IL-27 in patients who respond well to treatment [124]. Furthermore IFN-β promotes IL-27 which inhibits pathogenic Th17 cells during EAE. IFN-β therapy reduces relapse rate by approximately 30% however, not all patients respond to treatment [253]. An alternative firstline treatment is glatiramer acetate (GA). It is thought the therapeutic effect of GA is mediated by binding of the drug to MHC-II, thereby blocking T-cell

activation. Other studies suggest that GA has an overall immunosuppressive effect by inducing anti-inflammatory cytokines and Treg cells [254]. GA reduces relapses by approximately 30%. IFN-β and GA have been used as therapy for patients with a single demyelination event (MS is diagnosed after a second demyelination event) as prophylaxis against further episodes. One study has shown that IFN-β can reduce further demyelination events over 3 years by 15% [255].

Several mouse models have been developed to further understand the pathogenesis of MS. EAE is a commonly used mouse model for MS and has been employed during the development of novel therapeutics, including fingolimod and Tysabri. Fingolimod is a functional antagonist for sphingosine-1-phosphate (S1P) and has shown superior efficacy at preventing relapses in comparison with IFN-β [256, 257]. Fingolimod sequesters lymphocytes in the lymph node, thereby preventing the infiltration of pathogenic T-cells into the CNS [258]. Tysabri is a monoclonal antibody that binds to very late antigen 4 (VLA-4). VLA-4 is essential for the adhesion of leukocytes to the interior of the vasculature and blocking it prevents the egress of immune cells into inflamed tissue [259, 260]. Tysabri is very effective at attenuating the clinical signs of EAE and is also very efficacious at reducing relapse rates in RRMS patients [261]. Tysabri has also revealed the limitations of mouse models; while mice treated with Tysabri have no drastic side effects, in humans it increases the risk of developing progressive multifocal leukoencephalopathy [262, 263]. Therefore, Tysabri has been licensed as a therapy for patients with aggressive disease, who do not respond to other lower risk treatments.

1.11 Experimental autoimmune encephalomyelitis

EAE is a demyelinating autoimmune disease which is used as a mouse model for MS. It is induced in susceptible strains of mice by immunisation with myelin-antigen emulsified with complete Freund's adjuvant (CFA). The myelin-antigens used range from single polypeptides, such as myelin oligodendrocyte glycopeptide (MOG) and proteolipid peptide (PLP), to whole spinal cord homogenates [264]. Immunisation of different mouse strains with various myelin antigens results in different forms of disease, acute, chronic or relapsing remitting. C57BL/6 mice immunized with myelin oligodendrocyte glycoprotein MOG peptide 35-55 develop disease that is first severe and acute and then moderate and

chronic. SJL mice develop a clinically relevant relapsing remitting course of disease after immunisation with proteolipid protein (PLP) peptide 139-151 [265].

The pathogenesis of EAE is primarily dependent on myelin-reactive T-cells and can be induced in naive mice by the adoptive transfer of MOG-specific $CD4^+$ T-cells from mice with EAE [266]. The disease is mediated by the infiltration of T-cells into the CNS of mice. Once inside the CNS, antigen-specific T-cells are restimulated by endogenous myelin antigens and APC, and mediate their pathogenic effects. These include the production of pro-inflammatory cytokines and chemokines which opens the blood brain barrier and recruits inflammatory cells such as neutrophils and macrophages. These cells cause tissue damage and result in the loss of cognitive function associated with clinical disease [267, 268].

Th1 cells were initially thought to mediate disease as IL-12p40$^{-/-}$ mice are resistant to EAE. This compromises the signalling of IL-12, therefore inhibiting the development of Th1 cells. Furthermore, Horwitz et al showed that overexpression of IFN-γ in the CNS induced spontaneous demyelination similar to that seen in MS and EAE [269]. However, this hypothesis was challenged by the fact that IFN-$\gamma^{-/-}$ mice develop exacerbated clinical disease [270]. IL-12p40 is a subunit of both IL-12 and IL-23 therefore both Th1 cells and Th17 cells are affected by its absence. Recent research has shown that the loss of IL-12p35, which is unique to IL-12 and not IL-23, has no effect on induction of EAE [271].

Cua et al have shown that IL-23p19$^{-/-}$ mice were resistant to induction of EAE and therefore IL-23, not IL-12, was shown to be a key innate cytokine in the pathogenesis of EAE [39]. Furthermore, IL-23 driven IL-17 cells were shown to induce EAE when adoptively transferred into naive mice [36]. Exposure of IL-17 to human endothelial cells reduces the expression of the protein occludin, which is involved in maintaining tight junctions [269]. This suggests that IL-17 may mediate the entry of cells into the CNS by breaking down the blood brain barrier. The relative importance of Th1 and Th17 cells in the pathogenesis of EAE is still unclear. A recent paper by Kroenke et al demonstrated that EAE could be induced by transferring either MOG-specific Th1 or MOG-specific Th17 cells [272]. Although both subsets induced demyelination and paralysis, Th1 cells recruited macrophages to the CNS, whereas Th17 cells recruited neutrophils. The same report has shown that GM-CSF can mediate EAE in the absence of both IFN-γ and IL-17 production.

Taken together, these studies describe EAE as a heterogeneous disease with many different mechanisms that mediate pathology.

EAE has also helped in the understanding of the regulation of autoimmune disease through the use of mice deficient in various immune regulators. Bettelli et al observed that IL-10 has a critical role in restraining the clinical symptoms of EAE [273]. They showed that IL-10-deficient mice acquired a much more severe disease than WT mice, moreover, artificially overexpressing IL-10 in transgenic mice rendered them immune to the induction of EAE. In an elegant experiment, Cua et al showed that EAE could be completely prevented by the expression of IL-10 in the CNS by adenovirus [274].

IL-27 is an important Th1-enhancing cytokine but studies in EAE have helped to define an anti-inflammatory role for this cytokine. Administration of IL-27 attentuates the clinical symptoms of EAE in WT mice [275] and the clinical course of EAE is exacerbated in mice deficient in the IL-27 receptor (WSX1) [276]. Batten et al also showed that the exacerbated symptoms of EAE were associated with enhanced IL-17 production in $WSX^{-/-}$ mice. EAE has also enhanced the understanding of the role of macrophage activation in autoimmune diseases. The transfer of M2 macrophages significantly reduced the symptoms of EAE [182, 183] and therapeutics that enhanced the generation of M2 macrophages are capable of ameliorating the symptoms of EAE [184]. These studies suggest the importance of EAE as a model for analysing the role of the immune system in the pathogenesis of autoimmune diseases.

1.12 Aim of study

Evidence from genetically modified mice has established the importance of NOD1 and NOD2 in the detection of pathogenic bacteria. Although TLRs are more potent activators of the innate immune response, NOD1 and NOD2 have a significant modulatory effect on the potentiation of innate and adaptive immune responses. Therefore, it is surprising that a loss of function mutation of NOD2 is considered to have a protective role against the chronic inflammation associated with Crohn's disease. The mechanism behind the role of NOD2 activation is still not fully understood; one theory suggests that NOD2 is involved in inducing the anti-inflammatory IL-10 in response to PGN stimulation, therefore preventing pathogenic inflammation [234, 235]. This suggests that a NOD2 agonist may have natural anti-inflammatory mechanisms that could be useful therapeutically.

NOD1 and NOD2 share the same signalling pathways, suggesting that NOD1 agonists may have a similar anti-inflammatory potential to NOD2 agonists. Thus far, the role for NOD1 in the protection against chronic inflammation or as a regulator of immune response has received little attention. The first aims of the present study were to:

- Examine the potential anti-inflammatory role of the NOD1 agonist TriDAP in the autoimmune model EAE.
- Examine the immunomodulatory effect of TriDAP on innate immune cells and T-cells.

In addition, recent studies have discovered the potential of NOD1/2 agonists to drive Th2 responses in vivo [214, 215]. Th2 immune responses promote the generation of M2 macrophages. The balance between M1 and M2 activation has significant effects on the immune responses to infection and tumours and on the development of autoimmunity. Furthermore, the activation of M2 macrophages has been implicated as one of the mechanisms by which bacteria can subvert the immune response during chronic infection. Thus far no study has looked at the potential of NOD1 to induce M2 activation. Therefore this study aimed to:

- Examine the effect of TriDAP on macrophage activation in vivo.
- Determine the mechanism by which TriDAP mediates macrophage activation in vivo.

Chapter 2:

Materials and methods

CHAPTER 2: Materials and methods

2.1 Materials

AMMONIUM CHLORIDE LYSIS SOLUTION

0.77 g ammonium chloride (Sigma) dissolved in 100 ml dH_20 and filter sterilised.

CELL CULTURE MEDIUM

Roswell Park Memorial Institute-1640 medium (RPMI; Biosera) was supplemented with 10% heat inactivated (56°C, 30 min) foetal calf serum (FCS, Biosera), 100 mM L-Glutamine (Sigma), 100 μg/ml penicillin/streptomycin (Sigma). RPMI was also supplemented with 50 μM β-mercapthoethanol (Sigma) when used for T-cell culture.

Hanks Buffered Salt Solution (HBSS, Sigma) was supplemented with 2% FCS.

ETHIDIUM BROMIDE/ACRIDINE ORANGE (EB/AO)

2.5 g of ethidium bromide (Sigma) and 2.5 g of acridine orange (Sigma) dissolved in 50 ml of 1X PBS

EDTA (25mM)

0.93 g EDTA (Sigma) dissolved in 50ml Baxters Water.

ELISA BLOCKING SOLUTION

1 g bovine serum albumin (BSA) added to 100 ml 1X PBS

5 g Marvel skimmed milk added to 100 ml 1X PBS

ELISA DEVELOPING SOLUTION

1 OPD tablet (Sigma) dissolved in 25 ml of phosphate citrate buffer with 7 µl of hydrogen peroxide (H_2O_2; Sigma).

ELISA STOPPING SOLUTION (1M H_2SO_4)

26.47 ml 18 M H_2SO_4 with 473.26 ml dH_2O.

ELISA WASHING BUFFER

500 ml 20x PBS, 5 ml Tween (Sigma) made up to 10 L with dH_2O.

FACS BUFFER

500 ml of sterile 1X PBS supplemented with 0.1% azide and 2% FCS.

MACS BUFFER

10 ml FCS, 5 ml 25 mM EDTA added to 500 ml sterile 1X PBS.

PERITONEAL LAVAGE BUFFER

500 ml of sterile 1X PBS supplemented with 100 µg/ml penicillin/streptomycin (Sigma).

PHOSPHATE BUFFERED SALINE (PBS)

20X stock was used for ELISA solutions: 800 g sodium chloride (NaCl, Sigma), 92 g sodium hydrogen phosphate (Na_2HPO_4, Sigma), 20 g potassium dihydrogen phosphate (KH_2PO_4, Sigma), 20 g potassium chloride (KCl, Sigma) all dissolved in 5 L dH_2O and adjusted to pH 7.

Sterile PBS (Sigma) was used for mouse injections, FACS buffer, MACS buffer, lavages and perfusions.

Sterile 10x PBS (Sigma) was used to make up stock isotonic Percoll.

PHOSPHATE CITRATE BUFFER

10.19 g anhydrous citrate acid (Sigma), 36.69 g hydrous sodium hydrogen phosphate ($Na_2HPO_4.12H_2O$, Sigma) made up in 1 L of dH20 and adjusted to pH 5.

PERCOLL SOLUTIONS

Stock isotonic percoll (SIP) was made by mixing 1 part 10x PBS to 9 parts Percoll (GE Healthcare). Other densities of Percoll were made using the formula below. For example, if you require 100ml of 1.088 g/ml density Percoll,

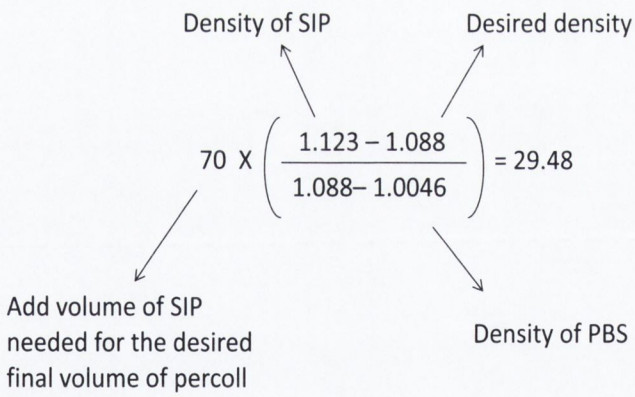

Therefore, 70 ml SIP + 29.38 ml 1x PBS = 99.38 ml 1.088 g/ml Percoll.

Table 2.1.1Recombinant murine cytokines

Cytokine	Supplier	Conc. in vitro	Dose in vivo
IL-1β	R&D	10 ng/ml	100 ng/mouse
IL-23	R&D	10 ng/ml	100 ng/mouse
IL-4	Miltynei	n/a	5 µg/mouse
IL-10	R&D	n/a	200 ng/mouse
IL-2	R&D	10U/ml = 5 ng/ml	n/a
GM-CSF	In house	20 ng/ml	n/a
M-CSF	In house	20% v/v	n/a

Table 2.1.2 Small molecule inhibitors

Inhibitor	Target	Supplier	Conc in vitro
SB203580	p38	Jena Bioscience	500 nM
ZSTK 474	pi3K	Selleckchem	50 nM

Table 2.1.3 Real-time PCR primers

Protein	Gene	Product code	Ref. Seq	Supplier
18S rRNA	18S	4319413E	X03205.1	ABI
Arginase 1	Arg1	Mm00475988_m1	NM_007482.3	ABI
Relm-α	Retnla	Mm00445109_m1	NM_020509.3	ABI
iNOS	Nos2	Mm00440502_m1	NM_010927.3	ABI
TGF-β	Tgfb1	Mm00441724_m1	NM_011577.1	ABI
TNF-α	Tnf	Mm00443258_m1	NM_013693.2	ABI
IL-1β	Il1b	Mm00434228_m1	NM_008361.3	ABI
IL-12p40	Il12b	Mm00434174_m1	NM_008352.2	ABI
IL-4	Il4	Mm00445259_m1	NM_021283.2	ABI
IL-10	Il10	Mm00439614_m1	NM_010548.2	ABI

Table 2.1.4 PRR ligands

PRR Ligand	PRR	Supplier	Conc. in vitro	Dose in vivo
CpG	TLR9	Sigma-genosys	5 µg/ml	n/a
LPS	TLR4	Enzo	100 or 500 ng/ml	100 ng /mouse
Pam3CSK	TLR2 & TLR1	Invivogen	500 ng/ml	n/a
Zymosan	TLR2 & Dectin-1	Invivogen	10 µg/ml	n/a
TriDAP	NOD1	Invivogen	100 µg/ml	100 µg /mouse
Heat killed *M. tuberculosis*	TLR2, TLR4 & NOD2	Difco	25 µg/ml	400 µg /mouse

Table 2.1.5 Antigens

Antigen	Supplier	Conc. in vitro	Dose in vivo
MOG_{35-55}	Cambridge	2, 10 or 50 µg/ml	150 µg/mouse
OVA protein	Sigma-aldrich	25 µg/ml	n/a

Table 2.1.6 NA/LE Antibodies

Antibody	Clone	Supplier	Conc in vitro	Dose in vivo
Anti-IL-4	BVD4	Bioceros	n/a	550 µg/mouse
Anti-CD3e	145-2C11	BD Pharmigen	1 µg/ml	n/a
Anti-CD28	37.51	BD Pharmigen	2 µg/ml	n/a

Table 2.1.7 ELISA antibodies, standards and blocking solutions.

Cytokine	Capture Antibody	Block	Detection Antibody	Standard	Supplier
IL-1β	4µg/ml	1% BSA	2.5 µg/ml	1000 pg/ml	R&D
IL-23	4 µg/ml	1% BSA	100 ng/ml	2500 pg/ml	R&D
IL-27	2µg/ml	1% BSA	1 µg/ml	1000 pg/ml	R&D
IL-10	4µg/ml	1% BSA	300 ng/ml	2000 pg/ml	R&D
IL-12p40	1 µg/ml	5% Marvel	1 µg/ml	2500pg/ml	BD Pharmigen
IL-12p70	4 µg/ml	1% BSA	400 ng/ml	1500 pg/ml	R&D
IL-17	2µg/ml	1% BSA	400 ng/ml	1000 pg/ml	R&D
IFN-γ	1 µg/ml	5% Marvel	1 µg/ml	10 ng/ml	BD Pharmigen
TNF-α	800 ng/ml	1% BSA	200 ng/ml	2000 pg/ml	R&D
GM-CSF	2 µg/ml	1% BSA	50 ng/ml	500 pg/ml	R&D
IL-6	1 µg/ml	5% BSA	1 µg/ml	5000 pg/ml	BD Pharmigen

Table 2.1.8 Fluor-conjugated FACS antibodies

Specificity	Clone	Flurochrome	µl/1x10^6 cells	Supplier
IL-17	eBio17B7	APC	0.25	eBioscience
IFN-γ	XMG1.2	PerCp Cy 5.5	0.25	eBioscience
IL-4	11B11	PE	0.25	BD Pharmigen
IL-10	JES5-16E3	APC	0.25	eBioscience
Ki67	501A15	Alexa-647	0.25	eBioscience
FoxP3	FJK-165	APC	0.25	eBioscience
CD19	ID3	APC	0.25	eBioscience
CD80	16-10A1	PE	0.25	BD Pharmigen
CD86	GL1	FITC	0.25	BD Pharmigen
CD45RB	C36.16A	FITC	0.25	eBioscience
CD25	PC61.5	PE	0.25	eBioscience
CD4	RM4-5	V450	0.25	BD Pharmigen
CD4	GK1.5	APC-Cy7	0.25	BD Pharmigen
CD3	500A2	PeCy7	0.25	eBioscience
CD11b	M1/70	Alexa-780	0.25	eBioscience
CD11b	M1/70	APC	0.25	eBioscience
CD11c	N418	FITC	0.25	eBioscience
F480	BM8	PeCy7	0.25	eBioscience
γδ-TCR	GL3	PE	0.25	BD Pharmigen
GR1	RB6-8C5	PE	0.25	eBioscience
MHC-II/IA-IE	2G9	FITC	0.05	BD Pharmigen
MHC-II/IA-IE	MS/114.15.2	Pacific Blue	0.05	eBioscience
Ly6C	HK1.4	PerCP-Cy5.5	0.25	eBioscience
Ly6G	1A8	PE	0.25	BD-Pharmigen
Ly6G	1A8	Pacific Blue	0.25	Biolegend
PD-L2	I22	FITC	0.25	eBioscience
Dectin-1	n/a	APC	0.25	R&D
Siglec-F	E50-2440	PE	0.25	BD-Pharmigen

Table 2.1.9 Biotin-antibody cocktails used for the purification of cells by negative magnetic selection

Purified population	Targets of antibody cocktail	Supplier
Pan T-cell	CD11b, CD11c, CD19, CD45R, CD49b, CD105, MHC-II, Ter-119	Miltenyi Biotech
$CD4^+$ T-cell	CD8a, CD11b, CD11c, CD19, CD45R, CD49b, CD105, MHC-II, Ter-119	Miltenyi Biotech

Table 2.1.9 Reagents for restimulation of cells for intracellular staining

Reagent	Concentration in vitrol	Supplier
PMA	10 ng/ml	Sigma
Ionomycin	1 µg/ml	Sigma
Brefeldin A	5 µg/ml	Sigma

2.2 Mice

Specific pathogen-free C57BL/6 and BALB/c mice were purchased from Harlan UK Ltd (Bicester, UK). The mice were maintained according to the guidelines and regulations of the Irish Medical Board and experiments were carried out under licence with the approval of Trinity College Dublin Bioresources Ethics Committee. Mice were sacrificed by cervical dislocation or by asphyxiation with CO_2 except when an intra-cardial perfusion was required, where the mice were euthanised with pentobarbital sodium. All animals used were age matched females at 8-12 weeks old at the initiation of experiments. IL-$10^{-/-}$ mice and DO11 OVA-transgenic mice were bred in-house on a C57BL/6 and BALB/c background, respectively. Age matched wild type mice were bred in-house as a control for any transgenic mice used.

2.3 Methods

2.3.1 General protocols for cell culture

2.3.1.1 Preparation of a single cell suspension

Organs (lymph nodes, spleens, brains etc.) were harvested from sacrificed mice using autoclaved instruments and collected in ice-cold RPMI. Organs were processed by pushing them through a sterile cell strainer (40 µm or 70 µm; Greiner) using the plunger from a sterile 5 ml syringe (Greiner). The cells were washed through the strainer with RPMI or PBS and pelleted by centrifugation (242 g, 5 min, Eppendorf 5810R). The pellet was then resuspended in RPMI for counting or ammonium chloride lysis solution to lyse red blood cells.

2.3.1.2 Red blood cell lysis

The red blood cells from single cell suspensions were lysed using ammonium chloride lysis solution. The pellet of cells was resuspended in 5 ml warm ammonium chloride lysis solution for 3 min. The cells were then washed with an excess of RPMI and pelleted by centrifugation (242 g, 5 min). The pellet was then resuspended in a appropriate volume of RPMI for counting.

2.3.1.3 Cell counting

Viable cells were counted by diluting 10 µl of cells in 190 µl EB/AO solution. The mixture was then placed in a haemocytometer (Hycor Biomedical). The numbers of viable cells (green) and numbers of dead cells (orange) in the nine squares were counted using a UV-fluorescent microscope.

No. Cells/ml= Count x Dilution Factor x 10^4

2.3.2 Cell culture

Single cell suspensions were cultured in RPMI in tissue culture plates (48 well -96 well; Greiner) or tissue culture flasks (T75 or T175; Greiner) in an incubator maintained at a constant temperature and atmosphere (37°C, 5% CO_2).

2.3.2.1 Generation of bone marrow derived dendritic cells

Bone marrow from the legs of C57BL/6 mice was flushed out using a syringe with a 27 G needle filled with RPMI. Any cell aggregates were broken down by syringing the cells up and down using a 19 G needle. The red blood cells were lysed as described in Section 2.3.1.2. The cells were then counted and cultured in a T175 flask at a concentration of $5x10^5$ cells/ml in 30ml of RPMI supplemented with 20 ng/ml of GM-CSF.

Another 20 ml of RPMI supplemented with 20 ng/ml of GM-CSF was added on d 3. On d 6 the supernatant was gently removed and 20ml of sterile PBS was added and the flask was agitated and the PBS and cells were removed and added to 10 ml of RPMI. 20ml of EDTA (Sigma) was added to the flask and incubated for 10 min at 37°C and 5% CO_2. The flask was agitated and the EDTA and cells were removed and added to 10 ml of RPMI. Both PBS and EDTA solutions were centrifuged (242 g, 5 min) and resuspended in 10 ml of RPMI. The cells were counted and cultured in a T175 flask at $5x10^5$ cells/ml in 30 ml of RPMI supplemented with 20 ng/ml of GM-CSF.

20 ml of RPMI supplemented with 20 ng/ml of GM-CSF was added on d 8. On d 10 the supernatant was pipetted over the bottom of the flask approximately five times before being removed and centrifuged (242 g, 5 min). Cells were resuspended in 10 ml of RPMI, counted and re-seeded in the appropriate cell culture plates. Cells were rested for at least 3 h before being stimulated as required.

2.3.2.2 Generation of bone marrow derived macrophages

Bone marrow from the legs of C57BL/6 mice was flushed out using a syringe with a 27G needle. The cell aggregates were broken down by syringing up and down using a 19G needle. The red blood cells were lysed as described in Section 2.3.1.2. The cells were counted and cultured in a petri dish at $1x10^6$ cells/ml in RPMI supplemented with 10% v/v M-CSF. On d 4 the supernatant was removed carefully and replaced with fresh RPMI supplemented with 10% v/v M-CSF. On d 7 the loose cells were washed away using RPMI and the adherent macrophages were scraped off, counted and re-seeded in the appropriate cell culture plates. The cells were allowed to rest for 3 h before being stimulated as required.

2.3.3 Intraperitoneal injections

Mice were injected intraperitoneally (i.p.) with a $27_{1/2}$ G micro tuberculin syringe filled with various reagents or cells depending on the experiment. Reagents were diluted in PBS and a total volume of 100 µl/mouse was injected.

2.3.3.1 The isolation of peritoneal cells by peritoneal lavage

The peritoneal cavity was used as a source of either treated or untreated cells. Naive mice or mice which had been injected with a particular treatment (for example, TriDAP) were sacrificed by asphyxiation with CO_2 and carefully dissected to reveal the intact peritoneal cavity. 5 ml of ice-cold peritoneal lavage buffer was injected into the peritoneal cavity using a 27 G needle attached to a 5 ml syringe barrel. The needle was carefully removed and the mouse was gently shaken to encourage the removal of peritoneal cells. The needle was reinserted and as much buffer as possible was removed (approximately 4 ml). The cell suspension was kept on ice as much as possible to prevent the adherence of macrophages to plastic. The peritoneal exudate cells (PEC) were pelleted by centrifugation (242 g, 5 min) and resuspended in RPMI. The PEC were counted and either seeded in tissue culture plates for further stimulation or added to TRIzol (Invitrogen) for the isolation of RNA.

Table 2.3.1 Panel of fluor-conjugated antibodies used for analysing the PEC

Specificity	Clone	Flurochrome	µL/1x10^6 cells	Supplier
MHC-II/IA-IE	2G9	FITC	0.05	BDPharmingen
Ly6G	1A8	PE	0.25	BDPharmingen
F480	BM8	PeCy7	0.25	eBioscience
CD11b	M1/70	Alexa780	0.25	eBioscience
Ly6C	HK1.4	PerCP-Cy5.5	0.25	eBioscience
CD19	ID3	APC	0.25	eBioscience
LIVE/DEAD	n/a	V500	0.05	Life Tech.

2.3.4 Subcutaneous injections

Mice were injected subcutaneously (s.c.) using a $27_{1/2}$ G micro tuberculin syringe filled with various reagents or cells depending on the experiment. Reagents were diluted in PBS and a total volume of 100 µl/mouse was injected. In the case of EAE induction, 200 µl of reagent was injected using a 19 G needle attached to a 1 ml syringe barrel.

2.3.5 Footpad injections

Mice were injected s.c. in the footpad using a $27_{1/2}$ G micro tuberculin syringe filled with various reagents depending on the experiment. Reagents were diluted in PBS and a total volume of 25 µl was injected per footpad for a total of 50 µl per mouse. The draining popliteal lymph nodes were then taken at the required timepoint. The lymph nodes were processed and the single cell suspension was used as required.

2.3.5.1 In vivo stimulation of γδ T-cells

C57BL/6 were injected subcutaneously in the footpad with either PBS, TriDAP (100 µg), IL-1β (100 ng) and IL-23 (100 ng) or a combination of IL-1β, IL-23 and TriDAP. The mice were sacrificed after 4 h and the draining popliteal lymph nodes were removed. The organs were processed as described in Section 2.3.1.1. The cells were then stained with fluor-conjugated antibodies as described in Section 2.3.11. The antibodies used and concentrations they were used at are shown in Table 2.3.2.

Table 2.3.2 Panel of fluor-conjugated antibodies for the analysis of γδ T-cells ex vivo

Specificity	Clone	Flurochrome	µL/1x10^6 cells	Supplier
IFN-γ	XMG1.2	PerCPcy5.5	0.25	eBioscience
IL-17A	17B7	APC	0.25	eBioscience
CD3	145-2C11	PeCy7	0.25	eBioscience
Live/Dead	N/A	V500	0.05	Life Tech.
γδ -TCR	GL3	PE	0.25	BDPharmingen

2.3.6 Protocols associated with EAE

2.3.6.1 Actively induced EAE

C57BL/6 mice were injected s.c. with MOG_{35-55} (AnaSpec Inc., 100 µg) emulsified in complete Freund's adjuvant (CFA, Chondrex Inc) at a ratio of 1:1. Mice were also injected i.p. with pertussis toxin (PT, Kaketsuken Japan, 500 ng) on d 0 and 2. Clinical score was measured every day as follows: 1 = limp tail, 2 = altered gait, 3 = paralysis of single limb, 4 = paralysis of two limbs, 5 = paralysis of three or more limbs/death.

2.3.6.1.2 Passively induced EAE

C57BL/6 mice were injected s.c. with MOG_{35-55} (AnaSpec Inc., 100 µg) emulsified in CFA (Chondrex Inc.) at a ratio of 1:1. Mice were sacrificed d 10 post injection and the inguinal, brachial and auxiliary lymph nodes and spleen were removed. $150x10^6$ lymphocytes and $350x10^6$ splenocytes were cultured in a T75 flask in 50 ml RPMI. The cells were incubated in the presence of MOG_{35-55} (100 µg/ml), IL-1β (10 ng/ml) and IL-23 (10 ng/ml) for 72 h. The cells were removed from culture and counted. The cells were washed in PBS and injected i.p. into naive C57BL/6 mice ($15x10^6$ cells/mouse). Clinical score was measured every day as follows: 1 = limp tail, 2 = altered gait, 3 = paralysis of single limb, 4 = paralysis of two limbs, 5 = paralysis of three or more limbs/death.

2.3.6.2 Mononuclear cell isolation from the central nervous system

Mice were anaesthetised with an i.p. injection of 40 µl of Pentobarbitol Sodium (Euthethal) before being perfused intracardially with 10 ml of ice cold sterile PBS. The brain was placed in approximately 2 ml of HBSS and processed as described in Section 2.3.1.1. Cells were centrifuged (242 g, 5 min) and resuspended in a solution of collagenase D (1 mg/ml; Roche) and DNAse I (10 µg/ml; Sigma). Cells were incubated at 37°C for 1 hour with gentle agitation. Cells were washed with HBSS and centrifuged (242 g, 5 min).

Cells were resuspended in 1088 g/ml Percoll. This was underlaid with SIP before being overlaid with 1.072 g/ml Percoll, 1.030 g/ml Percoll and finally with 1x PBS. The gradient was then centrifuged (1250 g for 45 min). Mononuclear cells were taken from the 1.088:1.072 g/ml and 1.072:1.030 g/ml interfaces. Cells were washed twice in HBSS before being resuspended in RPMI for counting. Cells were then surface-stained and stained intracellularly with fluor-conjugated antibodies (Table 2.2.3) as described in Section 2.3.11.

Table 2.2.3 The panel of fluor-conjugated antibodies used for analysing mononuclear brain cells ex vivo

Specificity	Clone	Flurochrome	µL/1x10^6 cells	Supplier
IL-17	eBio17B7	APC	0.25	eBioscience
IFN-γ	XMG1.2	PerCp Cy 5.5	0.25	eBioscience
Live/Dead	N/A	V500	0.05	Life Tech
CD4	RM4-5	V450	0.25	BD Horizon
CD3	500A2	PeCy7	0.25	eBioscience

2.3.6.3 The transfer of peritoneal macrophages into mice with EAE

C57BL/6 mice were injected i.p. with PBS, TriDAP (100 μg) or LPS (100 ng) on d 0, 1, 2, 3 and 4. Another group of mice were injected i.p. with IL-4c (IL-4 and αIL-4; 5 μg and 25 μg, respectively) on d 0 and 2. Total peritoneal macrophages were purified from the treated mice as described in Section 2.3.7.3. The cells were counted and resuspended in PBS at a concentration of $5x10^6$/ml. 200 μl of cell suspension was injected into mice with EAE s.c. near the site of the original MOG and CFA injection on d 0 and 6 post induction of EAE.

2.3.6.4 Immunisation of mice with MOG and CFA for the isolation of antigen-specific T-cells

C57BL/6 mice were injected s.c. with MOG_{35-55} (100 μg) emulsified in CFA at a ratio of 1:1. Mice were sacrificed on d 7 post immunisation and a single cell suspension was formed from the spleen and the inguinal, brachial and auxiliary lymph nodes as described in Section 2.3.1.1. T-cells were then purified and used as required.

2.3.7 Cell Purification

2.3.7.1 Purification of $CD4^+$ or $CD3^+$ T-cells using negative magnetic selection

$CD4^+$ and $CD3^+$ T-cells were purified by negative selection using the magnetic sorting kits (MACS) available from Miltenyi Biotech. The following is the basic protocol for sorting either cell population using the reagents described in Table 2.1.9.

Inguinal, cervical, brachial, auxiliary and popliteal lymph nodes and spleens were isolated from either naive or MOG immunized C57BL/6 mice as required. Organs were processed as described in Section 2.2.1. The single cell suspension was counted, centrifuged (242 g, 5 min) and washed with MACS buffer to ensure the removal of any RPMI. Cells were pelleted by centrifugation (242 g, 5 min) and resuspended in the appropriate amount of MACS buffer (40 µl/10^7 cells). The appropriate amount of Pan T-cell or $CD4^+$ T-cell biotin-antibody cocktail (10 µl/10^7 cells; Miltenyi Biotech) was added and the cells were incubated for 10 min at 4°C. MACS buffer was added (60 µl/10^7 cells). Then the appropriate amount of Anti-Biotin Microbeads (20 µl/10^7 cells; Miltenyi Biotech) was added and the cells were incubated for 15 min at 4°C. Finally the cells were washed in MACS buffer and pelleted by centrifugation (242 g, 5 min). The cells were resuspended in the appropriate volume of MACS buffer (500 µl/10^8 cells).

Cells were filtered through a cell strainer (70 µm; Cellmetrics) onto a magnetised LS column (Miltenyi Biotech) and the column was washed three times with 3 ml of MACS buffer. All of the eluent was collected which represented the enriched $CD4^+$/$CD3^+$ T-cells. These cells were resuspended in RPMI and counted. Cell purity was checked using fluor-conjugated antibodies specific for CD3 or CD4 and analysed by flow cytometry. The purity of any cells used was > 97%.

Fig 2.2.1 Sample purities for $CD3^+$ T-cells (A) and $CD4^+$ T-cells (B) sorted by negative magnetic selection

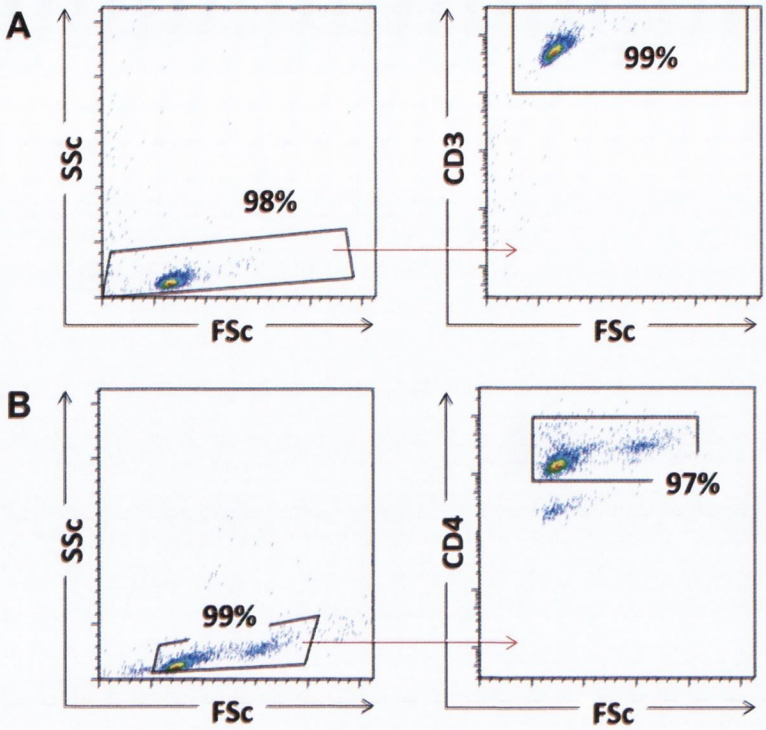

2.3.7.2 Purification of naive T-cells by FACS

Inguinal, cervical, brachial, auxiliary and popliteal lymph nodes and spleens were isolated from naive C57BL/6 or BALB/c mice as required. Organs were processed as described in Section 2.3.1.1). The single cell suspension was counted, centrifuged (242 g, 5 min) and washed with PBS to ensure the removal of any RPMI.

Cells were resuspended in 2.5 ml of PBS (up to 5 x 10^7 cells) and incubated with FC block (12.5 µl/2.5 ml; BD Biosciences) for 10 min to prevent the unspecific binding of antibodies to the FcγIIR. The appropriate panel of fluor-conjugated antibodies (Table 2.2.4) was then added and the cells were incubated at RT for 15 min. The cells were then washed in an excess of PBS. The cells were pelleted by centrifugation (242 g, 5 min) and resuspended in 1 ml of RPMI (up to 5 x 10^7 cells). Naive T-cells ($CD4^+CD25^-CD45RB^{int-hi}$) were sorted by FACS using the gating strategy shown (Fig 2.2.2) using a MoFlow flow cytometer (Beckman Coulter). The cells were collected in RPMI, counted and used as necessary.

Table 2.2.4 The panel of fluor-conjugated antibodies used for sorting naive T-cells

Specificity	Clone	Flurochrome	µL/5x10^7 cells	Supplier
CD4	GK1.5	PeCy7	10	BD-Pharmigen
CD25	PC61.5	PE	10	eBioscience
CD45RB	C363.16A	FITC	10	eBioscience

Fig 2.2.2 The gating strategy for sorting naive T-cells by FACS

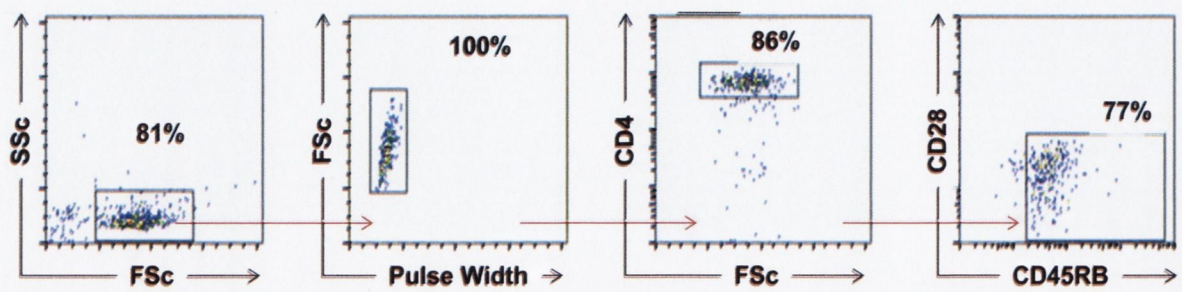

2.3.7.3 Purification of peritoneal macrophages by FACS

PEC were harvested from treated or untreated mice as described previously (Section 2.3.3.1). The single cell suspension was counted, pelleted by centrifugation (242 g, 5 min) and resuspended in 2.5 ml of PBS (up to 5 x 10^7 cells). The cells were then incubated with FC block (12.5 µl/2.5 ml; BD Biosciences) for 10 min to prevent the unspecific binding of antibodies to the FcγIIR. The appropriate panel of fluor-conjugated antibodies (Table 2.2.5) was then added and the cells were incubated at RT for 15 min. The cells were then washed in an excess of PBS. The cells were pelleted by centrifugation (242 g, 5 min) and resuspended in 1 ml of RPMI (up to 5 x 10^7 cells). Large peritoneal macrophages ($CD11b^+F480^+Gr1^-MHC\text{-}II^-$) or total peritoneal macrophages ($CD11b^+F480^+Gr1^-$) were sorted by FACS using the gating strategies shown in Fig 5.2.1 and Fig 5.2.2 using a MoFlow flow cytometer (Beckman Coulter). The cells were collected in RPMI, counted and used as necessary.

Table 2.2.5 Panel of fluor-conjugated antibodies used for sorting peritoneal macrophages

Specificity	Clone	Flurochrome	µL/5x10^7 cells	Supplier
MHC-II/IA-IE	2G9	FITC	10	BD-Pharmigen
GR1	RB6-8C5	PE	10	eBioscience
F480	BM8	PeCy7	10	eBioscience
CD11b	M1/70	Alexa780	10	eBioscience

2.3.7.4 Purification of peritoneal neutrophils

C57BL/6 mice were injected i.p. with 9% casein to recruit neutrophils to the peritoneal cavity. After 15 h a second i.p. injection of 9% casein was administered, and 3 h after the second injection the peritoneal cavity was lavaged as described previously (Section 2.3.3.1). The cells were resuspended in 62% SIP (62 ml SIP and 38 ml 1X PBS) and centrifuged (2100 g, 25 min, no brake). Three layers were formed; the top layer contained mononuclear cells (macrophages, lymphocytes etc.), the middle layer contained polymorphonuclear cells (neutrophils, eosinophils etc.) and the bottom layer contained erythrocytes. The middle layer was pipetted into a fresh tube and washed with an excess of RPMI. The cells were centrifuged (242 g, 5 min), resuspended in the appropriate amount of RPMI and counted. The cells were then used as required. The purity of neutrophils ($GR1^{hi}CD11b^{+}$) retrieved was > 93%.

Fig 2.2.3 Sample purities for neutrophils purified by continuous Percoll gradient

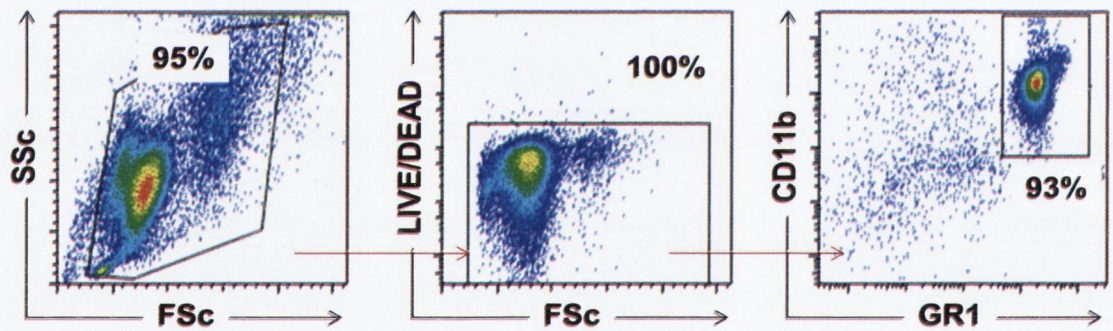

2.3.7.5 Depletion of innate cells from the PEC by FACS

PEC were harvested from naive C57BL/6 mice as described previously (Section 2.3.3.1). The single cell suspension was counted, pelleted by centrifugation (242 g, 5 min) and resuspended in 2.5 ml of PBS (up to 5 x 10^7 cells). The cells were then incubated with FC block (12.5 µl/2.5 ml; BD Biosciences) for 10 min to prevent the unspecific binding of antibodies to the FcγIIR. The cells were then split in half and the appropriate panel of fluor-conjugated antibodies (Table 2.26 and Table 2.2.7) was added to each tube. The cells were incubated at RT for 15 min. The cells were then washed in an excess of PBS, pelleted by centrifugation (242 g, 5 min) and resuspended in 1 ml of RPMI each (up to 5 x 10^7 cells).

PEC cells were then depleted of DC, eosinophils, macrophages or neutrophils by FACS according to the gating strategies described in Fig 2.2.4 using a MoFlow flow cytometer (Beckman Coulter). The cells were collected in RPMI, counted and used as required.

Table 2.2.6 Panel of fluor-conjugated antibodies used for depleting DC and eosinophils by FACS

Specificity	Clone	Flurochrome	µL/5x10^7 cells	Supplier
CD11c	N418	FITC	10	eBioscience
Siglec F	E50-2440	PE	10	BDPharmingen
CD11b	M1/70	Alexa-780	10	eBioscience

Table 2.2.7 Panel of fluor-conjugated antibodies used for depleting peritoneal macrophages and neutrophils by FACS

Specificity	Clone	Flurochrome	µL/5x10^7 cells	Supplier
MHC-II/IA-IE	2G9	FITC	10	BDPharmingen
GR1	RB6-8C5	PE	10	eBioscience
F480	BM8	PeCy7	10	eBioscience
CD11b	M1/70	Alexa780	10	eBioscience

Fig 2.2.4 The gating strategy used to deplete (A) neutrophils, (B) macrophages, (C) DC and (D) eosinophils from the total PEC

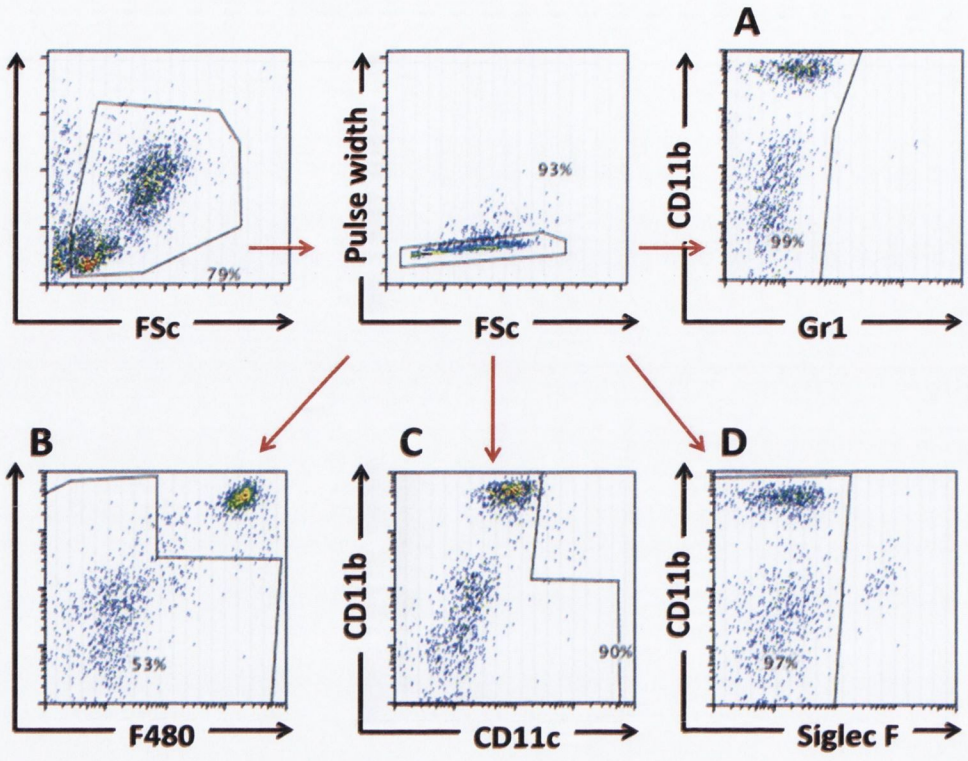

2.3.8 In vitro cell stimulations

2.3.8.1 Stimulation of BMDC with TLR agonists and TriDAP

BMDC were generated as described in Section 2.3.2.1. Cells were counted and resuspended in RPMI at a concentration of $1x10^6$/ml. The cell suspension was added to the wells of a 96 round-bottom tissue culture plate (200 µl/well). Cells were incubated in the absence or presence of TriDAP (100 µg/ml) for 1 h before the addition of RPMI alone or various TLR agonists (see Table 2.1.4 for concentrations). The final volume in the well was 250 µl. All treatments/controls were carried out in triplicate. After 24 h the cells were centrifuged (242g, 5min) and supernatants were removed. The concentrations of various cytokines were quantified by ELISA.

2.3.8.2 Stimulation of BMM with TriDAP or LPS

BMM were generated as described in Section 2.3.2.2. Cells were counted and resuspended in RPMI at a concentration of $1x10^6$/ml. The cell suspension was added to the wells of a 96 round-bottom tissue culture plate (200 µl/well). BMM were incubated with or without TriDAP (100 µg/ml) or LPS (500 ng/ml) in a final volume of 250 µl/well. All treatments/controls were carried out in triplicate. After 24 h the cells were centrifuged (242g, 5min) and supernatants were removed. The concentrations of various cytokines were quantified by ELISA.

2.3.8.3 Stimulation of PEC in vitro with TriDAP or LPS

PEC were isolated as described in Section 2.3.3.1. PEC were counted and resuspended in RPMI at a concentration of $1x10^6$/ml. The cell suspension was added to 96 well plates (200 µl/well) or 48 well plates (500 µl/well) for stimulation. PEC were incubated with or without TriDAP (100 µg/ml) or LPS (500 ng/ml). Other experiments included the addition of the p38 inhibitor SB203508 (500 nM; Jena Bioscience) or the Pi3K inhibitor ZSTK 474 (50 nM; Selleckchem). The final volume per well was 250 µl (96 well plate) or 550 µl (48-well plate). All treatments/controls were carried out in triplicate. The cells were centrifuged (242 g, 5 min) and supernatants were removed at the timepoints required. The concentrations of various cytokines in the supernatant were quantified by ELISA. Supernatants were also kept to be added to $CD4^+$ T-cells as described in Section 2.3.9.3. TRIzol was added to the remaining cells and RNA was isolated as described in Section

2.3.14.1. Real-time PCR was then used to measure the relative expression of a variety of different genes (Section 2.3.14.3).

2.3.8.4 Stimulation of peritoneal neutrophils

Neutrophils were isolated as described in Section 2.3.7.4. Cells were counted and resuspended in RPMI at a concentration of $1x10^6$/ml. The cell suspension was added to the wells of round bottom 96 well plates (200 µl/well). Neutrophils were incubated with or without TriDAP (100 µg/ml) or LPS (500 ng/ml) at a final volume of 250 µl. All treatments/controls were carried out in triplicate. After 24 h the supernatants were removed and the concentrations of various cytokines were quantified by ELISA.

2.3.8.5 Stimulation of depleted PEC

PEC cells were depleted of various innate immune cells as described in Section 2.3.7.5. Cells were counted and resuspended in RPMI at a concentration of $1x10^6$/ml. The cell suspension was added to the wells of round bottom 96 well plates (200 µl/well). Depleted PEC were incubated with or without TriDAP (100 µg/ml) or LPS (500 ng/ml) at a final volume of 250 µl. All treatments/controls were carried out in triplicate. After 24 h the supernatants were removed and the concentrations of various cytokines were quantified by ELISA.

2.3.9 T-cell stimulations

2.3.9.1 In vitro stimulation of $CD4^+$ T-cell

T-cells were stimulated in vitro with a combination of plate bound αCD3 and soluble αCD28. 50 µl of αCD3 (1 µg/ml) diluted in sterile PBS was added to wells and incubated for 4 h at 37°C. The wells were then washed twice with excess PBS before the addition of T-cells and soluble αCD28.

2.3.9.2 Stimulation of $CD4^+$ T-cells in the presence of TriDAP

$CD4^+$ T-cells from C57BL/6 mice immunized with MOG and CFA were purified by negative magnetic selection as described in Section 2.3.7.1. $CD4^+$ T-cells were counted and resuspended in RPMI at a concentration of $1x10^6$cells/ml. Cells were seeded in round-

bottom tissue culture plates (200 µL/well). $CD4^+$ T-cells were stimulated with plate-bound αCD3 (1 µg/ml) and soluble αCD28 (2 µg/ml) in the absence or presence of TriDAP (100 µg/ml). All treatments/controls were carried out in triplicate. The supernatant was removed after 72 h and the concentrations of various cytokines were quantified by ELISA.

2.3.9.3 Stimulation of $CD4^+$ T-cells in the presence of supernatant from PEC

Naive $CD4^+$ T-cells from naive C57BL/6 mice were purified by FACS as described in Section 2.3.7.2. The purified cells were then labelled using CTV as described in Section 2.3.12.1. $CD4^+$ T-cells were counted and resuspended in RPMI at a concentration of $2x10^6$cells/ml. Cells were seeded in round-bottom tissue culture plates (100 µl/well) and stimulated with IL-2, IL-2 and plate bound αCD3 or IL-2, plate bound αCD3 and soluble αCD28. In addition, the $CD4^+$ T-cells were incubated in the absence or presence of supernatant from TriDAP-treated, LPS-treated or untreated-PEC (Section 2.3.8.3). After 72 h the cells were centrifuged (242 g, 5 min) and the supernatant was removed. The concentrations of various cytokines were quantified by ELISA.

The cells were then surface-stained, fixed, permeabilised and stained intracellularly with fluor-conjugated antibodies (Table 2.2.8) using the protocols described in Section 2.3.11. The cells were then analysed by flow cytometry.

Table 2.2.8 Panel of fluor-conjugated antibodies used for the FACS analysis of $CD4^+$ T-cells stimulated in the presence of supernatant from treated PEC

Specificity	Clone	Flurochrome	µL/1x10^6 cells	Supplier
CD4	GK1.5	APC-Cy7	0.25	BDPharmigen
CD3	145-2C11	PeCy7	0.25	eBioscience
Live/Dead	n/a	V500	0.05	Life Tech
IL-10	JES5-16E3	APC	0.25	eBioscience
IL-4	11B11	PE	0.25	BDPharmigen

2.3.10 T-cell and APC co-cultures

2.3.10.1 Antigen presentation assay with stimulated BMDC and $CD4^+$ T-cells

BMDC were generated as described in Section 2.3.2.1. The BMDC were counted and resuspended in RPMI at a concentration of 2.5 x 10^5 /ml. The cells were then added to the wells of 96-well round bottom tissue culture plates (200 µl/well). BMDCs were cultured for 16 h with either medium or MOG (25 µg/ml) in the absence or presence of TriDAP (10 or 100 µg/ml) in a final volume of 250 µl. The cells were washed and incubated with $CD4^+$ T-cells purified from MOG-immunized mice as described in Section 2.3.7.1. $CD4^+$ T-cells were added at a ratio of 1:10 (BMDC:T-cell). All treatments/controls were carried out in triplicate. After 72 h the supernatant was removed and the concentrations of various cytokines were quantified by ELISA. An additional plate was set up to measure IL-2 production and T-cell proliferation. 50 µL was removed from the second replicate after 24 h and the concentration of IL-2 was quantified by ELISA. The 50 µl of supernatant was replaced by [^{3}H] thymidine (1 µl/well) diluted in RPMI. After another 48 h the cells were harvested and the incorporation of [^{3}H] thymidine was measured as described in Section 2.3.12.2.

2.3.10.2 Antigen-specific restimulation of cells from mice with EAE

Inguinal lymph nodes from mice with EAE were processed as described in Section 2.3.1.1. Cells were counted and resuspended in RPMI at a concentration of 1x10^6 cells/ml. Cells were added to the wells of 96-well tissue culture plates (200 µl/well). Cells were cultured with either medium alone, MOG (2, 10, 50 µg/ml) or PMA (10 ng/ml) and αCD3 (1 µg/ml). All treatments/controls were carried out in triplicate. After 72 hours the supernatants were removed and concentrations of cytokines were quantified by ELISA.

2.3.10.3 Co-culture of *M. tuberculosis* stimulated BMDC and purified T-cells

BMDC were generated as described in Section 2.3.2.1. The BMDC were counted and resuspended in RPMI at a concentration of 5 x 10^5 /ml. The cells were added to the wells of round-bottom 96-well tissue culture plates (100 µl/well). The BMDC were incubated in the absence or presence of TriDAP (100 µg/ml) at a final volume of 200 µl. After 16 h either RPMI alone or heat-killed *M.tuberculosis* (25 µg/ml) was added to the cell culture. After 6 h the BMDC were washed and incubated with purified pan-T-cells (Section

2.3.7.1). T-cells were added at a ratio of 1:4 (BMDC:T-cell). All treatments/controls were carried out in triplicate. After 72 the supernatant was removed and the concentrations of cytokines were quantified by ELISA. The additional plate was used to measure T-cell proliferation; after 24 h 50 µl of supernatant was removed and replaced with [^{3}H] thymidine (1 µl/well) diluted in RPMI. After another 48 h the cells were harvested and the incorporation of [H]^3 thymidine was measured (Section 2.3.12.2).

2.3.10.4 Co-culture of LPM with OVA-specific CD4$^+$ T-cells

PEC were isolated from PBS- or TriDAP-treated BALB/c mice as described in Section 2.3.3.1. LPM were purified from the total PEC by FACS as described in Section 2.3.7.3. The LPM were counted and resuspended in RPMI at a concentration of 5x10^5 cells/ml. The LPM were seeded in round-bottom 96-well tissue culture plates (100 µl/well). CD4$^+$ T-cells from DO11 OVA-transgenic mice were purified by negative magnetic selection (Section 2.3.7.1). The purified CD4$^+$ T-cells were labelled with CTV (Section 2.3.12.1) and added to the LPM culture at a ratio of 4:1 (T-cell:LPM). The co-culture was incubated in the presence or absence of OVA protein (50 µg/ml) for 72 h. All treatments/controls were carried out in triplicate. The cells were then surface-stained with a panel of fluor-conjugated antibodies (Table 2.2.9) using the protocols described in Section 2.3.11. The proliferation of CD4$^+$ T-cells was measured by the dilution of CTV labelling.

Table 2.2.9 Panel of fluor-conjugated antibodies used for the co-culture of LPM and OVA-specific CD4$^+$ T-cells

Specificity	Clone	Flurochrome	µL/1x10^6 cells	Supplier
CTV	n/a	V450	n/a	Invitrogen
CD4	GK1.5	APC-Cy7	0.25	eBioscience
CD3	145-2C11	PeCy7	0.25	eBioscience
Live/Dead	n/a	V500	0.05	Life Tech

2.3.11 FACS Analysis

Cells were analysed by multi-colour flow cytometry. Cells were stained in sterile FACS tubes (BD Biosciences) in a volume of 50 µl/1x10^6 cells unless stated otherwise. Fluorescence minus one (FMO) controls were used to define gating boundaries.

2.3.11.1 The discrimination of live and dead cells

Live and dead cells were discriminated using the LIVE/DEAD Aqua Cell Stain Kit (Life technologies). Cells were stained in 50 µl of PBS with LIVE/DEAD reagent (0.05 µl/1x10^6 cells) for 25 min at RT in the dark. The cells were then washed in an excess of FACS buffer and pelleted by centrifugation (242 g, 5 min). The supernatant was removed and the cells were surface-stained, fixed etc. as required. LIVE/DEAD Aqua is detected in the V500/Am-Cyan channel (excitation/emission; 375/512 nm). LIVE/DEAD binds dead cells with a higher affinity than with live cells and therefore can be separated during acquisition. Cells that were killed by incubating them for 10 min in ammonium chloride solution were added to a tube of live cells and stained with LIVE/DEAD as a compensation control.

2.3.11.2 Surface marker staining

Cells were counted and pelleted by centrifugation (242 g, 5 min). The cells were resuspended in FACS buffer and non-specific binding was blocked by incubating cells with FC block (1 µg/ml; BD Pharmingen) for 15 min at RT. Surface staining was carried out at RT for 15 m in the dark using the appropriate concentration of fluor-conjugated antibody (Table 2.1.8). Cells were then washed with FACS buffer and pelleted by centrifugation (242 g, 5 min). The cells were then resuspended in FACS buffer for acquisition or further intra-nuclear/intracellular staining.

2.3.11.3 Intra-nuclear staining

For intra-nuclear staining, cells were fixed and permeabilised using the FoxP3 Fixation/Permeabilisation Kit (eBioscience). Cells were resuspended in 1 ml of fix/perm working buffer and incubated at 4°C for 1 h in the dark. Cells were then washed with 2 ml of permeabilisation buffer and pelleted by centrifugation (242 g, 5 min). The cells were resuspended in 100 µl of permeabilisation buffer and the appropriate concentration of fluor-conjugated antibody was added (Table 2.1.8). The cells were then incubated at 4°C for 1 h in the dark. The cells were washed with 2 ml of permeabilisation buffer, washed

twice with FACS buffer and pelleted by centrifugation (242 g, 5 min). Cells were then resuspended in FACS buffer for acquisition.

2.3.11.4 Stimulation of cells for intracellular cytokine staining

Cells were restimulated prior to staining with fluor-conjugated antibodies if the production of intracellular cytokine was to be investigated. T-cells were restimulated with PMA (10 ng/ml) and ionomycin (1 µg/ml) in RPMI supplemented with β-mercapthoethanol. In addition, cells were incubated in the presence of brefeldin A (5 µg/ml) to inhibit the golgi apparatus. The cells were incubated for 5 h at 37°C and 5% CO_2 before being washed twice with FACS buffer. The cells were then pelleted by centrifugation (242 g, 5 min) and resuspended in FACS buffer for staining.

2.3.11.4.1 Intracellular staining

For intracellular staining, cells were fixed and permeabilised using a Fix & Perm kit (Dako). Cells were resuspended in 50 µl of the fixation buffer for 15 min at RT in the dark. The cells were washed with FACS buffer and pelleted by centrifugation (242 g, 5min). The cells were resuspended in permeabilisation buffer and the appropriate concentration of fluor-conjugated antibody was added (Table 2.1.8). Cells were incubated at RT for 15 min in the dark. The cells were washed in FACS buffer and pelleted by centrifugation (242 g, 5 min). The cells were then resuspended in FACS buffer for acquisition.

2.3.11.4.2 Intracellular staining of YM1

Cells were surface-stained and fixed as described previously (Section 2.3.11). The YM1-specific antibody (R&D) was conjugated with an Alexa-fluor 647 fluorochrome up to 30 mins before staining. The conjugation of the antibody was done according to the manufacturer's instructions using a Zenon Goat IgG labelling Kit (Life Technologies). The cells were resuspended in permeabilisation buffer and the fluor-conjugated anti-YM1 antibody was added (0.5 µl/1x10^6 cells). Cells were then incubated at 4°C for 15 min in the dark. The cells were washed twice with FACS buffer and pelleted by centrifugation (242 g, 5 min). The cells were then resuspended in FACS buffer for acquisition.

2.3.11.4.3 Intracellular staining of relm-α

Cells were surface-stained and fixed as described previously (Section 2.3.11). The cells were resuspended in permeabilisation buffer and the biotin-labelled relm-α-specific antibody (0.5 µl/1x10^6 cells; Peprotech) was added. The cells were then incubated at 4°C for 15 min in the dark. The cells were washed with FACS buffer and resuspended in permeabilisation buffer. A secondary PE-conjugated strepavidin-labelled antibody (0.5 µl/1x10^6 cells; eBioscience) was added. The cells were then incubated at 4°C for 15 min in the dark. The cells were washed twice with FACS buffer and pelleted by centrifugation (242 g, 5 min). The cells were then resuspended in FACS buffer for acquisition.

Table 2.2.10 Panel of fluor-conjugated antibodies used for the staining of YM1 an relm-α in peritoneal macrophages

Specificity	Clone	Flurochrome	µL/1x10^6 cells	Supplier
MHC-II/IA-IE	2G9	FITC	0.25	BDPharmingen
Ly6G	1A8	Pacific Blue	0.25	BDPharmingen
F480	BM8	PeCy7	0.25	eBioscience
CD11b	M1/70	Alexa780	0.25	eBioscience
Ly6C	HK1.4	PerCP-Cy5.5	0.25	eBioscience
YM1	n/a	Alexa-647	0.5	R&D
Relm-α	n/a	2° PE	0.5	Perprotech

2.3.11.4 Acquisition and analysis of FACS data

Flow cytometric acquisition was carried out on a FacsCanto flow cytometer (BD Biosciences) according to the manufacturer's instructions. Compensation was calibrated using individually stained Comp Beads (BD Biosciences) on the FacsDiva Software (BD Biosciences). Results were analysed using FloJo (Stanford University) software. Debris was excluded from analysis by applying a FSc and SSc gate. Dead cells and doublet cells were excluded by their LIVEDEAD staining and pulse width profile, respectively. Percentages and total numbers of cells were calculated on the basis of live single cells. FMO controls

were used as a guide for gating strategies. Analysis included back-gating to ensure cell populations matched with their requisite FSc and SSc profiles.

2.3.12 Measurement of cell proliferation

2.3.12.1 Labelling of cells with CTV

Purified T-cells were labelled with a fluorescent membrane dye called cell trace violet (CTV; Invitrogen) to measure proliferation. As cells proliferate the CTV labelling is split between the newly divided cells, therefore new cells have less CTV on their surface.

Cells were washed twice with PBS to ensure the removal of protein. Cells were resuspended in 5 ml of warm PBS (up to $1x10^8$ cells). A 2X dilution of CTV (2mM) was made in 5 ml warm PBS. The 5 ml CTV solution was added to the cell suspension, cells were incubated for 3 min and the labelling was stopped by adding 3 ml of FCS. The cells were then washed in an excess of RPMI and centrifuged (242 g, 5 min). The cells were then resuspended in RPMI and cultured as required.

2.3.12.2 The measurement of proliferation by the incorporation of [^{3}H] thymidine

Thymidine is used by cells to synthesise DNA during proliferation. Radioactive thymidine can be used to measure how much thymidine has been incorporated by the cell and therefore quantify how much proliferation has taken place. 2.5 μCi/ml of [^{3}H] thymidine (Amersham Pharmacia Biotech) was added to T-cell cultures 48 h after stimulation. At the end of culture, the cells were aspirated onto a glass fibre filter (Wallac) using an automatic cell harvester. The filters were allowed to dry on a heating block at 60°C before being sealed in plastic bags containing non-aqueous BetaScint scintillation fluid (5ml; Wallac). The incorporation of [^{3}H] thymidine was quantified using a Beta-plate scintillation counter (Wallac). Results were expressed as mean counts per min (CPM) of [^{3}H] thymidine incorporation for triplicate T-cell stimulations.

2.3.13 Enzyme linked immunosorbent assay (ELISA)

The concentrations of murine IL-1β, IL-27, IL-23, IL-10, IL-12p40, IL-12p70, IL-17, IFN-γ, TNF-α, IL-6 and GM-CSF were measured using pairs of rat anti-mouse capture and detection antibodies specific for the cytokine in question (Table 2.1.7). High-binding 96-well microtiter plates (Greiner Bio-one) were coated overnight at 4°C with 50 µL of the appropriate capture antibody.

The plates were washed with ELISA wash buffer and blocked with 200 µL of the appropriate blocking reagent (Table 2.1.7) for 2 hours at RT. Plates were washed with ELISA wash buffer and sample supernatants were added (50 µL/well). In some cases supernatants were diluted with sterile PBS before being put onto the coated plates. Cytokine standards were added in triplicate (50 µL/well) at the appropriate top working standard and serially diluted. Supernatants and standards were incubated at 4°C overnight.

After washing with ELISA wash buffer, 50 µL of the appropriate concentration of biotinylated detection antibody was added for 2 hours at RT. After washing with ELISA wash buffer, 50 µL of horse radish peroxidase-conjugated streptavidin was added (1:1000 dilution BD Pharmigen, 1:200 dilution R&D) for 20 min at RT in the dark. The plates were washed with ELISA wash buffer and 50 µL of ELISA developing solution was added. The reaction was stopped at an appropriate time using ELISA stop solution. Absorbance was read at 492 nm on a Versamax Tunable Microplate Reader (Molecular Devices) using SoftMax Pro software. Concentration of the cytokine was determined using the standard curve.

2.3.14 Gene expression assays using real-time PCR

2.3.14.1 RNA isolation

RNA was isolated from cells using the TRIzol/chloroform method. Cells were collected in TRIzol (500 µl/ $1x10^6$ cells; Life Technologies) in sterile RNAse-free tubes. 200 µl of chloroform (Sigma) was added and the tubes were shook vigorously for approximately 15 sec. The tubes were allowed to stand for 5 min before being centrifuged (12000 g, 15 min, 4°C). The top aqueous layer was removed (approximately 250 µl) and added to a fresh RNAse-free tube containing 250 µl of iso-propanol (Sigma). The solution was mixed by inverting and allowed to stand for 10 min. The tubes were then centrifuged (12000 g, 10 min, 4°C). The supernatant was decanted and 500 µl of 75% ethanol was added. The tubes were briefly vortexed before being centrifuged (7500 g, 5 min, 4°C). The supernatant was decanted and the pellets were allowed to dry for approximately 10 min. The pellet was then resuspended in 30 µl of RNAse-free water. The concentration of RNA was determined spectrophotometrically using a Nanodrop (Thermo Scientific) according to the manufacturer's instructions. The purity of the RNA was determined by the 260/280 absorbance ratio.

2.3.14.2 Reverse transcription PCR

Approximately 1 µg of RNA was reverse transcribed into cDNA using the High Capacity cDNA Reverse Transcriptase Kit (Applied Biosystems) according to the manufacturer's instructions. The PCR reaction was carried out in a Peltier I thermal cycler (Dyad). The cDNA was diluted 1:8 with DNAse–free water and stored at -80°C.

2.3.14.3 Real-time PCR

The expression of specific mRNA was quantified by the expansion of specific cDNA transcripts using real-time PCR. Real-time PCR was carried out on a ABI 7500 Fast Real Time PCR System using pre-made Taqman Gene Expression Assays (Table 2.1.3) using the appropriate reagents from Applied Biosystems according to the manufacturer's instructions. Each sample was measured in triplicate. The abundance of mRNA in each sample was normalised by the measurement of an endogenous control (18S rRNA). The relative expression of each gene was then normalised to a control, for example untreated cells.

Chapter 3:

The effect of the NOD1 agonist TriDAP on the clinical symptoms of EAE

CHAPTER 3: The effect of the NOD1 agonist TriDAP on the clinical symptoms of EAE

3.1 Introduction

The NLRs are a unique family of cytosolic PRRs which detect PAMPs and DAMPs. The NOD receptors are a subfamily of the NLRs which contain a conserved NOD domain and include the proteins NOD1 and NOD2 [188, 189]. NOD1 and NOD2 are constitutively expressed across a wide range of cells, however, myeloid and epithelial cells express them in larger amounts. Their specific function is to detect components of bacterial PGN, therefore, they play an essential role in protecting against bacterial pathogens, such as *Helicobacter pylori* and *Listeria monocytogenes* [221, 277]. Ligation of NOD1 and NOD2 with their respective ligands results in the activation of RIP2 and CARD9, which in turn activate the NFkB transcription factor and MAP kinases [190]. This signalling results in the induction of anti-microbial peptides, chemokines and cytokines as well as the synergistic enhancement of TLR-mediated pro-inflammatory cytokine secretion [193, 207, 221]. The activation of NOD1 and NOD2 can also facilitate the induction of adaptive immune responses by enhancing TLR-mediated-cytokine production by DC [211].

Although NOD1 and NOD2 agonists have been shown to activate NFkB and induce the production of inflammatory mediators, they are weak adjuvants in comparison with TLR agonists [206, 211, 278]. Both NOD1 and NOD2 activation, however, have been implicated in the activation of adaptive immune responses. Defining the mechanism behind NOD1 and NOD2 adjuvanticity has proven complex; studies on NOD1 deficient mice have suggested that NOD1 is important for driving Th1, Th17 and Th2 immune responses [279]. Geddes et al showed that Th17 responses elicited by *Citrobacter rodentium* infection were dependent on NOD1 and NOD2 activation [217]. Other studies have shown that administration of a NOD1 agonist alone drives predominantly Th2 responses in vivo. Specifically, Magalhaes et al showed that the induction of Th2 immunity in response to NOD1 activation was mediated by stromal cell derived TSLP [215]. Furthermore, the adjuvant activity of CFA has been shown to be partially dependant on NOD1 and NOD2 activation [212], and more recently, Shaw et al have implicated NOD1 and NOD2 in the induction of EAE. Mice deficient in RIP2, an important kinase in the NOD1 signalling pathway, are highly resistant to EAE [280]. Collectively,

these studies implicate NOD1 activation in modulating adaptive immune responses in a variety of circumstances, including infection and autoimmunity.

The immunostimulatory capacity of NOD1 and NOD2 agonists is well characterised, however, evidence is mounting for an inhibitory or homeostatic role for NOD2. Genetic studies have shown a link between loss of function mutations in CARD15 and a risk of developing Crohn's disease [225, 226]. CARD15 encodes the ligand binding domain of NOD2 and the mutation prevents proper binding of MDP, therefore preventing the proper activation of the receptor. Pellino3, a protein essential for NOD2 signalling, was also decreased in Crohn's patients but not patients with ulcerative colitis, suggesting that NOD2 is linked specifically to Crohn's disease pathogenesis [202]. Furthermore, it has been shown that a knock-in of the CARD15 mutation can lead to exacerbated NFkB activation and increased IL-1β production in mice [233]. Moreover, administration of a NOD2 ligand can negatively regulate TLR2-mediated IL-12 production, while mice with the CARD15 mutation have enhanced IL-12 production and Th1 responses. Wanatabe et al also demonstrated that administration of a NOD2 agonist can attenuate murine experimental colitis by downregulating TLR2, TLR4, TLR9 and TLR5-mediated cytokine production [281]. These studies suggest that NOD2 signalling has a protective effect during Crohn's disease, possibly by modulating the production of pro-inflammatory cytokines, IL-12 and IL-1β. However, this hypothesis is controversial as numerous studies show NOD2 ligands can enhance the TLR-mediated production of pro-inflammatory cytokines, including IL-12 and IL-1β [282]. Recent work by Brain et al suggests that NOD2 activation can induce the expression of microRNA-29 which protects against Crohn's pathogenesis by inhibiting IL-23 production. Furthermore, Crohn's patients with the CARD15 mutation fail to express microRNA-29 and produce enhanced levels of IL-12p40. Loss of function mutations have also been found in the genes encoding NOD1. These mutations have been associated with asthma and atopic eczema, but it is unclear how they are implicated in disease [237]. As NOD1 and NOD2 share many downstream signalling pathways it is possible that they play similar roles in modulating the immune response. However, a regulatory role for NOD1 has yet to be investigated. In this study EAE was used as a model of inflammatory autoimmune disease to investigate the effect of NOD1 activation during chronic inflammation.

EAE is a demyelinating disease which is used as a mouse model for MS. The disease is induced by a s.c. injection of CFA emulsified with the auto-antigen MOG [265]. The resulting inflammatory response generates myelin-reactive T-cells in the periphery of the mouse, which then traffic to the brain and mediate pathogenesis. IL-17 and IFN-γ are produced by these infiltrating effector T-cells during EAE [36]. The activation of the IL-17 and IFN-γ producing effector T-cells is dependent on the secretion of cytokines from innate immune cells during the initial inflammatory response. IL-12 is essential for Th1 differentiation and therefore IFN-γ production, [270] while IL-1β, IL-6 and IL-23 are important for the development of Th17 cells during EAE [41]. IL-17, an important mediator of pathology during EAE, is now a drug target for MS. The role of IFN-γ is more complex, with studies showing that it can have a pathogenic and protective effect in the EAE model [272, 283, 284]. In addition, the symptoms of EAE can be ameliorated by the production of innate anti-inflammatory cytokines such as IL-10 or IL-27 [273, 275].This study investigated the effect of the NOD1 agonist TriDAP on EAE and the associated adaptive immune responses.

3.2 Results

3.2.1 The effect of the NOD1 agonist TriDAP on antigen-specific immune responses in vivo and the clinical course of EAE.

NOD1 has been implicated in promoting the adaptive immune response, however, the exact mechanism by which this receptor modulates adaptive immunity is still controversial. There is growing evidence that the absence of NOD1 has an important effect on Th1, Th17 and Th2 immunity. NOD1 is important for the generation of Th17 cells in response to *C. rodentium* infection [217] and NOD1 agonists have been shown to drive the generation of Th2 cells in vivo [215] and Th1 cells in vitro [279]. This study was designed to investigate the effects the NOD1 agonist TriDAP on the adaptive immune responses that mediate EAE. C57BL/6 mice were injected s.c. on d 0 with MOG emulsified in CFA. TriDAP was administered within the MOG emulsion on d 0 and mice were given further s.c. injections of TriDAP on d 1, 2 and every second day thereafter. A second group of mice were treated with PBS on the same days as a control. The clinical scores and weights were recorded daily to measure disease severity.

In vivo mouse models are inherently variable and to combat this clinical scores and weights from four separate experiments were combined (n=20). TriDAP-treated mice had a significantly decreased clinical score at the peak of disease on d 12 in comparison to PBS-treated mice (Fig 3.1; $P < 0.001$). Similarly, TriDAP-treated mice had significantly decreased weight loss from d 9 onwards (Fig 3.1; $P < 0.01$).

The severity of EAE is associated with infiltration of pathogenic Th17 and Th1 cells into the brains of mice. The results shown in Fig 3.2 and Fig 3.3 are representative of two independent experiments that were used to investigate cytokine production in the brain and MOG-specific responses in the periphery of mice with EAE. All mice injected with PBS became ill, peaking on d 12 with an average clinical score of 3.8. Mice had an average clinical score of 3 when sacrificed on d 13 (Fig 3.2). Mice that were treated with TriDAP had a significantly decreased clinical score in comparison with mice treated with PBS, achieving statistical significance on d 5 and continuing until sacrifice on d 13 (Fig 3.2; $P < 0.001$). Mice injected with TriDAP had a peak average clinical score of 1, significantly decreased in comparison with PBS-treated controls (Fig 3.2; $P < 0.001$). There was also a

significant reduction in weight loss in mice treated with TriDAP in comparison with mice treated with PBS (Fig 3.2; $P < 0.001$).

The mice were sacrificed on d 13 and perfused intra-cardially with ice-cold PBS to clear the blood vessels surrounding brain. Mononuclear cells from the brain tissue were purified using a percoll gradient and then pooled. Cells were stimulated with PMA and ionomycin in the presence of brefaldin A for 5 h before being surface-stained with antibodies specific for CD3 and CD4. Cells were then stained intracellularly with antibodies specific for IL-17 and IFN-γ and analysed by flow cytometry. Results show that there was a decrease in the frequency of IL-17$^+$, IFN-γ$^+$ and IL-17$^+$IFN-γ$^+$ cells in the brains of mice treated with TriDAP in comparison with PBS-treated mice (Fig 3.3A).

To investigate MOG-specific responses in the periphery, cells from the inguinal lymph nodes of mice were processed and co-cultured in the presence of increasing concentrations of the antigen MOG. After 72 h the concentrations of IL-17, IFN-γ and TNF-α were quantified by ELISA. There was a significant decrease in the concentration of MOG-specific IL-17, IFN-γ and TNF-α produced by lymph node cells from TriDAP-treated mice (Fig 3.3B; $P < 0.001$). In summary, TriDAP administration significantly reduced the severity of disease, decreased autoantigen-specific IL-17 and IFN-γ production in the inguinal lymph nodes and reduced the percentage of IL-17- and IFN-γ-producing T-cells infiltrating the brains of mice with EAE.

3.2.2 The effect of TriDAP on cytokine production by T-cells from MOG-immunized mice

In order to examine the possible mechanism behind TriDAP-mediated inhibition of Th1 and Th17 cells during EAE, an in vitro study was designed to investigate whether TriDAP could affect the production of IL-17 and IFN-γ by activated CD4$^+$ T-cells. T-cells were obtained from mice d 7 post immunisation with MOG and CFA. CD4$^+$ T-cells were purified from the inguinal lymph nodes by MACS separation. The T-cells were incubated with or without TriDAP for 1 h before the addition of either medium or αCD3 and αCD28. The supernatants were harvested after 72 h and the concentrations of IL-17 and IFN-γ were quantified by ELISA.

As expected, $CD4^+$ T-cells from mice immunized with MOG and CFA produced substantial concentrations of IL-17 and IFN-γ in response to stimulation with αCD3 and αCD28 (Fig 3.4). TriDAP alone did not induce the production of IL-17 or IFN-γ by CD4+ T-cells. TriDAP had no effect on the production of IL-17 by $CD4^+$ T-cells in response to αCD3 and αCD28. However, TriDAP significantly enhanced the production of IFN-γ by $CD4^+$ T-cells in response to αCD3 and αCD28 (Fig 3.4; $P < 0.01$ versus medium).

3.2.3 The effect of TriDAP on the ability of DC to present antigen to antigen-specific T-cells.

As established in section 3.2.1, TriDAP administration attenuated the symptoms of EAE. Importantly, TriDAP-induced attenuation was associated with a decrease in IL-17 and IFN-γ producing T-cells in the brain of experimental mice. Peripheral antigen-specific IL-17, TNF-α and IFN-γ production was also reduced in response to TriDAP treatment. This data indicates that TriDAP may modulate the induction of adaptive immunity during the development of EAE. Myeloid cells express large amounts of NOD1, therefore, it is possible that TriDAP may manipulate adaptive immune responses via the modulation of innate immune myeloid cells. DC are well characterised as one of the primary myeloid cells of the innate immune system, capable of driving the proliferation of T-cells by presenting antigen and polarising T-cell responses by producing cytokines [123]. BMDC can present MOG to T-cells harvested from a mouse immunized with MOG and CFA [285-287]. The presentation of MOG by BMDC drives the proliferation and activation of the MOG-specific cells. Furthermore, BMDC pulsed with the auto-antigen MOG are capable of inducing EAE. These observations suggest a major role for DC during the induction of EAE, thus, a study was designed to investigate the effect of TriDAP on the ability of a DC to present MOG to a MOG-specific T-cell.

BMDC were cultured for 24 h with or without MOG in the presence or absence of TriDAP. The BMDC were washed and co-cultured with purified $CD4^+$ T-cells from mice immunized with MOG and CFA. Supernatants were harvested after 72 h and cytokine production was quantified by ELISA. The proliferation of T-cells was measured by the incorporation of $[^3H]$ thymidine. BMDC pulsed with MOG alone increased the incorporation of thymidine by MOG-specific T-cells, indicating an increase in the proliferation of these cells (Fig 3.5).

BMDC pulsed with MOG also induced the production of IL-17, IFN-γ and IL-2 by MOG-specific T-cells. TriDAP-treated BMDC pulsed with MOG induced the production of similar concentrations of IL-17, IFN-γ and IL-2 from T-cells when compared with untreated-BMDC. Similarly, there was no difference in the proliferation of T-cells that were co-cultured with TriDAP-treated BMDC in comparison with T-cells cultured with untreated-BMDC (Fig 3.5). In summary, NOD1 activation did not affect the ability of BMDC to induce antigen-specific T-cells to proliferate or produce IL-17, IFN-γ or IL-2.

3.2.4 The effect of TriDAP on the ability of DC to respond to *M. tuberculosis*

Certain bacteria can subvert immune responses to allow chronic infection. The mechanisms of subversion vary from active suppression of immune responses, to inducing tolerance to bacterial components. LPS, for example, has been shown to negatively regulate the innate immune system when administered chronically; a phenomenon known as endotoxin tolerance [288]. Endotoxin tolerance is also thought to be a fail-safe mechanism to restrain excess inflammation in parts of the host colonised by commensal bacteria, such as the gut.

EAE is typically induced by immunising mice with the auto-antigen MOG using CFA as an adjuvant. CFA contains heat-killed *M. tuberculosis* (Mtb), a powerful stimulator of the innate immune system. Both NOD1 and NOD2 have been implicated in the immunostimulatory capability of CFA [279]. In the present study, it was hypothesised that administration of a NOD1 agonist during the induction of EAE may be causing immune cells to become tolerant to further stimulation by NOD1 agonists, therefore reducing the effect of CFA during MOG immunisation. Hence, this study investigated the effect of NOD1 activation on Mtb-induced cytokine production by BMDC.

Mtb can induce the production of IL-1β and IL-23 by BMDC and both cytokines have been shown to be essential in driving an IL-17 response during EAE [39, 41]. Mtb also induces the production of IL-10 by BMDC. IL-10 suppresses inflammation and has been shown to attenuate EAE [274]. BMDC were cultured in the presence or absence of TriDAP for 16 h before the cells were washed and recultured with or without Mtb. Supernatants were removed after 24 h and the concentrations of IL-1β, IL-23 and IL-10 were quantified by ELISA.

BMDC cultured in the presence of Mtb produced significant amounts of IL-1β, IL-23 and IL-10 (Fig 3.6). BMDC stimulated with TriDAP only did not produce detectable concentrations of IL-1β, IL-23 or IL-10. Pre-treatment with TriDAP decreased the concentration of IL-23 produced by BMDC in response to Mtb, however, the difference was not significant in comparison with BMDC treated with Mtb alone (Fig 3.6). Interestingly, BMDC which were pre-treated with TriDAP produced significantly more IL-1β in response to Mtb than BMDC cultured with Mtb alone (Fig 3.6; $P < 0.001$). BMDC pre-treated with TriDAP produced the same concentration of IL-10 in response to Mtb as BMDC treated with Mtb alone (Fig 3.6).

TriDAP pre-treatment does not significantly reduce the production of Mtb-mediated IL-17 polarising cytokines by BMDC, suggesting that TriDAP cannot induce tolerance to further NOD1 stimulation. These results suggest that, rather than reducing the ability of BMDC to activate T-cells in response to Mtb, TriDAP can enhance the development of Th17 cells by increasing Mtb-mediated IL-1β production. To test this hypothesis, BMDC were cultured in the presence or absence of TriDAP for 16 h before the addition of either medium or Mtb. After 6 h the BMDC were washed and cultured with purified $CD3^+$ T-cells from naive C57BL/6 mice. Supernatants were harvested after 72 h and the production of IFN-γ, IL-17 and IL-10 was quantified by ELISA. The proliferation of T-cells was measured by the incorporation of $[^3H]$ thymidine. As expected, BMDC cultured with Mtb alone induced the production of IL-17 and IFN-γ by $CD3^+$ T-cells (Fig 3.7). When BMDC were incubated with TriDAP prior to stimulation with Mtb, the concentrations of IL-17 and IFN-γ produced by $CD3^+$ T-cells were reduced, but were not significantly different than the concentrations produced in response to Mtb alone (Fig 3.7). There was no significant difference in the concentration of IL-10 detected in response to BMDC stimulated with Mtb or a combination of TriDAP and Mtb. Similarly, there was no significant difference in the proliferation of $CD3^+$ T-cells cultured with BMDC stimulated with Mtb alone in comparison with $CD3^+$ T-cells cultured with BMDC incubated with both TriDAP and Mtb (Fig 3.7).

TriDAP enhanced the Mtb-mediated production of IL-1β by BMDC. Although IL-1β is a Th17 polarising cytokine, TriDAP did not enhance the ability of Mtb-stimulated BMDC to induce the production of IL-17 or IFN-γ by T-cells. In addition, Mtb-stimulated BMDC still induced the proliferation of T-cells after incubation with TriDAP. In summary, TriDAP did not significantly affect the ability of Mtb-stimulated BMDC to activate T-cells.

3.2.5 The effect of TriDAP on IL-1β and IL-23-mediated IL-17 production in vivo.

IL-1β and IL-23 have been shown to be important for the generation of Th17 responses during EAE. Mice deficient in IL-23p19, a subunit of mature IL-23, are resistant to EAE [39]. Furthermore, T-cells cultured with IL-23 become highly encephalogenic IL-17-producing T-cells when transferred into naive mice [36, 39]. Similarly, IL-1RI-deficient mice have lower incidence of EAE and fail to generate a robust Th17 population in response to EAE induction [41]. This in part reflects the role of IL-1β working with IL-23 to induce the production of innate IL-17 by γδ T-cells [287]. γδ T-cells are a subset of T-cells characterised by the unique expression of the γδ-TCR. They play an important role during the pathogenesis of EAE by promoting the activation of pathogenic Th17 cells by secreting innate IL-17 [55]. As shown in Fig 3.2, TriDAP can attenuate the production of IL-17 during EAE. Therefore, this study investigated the effect of TriDAP on IL-17 production by γδ T-cells in vivo.

C57BL/6 mice were injected in the footpad with IL-1β and IL-23 or a combination of IL-1β, IL-23 and TriDAP. Control mice were injected with PBS alone to measure background cytokine production. After 4 h mice were sacrificed and the draining popliteal lymph nodes were taken and processed. Cells were incubated with brefaldin A for 5 h before being stained with antibodies specific for CD3 and γδ-TCR. Cells were also stained intracellularly with antibodies specific for IL-17 and IFN-γ. Increased percentages of IL-17$^+$ γδ T-cells were observed in mice injected with IL-1β and IL-23 in comparison with mice injected with PBS alone (Fig 3.8). The addition of TriDAP had no effect on the percentage of IL-17$^+$ γδ T-cells observed in response to IL-1β and IL-23 injection (Fig 3.8). In summary, activation of NOD1 had no effect on the cytokine-mediated activation of γδ T-cells in vivo.

3.3 Discussion

Pattern recognition receptors have evolved to detect the invasion of host tissue by foreign microbes. In theory, detection of microbes leads to an inflammatory response specific to the microbe encountered. Furthermore, the specificity of this interaction leads to the discrimination of PAMPs and non-pathogenic foreign bodies such as allergens. However, in reality the interaction between the mammalian immune system and the microbial world is much more complex. Genetic studies have provided useful information on the factors that may play a role in immunological tolerance and regulation. For example, it has been shown that loss of function mutations in the NOD2 gene leads to an increased risk of developing Crohn's disease [226]. NOD2 is a PRR responsible for detecting MDP, a component of bacterial cell wall [227], and while the conventional role for a PRR may be pro-inflammatory these studies imply a regulatory role for NOD2. Mouse studies have shown that NOD2 mutations increase inflammatory mediators in the gut [233] and that administration of a NOD2 agonist can ameliorate experimental colitis [281]. These discoveries open up the possibilities of exploiting PRR agonists as therapies against inflammatory disorders such as Crohn's disease. NOD1 is strongly associated with another inflammatory disorder, asthma. However, the exact role of NOD1 during disease has yet to be elucidated. As NOD1 and NOD2 share signalling pathways it is possible that NOD1 also has a role in immune regulation.

This study has shown that administration of the NOD1 agonist TriDAP can ameliorate the clinical symptoms of EAE. EAE is a well characterised autoimmune model which is used as a mouse model of multiple sclerosis. These results suggest that NOD1 may have a hitherto undocumented effect on experimental autoimmune disease.

Pathogenesis of EAE involves an initial innate immune response to CFA, which generates pathogenic MOG-specific Th1 and Th17 cells. This study demonstrated that administration of TriDAP to mice with EAE inhibits IL-17 and IFN-γ production by MOG-specific $CD4^+$ T-cells. The mechanism by which NOD1 mediates this effect has not yet been elucidated. NOD1 is expressed in a variety of cells including lymphocytes, however, TriDAP did not suppress the production of IL-17 and IFN-γ when incubated with $CD4^+$ T-cells in vitro. In fact, this study showed that TriDAP enhanced the production of IFN-γ by $CD4^+$ T-cells from a mouse immunized with MOG. This finding conflicts with data showing

a reduction in IFN-γ in TriDAP-treated mice with EAE. As the T-cells that were treated in vitro were harvested from a MOG-immunized mouse, this result suggests that TriDAP does not reduce the production of pathogenic cytokines by memory T-cells which have already been polarised and activated. Therefore, it can be concluded that TriDAP does not mediate an attenuating effect on EAE by directly suppressing encephalogenic T-cells.

DC are professional APC and play a central role in the activation of T-cells. MOG-specific T-cell activation is dependent on the presentation of MOG by APCs. Furthermore, the transfer of activated BMDC pulsed with MOG has been shown to induce EAE [286, 289]. NOD2 ligands have been shown to modulate BMDC activation and reduce their ability to activate OVA specific T-cells [125]. Therefore it was hypothesised that NOD1 may mediate a similar effect on DC during EAE and thereby reduce MOG-specific T-cell responses. However, this study demonstrated that culture of BMDC with TriDAP did not affect their ability to induce IL-17 and IFN-γ production by MOG-specific T-cells from mice immunized with MOG and CFA. This indicates that TriDAP has no effect on the capability of BMDC to present antigen, and suggests that TriDAP is not mediating the suppression of EAE by modulating the ability of DC to present antigen.

RIP2 is a kinase activated in response to NOD1 ligation and is essential for NOD1-mediated NFkB activation. Shaw et al recently suggested that NOD1 activation is involved in the induction of EAE by showing that RIP2-deficient mice are highly resistant to EAE [280]. As the present study shows that the administration of TriDAP during the induction and course of EAE can ameliorate disease, it is possible that pre-treatment with a NOD1 agonist may suppress CFA-mediated innate immune responses during EAE. Endotoxin tolerance is a well-known phenomenon, where repeated activation of innate immune cells with LPS can lead to the resistance of cells to further activation. Heat-killed Mtb is the primary immunostimulatory component of CFA and has been shown to activate NOD1. It is possible that repeated activation of NOD1 may compromise the capability of CFA to drive EAE induction via endotoxin tolerance.

The polarisation of the pathogenic Th17 cells during EAE is promoted by IL-1β and IL-23. The production of these cytokines by DC can be induced by heat-killed Mtb, the primary immunostimulatory component of CFA [41, 287]. The present study demonstrated that initial stimulation of BMDC with TriDAP does not compromise the stimulatory capability

of heat-killed Mtb. In fact, TriDAP enhanced the production of Mtb-mediated IL-1β. This data indicates that, in contrast to the TriDAP-mediated reduction of IL-17 production observed during EAE, TriDAP should have the potential to exacerbate rather than reduce Mtb-mediated Th17 polarisation. However, the results of the present study indicate that TriDAP may be reducing Mtb-mediated IFN-γ and IL-17 production by T-cells, although any changes observed were not significant.

The immunosuppressive cytokine IL-10 can be produced in response to innate cell activation and is primarily involved in suppressing excess inflammation [81, 82, 290]. IL-10 has been shown to ameliorate the course of EAE [274] and therefore the production of this cytokine was investigated as a potential mechanism for the TriDAP-mediated amelioration of EAE. TriDAP alone did not induce production of IL-10 by BMDC. Furthermore, TriDAP could not modulate Mtb-mediated production of IL-10 by BMDC, nor modulate the production of IL-10 by T-cells in response to Mtb-stimulated BMDC. In conclusion, the results of this study indicate that TriDAP-treated BMDC cannot modulate the production of IL-17, IFN-γ or IL-10. Although NOD1 activation is having a significant effect on EAE, it is possible that the effect is not mediated via DC.

This study has revealed a dichotomy between the effects of TriDAP in vitro and the amelioration of EAE in vivo. The in vitro evidence presented thus far has shown an enhancement of IFN-γ production by T-cells and an enhancement of Mtb-mediated IL-1β in response to TriDAP. The effect of TriDAP on cytokine production in vivo was investigated by co-administering TriDAP with IL-1β and IL-23. IL-1β and L-23 drive IL-17 production by γδ T-cells in vivo, however, TriDAP had no effect on this response.

This study showed that NOD1 activation can significantly attenuate EAE. This result is worthy of further investigation as several novel therapeutics for MS, such as fingolimod, have been developed using EAE as a disease model [257, 291]. PAMPs have already been exploited as immunotherapeutics; CpG is currently undergoing clinical trials for the treatment of asthma [292]. However, the mechanism by which TriDAP attenuates EAE is still unclear. Although in vitro experimentation suggested that TriDAP had an effect on T-cells directly, the data showed that TriDAP enhanced the production of cytokines rather than reducing them. It has been previously reported that NOD receptor agonists have the potential to attenuate BMDC responses [281], but this study demonstrated that NOD1 did

not significantly modulate the ability of BMDC to produce pro-inflammatory cytokines or drive IL-17 or IFN-γ production by T-cells. This suggests that NOD1 activation may mediate its effect via a cell type other than DC. Although DC have been used extensively to characterise the function of NOD1, recent studies have shown that it has a role in activating macrophages, eosinophils and epithelial cells [125, 205, 214, 215, 239, 281]. BMDC culture limits the variety of cells upon which TriDAP can act, therefore, further studies have focused on the effect of NOD1 activation on a more heterogeneous population of cells.

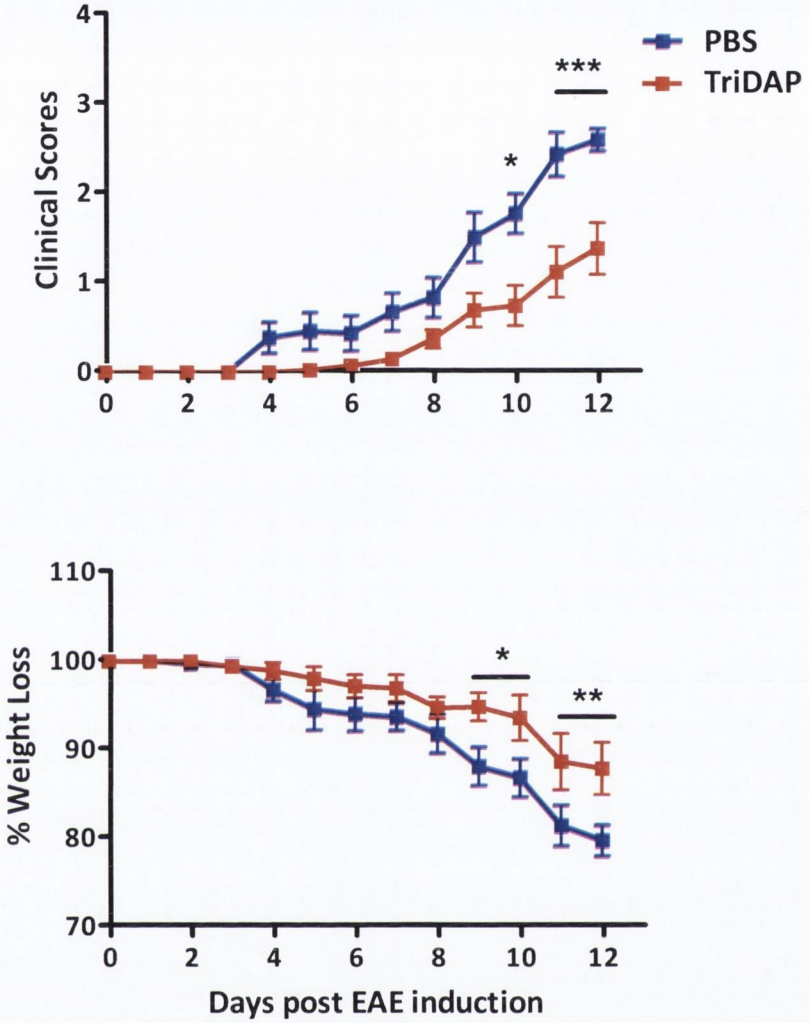

Fig 3.1 Admistration of TriDAP attenuates the symptoms of EAE. EAE was induced in C57BL/6 mice by s.c. injection of MOG (100 µg) emulsified in CFA, followed by an i.p. injection of PT (500 ng) on d 0 and 2. One group of mice was treated with TriDAP (100 µg), which was administered with the MOG emulsion on d 0 and injected s.c. on d 1, 2 and every second day thereafter. A second group was treated with PBS in a similar fashion. Clinical scores and weights were checked daily. Statistical significance was calculated using 2 way ANOVA with repeated measures and Bonferroni post-test. *=P < 0.05, *=P < 0.01***=P < 0.001 versus PBS. Results shown are the mean values from 4 independent experiments (n=20).

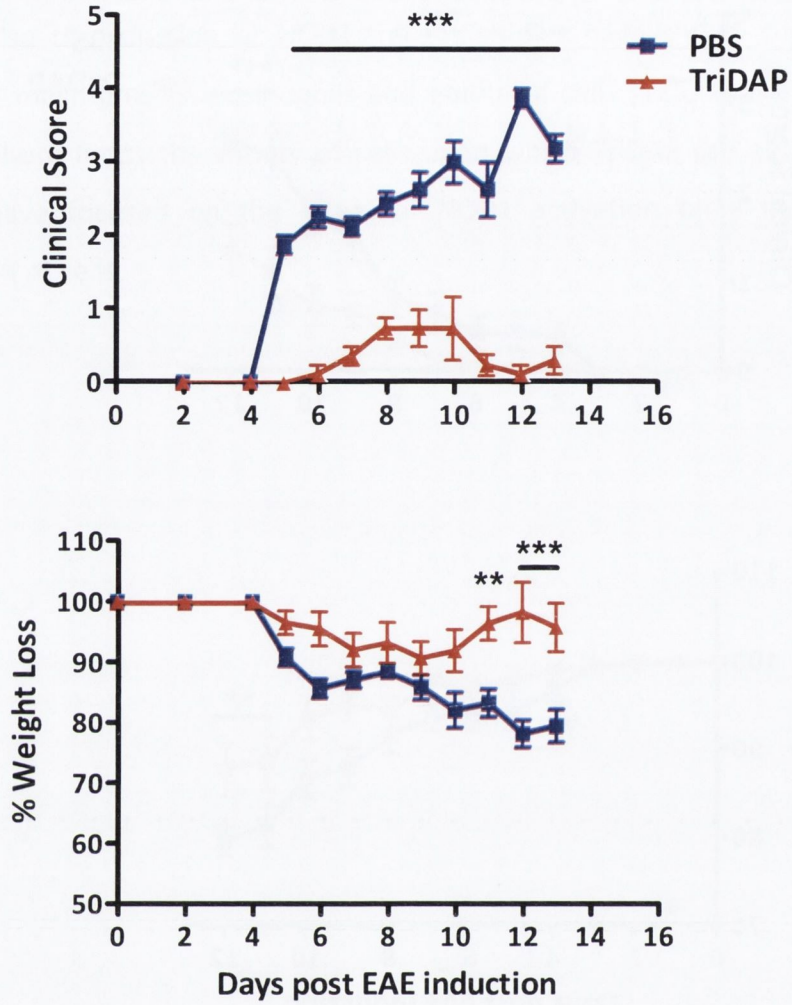

Fig 3.2 Admistration of TriDAP attenuates the symptoms of EAE. EAE was induced in C57BL/6 mice by s.c. injection of MOG (100 µg) emulsified in CFA, followed by an i.p. injection of PT (500 ng) on d 0 and 2. One group of mice were treated with TriDAP (100 µg), which was administered with the MOG emulsion on d 0 and injected s.c. on d 1, 2 and every second day thereafter. A second group was treated with PBS in a similar fashion. Clinical scores and weights were checked daily. Statistical significance was calculated using a repeated measures two-way ANOVA with a Bonferroni post test. **=$P < 0.01$, ***= $P < 0.001$ versus PBS. This figure is representative of 2 independent experiments, each one with n=5.

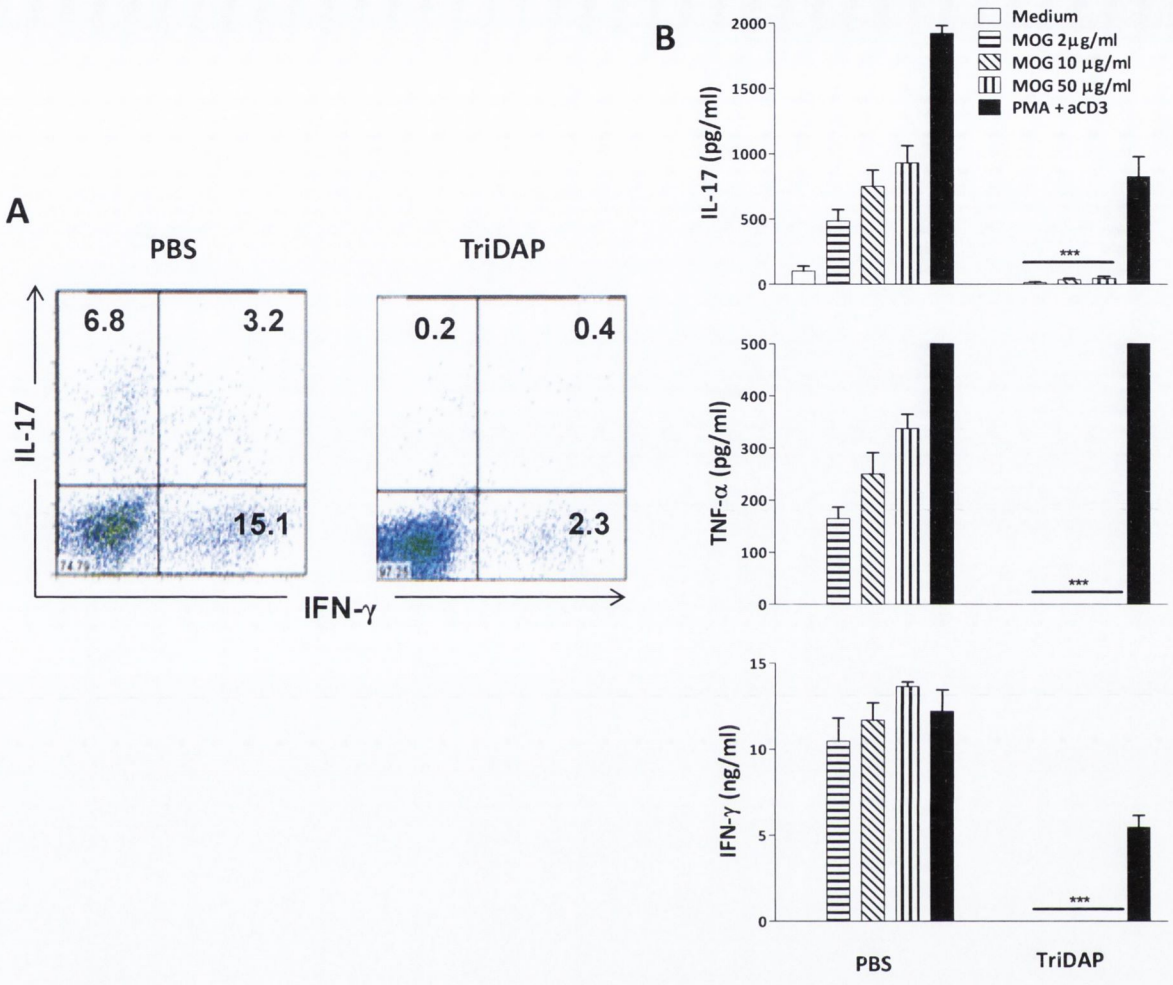

Fig 3.3 Administration of TriDAP supresses IL-17 and IFN-γ production by T-cells in the brains and lymph nodes of mice with EAE. EAE was induced and mice treated as described in Fig 3.2. Mice were sacrificed and perfused with PBS on d 13. A) Mononuclear cells were prepared from the brains of mice and pooled together into their respective groups. Cells were stimulated with PMA and ionomycin in the presence of brefeldin A for 5 h. Cells were surface stained with antibodies specific for CD3 and CD4 and stained intracellularly with IFN-γ- and IL-17-specific antibodies. Plots shown were gated on $CD3^+CD4^+$ cells. B) Lymph node cells were stimulated with increasing concentrations of MOG (2, 10 and 50 µg/ml) or PMA (10 ng/ml) and αCD3 (1 µg/ml). Supernatants were removed after 72 h and the concentrations of cytokines were quantified by ELISA (n=5). Statistical significance was calculated using a two-way ANOVA with Bonferroni post test. *** = $P < 0.001$ vs PBS injected mice. This figure is representative of 2 independent experiments.

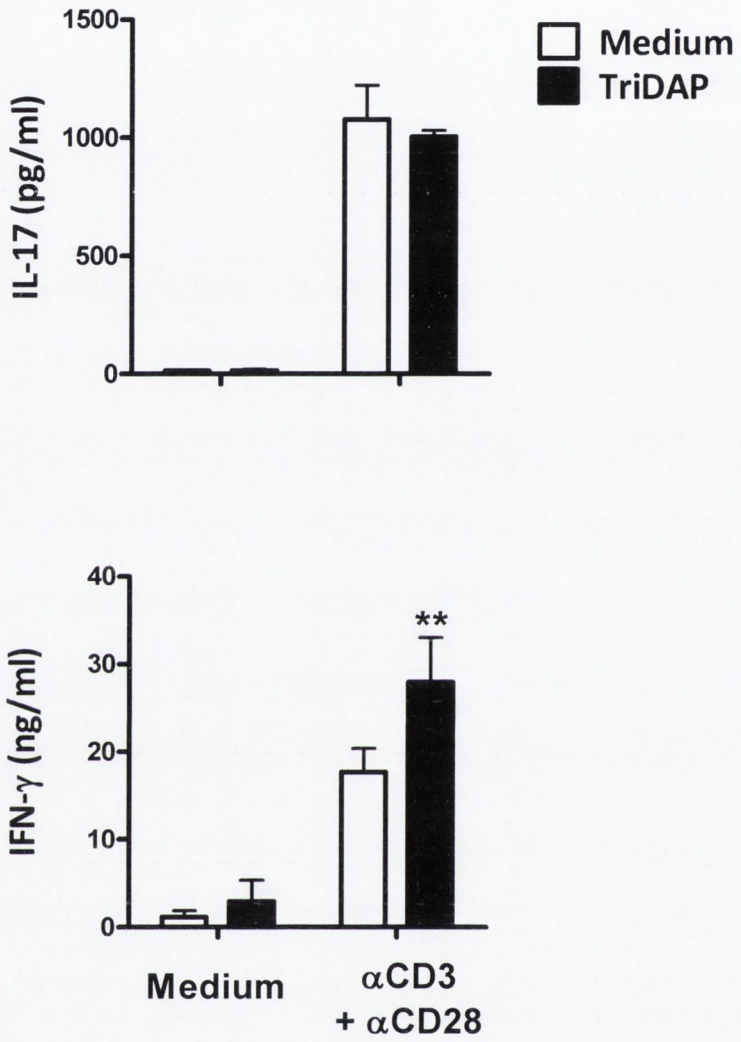

Fig 3.4 TriDAP enhances the production of IFN-γ but not IL-17 by CD4⁺ T-cells from MOG-immunised mice. C57BL/6 mice were immunised by s.c. injection of MOG (100 μg) emulsified in CFA. The mice were sacrificed on d 7 and CD4 T-cells were purified from their inguinal lymph nodes. The purified CD4 T-cells were incubated with or without TriDAP (100 μg/ml) for 1 h before the addition of either medium or αCD3 (1 μg/ml) and αCD28 (1 μg/ml). The supernatants were removed after 72 h and the concentrations of cytokines were quantified by ELISA. Each combination was examined in triplicate. Statistical significance was calculated using 2 way ANOVA and Bonferroni post-test. **=$P < 0.01$ versus medium and αCD3/CD28. This figure is representative of 2 independent experiments.

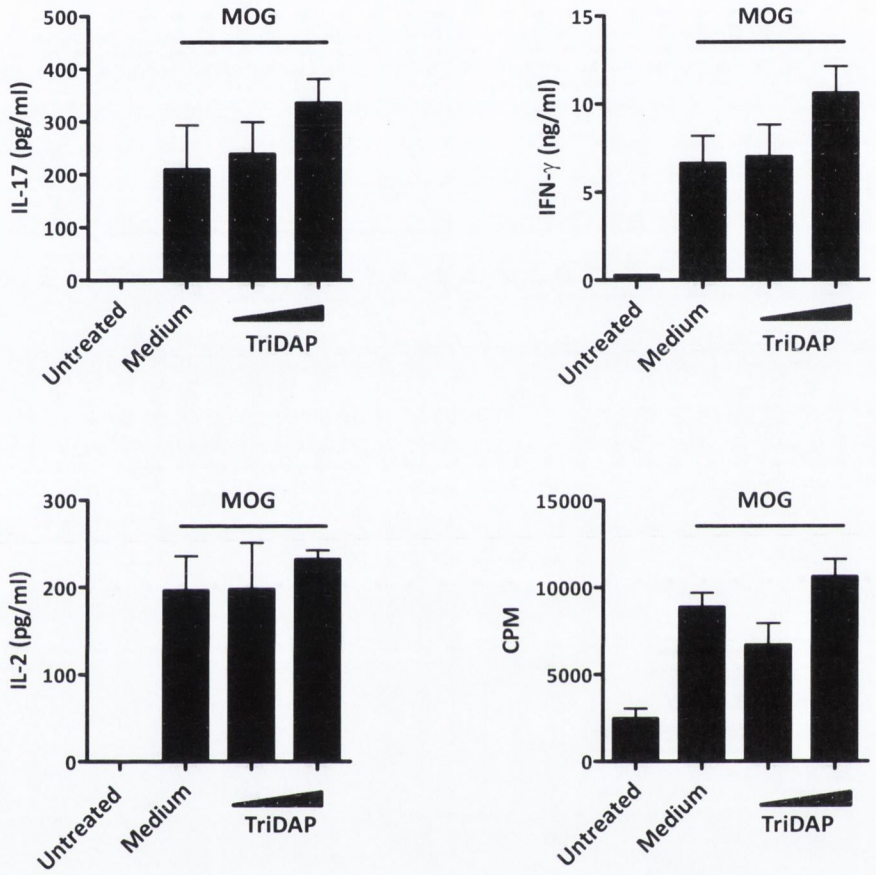

Fig 3.5 The treatment of BMDC with TriDAP does not modulate their ability to induce antigen-specific T-cell responses. BMDC generated from C57BL/6 mice were cultured with or without TriDAP (10 μg/ml, 100 μg/ml) in the presence of MOG (25 μg/ml) for 16 h. In addition cells were left completely untreated as a negative control. The BMDC were washed and incubated with $CD4^+$ T-cells from MOG-immunised mice at a ratio of 1:10 (BMDC:$CD4^+$). After 72 h the supernatants were removed and cytokine concentrations were quantified by ELISA. Each combination was examined in triplicate. The incorporation of [^{3}H] thymidine was used to measure proliferation. This figure is representative of 3 independent experiments.

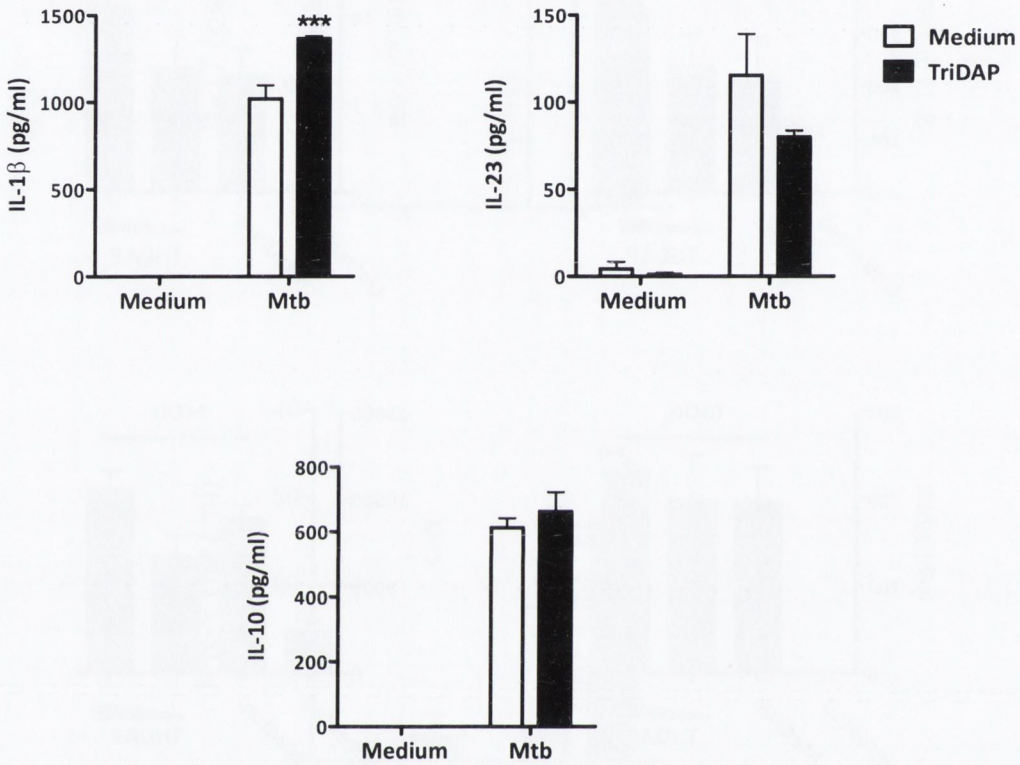

Fig 3.6 TriDAP enhances Mtb-induced production of IL-1β by BMDC. BMDC generated from C57BL/6 were cultured in the absence or presence of TriDAP (100 μg/ml) for 16 h before the addition of either medium or Mtb (25 μg/ml). Supernatants were removed at 24 h after stimulation with Mtb and the concentrations of cytokines were quantified by ELISA. Each combination was examined in triplicate. Statistical significance was calculated using two-way ANOVA with Bonferroni post-test. ***=$P < 0.001$ versus medium treated cells. This figure is representative of 3 independent experiments.

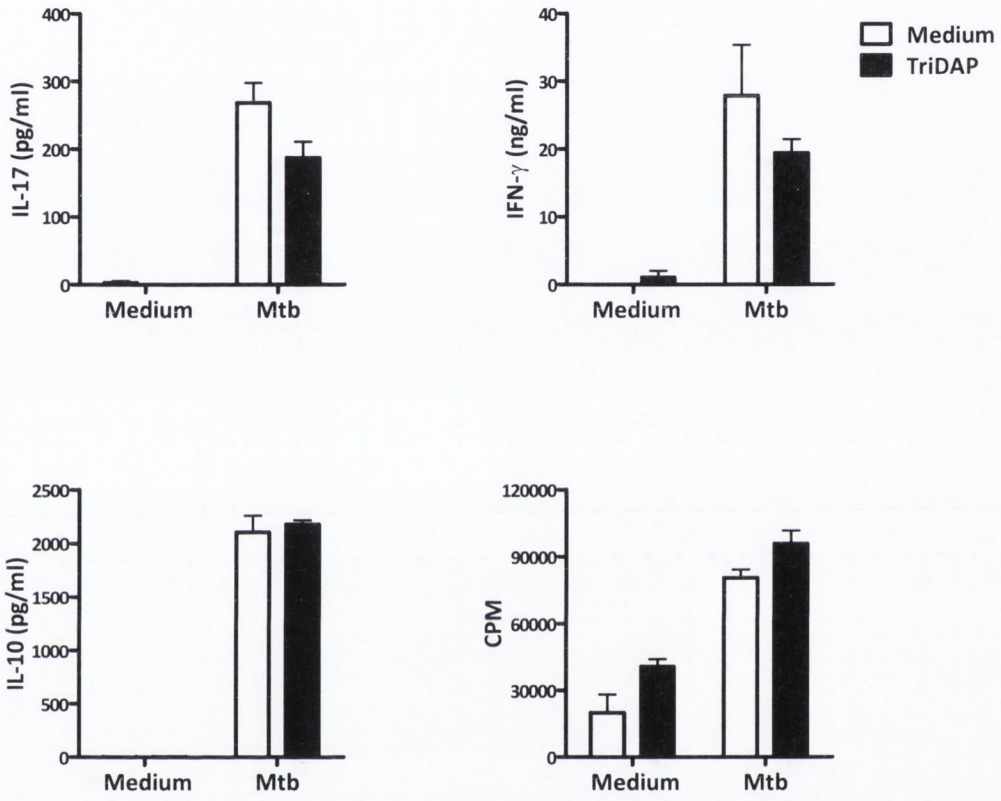

Fig 3.7 TriDAP does not significantly modulate the ability of BMDC stimulated with Mtb to induce the production of IL-17, IL-10 and IFN-γ from CD3$^+$ T-cells. BMDC generated from C57BL/6 mice were incubated for 16 h in the presence or absence of TriDAP (100 μg/ml). The cells were then incubated with or without Mtb (25 μg/ml) for 6 h. The BMDC were washed and incubated with purified CD3$^+$ cells from C57BL/6 mice at a ratio of 1:4 (BMDC:CD3$^+$). Each combination was examined in triplicate. After 72 h the supernatant was removed and cytokine concentrations were quantified by ELISA. The incorporation of [^{3}H] thymidine was used to measure proliferation. Statistical significance was calculated using a two-way ANOVA with a Bonferroni post test. This figure is representative of 3 independent experiments.

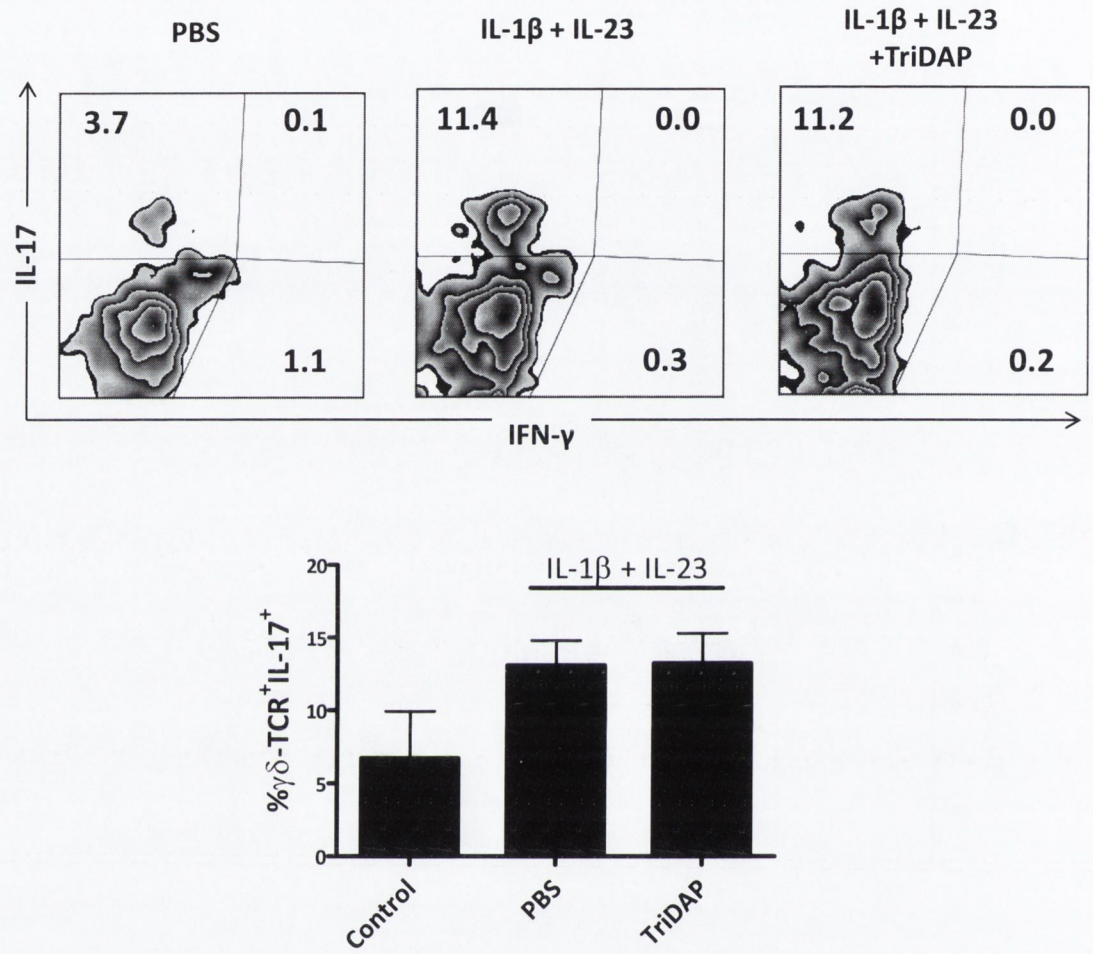

Fig 3.8 Administration of TriDAP has no effect on the ability of IL-1β and IL-23 to drive IL-17 production from γδ T-cells in vivo. C57BL/6 mice were injected in the footpad with IL-1β (100 ng) and IL-23 (100 ng), in combination with either PBS or TriDAP (100μg). Control mice were injected with PBS alone. After 4 h the mice were sacrificed and the popliteal lymph nodes were processed. The single cell suspension was stimulated with PMA, ionomycin in the presence of brefeldin A for 5 h. Cells were surface-stained with antibodies specific for CD3 and γδ-TCR and were stained intracellularly with antibodies specific for IL-17 and IFN-γ. The cells were then analysed using flow cytometry. FACS plots shown are gated on $CD3^+$ γδ-TCR^+ cells and representative of n=3. Statistical significance was calculated using one-way ANOVA and Tukey post test. This figure is representative of 2 independent experiments.

Chapter 4

The effect of the NOD1 agonist TriDAP on the production of cytokines by innate immune cells

CHAPTER 4: The effect of the NOD1 agonist TriDAP on the production of cytokines by innate immune cells

4.1 Introduction

NOD1 is a cytosolic receptor and part of the NLR family. It has been shown to recognise components of peptidoglycan; the main component of bacterial cell wall. The specific ligand for NOD1 is d-glutamyl-meso-diaminopimelic acid (DAP) [188, 207]. The NOD1 receptor contains a conserved caspase-recruitment domain (CARD) and binds its ligand via leucine-rich repeats. Upon binding of the ligand, the receptor oligomerises and interacts with other CARD-containing proteins in the cell. One of these proteins is the kinase RIP2 [293, 294]. NOD1 activation induces the ubiquitination of RIP2 via the adaptor protein TRAF6. Upon ubiquitination RIP2 activates a signalling cascade which results in the translocation of the transcription factor NFkB to the nucleus [200]. NOD1 can also activate the mitogen activated protein kinases (MAPK) p38, ERK and JNK, in a CARD9 dependent or RIP2 dependent manner [190, 201, 294-296].

Activation of either the MAPK or NFkB is known to activate innate immune cells and induce the production of immunostimulatory mediators, therefore the consensus view is that activation of NOD1 results in an inflammatory response similar to that elicited by the activation of other PRR. Agonists for NOD1, however, are weakly immunostimulatory in comparison with TLR agonists. Activation of NOD1 in BMDC and BMM results in the production of low concentrations of cytokines and chemokines [125, 211]. However, NOD1-deficient mice are more prone to certain bacterial infections which suggests that NOD1 signalling plays a significant role during bacterial infection [205, 219, 297]. In addition, NOD1 has been implicated in the production of anti-microbial peptides, nitric oxide and pro-inflammatory cytokines such as IL-1β, IL-8 and IL-6 [193, 217, 297, 298].

The current thinking is that NOD1 mediates protection against bacterial infection by modulating the response of cells to TLR agonists. A number of studies have shown that TLR-stimulated IL-12 and IL-1β production can be synergistically enhanced by the co-administration of NOD1 agonists [206, 211, 278]. While administration of NOD1 agonists alone does not induce significant production of cytokines or chemokines in vitro, in vivo administration of NOD1 agonists results in a substantial immune response. NOD1 activation in vivo results in recruitment of neutrophils, the activation of macrophages and

the polarisation of Th2 cells [203, 208, 214, 215]. The discrepancy between in vitro and in vivo NOD1 activation may be explained by the absence of many NOD1 expressing cells during in vitro cell culture. In fact, NOD1 dependent responses to *L. monocytogenes* are found to be mediated by endothelial cells and not by primary innate immune cells such as DC [299]. Furthermore, Magalhaes et al showed that NOD1 agonists fail to induce Th2 immunity when NOD1 is absent from the stromal compartment of mice [215]. NOD1 agonists have also been shown to activate eosinophils directly but only when cultured in the presence of epithelial cells[239]. These studies suggest that NOD1-mediated immune responses are dependent on the interaction of a variety of cell types.

The results presented in chapter 3 of this study demonstrated that administration of a NOD1 agonist could attenuate the production of IL-17 and IFN-γ in vivo, however, attempts to replicate this using in vitro assays was unsuccessful. This illustrates the complexity of NOD1-mediated immune responses and suggests that a variety of cell types may be involved in NOD1-mediated responses in vivo. Therefore this study investigated the possibility that the NOD1 agonist TriDAP could activate a variety of different immune cells, and whether the perception of NOD1 as a weak immunostimulator reflects the limitations of using in vitro assays with a single cell type.

This study investigated the effect of the NOD1 agonist TriDAP on cytokine production by BMDC and BMM. In addition, the peritoneal cavity was used as a source of primary murine cells to investigate the NOD1-mediated responses of a heterogeneous cell population. Cells obtained by a peritoneal lavage contain a mixture of immune cells including B-cells, T-cells, DCs, macrophages, NK cells, eosinophils, neutrophils and mast cells.

4.2 Results

4.2.1 The effect of TriDAP on TLR-stimulated cytokine production by BMDC

A number of studies have demonstrated that NOD1 agonists alone have little or no effect on the production of cytokines by BMDC [125, 278]. However, NOD1 activation is thought to modulate the immune response by synergistically enhancing TLR-mediated cytokine production. Watanabe et al also showed that NOD2 activation could inhibit the production of TLR-stimulated cytokines [125]. Fig 3.6 of the previous chapter showed that TriDAP only has a significant effect on Mtb-mediated IL-1β production by BMDC, therefore this study was designed to investigate if the NOD1 agonist TriDAP can modulate the production of IL-12, IL-23 and IL-1β in response to a variety of TLR. The production of anti-inflammatory mediators IL-10 and IL-27 was also measured to assess whether NOD1 activation could also modulate anti-inflammatory cytokine production. Murine BMDC were incubated in the absence or presence of TriDAP for 1 h prior to incubation with a range of TLR ligands. After 24 h the supernatants were removed and the concentrations of IL-1β, IL-23, IL-12p40, IL-12p70, IL-10 and IL-27 were quantified by ELISA.

Consistent with published reports [278], TriDAP alone failed to induce a quantifiable concentration of any cytokine examined. TLR agonists LPS, CpG, and Zymosan induced the production of IL-12p40, IL-12p70, IL-23 and IL-1β by BMDC (Fig 4.1 and 4.2). The TLR2 agonist Pam3CSK, however, only induced the production of IL-1β. TriDAP significantly enhanced the production of LPS-mediated IL-12p40, IL-12p70, IL-1β and IL-23 (Fig 4.1 and 4.2; all $P < 0.001$). In addition, TriDAP also enhanced the production of LPS-mediated IL-10 and IL-27 (Fig 4.3; n.s. and $P < 0.001$, respectively). Similarly, the CpG-mediated production of IL-12p40, IL-12p70, IL-1β, IL-23, IL-10 (n.s.) and IL-27 was significantly enhanced in the presence of TriDAP (Fig 4.1-4.3; all $P < 0.001$). These results confirm that TriDAP alone does not induce cytokine production by BMDC in vitro, but enhances TLR4 and TLR9-induced cytokine production. Interestingly, TriDAP only significantly enhanced zymosan-mediated production of IL-23 ($P < 0.001$) IL-10 ($P < 0.001$) and IL-12p70 ($P < 0.01$) (Fig 4.1-4.3), suggesting that different TLR are modulated to different degrees by NOD1 activation. Watanabe et al described that NOD2 activation could decrease the production of Pam3CSK-mediated cytokine production [125], however, we observed that NOD1 activation induced the production of IL-23 ($P < 0.05$) and IL-12p40 (n.s.) in

combination with Pam3CSK, and Pam3CSK mediated IL-1β production was enhanced in the presence of TriDAP (Fig 4.1-4.3; $P < 0.001$).

These results suggest that NOD1 activation alone is insufficient for the production of cytokines by BMDC. The data establishes that NOD1 activation can synergise with certain TLR agonists including LPS and CpG to enhance cytokine production. However, NOD1 modulated the production of different cytokines depending on the TLR agonist used. Interestingly, the effect of NOD1 was not limited to pro-inflammatory mediators; IL-10 and IL-27 production was enhanced in the presence of TriDAP. This study also showed that NOD1 cannot reduce Pam3CSK-mediated cytokine production.

4.2.2 The effect of TriDAP on cytokine production by BMM

Although NOD1 agonists have been shown to weakly activate innate immune cells in vitro, studies using *C. pneumonia* and *M. tuberculosis* infection have shown that NOD1 can activate macrophages in vivo [203, 299]. The present study investigated the effect of NOD1 activation on cytokine production by BMM in vitro. LPS was used as a positive control for cytokine production by BMM. BMM were cultured in the presence or absence of either TriDAP or LPS. After 24 h the supernatants were removed and the concentrations of IL-10, IL-12p40, IL-23, IL-1β, IL-6, TGF-β and IL-27 were quantified by ELISA.

IL-23 and TGF-β were produced by BMM in response to TriDAP but the concentrations were not statistically significant (Fig 4.4). IL-1β, IL-23, IL-6, IL10 and IL-12p40 were not detected in response to TriDAP. IL-27 was the only cytokine produced consistently by BMM in response to TriDAP (Fig 4.4; $P < 0.05$ versus untreated BMM). In contrast, BMM incubated with LPS produced significant concentrations of IL-10, IL-12p40, IL-6, IL-1β ($P < 0.05$) and IL-27 in comparison with untreated BMM (Fig 4.4, all $P < 0.001$ unless stated). TGF-β was not detected in response to LPS. In summary, this study establishes that IL-27 is produced by BMM in response to TriDAP. In contrast, BMM produced a range of pro- and anti-inflammatory cytokines in response to LPS.

4.2.3 The effect of TriDAP on cytokine production by peritoneal exudate cells.

NOD1 agonists alone are weakly immunostimulatory in vitro, failing to induce the production of cytokines by BMDC (Fig 4.1-4.3), however, NOD1 activation resulted in the production of IL-27 from BMM (Fig 4.4), suggesting that NOD1 agonists have the potential to activate certain immune cells in vitro. NOD1 agonists can modulate immune responses effectively when administered in vivo [214], therefore, it is possible that NOD1-mediated immune responses may depend on complex interplay between a variety of cell types or perhaps previous in vitro studies have not included NOD1-responsive cells. Thus, this study investigated the effect of the NOD1 agonist TriDAP on a heterogeneous cell population derived from the peritoneal cavity. The peritoneal cavities of C57BL/6 mice were lavaged to retrieve a population of cells that included macrophages, neutrophils, eosinophils, DC, NK cells, B-cells and T-cells. The peritoneal exudate cells (PEC) were incubated in the presence or absence of TriDAP or, as a positive contol for cytokine production, LPS. The supernatants were harvested after 1, 3, 5, and 24 h and the concentrations of IL-6, IL-10, IL-23, IL-12p70, IL-4, IL-13, TGF-β, TNF-α, IL-33, TSLP and IL-27 were quantified by ELISA.

Incubation of PEC with LPS for as little as 1 h resulted in significant production of IL-6, IL-10 ($P < 0.05$), TNF-α and IL-27 ($P < 0.05$) (Fig 4.5; $P < 0.001$ unless stated). In contrast to BMDC and BMM, TriDAP induced the production of significant concentrations of IL-6, TNF-α and IL-10 by PEC (Fig 4.5; all $P < 0.001$ versus untreated PEC). The production of IL-6 in response to TriDAP was measurable after 1 h and reached concentrations comparable with those produced by LPS after 5 h (~12 ng/ml). TriDAP-treated PEC produced significant concentrations of IL-10 after 5 h (~400 pg/ml) but did not produce concentrations of this cytokine that were comparable with those produced by LPS-treated PEC. The concentrations of TNF-α produced in response to TriDAP peaked after 1 h (~250 pg/ml) and were significantly less than those produced in response to LPS (Fig 4.5; $P < 0.001$). After 24 h TNF-α was no longer detected (Fig 4.5). Neither LPS nor TriDAP induced the production of TGF-β, IL-23 or IL-4 by PEC (Fig 4.5). Similarly, the Th2 polarising cytokines IL-13, TSLP and IL-33 were not detected in response to either TriDAP or LPS stimulation. The production of IL-12p70 in response to LPS was observed at the 5 h timepoint only, while TriDAP could not induce any detectable IL-12p70. These results suggest that the NOD1 agonist TriDAP alone can induce the production of significant

concentrations of IL-10, IL-6 and TNF-α by PEC in vitro. Although the concentrations of IL-10 and TNF-α are not comparable with the concentrations produced in response to LPS, the data suggests that a NOD1 agonist has the potential to induce the production of significant concentrations of these cytokines.

GM-CSF and IFN-γ play an important role in the classical or M1 activation of macrophages [137, 149]. The M1 activation of macrophages promotes phagocytosis and production of pro-inflammatory cytokines [149]. To examine the effect NOD1 activation has on the production of GM-CSF and IFN-γ, PEC were incubated with or without TriDAP. PEC were also incubated in the presence of LPS as a positive control for cytokine production. After 24 h the supernatants were removed and the concentrations of GM-CSF and IFN-γ were measured by ELISA.

TriDAP and LPS had no effect on the production of IFN-γ by PEC (Fig 4.6). Similarly, TriDAP had no effect on the production of GM-CSF by PEC (Fig 4.6). In contrast, LPS induced significant concentrations of GM-CSF in comparison with untreated PEC (Fig 4.6; $P < 0.01$).

4.2.4 The effect of p38 MAPK and phosphoinositide-3 kinase inhibitors on TriDAP-mediated cytokine production by PEC.

This study has shown that TriDAP induced the production of IL-10 and IL-6 by PEC (Fig 4.5). NOD1 activation has been shown to result in the activation of the MAPK p38 [190, 296, 297]. In addition, the activation of p38 has been implicated in the regulation of IL-10 and IL-6 production [300, 301]. Similarly, phosphoinositide-3 kinase (pi3K) has been implicated in the production of IL-10 [12]. Therefore, specific inhibitors of the signalling proteins p38 and pi3K were used to investigate their role in NOD1-mediated cytokine production. LPS was used as a positive control for IL-10 and IL-6 production. PEC harvested from C57BL/6 mice were incubated with or without TriDAP or LPS, in the presence or absence of the p38 inhibitor SB203580, the pi3K inhibitor ZSTK-474 or the vehicle control, DMSO.

Consistent with the data shown in Fig 4.5, TriDAP and LPS induced the production of IL-6 and IL-10 by PEC (Fig 4.7). TriDAP-mediated IL-6 production was completely dependent on p38 activation; incubation of cells with the p38 inhibitor significantly reduced the concentration of IL-6 produced in response to TriDAP to background concentrations (Fig 4.7; $P < 0.001$). The addition of the pi3K inhibitor had no effect on the production of IL-6

in response to TriDAP (Fig 4.7). Similarly, the production of IL-10 in response to TriDAP was completely dependent on p38 activation (Fig 4.7; $P < 0.001$ versus DMSO). The addition of the pi3K inhibitor significantly reduced the production IL-10 in response to TriDAP (Fig 4.7; $P < 0.001$ versus DMSO), however, it was significantly less than the reduction elicited by the p38 inhibitor (Fig 4.7; $P < 0.01$ versus p38 inh). Although the addition of either the p38 inhibitor or pi3K inhibitor reduced the production of TNF-α in response to TriDAP, neither were statistically significant in comparison with DMSO controls. Inhibition of either pi3K or p38 reduced the production of IL-10 in response to LPS (Fig 4.7; both $P < 0.001$ versus DMSO).These results indicate that the induction of cytokine production in response to TriDAP is dependent on p38 signalling. A number of papers have reported that SB203508 can inhibit RIP2 in addition to p38 [293, 302]. This suggests that RIP2 may be involved in the TriDAP-mediated production of IL-6 and IL-10. Therefore further study with other more specific inhibitors may be required to ensure that p38 is essential for TriDAP–mediated IL-6 and IL-10 production and that the change observed in this study is not due to inhibition of RIP2 alone. In addition, pi3K seems to have a partial role in TriDAP-mediated IL-10 production.

4.2.5 The role of different innate cells in TriDAP-mediated IL-10 and IL-6 production

The results shown in Fig 4.5 and Fig 4.7 demonstrated that TriDAP can induce the production of IL-10 and IL-6 from PEC. However, it is unclear which cell is producing the cytokines in response to TriDAP. As NOD1 is expressed highly in myeloid cells, different myeloid cells were systematically depleted from total PEC before stimulating with TriDAP. PEC from C57BL/6 mice were stained with antibodies specific for CD11b, SiglecF, F480, Ly6G, and CD11c. The total PEC were then depleted of either neutrophils ($CD11b^{+}Ly6G^{hi}$), DC ($CD11b^{+}CD11c^{hi}$), macrophages ($CD11b^{+}F480^{+}Ly6G^{-}$) or eosinophils ($CD11b^{+}SiglecF^{+}$). The depleted cell preparations were then cultured separately in the presence or absence of either TriDAP or LPS. The depleted PEC were then compared with total PEC cultured under the same conditions. After 24 h the supernatants were harvested and the concentrations of IL-10 and IL-6 were quantified by ELISA.

Consistent with the results of Fig 4.5, TriDAP and LPS induced the production of IL-10 and IL-6 by total PEC (Fig 4.8). IL-6 was not detected in response to LPS or TriDAP after the PEC was depleted of macrophages (Fig 4.8). Furthermore, PEC depleted of either eosinophils,

neutrophils or DC retained the ability to produce IL-6 in response to either LPS or TriDAP (Fig 4.8), suggesting that macrophages are the primary producers of IL-6. LPS-induced IL-6 production was increased in the absence of eosinophils, neutrophils or DC (Fig 4.8; $P < 0.001$ versus total PEC). Similarly, TriDAP-induced IL-6 production was significantly increased in the absence of eosinophils (Fig 4.8; $P < 0.001$ versus total PEC). IL-10 was not detected in response to TriDAP after the PEC was depleted of macrophages (Fig 4.8). Although IL-10 was detected in response to LPS in the absence of macrophages, the concentrations of IL-10 were reduced by 84% (Fig 4.8; $P < 0.001$). Depletion of eosinophils, neutrophils or DC increased the concentration of IL-10 produced in response to either LPS or TriDAP (Fig 4.8; all $P < 0.001$ versus total PEC). These results strongly suggest that macrophages are responsible for the production of IL-6 and IL-10 by PEC in response to TriDAP.

4.2.6 The effect of TriDAP on cytokine production by peritoneal macrophages.

The results from Fig 4.8 indicate that macrophages are required for the TriDAP-mediated IL-10 and IL-6 production by PEC. However, it is possible that the production of cytokines in response to TriDAP was mediated by macrophages but produced by another cell type. The results from Fig 4.4 show that BMM cannot produce IL-6 or IL-10 in response to TriDAP, suggesting that macrophages are not the primary producers of these cytokines in the PEC. However, BMM are phenotypically different from primary macrophages, due to the addition of M-CSF during their differentiation from bone marrow cells. Therefore, this study investigated the effect of TriDAP on a purified population of primary peritoneal macrophages. PEC from C57BL/6 mice were stained with antibodies specific to F480, CD11b and GR1. Macrophages ($CD11b^{+}F480^{+}Gr1^{-}$) were purified by FACS and incubated in the absence or presence of either TriDAP or LPS. Total PEC was also incubated separately in the presence or absence of either TriDAP or LPS as a positive control for the production of IL-10 and IL-6.

Consistent with the results shown in Fig 4.5, LPS and TriDAP induced the production of IL-10 and IL-6 by total PEC (Fig 4.9). Purified peritoneal macrophages produced significant concentrations of IL-10 in response to TriDAP and LPS (Fig 4.9; both $P < 0.001$ versus untreated macrophages). Although TriDAP and LPS also induced the production of IL-6 by purified peritoneal macrophages, the concentration was not significantly higher than

background concentrations (Fig 4.9). As shown in Fig 4.4, incubation of BMM with TriDAP failed to induce the production of any cytokines measured, nonetheless these results demonstrate that NOD1 activation can directly induce primary peritoneal macrophages to produce IL-10.

4.2.7 The effect of TriDAP on peritoneal neutrophils

A recent study has shown that neutrophils are an important source of NOD2-dependent IL-10 during polymicrobial sepsis [303]. NOD1 and NOD2 share the same signalling pathways, therefore, it is possible that a NOD1 agonist could induce IL-10 production by neutrophils. In order to investigate whether NOD1 agonists could induce the production of IL-10 or IL-6 from neutrophils, C57BL/6 mice were injected i.p. with 9% casein. After 15 h a second i.p. injection of 9% casein was administered, and 3 h after the second injection the peritoneal cavity was lavaged with ice-cold PBS. Granulocytes were purified using a percoll gradient. The purity of $Gr1^{hi}$ neutrophils was routinely > 90% (Fig 2.2.3). The cells were then cultured in the absence or presence of TriDAP or LPS. Supernatants were harvested after 24 h and the concentrations of IL-10 and IL-6 were quantified by ELISA. In contrast to purified peritoneal macrophages, neutrophils failed to produce IL-10 or IL-6 in response to TriDAP (Fig 4.10). Neutrophils produced IL-6 in response to LPS (Fig 4.10; $P < 0.001$ versus untreated neutrophils). LPS did not induce IL-10 production by neutrophils (Fig 4.10). This result suggests that NOD1 does not directly activate neutrophils to produce IL-10 or IL-6.

4.2.8 The effect of supernatant from TriDAP treated PEC on the polarisation of $CD4^+$ T-cells

Having successfully established that TriDAP can modulate the production of cytokines by PEC (Fig 4.5), the effect of TriDAP-activated PEC on modulating adaptive immune responses was investigated. The peritoneal cavities of C57BL/6 mice were lavaged with ice-cold PBS, and the PEC were incubated in the absence or presence of, TriDAP or LPS. The supernatants were harvested after 24 h. Spleens, inguinal and brachial lymph nodes were processed from a naive C57BL/6 mouse. The single cell culture was stained with antibodies specific for CD4, CD25 and CD45RB. $CD4^+CD25^-CD45RB^{int}$ cells were sorted by FACS. The naive T-cells were cultured with supernatants (1 in 2 dilution) from either TriDAP-treated, LPS-treated or untreated PEC. T-cells incubated without any supernatant

served as a control. In addition, T-cells were cultured in the presence of IL-2, IL-2 and αCD3 or IL-2, αCD3 and αCD28. The supernatants were harvested after 72 h, and the concentrations of IL-17, IFN-γ, IL-10 and IL-4 were quantified by ELISA.

When supernatant (s/n) from untreated PEC was added to the culture, T-cells produced significantly less IFN-γ in response to either IL-2 and αCD3, or IL-2, αCD3 and αCD28 (Fig 4.11; $P < 0.05$ and $P < 0.01$, respectively). In addition, s/n from untreated PEC induced IL-10 and IL-4 production by T-cells stimulated with the combination of IL-2, αCD3 and αCD28 (Fig 4.11; both $P < 0.001$). S/n from TriDAP-treated PEC had a similar effect; in the presence of IL-2, αCD3 and αCD28, T-cells produced significantly more IL-10 and IL-4 and reduced the production of IFN-γ in comparison with T-cells stimulated in the absence of s/n (Fig 4.11; $P < 0.001$, $P < 0.001$, $P < 0.01$, respectively). When compared with s/n from untreated PEC, s/n from TriDAP-treated PEC induced significantly greater concentrations of IL-10 by T-cells stimulated with either IL-2 and αCD3 or IL-2, αCD3 and αCD28 (Fig 4.11; $P < 0.001$ and $P < 0.01$, respectively). In addition, s/n from TriDAP-treated PEC induced the production of IL-17 by T-cells stimulated with either IL-2 and αCD3 or IL-2, αCD3 and αCD28 (Fig 4.10; $P < 0.05$ and $P < 0.001$, respectively).

In contrast, s/n from LPS-treated PEC did not suppress but enhanced IFN-γ production by T-cells stimulated with IL-2 and αCD3 (Fig 4.11; $P< 0.01$). In addition, s/n from LPS-treated PEC induced the production of IL-17 from T-cells, even in the absence of αCD3 ($P< 0.01$). In comparison with s/n from TriDAP-treated PEC, s/n from LPS-treated PEC induced significantly more IL-17 production by T-cells stimulated with either IL-2 and αCD3 or IL-2 αCD3 and αCD28 (Fig 4.11; both $P < 0.001$). S/n from LPS-treated PEC did not induce the production of IL-4 in the absence of αCD28, however, s/n from LPS-treated PEC induced the production of IL-4 by T-cells stimulated with IL-2, αCD3 and αCD28, but the production of IL-4 was significantly less than that produced in response to s/n from untreated or TriDAP-treated PEC (Fig 4.11; both $P < 0.001$). While large concentrations of IL-10 were detected in cultures with s/n from LPS-treated PEC, the concentrations did not change significantly with the addition of αCD3 or αCD28.

T-cells alone produced only IFN-γ in response to the combination of αCD3 and IL-2, and significantly higher concentrations of IFN-γ in response to the combination of IL-2, αCD3

and αCD28. IL-10, IL-4 and IL-17 were not produced by T-cells stimulated with any combination of IL-2, αCD3 or αCD28, in the absence of supernatants (Fig 4.11).

The production of IL-10 and IL-4 by $CD4^+$ T-cells was also confirmed by flow cytometry. Purified $CD4^+CD25^-CD45RB^{int}$ cells were labelled with cell trace violet (CTV) before being incubated in the presence of s/n from either TriDAP-treated, LPS-treated or untreated PEC and stimulated with IL-2, IL-2 and αCD3 or IL-2 αCD3 and αCD28. After 72 h the cells were stimulated with PMA and ionomycin for 5 h in the presence of brefaldin A. The cells were than stained intracellularly with antibodies specific for IL-4 and IL-10. CTV^+CD4^+ cells were then analysed by flow cytometry.

The addition of s/n from untreated PEC to T-cells stimulated with IL-2, αCD3 and αCD28 increased the frequency of IL-4+, IL-10+ and IL-10+IL-4+ CD4+ T-cells in comparison with T-cells stimulated in the absence of s/n (Fig 4.12). When compared with s/n from untreated PEC, s/n from TriDAP-treated PEC, in combination with either IL-2 and αCD3 or IL-2, αCD3 and αCD28, increased the frequency of $IL\text{-}4^+$, $IL\text{-}10^+$ and $IL\text{-}10^+IL\text{-}4^+$ $CD4^+$T-cells (Fig 4.12), confirming the results shown in Fig 4.11. In addition, s/n from LPS-treated PEC did not increase the frequency of $IL\text{-}10^+$ $CD4^+$ T-cells (Fig 4.12), confirming that the IL-10 detected by ELISA in Fig 4.11 was contained in the s/n from PEC and not produced by the $CD4^+$ T-cells. In summary, this data suggests that untreated PEC secrete factors that inhibit IFN-γ producing Th1-like responses and drive IL-4 and IL-10 producing Th2-like responses. Stimulation of PEC with TriDAP enhances their ability to drive the IL-4 and IL-10 producing Th2-like response, but in addition, TriDAP-treated PEC can induce the production of IL-17 by activated CD4+ T-cells. In contrast, LPS enhances the ability of PEC to drive the production of IFN-γ and IL-17, while reducing the production of IL-4.

4.3 Discussion

NOD1 is a cytosolic PRR important for the detection of bacterial cell wall. NOD1 deficient mice have increased susceptibility to a variety of bacterial infections such as *H.pylori* and *L. monocytogenes*, indicating that NOD1 is important for the recognition and clearance of bacteria. NOD1 agonists have been shown to be weak inducers of pro-inflammatory cytokines, therefore, it is unclear how important cytokine production is during NOD1 mediated response to infection. The results shown in chapter 3 demonstrated that the NOD1 agonist TriDAP significantly attenuated the symptoms of EAE and inhibited the generation of IL-17 and IFN-γ producing T-cells, indicating that NOD1 activation has a suppressive effect on Th1 and Th17 cells. However, experiments investigating the effect of TriDAP on CFA-mediated BMDC responses were inconclusive. The present study investigated cytokine production in response to TriDAP by a variety of innate immune cell types and revealed that a NOD1 agonist cannot induce cytokine production by BMDC but can induce cytokine production by BMM and peritoneal macrophages.

DC are important regulators of adaptive immunity. They drive T-cell activation by presenting antigen and provide the third signal for T-cell polarisation. For example, IL-12 production by DC induces the polarisation of Th1 cells. These cytokines are produced in response to PRR activation, such as the activation of TLR4 by LPS. This study confirmed the effectiveness of TLR agonists as potent inducers of innate cytokine production but demonstrated that the NOD1 agonist TriDAP was a poor inducer of cytokine production by BMDC. It has been proposed that NOD1 contributes to the immune response by modulating the production of TLR-mediated pro-inflammatory cytokines rather than directly inducing cytokine production [206, 211, 278, 299]. The present study found that TriDAP alone did not induce the production of pro-inflammatory cytokines but enhanced TLR4 and TLR9-mediated IL-1β, IL-12 and IL-23 production by BMDC. These cytokines are involved in polarising the adaptive immune response; IL-12 can induce Th1 type immunity, while IL-1β and IL-23 are involved in generating Th17 cells.

Interestingly, TLR-mediated IL-10 and IL-27 production by BMDC were also enhanced in response to TriDAP. IL-10 is a potent suppressor of innate immune cell activation, while IL-27 can induce IL-10 production by CD4+ T-cells and suppress Th17 responses[81, 124, 275, 304]. These results suggest that NOD1 enhances not only TLR-mediated pro-inflammatory responses but also enhances TLR-mediated anti-inflammatory responses.

Wantanabe et al described a role for NOD receptors in attenuating TLR-mediated cytokine production by BMDC [125], however, the present study suggests that NOD1 agonists can only enhance the response of DC to TLR-stimulation rather than attenuating it. Importantly, these findings indicate that DC cannot respond to NOD1 agonists alone, therefore, any effect elicited by TriDAP via DC must be made in the presence of a second signal from TLR stimulation.

Like DC, macrophages are innate immune cells that modulate adaptive immunity by secreting cytokines in response to PAMPs. The present study confirmed that BMM can produce cytokines associated with T-cell polarisation; LPS induced the production of IL-10, IL-12p40 and IL-6 by BMM, which are involved in the polarisation of Th2, Th1 and Th17 cells, respectively [44, 74, 305]. Similar to BMDC, BMM did not produce IL-10, IL-6, IL-1β, IL-23 or IL-12p40 in response to TriDAP alone. In contrast to BMDC, IL-27 was produced by BMM in response to TriDAP alone. This result indicates that NOD1 agonists can activate BMM, without the need of a second signal from TLR agonists. IL-27 is a cytokine that can modulate the polarisation of $CD4^+$ T-cells. IL-27 suppresses IL-17 and promotes IL-10 and IFN-γ production by CD4 T-cells [50, 306, 307]. Importantly, the clinical symptoms of EAE are enhanced in mice deficient in the IL-27 receptor (WSX1), highlighting an important role for this cytokine in regulating autoimmune responses. Thus, NOD1 agonists could potentially modulate adaptive immune responses during EAE via the production of IL-27 by macrophages. These results also established that macrophages, rather than DC, should be the focus of further investigations into the immunomodulatory role of NOD1 agonists.

Although both BMDC and BMM originate from the same precursors in the bone marrow, they are generated using GM-CSF and M-CSF, respectively, and respond differently to TLR stimulation. Consistent with previous reports [149], the present study showed that LPS induced the production of high concentrations of IL-10 and IL-6 and low concentrations of IL-23 and IL-1β by BMM, while the same stimulation had the opposite effect on BMDC. These differences are thought to be dependent on the suppressive nature of M-CSF; BMM degrade IKK at a much slower rate than BMDC, therefore preventing NFkB activation [149]. As IL-27 is produced in response to NFkB activation [308, 309] and NFkB is involved in the NOD1 signalling pathway [190], the suppression of NFkB does not explain why IL-27 is produced by BMM in response to TriDAP but not by BMDC. The most

likely explanation is that either M-CSF or GM-CSF alters the expression of NOD1 or that it is easier for NOD1 agonists to enter the cytosol of BMM.

The peritoneal cavity contains a heterogeneous population of immune cells including NK cells, mast cells, B-cells, T-cells, eosinophils, neutrophils, DC and macrophages. The PEC are fully differentiated resident cells, therefore, unlike the CSF-activated BMDC and BMM, may be more representative of the cell types that interact with NOD1 agonists during infection. The present study showed that LPS induced the production of IL-6, IL-10, IL-27, IL-12p70 and TNF-α by PEC, indicating that they can produce cytokines similar to those produced by BMM in response to LPS. However, this may not be surprising as the 20 % of the PEC is composed of macrophages. In contrast to both BMDC and BMM, PEC produced significant concentrations of IL-10 and IL-6 in response to TriDAP. This suggested that TriDAP may be inducing cytokine production from cells in the peritoneal exudate other than macrophages or DC. TriDAP-induced IL-6 production was detectable as early as 1 h and reached concentrations comparable with those elicited by LPS stimulation. TriDAP-induced IL-10 production was detectable at 5 h, 4 h after LPS-mediated IL-10 production.

The production of IL-6 in response to NOD1 activation is well characterised. NOD1-mediated IL-6 production has been shown previously in fibroblasts, periodontal ligament cells, BMM and BMDC [205, 207], and NOD1 deficient mice have been shown to have defective IL-6 production in response to *C. rodentium* and *S. Thyphium*-induced colitis [217]. There is more limited evidence of IL-10 production in response to NOD1 activation. Neutrophils have been shown to produce NOD2-dependent IL-10 in response to polymicrobial sepsis and loss of function mutations of NOD2 result in reduced TLR2-mediated IL-10 production [234, 303]. NOD2 agonists have not been shown to directly induce IL-10 production, but a mutation in NOD2 has been associated with inhibition of IL-10 production [310]. Loving et al concluded that NOD1 has no involvement in IL-10 production in response to bacterial infection [311]. Therefore, the production of IL-10 in response to TriDAP shown in the present study is a novel finding. IL-10 is a potent immunosuppressive cytokine, and has been shown to inhibit the clinical symptoms of EAE [273, 312, 313]. This suggests that IL-10 production may be responsible for the TriDAP-mediated attenuation of EAE observed in chapter 3. In addition, NOD1 mutations are strongly associated with the inflammatory diseases, such as asthma and IBD, and the

discovery of NOD1-mediated IL-10 production may shed some light on the regulatory role of NOD1 in these diseases.

The signalling pathway downstream of NOD1 involves the activation of MAPKs, including p38, ERK and JNK [295-297]. This study established that the NOD1-mediated cytokine production by PEC was dependent on p38 activation. The production of both IL-6 and IL-10 was completely abrogated in the presence of the p38 inhibitor SB203508. The addition of SB203508 had no effect on LPS-mediated IL-6 production, indicating that the inhibitor does not block TLR-induced IL-6. NOD1 also activates NFkB independently of p38 via the activation of RIP2 [190, 201, 294-296]. Some reports have shown that the p38 inhibitor SB203508 can block RIP2 activation. Therefore further investigation is required to demonstrate conclusively whether p38 or RIP2 is the essential signalling component mediating TriDAP-induced cytokine production. Pi3K has been implicated in the regulation of IL-10 production [314], and the present study showed that inhibition of Pi3K reduced the production of TriDAP-mediated IL-10 by approximately 50%. There have been no previous reports of a role for Pi3K in NOD1 activation, but the results of the present study highlight the need for further investigation into the involvement of Pi3K in NOD1 signalling.

The depletion of macrophages ($F480^{+}CD11b^{+}$) from PEC completely abrogated the production of IL-10 and IL-6 in response to TriDAP. The conclusion that macrophages are the primary mediator of NOD1-induced IL-10 and IL-6 production by PEC is consistent with the fact that LPS also failed to induce the production of these cytokines following depletion of macrophages. These results also demonstrated that IL-10 and IL-6 production in response to TriDAP and LPS increased when eosinophils, neutrophils or DC were depleted from the PEC. Although it is possible that these cells play a role in actively inhibiting cytokine production, an alternative explanation is that the numbers of macrophages in culture was increased when cell numbers were equalised after cell depletion.

TriDAP directly stimulated purified peritoneal macrophages to produce IL-10 in the absence of any other cell type, indicating that macrophages are the producers of IL-10 in the total PEC population and are not dependent on the presence of any other cell. IL-6 was not produced in significant concentrations in response to either TriDAP or LPS;

therefore, macrophages must be mediating the production of IL-6 by another cell type rather than producing it themselves. This result also highlights the difference in the response to TriDAP between BMM and isolated peritoneal macrophages. BMM failed to produce IL-10 in response to TriDAP, perhaps indicating that M-CSF can make BMM refractory to NOD1 activation. It is possible that the long period of time spent in culture may change the ability of a BMM to respond to NOD1 agonists. Importantly, these findings demonstrate that TriDAP has a significant effect on primary macrophages ex vivo.

The supernatant from PEC stimulated with either TriDAP or LPS had a substantial effect on cytokine production by $CD4^+$ T-cells in response to TCR activation. T-cells activated in the absence of PEC supernatant produced high concentrations of IFN-γ and low concentrations of IL-4, IL-10 and IL-17, indicating that they are primarily a Th1 phenotype. The addition of supernatant from untreated PEC reduced the production of IFN-γ and increased the production of IL-10 and IL-4, indicating a switch from a Th1 to a Th2 phenotype. The IL-4 and IL-10 was confirmed by flow cytometry to be produced by $CD4^+$ T-cells and did not come from the PEC supernatants. These findings indicate that untreated PEC have a propensity to polarise naive T-cells to Th2 cells. The production of IL-10 and IL-4 by TCR-activated T-cells was significantly enhanced when supernatants from TriDAP-treated PEC were added, however, the classic Th2 polarising cytokines IL-4 and IL-13 were not found in the supernatant of either untreated or TriDAP-treated PEC. TSLP is a cytokine produced by epithelial cells, which regulates Th2 polarisation via DC activation [28, 315]. NOD1 has been implicated in the production of TSLP [215], however, TSLP could not be detected in the supernatant of untreated or TriDAP-treated PEC. IL-10 plays a role in inhibiting Th1 responses, and as a result promotes Th2 polarisation [74, 305]. It is possible that TriDAP-treated PEC are promoting Th2 responses via the production of IL-10. In addition, no IL-12 was detected in supernatant from TriDAP-treated or untreated PEC, indicating that untreated or TriDAP-treated PEC does not have the capability to polarise Th1 cells. In contrast, supernatant from LPS-treated PEC enhanced the production of IFN-γ by TCR-stimulated T-cells. The Th1 polarising cytokines IL-12 and IL-27 were detected in the supernatants from LPS-treated PEC and may play a role in promoting IFN-γ production. Supernatant from LPS-treated PEC induced lower concentrations of IL-4 by TCR-stimulated T-cells in comparison with untreated or TriDAP-

treated PEC supernatants. IFN-γ can directly inhibit the polarisation of Th2 cells, therefore, the reduction in IL-4 production in response to LPS-treated PEC could be mediated by increased IFN-γ production.

Strikingly, supernatant from TriDAP-treated PEC promoted IL-17 production by TCR-stimulated T-cells. In addition, it has been reported that IL-6 and TGF-β play an important role in polarising Th17 cells. TriDAP and LPS induced the production of IL-6 but not TGF-β, but the supernatants from TriDAP-treated or LPS-treated PEC could still drive the production of IL-17 by TCR-activated T-cells. IL-6 induces RORγt and RORα, which are essential transcription factors in Th17 differentiation [42, 316]. TGF-β promotes Th17 differentiation by suppressing GATA3 and T-bet but has been shown to be dispensable for the activation of Th17 specific-transcription factors. Therefore, IL-6 is the most likely explanation for the TriDAP-mediated increase in IL-17 production. This result is consistent with the report of IL-6 dependent NOD1 mediated generation of Th17 cells during colitis [217].

The results of the present study indicate that unstimulated PEC cells promote Th2 polarisation and actively suppress Th1 polarisation. It has been shown that the Th2 associated cytokines IL-4 and IL-10 are involved in restricting Th1 responses to prevent indiscriminate immune responses and promote the resolution of inflammation. This suggests that unstimulated PEC may be involved in maintaining immune homeostasis. The present study demonstrated that LPS stimulated GM-CSF, IL-6, IL-12 and IL-27 production by PEC and induced the polarisation of IFN-γ- and IL-17-producing Th-cells. These results suggest that during an infection, LPS induces inflammatory responses by activating PEC. Interestingly, the findings of this study indicate that activation of NOD1 during infection may suppress Th1 responses and enhance the production of IL-10 and IL-4 by CD4 T-cells. This suggests NOD1 activation reinforces the homeostatic T-cell response observed with unstimulated PEC. However, NOD1 activation induced IL-6 production by PEC. IL-6 is a potent activator of inflammation, IL-6 deficient mice have a compromised acute phase reaction in response to infection or tissue damage [317]. TriDAP-treated PEC also promote IL-17 production by T-cells, possibly in response to the production of IL-6. The production of IL-17 may mediate any role that NOD1 plays in mounting an efficient adaptive immune response to infection.

This study highlights the different immune responses mounted in response to LPS and TriDAP. Only certain cell types produced cytokine in response to NOD1 activation alone; peritoneal macrophages and BMM produced cytokine in response to TriDAP but BMDC required a second signal from TLR agonists. NOD1 activation was poorly immunostimulatory in terms of pro-inflammatory cytokine production, only resulting in the production of IL-6. LPS, in contrast, induced the production of multiple pro-inflammatory cytokines and by a variety of cell types including neutrophils, peritoneal macrophages, BMM and BMDC. TriDAP induced the production of IL-10 by peritoneal macrophages which indicates that NOD1 activation can play a role in regulating inflammation. TriDAP also promoted Th2 responses and suppressed Th1 responses, indicating that NOD1 activation may play a role in restricting excessive inflammation during bacterial infection. NOD1 is a cytosolic PRR, therefore, would not be the first line of defence against infection as NOD1 agonists must enter the cytosol before they can be detected. This may indicate a role for NOD1 during the later stages of infection when inflammation must be resolved.

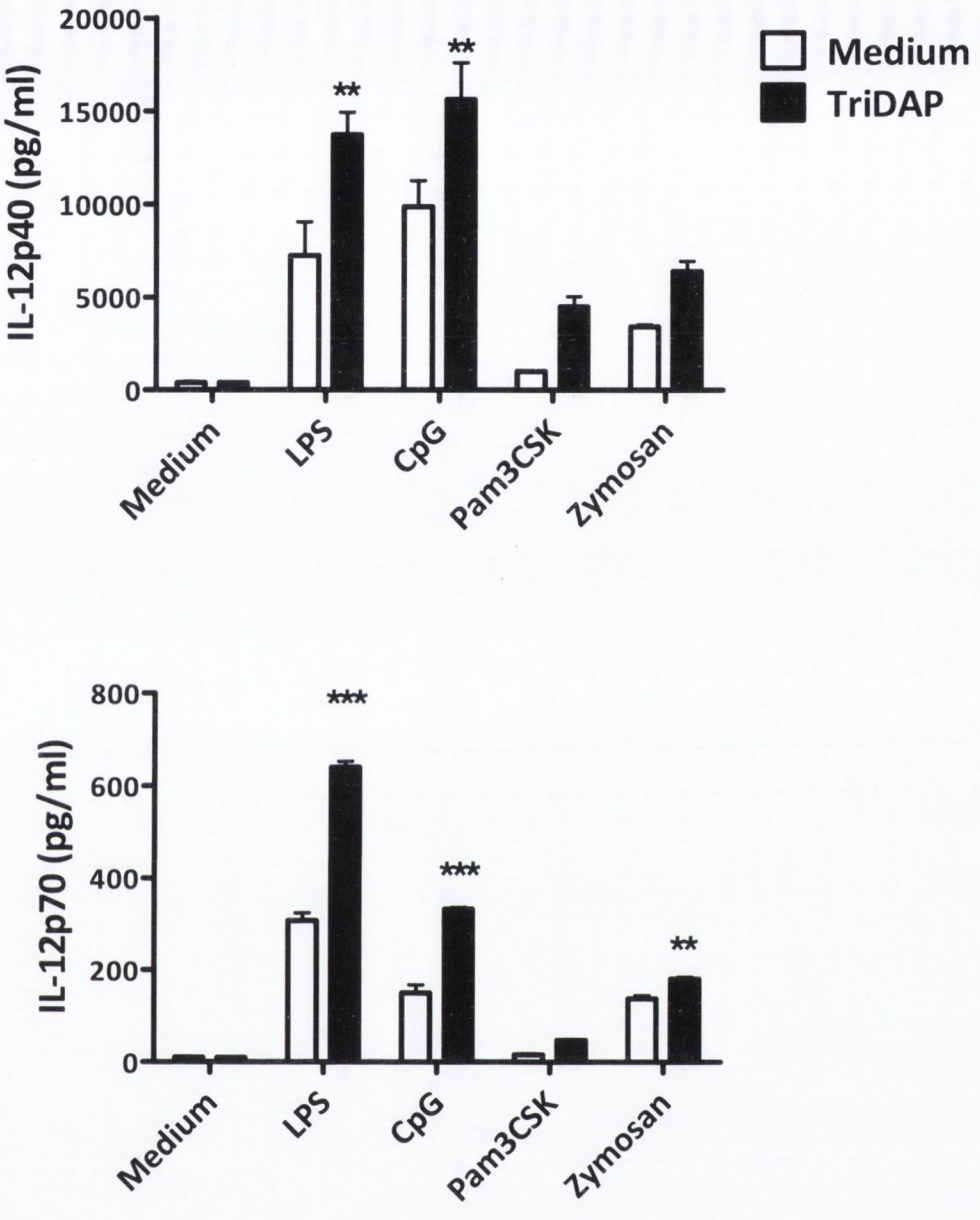

Fig 4.1 TriDAP synergises with TLR agonists to promote IL-12 production by BMDC. BMDC were incubated with or without TriDAP (100 μg/ml) for 1 h before the addition of either medium, LPS (100 ng/ml), CpG (1 μg/ml), Pam3CSK (500 ng/ml) or Zymosan (10 μg/ml). Each combination was examined in triplicate. Supernatants were removed after 24 h and cytokine concentrations were quantified by ELISA. Statistical significance was calculated using two-way ANOVA with Bonferroni post-test. **=$P < 0.01$, *** = $P < 0.001$ versus cells treated with medium. The results shown are representative of 3 or more independent experiments.

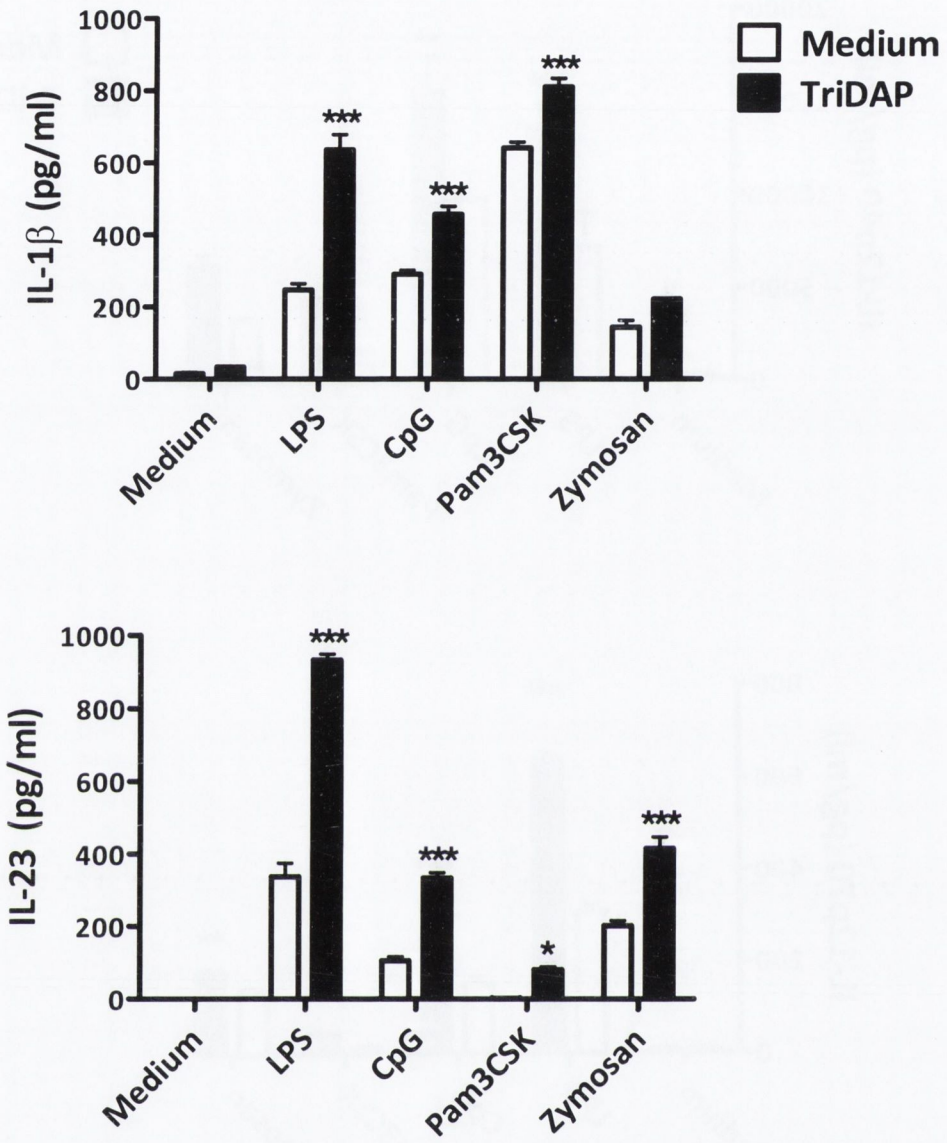

Fig 4.2 TriDAP synergises with TLR agonists to promote IL-1β and IL-23 production by BMDC. BMDC were incubated with or without TriDAP (100 μg/ml) for 1 h before the addition of either medium, LPS (100 ng/ml), CpG (1 μg/ml), Pam3CSK (500 ng/ml) or Zymosan (10 μg/ml). Each combination was examined in triplicate. Supernatants were removed after 24 h and cytokine concentrations were quantified by ELISA. Statistical significance was calculated using two-way ANOVA with Bonferroni post-test. *=$P < 0.05$, *** = $P < 0.001$ versus cells treated with medium. The results shown are representative of 3 or more independent experiments.

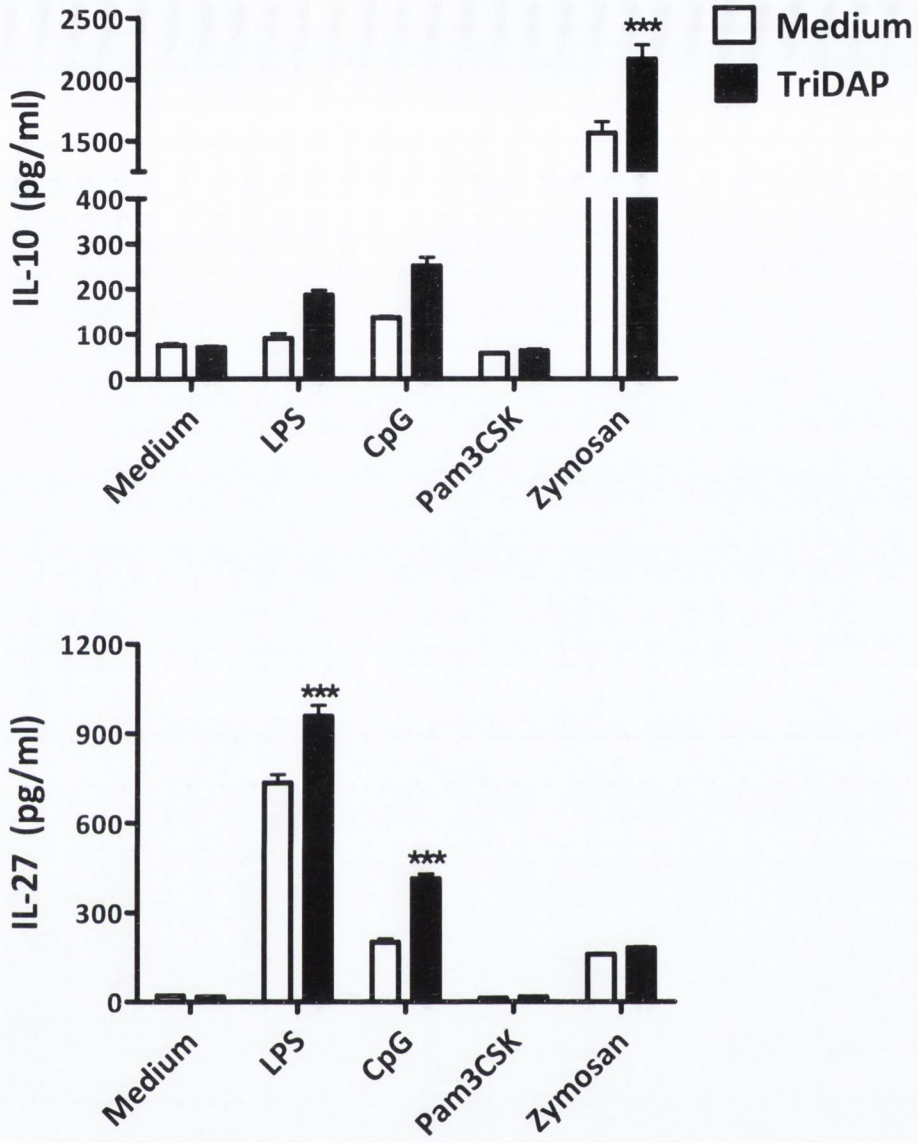

Fig 4.3 TriDAP synergises with TLR agonists to promote IL-10 and IL-27 production by BMDC. BMDC were incubated with or without TriDAP (100 μg/ml) for 1 h before the addition of medium, LPS (100 ng/ml), CpG (1 μg/ml), Pam3CSK (500 ng/ml) or Zymosan (10 μg/ml). Each combination was examined in triplicate. Supernatants were removed after 24 h and cytokine concentrations were quantified by ELISA. Statistical significance was calculated using two-way ANOVA with Bonferroni post-test. *** = $P < 0.001$ versus cells treated with medium. The results shown are representative of 3 or more independent experiments.

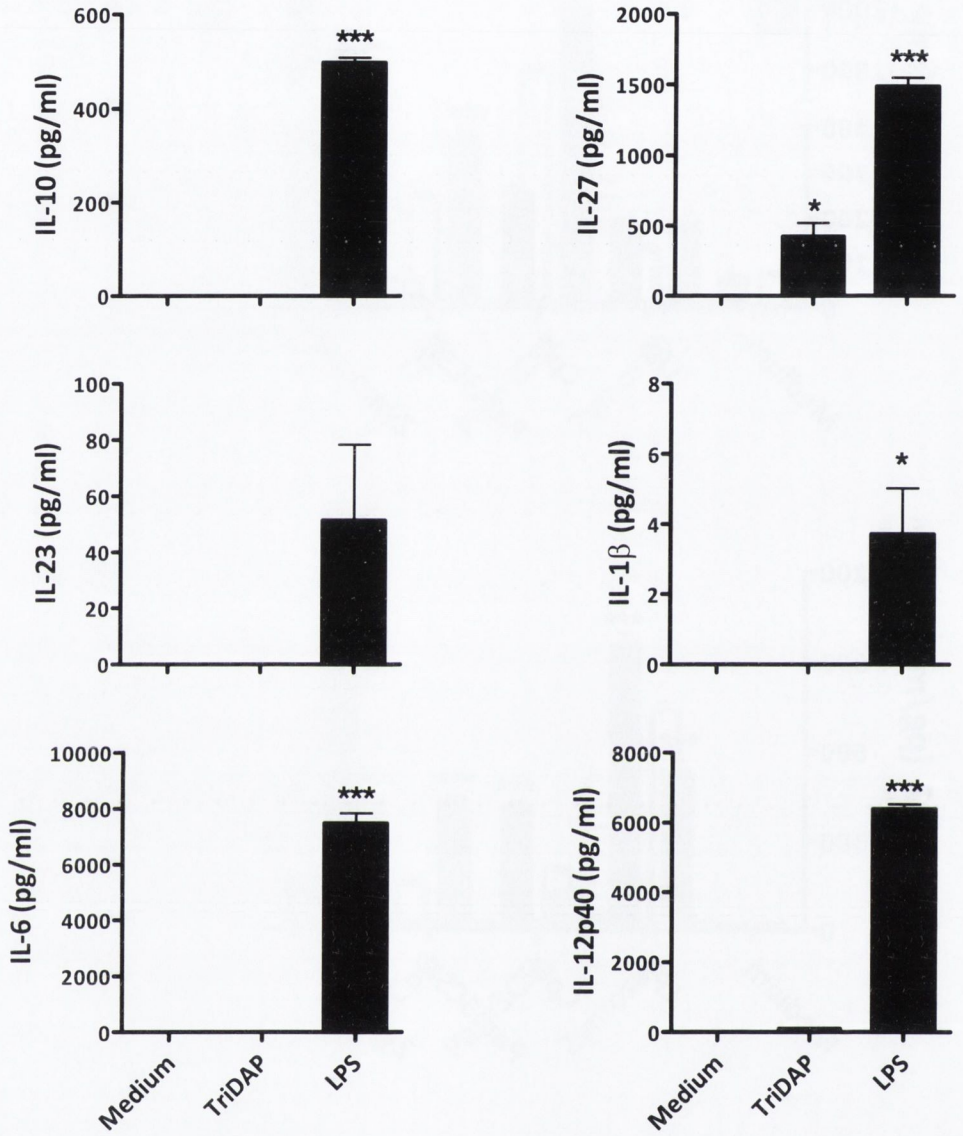

Fig 4.4 BMM produce IL-27 but not IL-10 or IL-6 in response to TriDAP alone. BMM were cultured with either medium, TriDAP (100 μg/ml) or LPS (500 ng/ml). Each combination was examined in triplicate. Supernatants were removed after 24h and cytokine concentrations were quantified by ELISA. Statistical significance was calculated using one-way ANOVA with a Tukey post test. *=$P < 0.05$, *** = $P < 0.001$ versus untreated cells. The results shown are representative of 3 independent experiments.

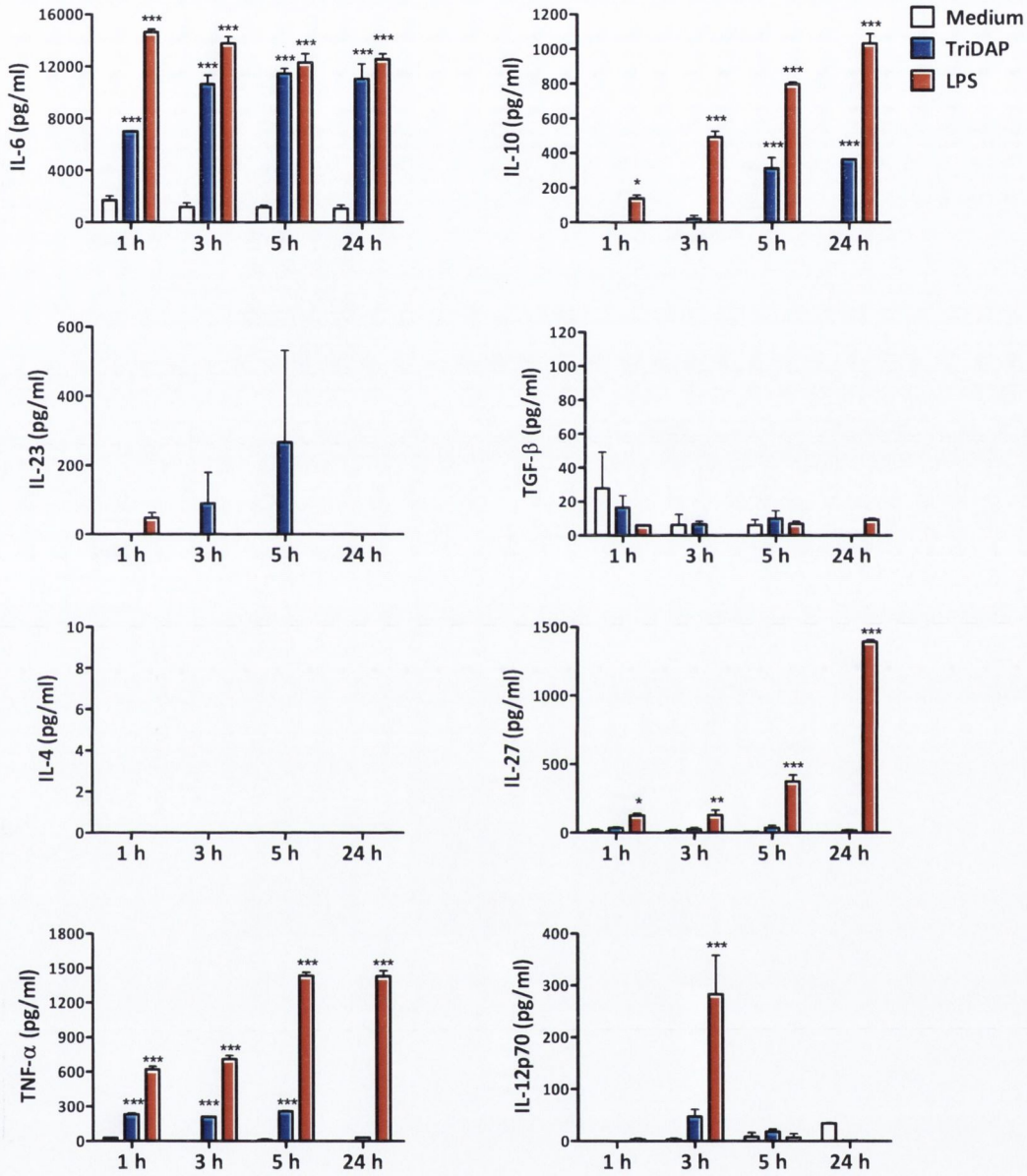

Fig 4.5 TriDAP induces the production of IL-6 and IL-10 by PEC. C57BL/6 mice were sacrificed and the peritoneal cavity was lavaged. PEC were cultured in the presence or absence of TriDAP (100 µg/ml) or LPS (500 ng/ml). Each combination was examined in triplicate. Supernatants were taken at 1, 3, 5 and 24 h. Concentrations of cytokines were quantified by ELISA. Statistical significance was calculated using repeated measures two-way ANOVA with a Bonferroni post test. *=$P < 0.05$, *** = $P < 0.001$ versus cells treated with medium. The results shown are representative of 3 independent experiments.

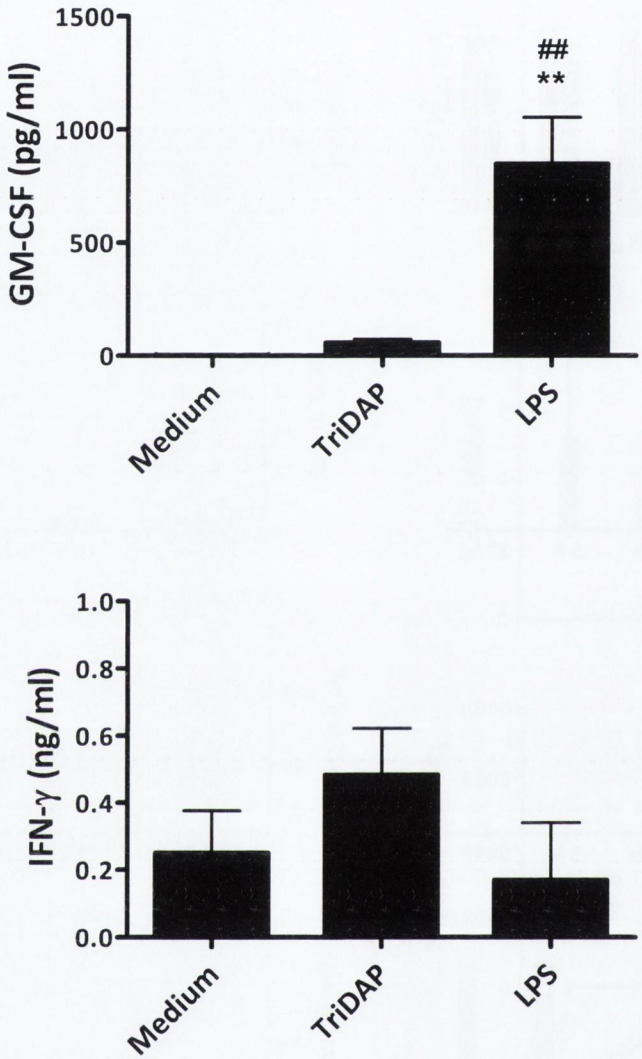

Fig 4.6 LPS induces GM-CSF production by PEC but TriDAP does not. C57BL/6 mice were sacrificed and the peritoneal cavity was lavaged. PEC were cultured in the presence or absence of TriDAP (100 μg/ml) or LPS (500 ng/ml). Each combination was examined in triplicate. Supernatants were taken after 24 h and the concentrations of cytokines were quantified by ELISA. Statistical significance was calculated using a one way ANOVA with a Tukey post test. ** = $P < 0.01$ versus untreated cells, ## = $P < 0.01$ versus cells treated with TriDAP. These results shown are representative of 3 independent experiments.

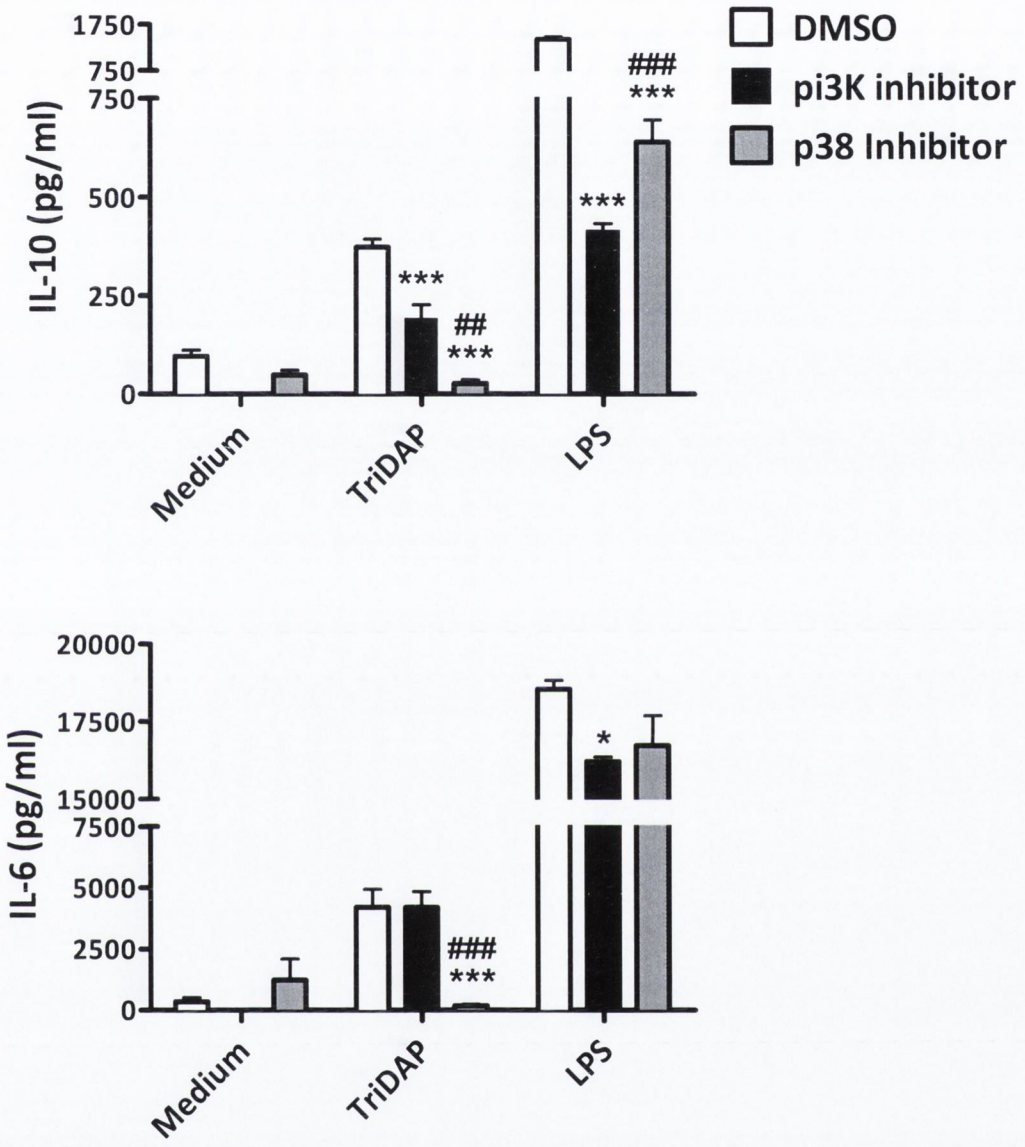

Fig 4.7 TriDAP-induced production of IL-6 and IL-10 by PEC is p38 dependent. C57BL/6 mice were sacrificed and the peritoneal cavity was lavaged. PEC were cultured with medium, TriDAP (100 μg/ml) or LPS (500 ng/ml) in the presence or absence of either DMSO, a p38 inhibitor (500 nM) or a pi3K inhibitor (50 nM). Each combination was examined in triplicate. Supernatants were taken at 24 h and the concentrations of cytokines were quantified by ELISA. Statistical significance was calculated using two way ANOVA with a Bonferroni post test. *=P < 0.05, *** = P < 0.001 versus cells treated with DMSO. ##=P < 0.01, ### = P < 0.001 versus cells treated with pi3K inh. These results shown are representative of 3 independent experiments.

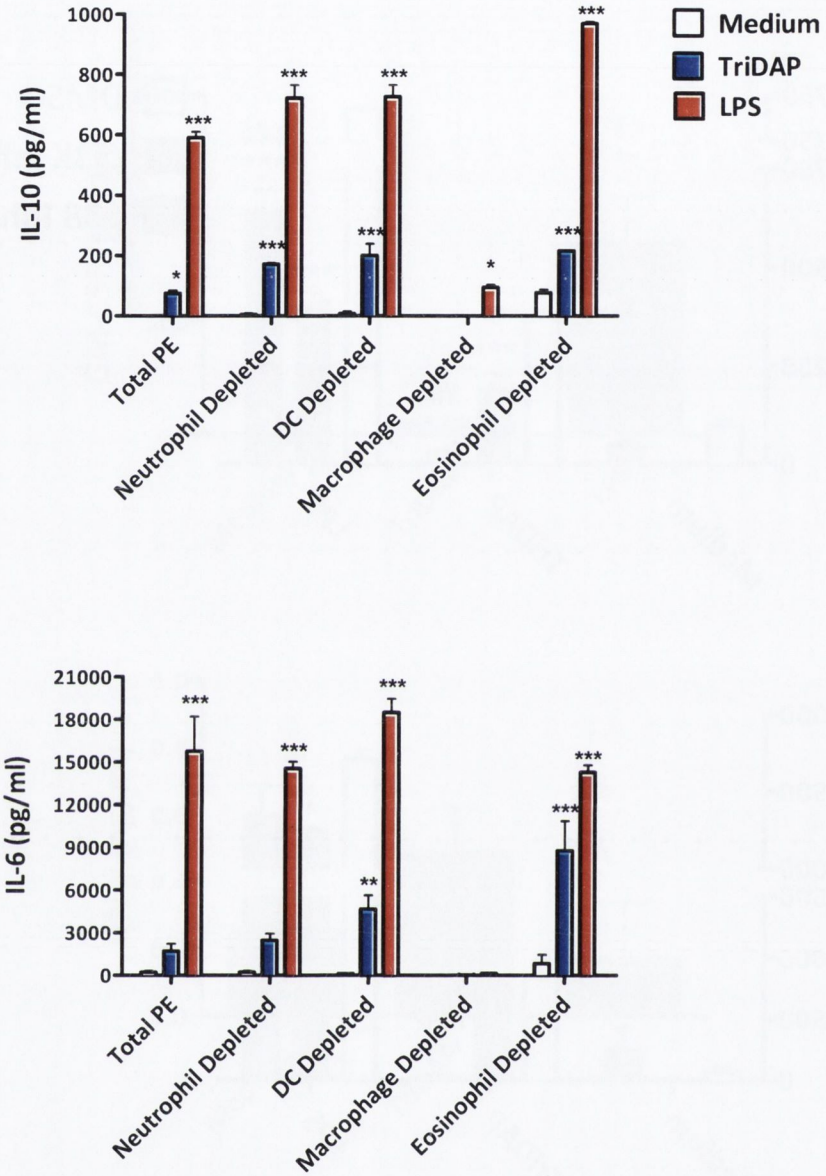

Fig 4.8 The TriDAP-induced production of IL-10 and IL-6 by PEC is dependent on the presence of macrophages. C57BL/6 mice were sacrificed and the peritoneal cavity was lavaged. The single cell suspension was surface-stained with antibodies specific to CD11b, F480, SiglecF, Ly6G and CD11c. The PEC were then depleted of different cell types by FACS. Various depleted PEC were then cultured in the presence or absence of TriDAP (100 μg/ml) or LPS (500 ng/ml). Each combination was examined in triplicate. Supernatants were taken at 24 h and the concentrations of cytokines were quantified by ELISA. Statistical significance was calculated using two way ANOVA with a Bonferroni post test. *= $P < 0.05$, **= $P < 0.01$, *** = $P < 0.001$ in comparison with untreated cells. The results shown are representative of 2 independent experiments.

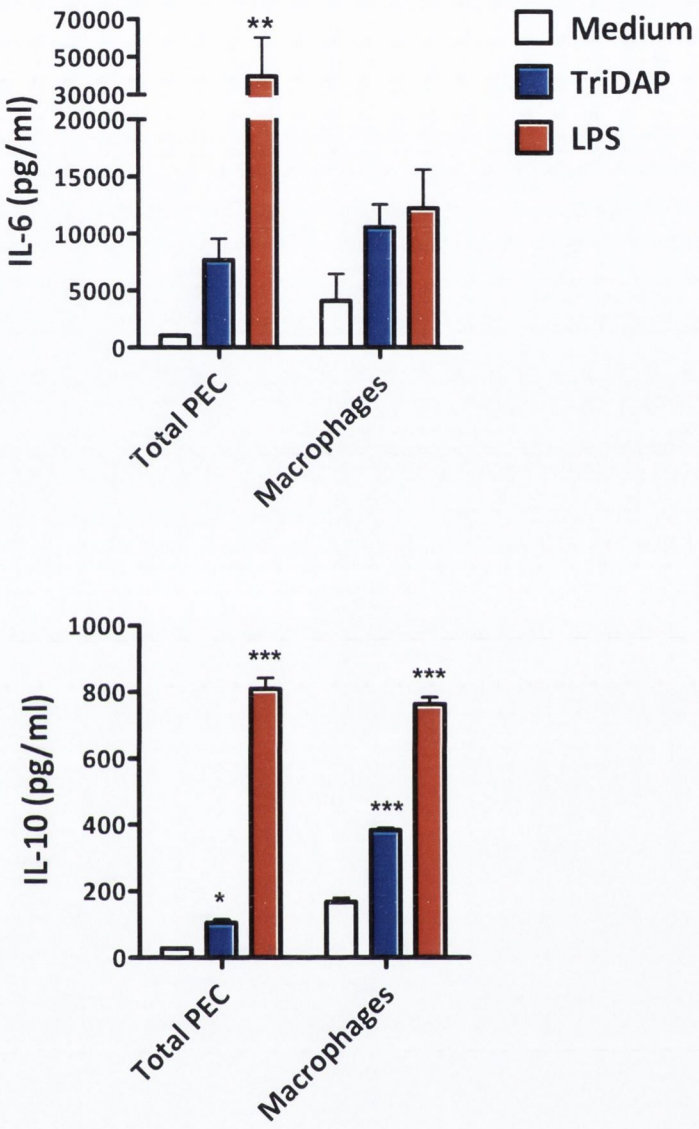

Fig 4.9 TriDAP induces IL-10 production by purified peritoneal macrophages. C57BL/6 mice were sacrificed and the peritoneal cavity was lavaged. PEC were stained with antibodies specific to CD11b, F480 and Gr1. Peritoneal macrophages ($CD11b^+F480^+GR1^-$) were purified by FACS. Purified macrophages or total PEC were cultured in the presence or absence of TriDAP (100 µg/ml) or LPS (500 ng/ml). Each combination was examined in triplicate. Supernatants were harvested after 24 h and the concentrations of cytokines were quantified by ELISA. Statistical significance was calculated using two-way ANOVA with a Bonferroni post test. *= $P < 0.05$, **= $P < 0.01$, *** = $P < 0.001$ versus cells treated with medium. The results shown are representative of 3 independent experiments.

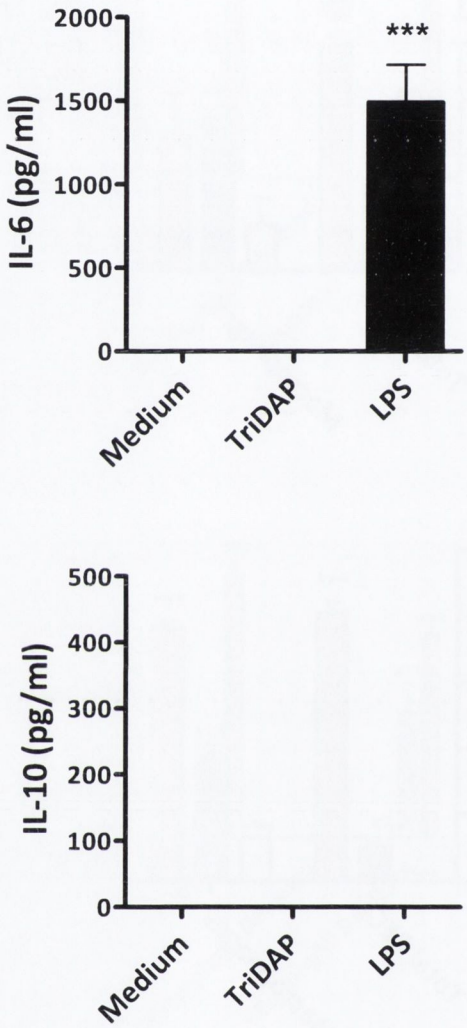

Fig 4.10 Neutrophils do not produce IL-10 or IL-6 in response to TriDAP. C57BL/6 mice were injected i.p. with 9% casein at 0 h and 15 h. At 18 h the peritoneal cavity was lavaged and neutrophils were purified using a percoll gradient. Purity was >90%. The cells were then cultured in the presence or absence of TriDAP (100 μg/ml) or LPS (500 ng/ml). Each combination was examined in triplicate. Supernatants were taken at 24 h and the concentrations of cytokines were quantified by ELISA. Statistical significance was calculated using a one-way ANOVA with a Tukey post test. ***= $P < 0.001$ versus cells treated with medium. The results shown are representative of 2 independent experiments.

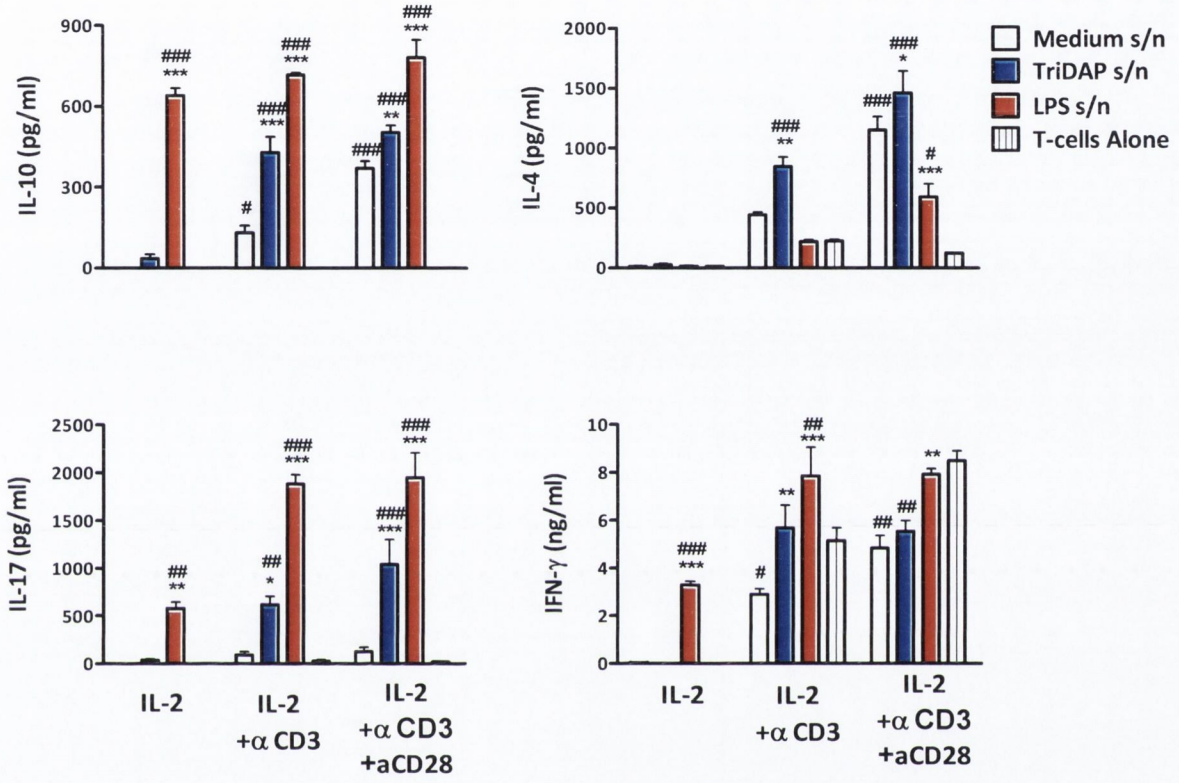

Fig 4.11 TriDAP-treated PEC induce IL-10, IL-4 and IL-17 production by TCR-stimulated CD4⁺ T-cells. C57BL/6 mice were sacrificed and the peritoneal cavity was lavaged. PEC were cultured in the presence or absence of TriDAP (100 μg/ml) or LPS (500 ng/ml). Supernatants were taken after 24 h and added to a culture of purified CD4⁺ T-cells. The T-cells were then cultured in the presence of either IL-2, IL-2 and αCD3 or IL-2 (10 U/ml), αCD3 (2 μg/ml) and αCD28 (1 μg/ml). Each combination was examined in triplicate. The supernatants were harvested after 72 h and the concentrations of cytokines were quantified by ELISA. Significance was calculated using two way ANOVA. *= $P < 0.05$, **= $P < 0.01$, *** = $P < 0.001$ in comparison with cells treated with medium s/n. #= $P < 0.05$, ##= $P < 0.01$, ### = $P < 0.001$ versus T-cells alone. The results shown are representative of 3 independent experiments.

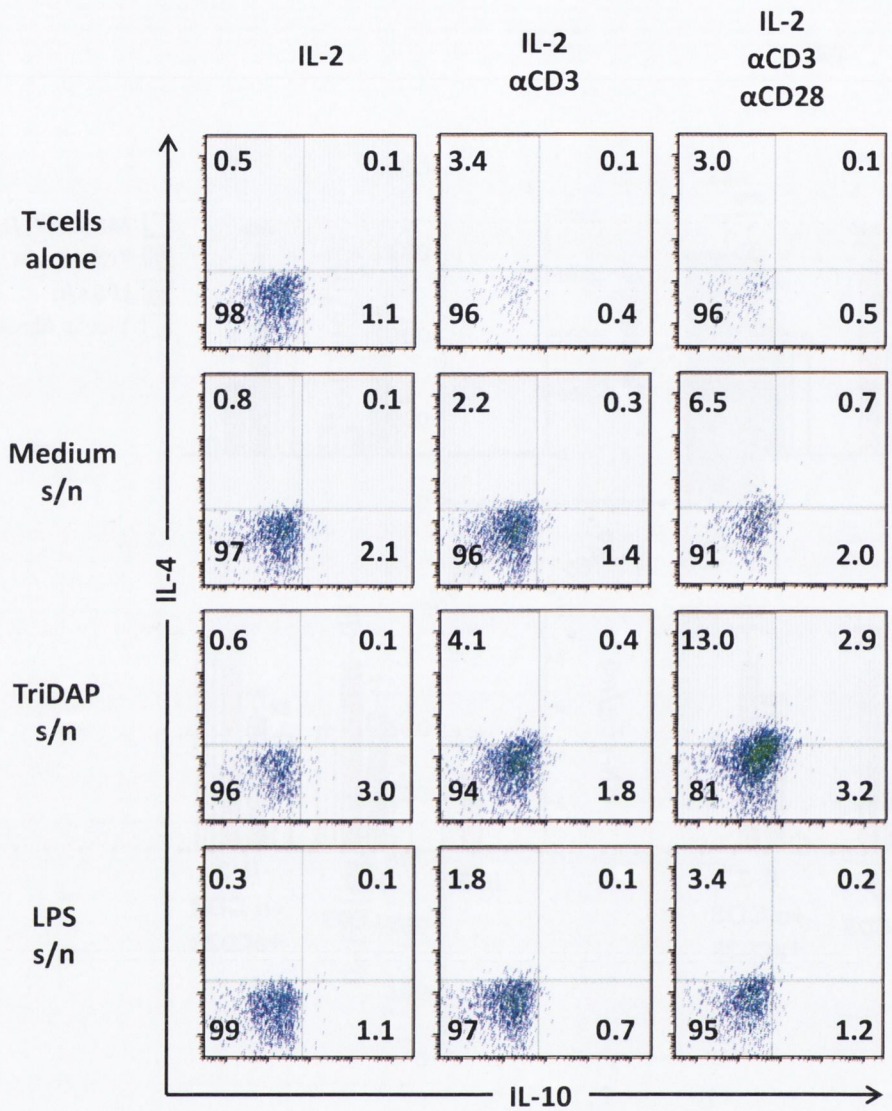

Fig 4.12 TriDAP-treated PEC induce the production of IL-10 and IL-4 by TCR-stimulated CD4⁺ T-cells. C57BL/6 mice were sacrificed and the peritoneal cavity was lavaged. PEC were cultured in the presence or absence of TriDAP (100 µg/ml) or LPS (500 ng/ml). Supernatants were taken after 24 h and added to a culture containing purified CD4⁺ T-cells stained with CTV. The T-cells were then cultured in the presence of either IL-2, IL-2 and αCD3 or IL-2 (10 U/ml), αCD3 (2 µg/ml) and αCD28 (1 µg/ml). After 72 h the cells were incubated for 5 h in the presence of PMA (10 ng/ml), ionomycin (1 µg/ml) and brefaldin A (5 ng/ml). The cells were surface-stained with antibodies specific for CD4 and intracellular-stained with antibodies specific for IL-4 and IL-10. All combinations were set up in triplicate before being pooled for analysis by flow cytometry. Plots shown were gated on $CD4^+CTV^+$ cells. The results shown are representative of 3 independent experiments.

Chapter 5

The effect of the NOD1 agonist TriDAP on the expansion and activation of macrophages

CHAPTER 5: The effect of the NOD1 agonist TriDAP on the expansion and activation of macrophages in vivo

5.1 Introduction

Macrophages are part of a highly complex network of innate immune cells which shape the adaptive immune response. They can present antigen and produce immune mediators which help to mount tailored responses to specific threats. Like other innate immune cells, macrophages have the capability to detect microbial pathogens by expressing a variety of PRRs such as TLRs NLRs and RLRs. When activated macrophages fall into two broad categories, pro-inflammatory classically activated M1 macrophages, and anti-inflammatory alternatively activated M2 macrophages. When activated by microbial molecular patterns such as LPS, macrophages become M1 activated and actively kill pathogens by producing reactive oxygen species such as nitric oxide [318]. M1 macrophages can also shape the adaptive immune response by presenting antigen directly to T-cells via MHC-II and by secreting T-cell polarising cytokines such as IL-12 [319]. In addition, the adaptive immune response can reciprocally regulate M1 macrophages; IFN-γ, a cytokine produced by Th1 cells, primes macrophages to respond to microbial products and propagate M1 activation [130].

Excessive inflammation can be hazardous to the host and therefore regulatory mechanisms have co-evolved with the immune response. Depending on environmental cues, macrophages can become regulatory cells which actively suppress the immune response and repair any collateral damage. These macrophages are broadly characterised as M2 macrophages or alternatively activated macrophages. M2 macrophages include several subsets; M2a macrophages are induced by the Th2-polarising cytokines IL-4 and IL-13 in response to parasites or extracellular bacteria and specialise in tissue repair and immunosuppression [172, 320]. M2b macrophages are induced in response to a combination of immune-complexes and TLR-agonists. M2b, in contrast to other M2 subsets, are not immunosuppressive but are poorly microbicidal in comparison with M1 macrophages [321]. IL-10, a well characterised immunosuppressive cytokine, induces the activation of M2c macrophages, which primarily suppress immune responses during excessive inflammation. Upon differentiation, M2 macrophages decrease the expression of NOS2 and upregulate the expression of arginase [322]. Arginase is an enzyme that

converts arginine to ornithine, depleting the microenvironment of the essential amino acid, starving surrounding cells and thereby limiting further immune responses [323]. M2 macrophages produce immunosuppressive proteins, such as relm-α and IL-10, to actively suppress innate immune cells and T-cell activation [159].

Classification of macrophages as either M1 or M2 is a simplification of a dynamic process. Macrophages are constantly changing in response to cues from the microenvironment to fulfil their role in a given circumstance. Chapter 4 of this study established that both BMM and peritoneal macrophages were capable of producing cytokines in response to the NOD1 agonist TriDAP. Interestingly, peritoneal macrophages specifically produced IL-10 in response to NOD1 activation, a novel mechanism by which NOD1 may regulate inflammation. Furthermore, the supernatant produced by TriDAP-treated PEC suppressed the production of IFN-γ and promoted the production of IL-4, IL-10 and IL-17 by $CD4^+$ T-cells. In light of these findings, this study explored the effects of NOD1 activation on peritoneal cells in vivo and investigated the phenotype and function of macrophages in vivo in response to NOD1 activation.

The peritoneal cavity contains a milieu of lymphoid and myeloid cells as well as a lining of epithelial cells known as the mesothelium. The myeloid and lymphoid cells are easily harvested and characterised. Approximately 50 % of the peritoneal exudates cells (PEC) from a naive mouse are B-cells and T-cells. The majority of the remaining cells are macrophages (20-30 %) but also include DCs, eosinophils, neutrophils, mast cells and NK cells. Peritoneal macrophages can be separated into two distinct subsets: small peritoneal macrophages (SPM) and large peritoneal macrophages (LPM) [100]. LPM and SPM can be distinguished from each other by the expression of CD11b, MHC-II and F480. LPM highly express CD11b and F480 but have low expression of MHC-II ($CD11b^{hi}F480^{hi}MHC\text{-}II^{lo}$). SPM express lower levels of F480 and CD11b but have high expression of MHC-II on their surface ($CD11b^{int}F480^{int}MHC\text{-}II^{hi}$) [100]. SPM turnover is rapid; during the steady state, the small numbers of monocytes which enter the peritoneal cavity differentiate into SPM, maintaining a small population. LPM are the dominant macrophage population during the steady state and have a long turnover time, however, there is currently no consensus on how the population of LPM are homeostatically maintained [109].

The established method for obtaining primary peritoneal macrophages involves the harvesting of cells after thioglycolate injection [324]. The sterile inflammation caused by thioglycolate recruits monocytes to the peritoneal cavity, where they differentiate into SPM. Four days after the injection of thioglycollate, LPM cannot be detected and SPM have become the dominant macrophage population in the peritoneal cavity. There are several explanations for the disappearance of the LPM population, including cell death, migration out of the cavity and increased adherence to the peritoneum, however, no conclusive evidence has been forthcoming. During certain infections both LPM and SPM are observed in the peritoneal cavity. Nguyen et al hypothesised that the population of LPM is maintained during infection because of the presence of IL-10. IL-10 induces the differentiation of infiltrating monocytes into LPM [109] (Fig 5.1.1) but there is currently no evidence that SPM can differentiate into LPM or vice versa. Other studies argue that local macrophage proliferation can occur under the right circumstances; Jenkins et al showed that infection with *L. sigmodontis*, a classical Th2 polarising pathogen, can induce the proliferation of LPM macrophages without the need to differentiate from monocytes. Upon further investigation, it was shown that proliferation of LPM was induced by IL-4 (Fig 5.1.1) [325].

Both SPM and LPM are phagocytic and can produce inflammatory cytokines and reactive oxygen species in response to stimuli [100]. SPM have a higher expression of MHC-II and are the more potent activators of antigen specific T-cells. LPM are more effective at clearing apoptotic cells and are thought to be involved in the resolution of inflammation [109]. There is also some evidence suggesting that SPM and LPM can be categorised as M1 and M2 macrophages, respectively. When restimulated ex vivo, LPM express the M2 markers arginase and relm-α, while SPM express M1 markers NOS2 and IL-12 [326]. Furthermore, LPM are preferentially activated and expanded in response to IL-4 or IL-10, which are both established M2 macrophage polarising cytokines. Conversely, SPM are expanded by LPS, a known activator of M1 macrophages.

This study investigated the effect of TriDAP administration in vivo on PEC, with particular attention to macrophage phenotype and function.

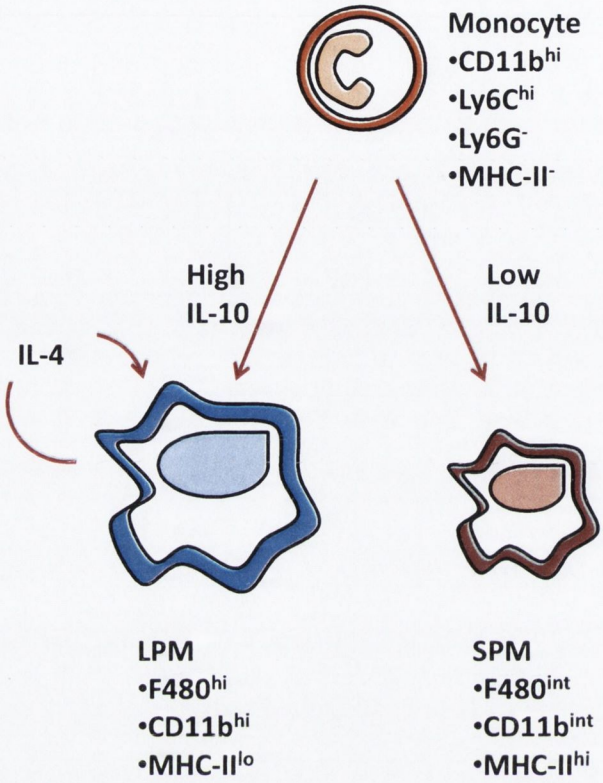

Fig 5.1.1 The maintenance of LPM and SPM, two distinct peritoneal macrophage subsets. Monocytes differentiate into either LPM or SPM depending on the concentration of IL-10 [109]. LPM may proliferate in response to stimulation by IL-4 [325].

5.2 Results

5.2.1 The characterisation of the innate immune cells from peritoneal cavity of naive mice

Multi-colour flow cytometry was used to identify the immune cell subsets within the peritoneal cavity. The peritoneal cavity was lavaged using ice cold PBS and kept on ice during handling to reduce the number of macrophages sticking to plastic. The cells were stained with a viability stain to prevent the acquisition of dead cells during FACS analysis. Cells were incubated with an Fc receptor blocking antibody to prevent non-specific staining of antibodies to the FcIIγ-receptor. The cells were then incubated with antibodies specific for Ly6C, Ly6G, F480, CD11b, MHC-II and CD19. Doublet cells were distinguished by their high Fsc width and were excluded. B-cells were excluded based on their high expression of CD19 and lymphocyte Fsc-Ssc profile (Fig 5.1). Non-myeloid cells were excluded by gating on $CD11b^+$ cells (Fig 5.1). $CD11b^+$ myeloid cells were broken into two subsets: $Ly6C^-$ resident cells and $Ly6C^+$ cells, which infiltrate from the blood. In untreated PEC, $Ly6C^+$ cells make up a very small percentage of the total cell population (Fig 5.1) but increase in number upon injection of a PAMP or inflammatory mediator such as LPS (Fig 5.1). The $Ly6C^+$ cells can be separated into specific cell types depending on their expression of Ly6G. Neutrophils express high levels of Ly6G and Ly6C and occupy a typical granulocyte position on Fsc and Ssc (Fig 5.1). Monocytes, however, are $Ly6G^-Ly6C^+$ (Fig 5.1). Monocytes do not express MHC-II but upregulate the protein when they differentiate into macrophages.

The $Ly6C^-CD11b^+$ subset contains LPM, SPM and eosinophils. Eosinophils express low levels of CD11b and F480 and can be further differentiated from other cells by their expression of Siglec-F and their unique high Ssc profile (Fig 5.1). LPM are the second most populous cell in the peritoneal cavity (10-20%; Fig 5.2B) after B-cells. LPM express high levels of CD11b and F480, have low expression of MHC-II and have a high Fsc and Ssc profile (Fig 5.1). SPM make up a smaller percentage (1-5%; Fig 5.2B) of the untreated peritoneal cavity but increase in number after an injection of LPS or thioglycolate. SPM and LPM both express similar amounts of CD11b but SPM have an intermediate expression of F480. In contrast to LPM, SPM express high levels of MHC-II and have a

lower Fsc and Ssc profile (Fig 5.1). SPM can also express low levels of Ly6C, an artefact of their differentiation from $Ly6C^+$ monocytes.

5.2.2 The characterisation of the peritoneal cavity 16 h after the injection of TriDAP or LPS

Ligation of the NOD1 receptor results in the activation of MAPK and NFkB. Although both of these signalling pathways induce the expression of pro-inflammatory genes and result in a strong immune response, in vitro NOD1 agonists have been shown to be weak innate immune stimulators in comparison with other PAMPs such as LPS [206, 211, 278, 279]. However, in vivo activation is not as well characterised. Similar to LPS, NOD1 activation induces the production of chemokines KC, MIP-2 and RANTES [208] in vivo. This suggests that TriDAP may induce the recruitment of neutrophils and other immune cells. This study was designed to examine the effect of injecting the NOD1 agonist TriDAP on cell recruitment into the peritoneal cavity and to compare this with the established effect of the TLR4 agonist LPS. C57BL/6 mice were injected i.p. with TriDAP, LPS or PBS as the vehicle control. The mice were sacrificed after 16 h and the peritoneal cavity was lavaged with ice-cold PBS. Cells were counted and stained with antibodies specific for CD19, CD11b, F480, Ly6C, Ly6G and MHC-II.

As expected, an injection of LPS significantly increased the numbers of cells within the peritoneal cavity after 16 h (Fig 5.2 A; $P < 0.05$). The increase in cell number was associated with an increase in the percentage of $CD11b^+$ myeloid cells from 25% to 60% of the total viable cells (Fig 5.2 B and C). LPS increased the percentage of neutrophils in the PEC by approximately 29% in comparison with mice injected with PBS (Fig 5.3; $P < 0.001$). Similarly, LPS increased the percentage of $Ly6C^+$ monocytes in the PEC by 19% in comparison with mice injected with PBS (Fig 5.3; $P < 0.001$). In addition, LPS decreased the percentage of LPM by 15% in comparison with mice injected with PBS (Fig 5.3; $P < 0.01$). There was no significant change in the percentage of eosinophils or SPM in response to the LPS injection. LPS significantly increased the numbers of neutrophils and monocytes by a factor of approx. 2.5 (Fig 5.4; both $P < 0.001$). Although the numbers of LPM decreased in response to LPS injection, the change was not statistically significant (Fig 5.4).

The injection of TriDAP also increased the numbers of cells within the peritoneal cavity after 16 h (Fig 5.2 A) and this was associated with an increase in the percentage of myeloid cells from 25% to 30% of the total viable cells (Fig 5.2 B). TriDAP increased the percentage of monocytes in the PEC by 9% in comparison with mice injected with PBS (Fig 5.3; $P < 0.01$). Similarly, TriDAP increased the percentage of neutrophils in the PEC by 9% in comparison with mice injected with PBS (Fig 5.3). TriDAP also decreased the percentage of LPM in the PEC by 10% in comparison with PBS injected mice (Fig 5.3; $P < 0.05$). When absolute numbers were calculated, TriDAP increased the numbers of both neutrophils and monocytes in comparison with mice injected with PBS (Fig 5.4). However, the increase in the numbers of these cells was not statistically significant.

After 16 h, LPS induced a more significant change in the PEC in comparison with TriDAP. Mice injected with LPS had a larger number of cells in the peritoneal cavity in comparison with mice injected with TriDAP (Fig 5.2 A; $P < 0.05$). Mice injected with LPS had a higher percentage of monocytes and a higher percentage of neutrophils in comparison with mice injected with TriDAP (Fig 5.3; $P < 0.001$ and $P < 0.01$, respectively). Similarly, mice injected with LPS had a higher absolute number of monocytes and neutrophils in the peritoneal cavity in comparison with mice injected with TriDAP (Fig 5.4; $P < 0.01$ and $P < 0.001$, respectively).

In summary, the injection of LPS induced an inflammatory response which was associated with an increase in neutrophils and monocytes in the peritoneal cavity after 16 h. In agreement with the literature, LPS also reduced the population of LPM in the cavity after 16 h. TriDAP had a similar, albeit weaker, effect. TriDAP significantly increased the percentage of monocytes in comparison with PBS injected controls; however, the increase in monocytes in response to LPS was significantly larger. This study suggests that TriDAP can induce a significant inflammatory response in vivo.

5.2.3 The characterisation of the peritoneal cavity 4 days after the injection of TriDAP or LPS

The classic protocol for harvesting large amounts of macrophages involves injecting thioglycollate into the peritoneal cavity of mice. Thioglycollate initially attracts large numbers of monocytes to the peritoneal cavity. After 4 days the inflammatory response resolves and the monocytes convert into SPM, leaving SPM as the dominant macrophage subset in the peritoneal cavity. A similar response is observed after the injection of LPS; firstly, neutrophils and monocytes are recruited to the site of peritoneal cavity, and after 4 days SPM become the dominant macrophage subset [100]. Other studies, however, have shown that monocytes can also differentiate into LPM, depending on the nature of the microenvironment [109]. The present study showed that TriDAP can recruit monocytes to the peritoneal cavity (Fig 5.2). Therefore, this study was extended to investigate the phenotype of peritoneal cells, including SPM and LPM, 4 days after repeated injection of TriDAP. C57BL/6 mice were injected i.p. on d 0, 1, 2 and 3 with TriDAP, LPS or PBS. The mice were sacrificed on d 4 and the peritoneal cavity was lavaged with ice-cold PBS. Cells were counted and stained with antibodies specific for CD19, CD11b, F480, Ly6C, Ly6G and MHC-II. The phenotype of the peritoneal cavity was then analysed using flow cytometry.

Mice injected with LPS had significantly higher numbers of cells in the peritoneal cavity on d 4 (Fig 5.5 A; $P < 0.01$). This increase in cell number was associated with an increase in the percentage of myeloid cells in the peritoneal cavity from 10% in mice injected with PBS to 20% in mice injected with LPS (Fig 5.5 B). In contrast with mice sacrificed after 16 h (Fig 5.3 and 5.4), monocytes ($CD11b^{+}LY6C^{+}Ly6G^{-}MHC\text{-}II^{-}$) were no longer detected after 4 days in mice injected with PBS, LPS or TriDAP. After 4 days the percentage of neutrophils remained higher in the peritoneal cavity of mice injected with LPS in comparison with PBS injected controls (Fig 5.6). Furthermore, LPS increased the absolute numbers of neutrophils in the peritoneal cavity in comparison with PBS injected controls (Fig 5.7; $P < 0.05$). By d 4 LPS had increased the percentage of SPM in the peritoneal cavity by 4% in comparison to PBS injected mice (Fig 5.6). Furthermore, the absolute numbers of SPM in the peritoneal cavity was increased in comparison with PBS injected mice (Fig 5.7). In contrast, the injection of LPS resulted in a 7% decrease of the percentage of LPM by d 4 (Fig 5.6; $P < 0.05$).

TriDAP increased the numbers of cells in the peritoneal cavity after 4 days (Fig 5.5 A). This was associated with an increase in the percentage of myeloid cells from 10% in PBS-treated mice to 34% in TriDAP-treated mice (Fig 5.5 B). In contrast to LPS, mice injected with TriDAP showed no significant change in the percentage or absolute numbers of neutrophils in the peritoneal cavity on d 4 (Fig 5.6 and 5.7). However, by d 4, TriDAP increased the percentage of SPM by 4% in comparison with PBS controls (Fig 5.6; n.s.). Furthermore, TriDAP increased the absolute numbers of SPM in the peritoneal cavity in comparison with PBS controls (Fig 5.7; n.s.). Notably, TriDAP increased the percentage of LPM in the peritoneal cavity by 15% in comparison with PBS controls (Fig 5.6; $P < 0.001$). This was associated with a significant increase in the absolute numbers of LPM in mice injected with TriDAP in comparison with PBS treated mice (Fig 5.7; $P < 0.05$).

In summary, 4 days post injection, LPS continued to result in increased frequencies and numbers of neutrophils in the peritoneal cavity, however, the population of monocytes, which made up approximately 20% of the peritoneal cells after 16 h, were no longer detected. Similarly, the monocytes, which made up approximately 10% of the peritoneal cells 16 h after injection with TriDAP, were not detected after 4 days. TriDAP and LPS both promoted a non-significant increase of SPM in the peritoneal cavity 4 days post i.p. injection. TriDAP significantly increased the percentage and numbers of LPM in the peritoneal cavity after 4 days. In contrast, LPS resulted in a decrease in the percentage of LPM by d 4. This data strongly indicates that, although the initial inflammatory response after the injection of TriDAP seems similar to that of LPS, TriDAP induces a different type of resolution phase which is characterised by the increase in LPM 4 days post exposure.

5.2.4 The characterisation of surface proteins expressed by LPM and SPM

Macrophages can process and present antigen via MHC-II to $CD4^+$ T-cells to promote an adaptive immune response. T-cell activation also requires the ligation of co-stimulatory molecules, such as CD80 and CD86, which are expressed by APCs, including macrophages. Therefore this study investigated the expression of the co-stimulatory molecules CD80 and CD86 on the surface of LPM and SPM. TriDAP significantly increased the numbers of LPM in the peritoneal cavity (Fig 5.7), therefore the effect of TriDAP on the expression of co-stimulatory molecules was also investigated. C57BL/6 mice were injected i.p. with

either PBS or TriDAP on d 0, 1, 2 and d 3. The mice were sacrificed on d 4 and the peritoneal cavity was lavaged with ice-cold PBS. The cells were surface-stained with antibodies specific for CD11b, F480, Ly6G, Ly6C, MHC-II, CD80 and CD86 and analysed by flow cytometry. The populations of LPM and SPM were gated as described in Fig 5.1.

LPM expressed lower levels of MHC-II in comparison with SPM (Fig 5.8). The average median fluorescence intensity (MFI) of MHC-II was 80% lower in LPM than in SPM (Fig 5.8; $P < 0.001$). The administration of TriDAP significantly increased the expression of MHC-II by SPM in comparison with PBS-treated mice (Fig 5.8; $P < 0.001$). The expression of MHC-II by LPM was unchanged after TriDAP administration (Fig 5.8). LPM expressed higher amounts of CD80 and CD86 in comparison with SPM (Fig 5.8). The average MFI of CD80 was 86.3% lower in SPM than in LPM (Fig 5.8; $P < 0.001$) and the average MFI of CD86 was 80.6% lower in SPM than in LPM (Fig 5.8; $P < 0.001$). The administration of TriDAP significantly decreased the expression of CD80 and CD86 by LPM in comparison with PBS-treated mice (Fig 5.8; both $P < 0.05$).

In summary, MHC-II was expressed in larger amounts on the surface of SPM than LPM, but LPM expressed larger amounts of the co-stimulatory molecules CD80 and CD86. The administration of TriDAP significantly increased the expression of MHC-II on SPM but not LPM, suggesting that SPM are more efficient at antigen presentation. TriDAP decreased the expression of both CD80 and CD86 by LPM, which may affect their ability to activate T-cells.

In addition to co-stimulatory molecules, APCs can produce co-inhibitory molecules to suppress T-cell activation. Programmed death ligand 2 (PD-L2) has been shown to inhibit T-cell proliferation and is a marker for M2 macrophage activation [327]. Dectin-1, a PRR which recognises fungal PAMPs, is also a marker for M2 macrophages [328]. It has been suggested that LPM and SPM macrophages can be categorised as M2 and M1 macrophages, respectively [326]. Therefore the present study examined the expression of the M2 markers PD-L2 and dectin-1 after TriDAP administration. PEC from mice injected with PBS or TriDAP were surface-stained with antibodies specific for CD11b, F480, Ly6G, Ly6C, MHC-II, dectin-1 and PD-L2 and analysed by flow cytometry. The populations of LPM and SPM were gated as described in Fig 5.1.

LPM expressed significantly higher amounts of both PD-L2 and dectin-1 in comparison with SPM (Fig 5.9). The average MFI of PD-L2 was 80% lower in SPM in comparison with LPM (Fig 5.9; $P < 0.001$). Similarly, the average MFI of dectin 1 was 69% lower in SPM in comparison with LPM (Fig 5.9; $P < 0.001$). TriDAP had no effect on the expression of dectin-1 by either LPM or SPM (Fig 5.9). TriDAP had no effect on the expression of PD-L2 by LPM; however, the expression of PD-L2 by SPM was significantly increased in response to TriDAP administration (Fig 5.9; $P < 0.01$ in comparison with PBS-treated mice). In summary, LPM expressed an increased level of the markers of M2 activation, dectin-1 and PD-L2, in comparison with SPM. In addition, TriDAP increased the expression of PD-L2 by SPM.

5.2.5 Injection of TriDAP induces the proliferation of LPM and SPM.

Having established that TriDAP can significantly increase the number of LPM in the peritoneal cavity, this study examined whether TriDAP induces the proliferation of these macrophages. Nguyen et al argue that under the right circumstances, monocytes can differentiate into LPM [109], however, a conflicting report showed that the replenishment of LPM in the peritoneal cavity is not due to their differentiation from either SPM or recruited monocytes [100]. Furthermore, Jenkins et al have shown that expansion of the LPM population in response to *L. sigmodontis* infection is not dependent on monocyte differentiation, but rather IL-4-dependent proliferation of the LPM [325]. IL-4c is a complex of recombinant IL-4 and α-IL4 antibody, which increases the half life of recombinant IL-4 in vivo. When injected into the peritoneal cavity IL-4c causes the proliferation of LPM [325]. To investigate TriDAP-induced LPM proliferation, C57BL/6 mice were injected with PBS or TriDAP on d 0, 1, 2 and 3. Another group of mice were injected with IL-4c on d 0 and 2, as a positive control for in situ LPM proliferation. Mice were sacrificed on d 4 and the peritoneal cavity was lavaged with ice-cold PBS. Cells were counted and surface-stained with antibodies specific for CD19, CD11b, F480, Ly6C, Ly6G and MHC-II. Cells were then stained intra-nuclearly with an antibody specific for Ki67. Ki67 is a protein involved in the cell cycle and is expressed in cells that are undergoing cell division [329].

Consistent with the data shown in Fig 5.6 and Fig 5.7, administration of TriDAP significantly increased the number of SPM (Fig 5.10; $P < 0.05$ in comparison with PBS

controls) and significantly increased the percentage and absolute number of LPM (Fig 5.10; $P < 0.01$ in comparison with PBS controls). Consistent with the literature, IL-4c induced a significant increase in the percentage of LPM in the peritoneal cavity; the percentage of LPM was increased by 15% in comparison with mice injected with PBS (Fig 5.10; $P < 0.05$). Furthermore, IL-4c increased the absolute numbers of LPM in the peritoneal cavity in comparison with mice injected with PBS (Fig 5.10; $P < 0.05$). There was no significant difference in the percentage or absolute numbers of LPM between mice injected with TriDAP and mice injected with IL-4c. However, in contrast to TriDAP, IL-4c did not induce any significant change in the percentage or absolute numbers of SPM in the peritoneal cavity (Fig 3.8). As shown previously, TriDAP did not change the percentage or absolute numbers of eosinophils in comparison with mice injected with PBS, however, IL-4c increased the percentage of eosinophils by 4% in comparison with PBS injected mice (Fig 5.10; $P < 0.05$).

Consistent with published findings, IL-4c increased the expression of Ki67 by LPM in comparison with mice injected with PBS (Fig 5.11; $P < 0.05$). Similarly, TriDAP increased the expression of Ki67 by LPM in comparison with mice injected with PBS (Fig 5.11; $P < 0.05$). The increase in Ki67 expression in response to TriDAP was comparable to that induced by IL-4c (Fig 5.11). Interestingly, SPM from mice injected with TriDAP had significantly increased expression of Ki67 in comparison with mice injected with PBS or IL-4c (Fig 5.11; $P < 0.05$).

In summary, TriDAP increased the percentage and absolute numbers of LPM and this was associated with an increase in Ki67 expression in LPM. TriDAP increased the expression of Ki67 by LPM as effectively as the positive control, IL-4c. Interestingly, TriDAP also increased the number of SPM in the peritoneal cavity. In addition, SPM expressed higher levels of Ki67 in response to TriDAP, establishing that TriDAP induces the proliferation of both SPM and LPM. These findings suggest that the increase in macrophages observed in the peritoneal cavity in response to TriDAP is due to the in situ proliferation of the cells rather than recruitment and de novo differentiation from monocytes.

5.2.6 The expression of the M2 markers relm-α and YM1 by LPM and SPM.

Macrophage activation can be split into two broad categories, M1 and M2 activation. M2 macrophages express several characteristic markers including relm-α and YM1 [330]. Several studies have attempted to categorise SPM and LPM as M1 or M2 macrophages, respectively. Spence et al showed that LPM can express the M2 marker YM1, whereas SPM express the M1 marker NOS2 [326]. Furthermore, Jenkins et al established that LPM can proliferate and express relm-α and YM1 in response to injection of IL-4 into the peritoneal cavity [325]. As shown in Fig 5.10, TriDAP injections increase the number of LPM in the peritoneal cavity to a similar extent as injections of IL-4. This study also showed that LPM constitutively express the M2 markers PD-L2 and dectin-1 (Fig 5.9). In order to assess if LPM are M2-like, this study compared the expression of relm-α and YM1 by LPM and SPM. In addition, the effect of TriDAP and LPS on relm-α and YM1 was investigated. C57BL/6 mice were injected with PBS, TriDAP or LPS on d 0, 1, 2 and 3. Mice were sacrificed on d 4 and the peritoneal cavity was lavaged with ice-cold PBS. Cells were incubated with brefaldin A for 5 h and then surface-stained with antibodies specific for CD19, CD11b, F480, Ly6C, Ly6G and MHC-II and stained intracellularly with antibodies specific for relm-α and YM1.

Relm-α and YM1 were both expressed by LPM from mice injected with PBS, as indicated by the significant difference in MFI in comparison with the FMO controls for YM1 and relm-α (Fig 5.12 A; $P < 0.01$ and $P < 0.001$, respectively). SPM did not express YM1 (Fig 5.12). SPM also express relm-α, indicated by the significant difference in MFI in comparison with the FMO control, but importantly, LPM expressed significantly more relm-α and YM1 when compared with SPM (Fig 5.12A; both $P < 0.001$).

While both TriDAP and LPS injections decreased the expression of YM1 in LPM, neither change was significant (Fig 5.12). LPS decreased the expression of relm-α by LPM by 63% (Fig 5.12; $P < 0.01$ in comparison with PBS controls) and the expression of relm-α by SPM by 35% (Fig 5.12; $P < 0.05$ in comparison with PBS injected controls). However, TriDAP had no effect on the expression of relm-α in either LPM or SPM (Fig 5.12).

In summary, LPM constitutively expressed the markers of M2 activation relm-α and YM1. As LPM are the dominant macrophage population at rest, this result indicates that the peritoneal cavity is a predominantly M2 environment during the steady state. TriDAP had

no effect on the expression of the M2 markers by LPM but maintained the expression of relm-α by SPM. In contrast, LPS decreased the expression of relm-α in both LPM and SPM. Consistent with the depletion of LPM in response to LPS (Fig 5.3,6 and 7), these results indicate that LPS shifts the resting equilibrium from an M2 phenotype to an M1 phenotype.

5.2.7 The effect of TriDAP on the expression of M2 and M1 associated mRNA

This study has demonstrated that in vivo administration of TriDAP expands the population of LPM, whereas i.p. injection of LPS reduces the number of LPM in the peritoneal cavity (Fig 5.5 and 5.6). Consistent with recent reports, the present study demonstrated that LPM expresses two markers of M2 activation, relm-α and YM1. Therefore it is possible that TriDAP expands the numbers of M2-like LPM, thereby enhancing the expression of M2 associated proteins by PEC, while LPS may cause a shift towards a predominantly M1 environment by reducing LPM and expanding SPM. To investigate this hypothesis, the expression of M2 markers arginase, relm-α, TGF-β and IL-10 by PEC were compared with the expression of M1 markers NOS2, IL-12, TNF-α and IL-1β using RT-PCR. C57BL/6 mice were injected i.p. with PBS, TriDAP or LPS on d 0, 1, 2 and 3. Mice were sacrificed on d 4 and the peritoneal cavity was lavaged with ice-cold PBS. RNA was isolated from the total PEC and converted into cDNA by reverse-transcription. The relative quantification of specific mRNA was measured using real-time PCR. Results were expressed relative to cells from PBS injected mice.

The injection of LPS into the peritoneal cavity induced a significant increase in the expression of M1 markers in comparison with mice injected with either PBS or TriDAP, with a 500-fold increase in the expression of NOS2 mRNA (Fig 5.13; $P < 0.01$). Furthermore, LPS significantly increased IL-12p40 mRNA expression by a factor of 6 ($P < 0.01$), increased TNF-α mRNA expression by a factor of 250 ($P < 0.001$) and increased IL-1β mRNA expression by a factor of 1600 ($P < 0.001$) in comparison with PBS controls (Fig 5.13). In contrast, TriDAP did not significantly change the expression of any of the M1 markers investigated (Fig 5.13).

TriDAP increased the expression of relm-α mRNA by a factor of 2 in comparison with PBS controls (Fig 5.13). In contrast, relm-α mRNA expression was decreased following LPS injection and was significantly lower in comparison with TriDAP injected mice (Fig 5.13; P

< 0.001). Injection of either LPS or TriDAP increased the expression of arginase mRNA by a factor of 20 in comparison with PBS controls (Fig 5.13; $P < 0.05$). Both TriDAP and LPS marginally increased the expression of TGF-β mRNA but the differences observed were not statistically significant. TriDAP marginally increased the expression of IL-10 in comparison with PBS injected mice, however, LPS increased the expression of IL-10 by a factor of 60 in comparison with PBS injected controls (Fig 5.13; $P < 0.01$).

The spleens of mice injected with TriDAP or LPS were harvested to investigate any changes in the expression of M2 and M1 markers. RNA was harvested from the splenocytes of mice injected with PBS, TriDAP or LPS. TriDAP administration significantly increased the expression of IL-10 by a factor of 3 and relm-α by a factor of 2 in comparison with PBS-treated controls (Fig 5.14; $P < 0.001$ and $P < 0.01$, respectively). In addition, TriDAP had no effect on the expression of NOS2 or IL-12p40 mRNA. LPS decreased the expression of relm-α and significantly increased the expression of IL-10 by a factor of 2 in comparison to PBS-injected mice (Fig 5.14; $P < 0.05$). LPS had no effect on the expression of NOS2 or IL-12p40 mRNA (Fig 5.14).

This study demonstrates that LPS can potently increase the expression of M1 markers in the PEC. The increase could be mediated in two different ways; LPS may directly induce the expression of M1 markers by macrophages, or LPS may shift the balance towards an M1 phenotype indirectly by decreasing the numbers of M2-like LPM in the PEC, as shown in Fig 5.7. TriDAP increased the expression of arginase without increasing any of the M1 markers. Furthermore, while LPS decreased the expression of relm-α, TriDAP maintained its expression. It is not possible to conclude from this data whether TriDAP is increasing the expression of the markers or merely increasing the numbers of macrophages that express these markers constitutively. Therefore, LPM were sorted from mice injected with TriDAP or LPS on d 0, 1, 2 and 3, and the expression of M1 and M2 markers were compared to PBS injected mice. Mice were sacrificed on d 4 and the peritoneal cavity was lavaged with ice-cold PBS. The single cell suspension was surface-stained with antibodies specific for F480, CD11b, MHC-II and GR1. $F480^{hi}CD11b^{hi}GR1^{-}MHC\text{-}II^{-}$ LPM were sorted by FACS (Fig 5.2.1). RNA was isolated from the purified cells and converted to cDNA. The numbers of LPM obtained from LPS-injected mice were too low to isolate sufficient RNA. The expression of M1 markers NOS2, IL-12 and IL-1β, and the expression of M2 markers arginase, relm-α and IL-10 were quantified relative to the PBS controls using RT-PCR.

LPM from TriDAP-injected mice increased the expression of arginase mRNA by a factor of 9 (Fig 5.15; $P < 0.01$), increased the expression of relm-α mRNA by a factor of 4 (Fig 5.15; $P < 0.05$) and increased the expression of IL-10 mRNA by a factor of 3 in comparison with PBS controls (Fig 5.15; $P < 0.05$). Furthermore, TriDAP did not significantly change the expression of IL-12p40 or IL-1β mRNA by LPM (Fig 5.15). The expression of NOS2 could not be detected by LPM from mice injected with either PBS or TriDAP (Fig 5.15).

Consistent with our previous results (Fig 5.12), this study suggests that the M2 marker relm-α is constitutively expressed by LPM and that injection of LPS can reduce this expression significantly. This study established that TriDAP can increase the expression of M2 markers by LPM in vivo, while leaving the expression of M1 markers unaffected. Conversely, LPS reduced the number of LPM and increased the expression of M1 markers in the PEC. Taken together, these experiments establish LPM as an M2-like macrophage population and suggest a role for NOD1 in their activation and expansion. In addition, administration of TriDAP i.p. increased the expression of relm-α and IL-10 in the spleen, suggesting that NOD1 activation may be eliciting a systemic effect on M2-macrophage activation.

5.2.8 The role of IL-4 in the TriDAP-induced expansion and M2 activation of LPM

IL-4 is a cytokine involved in the differentiation of Th2 cells and is produced by Th2 cells themselves. IL-4 also mediates the activation of M2 macrophages, inducing the expression of arginase, relm-α, IL-10 and IL-4 [134, 139]. IL-4 can induce LPM to proliferate and produce M2 markers such as relm-α [325]. A number of studies have implicated NOD1 activation in enhancing Th2 responses [214, 215], and we have shown in chapter 4 that TriDAP-treated PEC can induce the production of IL-4 by $CD4^+$ T-cells (Fig 4.10 and 4.11). It is possible that the expansion of LPM in response to TriDAP is dependent on IL-4 production, and that IL-4 was responsible for the TriDAP-mediated M2 activation of LPM. To test this hypothesis, C57BL/6 mice were injected with either PBS or TriDAP on d 0, 1, 2 and d 3. An additional group of mice were injected with TriDAP on d 0, 1, 2 and 3 and also injected with an IL-4 neutralising antibody (αIL-4) on d 0 and 2. Mice were sacrificed on d 4 and the peritoneal cavity was lavaged with ice-cold PBS. Cells were surface-stained with antibodies specific for F480, CD11b, Ly6C, Ly6G and MHC-II and analysed by flow cytometry. The populations of various cell types were analysed using the

gating strategy shown in Fig 5.1. The expression of M2 markers by LPM was also investigated by real-time-PCR. PEC were surface-stained with antibodies specific for F480, CD11b, MHC-II and GR1. $F480^{hi}CD11b^{hi}GR1^{-}MHC\text{-}II^{-}$ LPM were sorted by FACS using the gating strategy explained in Fig 5.2.1. RNA was isolated from the cells and converted to cDNA. The expression of M1 markers NOS2, IL-12p40, TNF-α and IL-1β as well as the expression of M2 markers arginase, relm-α, IL-10 and IL-4 were quantified using RT-PCR relative to the PBS injected controls.

Consistent with the earlier results, TriDAP significantly increased the percentage and numbers of LPM in the peritoneal cavity (Fig 5.16 and Fig 5.17; $P < 0.05$). Mice injected with a combination of TriDAP and αIL-4 had a smaller percentage and absolute number of LPM in the peritoneal cavity in comparison with mice injected with TriDAP alone, however, the difference was not significant (Fig 5.16 and Fig 5.17). In comparison with PBS-treated controls, TriDAP did not significantly increase the percentage of LPM in the presence of αIL-4 (Fig 5.16). While the addition of αIL-4 did not significantly reduce the TriDAP-mediated expansion of LPM, the small decrease in the percentage of LPM may indicate that IL-4 is playing some role.

Consistent with data shown in Fig 5.15, LPM from mice injected with TriDAP increased the expression of arginase mRNA and relm-α mRNA in comparison with LPM from PBS treated controls (Fig 5.18; $P < 0.01$). The TriDAP-induced expression of relm-α was significantly decreased to background levels in the presence of αIL-4 (Fig 5.18; $P < 0.05$). Similarly, TriDAP-mediated expression of arginase was reduced in the presence of αIL-4 (Fig 5.18). These results suggests that the TriDAP-induced expression of relm-α by LPM is dependent on IL-4 production. TriDAP increased LPM expression of IL-4 by a factor of 174 in comparison with LPM from PBS controls (Fig 5.18; $P < 0.05$), and this was significantly reduced in the presence of αIL-4 ($P < 0.05$; Fig 5.18). This suggests that IL-4 may establish an autocrine positive feedback loop in response to TriDAP. Consistent with the results shown in Fig 5.15, TriDAP did not significantly change the expression of TNF-α, IL-1β and IL-12p40 mRNA by LPM (Fig 5.18). Furthermore, TriDAP injection significantly decreased the expression of NOS2 in comparison with PBS controls (Fig 5.18; $P < 0.05$). Interestingly, the injection of TriDAP in combination with αIL-4 significantly increased IL-12p40 and IL-1β expressed in comparison with LPM from PBS injected mice (Fig 5.18; $P < 0.01$ and $P < 0.05$, respectively). Furthermore, the addition of αIL-4 significantly increased the TriDAP

induced expression of IL-1β in comparison with LPM from mice injected with TriDAP alone (Fig 5.18; $P < 0.05$). This data suggests that IL-4 can inhibit the production of these M1 markers.

PEC obtained from naive mice contain a large percentage of LPM (Fig 5.1), therefore, it is possible that TriDAP may induce IL-4 production from total PEC in vitro, which may activate macrophages to produce M2 markers, such as relm-α. To test this hypothesis PEC were incubated in the presence or absence of TriDAP or LPS. After 24 h RNA was isolated from the cells and converted to cDNA by reverse transcription. The expression of relm-α and IL-4 mRNA was measured by real-time PCR and normalised relative to the untreated control cells.

Neither TriDAP nor LPS had any effect on the expression of IL-4 mRNA by PEC (Fig 5.19). This result is consistent with previous data that indicates that IL-4 protein cannot be detected in the supernatant of TriDAP-treated PEC (Fig 4.5). Interestingly, both LPS and TriDAP significantly reduced the expression of relm-α mRNA (Fig 5.19; $P < 0.001$). These data indicate that IL-4 cannot be expressed by PEC in response to TriDAP in vitro. In addition, relm-α expression by PEC, which has been shown to be expressed in response to TriDAP in vivo, was decreased in response to TriDAP in vitro.

Arginase has been shown to be expressed in an IL-4 independent manner [331], therefore it is possible that TriDAP may mediate arginase expression in vitro, even in the absence of IL-4 production. To investigate this hypothesis PEC were cultured in vitro in the presence or absence of TriDAP or LPS and the expression of arginase was measured by real-time PCR. The expression of NOS2 was also measured as a control for M1 activation. The data discussed in chapter 4 showed that TriDAP-mediated cytokine production was dependent on p38, therefore PEC were also incubated with or without a p38 inhibitor (SB203508) in an attempt to block NOD1-mediated arginase expression. The p38 inhibitor was dissolved in DMSO, thus, DMSO was used as a vehicle control. After 24 h RNA was isolated from the cultured cells and converted to cDNA by reverse transcription. The expression of arginase and NOS2 mRNA was measured by real-time PCR and normalised relative to the untreated vehicle controls.

LPS induced an 11000 fold increase in the expression of NOS2 mRNA by PEC in comparison with untreated controls (Fig 5.20; $P < 0.001$). The increase of NOS2 mRNA

expression in response to LPS was significantly reduced in the presence of a p38 inhibitor (Fig 5.20; $P < 0.001$), however, the expression of NOS2 was still 5000 fold higher than the expression by untreated PEC (Fig 5.20; $P < 0.001$). TriDAP had no effect on the expression of NOS2 mRNA by PEC in comparison with untreated controls. LPS increased arginase mRNA expression by a factor of 30 in comparison with untreated controls (Fig 5.20; $P < 0.001$). The LPS-induced increase in arginase mRNA was reduced by 30% in the presence of a p38 inhibitor ($P < 0.001$), however the expression of arginase mRNA was still significantly increased in comparison with untreated controls (Fig 5.20; $P < 0.001$). This result indicates that LPS-induced arginase production is not completely dependent on p38. TriDAP increased arginase mRNA expression by a factor of 12 in comparison with untreated controls (Fig 5.20; $P < 0.001$). The addition of a p38 inhibitor reduced the expression of arginase in response to TriDAP to background levels (Fig 5.20).

These results demonstrate that administration of TriDAP in vivo induces the production of IL-4 by LPM. Although IL-4 has been shown to drive the proliferation of LPM (Fig 5.11), this study suggests that IL-4 is only partially responsible for the expansion of LPM in response to TriDAP. However, IL-4 is required for LPM to produce M2 markers in response to TriDAP. These data suggest that IL-4 is polarising LPM towards an M2 phenotype in two ways; firstly, IL-4 induces the expression of arginase, and relm-α, and secondly, by blocking the production of IL-1β in response to TriDAP. In addition, these results suggest that IL-4 may establish an autocrine positive feedback loop in response to TriDAP, which induces the production of additional IL-4. This process was only observed in vivo; stimulation of PEC with TriDAP in vitro did not elicit an increase in IL-4 mRNA expression. TriDAP induced the production of arginase in vitro in a p38 dependent manner, but not relm-α. This indicates that TriDAP only induces IL-4 and relm-α expression in vivo. It is possible that TriDAP-mediated IL-4 is dependent on indirect stimulation via bystander cells, which are absent in vitro.

5.2.9 The role of IL-10 in the TriDAP-induced expansion and M2 activation of LPM

The origin of LPM is still poorly understood. Our data and the data compiled by Jenkins et al indicate that LPM can proliferate in vivo [325], however, Nguyen et al argue that LPM differentiate from inflammatory monocytes under the correct conditions [109]. Monocytes normally differentiate into SPM during an inflammatory response but preferentially differentiate into LPM in the presence of IL-10. Although IL-4 is the classical activator of M2 macrophages, recent studies have shown that IL-10 can also induce the polarisation of macrophages towards an M2 phenotype [129, 143]. For example, *M. tuberculosis* has been shown to propagate M2 macrophages via autocrine IL-10 production [143]. As established in chapter 4, PEC can produce IL-10 in response to TriDAP, therefore it is possible that TriDAP-induced IL-10 may play a role in the expansion and activation of M2-like LPM by inducing the differentiation of infiltrating monocytes. This hypothesis was investigated by injecting WT C57BL/6 and IL-$10^{-/-}$ C57BL/6 mice with PBS or TriDAP on d 0, 1, 2 and 3 and quantifying the numbers of LPM in the peritoneal cavity. Another group of mice were injected in similar manner with LPS, which induces IL-10 production, but results in the differentiation of SPM rather than LPM. Mice were sacrificed on d 4 and the peritoneal cavity was lavaged using ice-cold PBS. Cells were surface-stained with antibodies specific for F480, Ly6G, Ly6C, CD11b and MHC-II. The cells were then analysed by flow cytometry.

As shown previously (Fig 5.6 and 5.7), administration of TriDAP increased the percentage and absolute numbers of LPM in the peritoneal cavity in comparison with PBS-injected mice (Fig 5.21A-C; $P< 0.001$ and $P < 0.05$, respectively). In contrast, TriDAP did not increase the percentage of LPM in IL-$10^{-/-}$ mice (Fig 5.21A and B; $P < 0.001$ in comparison with WT mice). Furthermore, there was no significant difference between the numbers of LPM in WT controls and IL-$10^{-/-}$ mice injected with TriDAP (Fig 5.21C). This suggests that the increase in number and percentage of LPM in response to TriDAP is dependent on IL-10. Consistent with previous results (Fig 5.6 and Fig 5.7), TriDAP increased the percentage and absolute number of SPM in the peritoneal cavity in comparison with PBS-injected mice (Fig 5.21A-C; $P < 0.01$ and $P < 0.001$, respectively). However, the absence of IL-10 did not significantly affect the TriDAP-mediated increase in percentage or number of SPM (Fig 5.21A-C). As shown previously (Fig.5.6 and Fig.5.7), administration of TriDAP has no significant effect on the percentage or number of neutrophils or eosinophils in

comparison with PBS injected mice (Fig 5.21B and C). However, the absolute number of eosinophils was increased in response to TriDAP in IL-10$^{-/-}$ mice, suggesting that IL-10 inhibits the proliferation or recruitment of eosinophils in response to TriDAP (Fig 5.21C).

Consistent with previous results, LPS increased the percentage of SPM in WT mice by an average of 5% in comparison with PBS-injected mice (Fig 5.21A and B; $P < 0.05$). In contrast to TriDAP-treated mice, the LPS-induced increase in the number of SPM was significantly enhanced in IL-10$^{-/-}$ mice in comparison with WT mice (Fig 5.21C; $P < 0.001$). LPS decreased the percentage and number of LPM in the peritoneal cavity, but the differences were not significant (Fig 5.21B and C). In contrast, LPS increased the numbers of LPM in IL-10$^{-/-}$ mice (Fig 5.22C; $P < 0.01$). Consistent with previous results (Fig 5.6 and Fig 5.7), the administration of LPS increased the percentage of neutrophils in the peritoneal cavity by an average of 7% in comparison with PBS-injected mice (Fig 5.21B; $P < 0.001$). LPS also increased the numbers of neutrophils in WT mice in comparison with PBS-injected mice (Fig 5.21C; $P< 0.001$). LPS recruited significantly more neutrophils to the peritoneal cavity in IL-10$^{-/-}$ mice compared with WT mice, increasing the percentage of neutrophils by an average of 13% and increasing their numbers by a factor of 10 (Fig 5.21B and C; $P < 0.001$).

IL-10 has been characterised as an M2 polarising cytokine [143, 332], therefore an experiment was designed to investigate the expression of M1 and M2 markers in the PEC of WT and IL-10$^{-/-}$ mice in response to TriDAP and LPS. WT C57BL/6 and IL-10$^{-/-}$ C57BL/6 mice were injected with PBS, TriDAP or LPS on d 0, 1, 2 and 3. Mice were sacrificed on d 4 and RNA was isolated from the PEC. The expression of M1 markers NOS2 and IL-1β mRNA and the expression of M2 markers arginase and relm-α mRNA were quantified using RT-PCR, and the data was normalised relative to WT mice injected with PBS.

As shown previously (Fig 5.13), TriDAP increased the expression of M2 markers arginase and relm-α by PEC from WT mice (Fig 5.22; $P < 0.01$). Furthermore, TriDAP did not significantly change the expression of M1 markers NOS2 and IL-1β in WT mice (Fig 5.22). In contrast, WT mice that were injected with LPS had non-significantly increased expression of NOS2 and IL-1β mRNA in comparison with PBS-treated controls (Fig 5.22). Basal relm-α expression was increased in IL-10$^{-/-}$ mice in the absence of any stimulus, suggesting an inhibitory role for IL-10 in the expression of relm-α (Fig 5.22). There was no

difference in the expression of relm-α between the WT and IL-10$^{-/-}$ mice in response to the administration of TriDAP (Fig 5.22), however, the high basal expression of relm-α observed in IL-10$^{-/-}$ mice was reduced in response to LPS. LPS-mediated NOS2 and IL-1β expression was enhanced in IL-10$^{-/-}$ mice, indicating that IL-10 has a role in suppressing the production of these M1 markers (Fig 5.23; $P < 0.01$ and $P < 0.001$, respectively). Interestingly, the TriDAP and LPS-mediated expression of arginase was enhanced in the absence of IL-10 (Fig 5.22; $P < 0.05$ and $P < 0.001$ in comparison with WT mice, respectively).

Having established that IL-10 is necessary for the TriDAP-mediated expansion of LPM (Fig 5.21A-C), an experiment was designed to investigate the effect of recombinant IL-10 on the populations of LPM and SPM in the peritoneal cavity. C57BL/6 mice were injected with either PBS or recombinant IL-10 on d 0 and d 2. The mice were sacrificed on d 4 and the peritoneal cavities were lavaged. PEC were surface-stained with antibodies specific for F480, Ly6G, Ly6C, CD11b and MHC-II. The populations of LPM and SPM were then analysed by flow cytometry using the gating strategy shown in Fig 5.1.

The administration of IL-10 significantly reduced the total numbers of cells in the peritoneal cavity in comparison with PBS-injected mice (Fig 5.23 A; $P < 0.05$). This was associated with a significant decrease in the numbers of LPM in the peritoneal cavity in comparison with PBS-injected mice (Fig 5.23 B; $P < 0.01$). IL-10 also reduced the percentages of LPM in the peritoneal cavity in comparison with PBS-injected mice (Fig 5.23 A and B). IL-10 had no effect on the percentage but reduced the absolute number of SPM in the peritoneal cavity in comparison with PBS-injected mice (Fig 5.23 A and B).

In summary, this study indicates that IL-10 has a suppressive effect on macrophage activation; the absence of IL-10 enhanced the expression of both M1 and M2 activation markers. The expansion of LPM in response to TriDAP was dependent on IL-10, but in contrast, the expansion of SPM in response to either TriDAP or LPS was restrained in the presence of IL-10. These results suggest that the TriDAP-mediated expansion of LPM, but not their activation, is dependent on IL-10 and provides evidence that IL-10 is an important inhibitor of SPM expansion. Recombinant IL-10 reduced the numbers of LPM in the peritoneal cavity, indicating that IL-10 alone is insufficient to expand the resident

population of LPM. Therefore, it is possible that other signals contribute to IL-10-dependent expansion of LPM in response to TriDAP.

5.2.10 The effect of TriDAP on the population of Treg cells in the peritoneal cavity

Treg cells are regulators of the immune system. Naturally occurring Treg (nTreg) cells are generated in the thymus but $CD4^+$ T-cells can also be converted to "inducible" Treg (iTreg) cells in the presence of certain ligands. These cells dampen inflammation and suppress inappropriate immune responses. Treg cells are characterised by the expression of the transcription factor FoxP3 and surface marker CD25 [333]. Studies have shown that macrophages can polarise $CD4^+$ T-cells into iTreg cells by the secretion of mediators such as retinoic acid, TGF-β and IL-10. M2 macrophages are also involved in the regulation of inflammation and are effective at generating iTreg cells [173, 326, 334]. It is possible that by expanding and activating M2 macrophages in the PEC, TriDAP may also expand a population of Treg cells. Conversely, LPS may deplete the population of Treg cells indirectly by depleting the population of M2 macrophages. C57BL/6 mice were injected i.p. with PBS, TriDAP or LPS on d 0, 1, 2 and 3. Mice were sacrificed on d 4 and the peritoneal cavity was lavaged with ice-cold PBS. The PEC were surface stained with antibodies specific for CD4 and CD25 and stained intra-nuclearly with a FoxP3-specific antibody. The cells were then analysed by flow cytometry.

Approximately 10% of the $CD4^+$ cells in the peritoneal cavity of mice injected with PBS were $CD25^+FoxP3^+$ Treg cells (Fig 5.24). TriDAP had no effect on the percentage of $CD25^+FoxP3^+$ Treg cells in the peritoneal cavity (Fig 5.24). LPS reduced the percentage of $CD25^+FoxP3^+$ Treg cells in the peritoneal cavity, but the change was not statistically significant (Fig 5.24). This data indicates that the injection of TriDAP or LPS has no significant effect on the percentage of Treg cells in the peritoneal cavity.

5.2.11 The effect of TriDAP on the ability of LPM to present antigen

LPM express less MHC-II than SPM, hence, are less capable of presenting antigen to a T-cell [109]. M2 macrophages have been shown to actively suppress the induction of adaptive immunity via the production of arginase and relm-α [159, 172, 323]. We have shown that TriDAP can expand a population of LPM which express the markers of M2 activation, therefore, an experiment was designed to investigate the effect of TriDAP on the ability of LPM to present antigen and induce T-cell proliferation. BALB/c mice were

injected i.p. with either PBS or TriDAP on d 0, 1, 2 and 3. The mice were sacrificed on d 4 and the peritoneal cavity was flushed with ice-cold PBS. The cells were surface-stained with antibodies specific for F480, GR1, CD11b and MHC-II. LPM ($F480^{+}CD11b^{+}GR1^{-}MHC\text{-}II^{-}$ cells) were purified by FACS using the gating strategy shown in Fig 5.2.1. The LPM were cultured with CTV-labeled OVA-specific $CD4^{+}$ T-cells purified from the spleen of a BALB/c DO-II transgenic mouse. The LPM and $CD4^{+}$ T-cells were cultured in the presence or absence of OVA for 72 h. The cells were harvested and stained with CD3 and CD4 specific antibodies and analysed by flow cytometry. The proliferation of $CD4^{+}$ T-cells was measured by the dilution of CTV staining.

LPM, from either PBS or TriDAP injected mice, did not induce the proliferation of $CD4^{+}$ T-cells in the absence of OVA (Fig 5.25). LPM from PBS-treated mice induced the proliferation of OVA-specific $CD4^{+}$ T-cells; 16% of $CD4^{+}$ T-cells underwent CTV dilution in response to co-culture with OVA and LPM (Fig 5.25). TriDAP treatment in vivo reduced the ability of LPM to induce proliferation of $CD4^{+}$ T-cells; only 4.9% of $CD4^{+}$ T-cells underwent CTV dilution in response to co-culture with OVA and LPM from TriDAP-treated mice (Fig 5.25). This data suggests that TriDAP expands a population of LPM that are less capable of presenting antigen, and therefore less capable of activating T-cells, in comparison with an LPM from a PBS-treated mouse.

5.2.12 The effect of macrophage transfer on the clinical symptoms of EAE.

LPM are the dominant resident macrophage in the peritoneal cavity and are thought to help maintain homeostatic equilibrium by engulfing apoptotic cells and suppressing excess inflammation [109, 326]. Consistent with the literature [326], this study showed that LPM constitutively express relm-α, an M2 activation marker which actively suppresses T-cell responses [159]. The administration of TriDAP expands this population of macrophages and induces the expression of arginase, relm-α and IL-10 (Fig 5.15). In addition, TriDAP administration reduces the ability of LPM to activate T-cells (Fig 5.25).LPS reduced the population of M2-like LPM, expanded the more pro-inflammatory M1-like SPM [100, 326] and induced the expression of M1 markers NOS2, IL-1β and IL-12 (Fig 5.6, 5.7 and 5.13).

M2-like macrophages have been shown to be immunosuppressive; Jiang et al showed that transfer of M2 macrophages could suppress the clinical symptoms of EAE and

associated pathogenic IL-17 and IFN-γ producing T-cells [183]. M1 macrophages produce IL-12 and IL-1β which are essential for the generation of pathogenic Th1 and Th17 T-cell responses during EAE [41]. Therefore an experiment was designed to examine the effect of TriDAP- or LPS-expanded macrophages on the course of EAE, using a cell transfer approach. Macrophages from mice injected with IL-4c were transferred as a positive control for M2 macrophages. C57BL/6 mice were injected with PBS, TriDAP or LPS on d 0 1, 2 and 3. An additional group of mice were injected with IL-4c on d 0 and 2. The mice were sacrificed on d 4 and the peritoneal cavity was lavaged with ice-cold PBS. The cells were surface stained with antibodies specific for F480, CD11b and GR1. Macrophages ($F480^+CD11b^+GR1^-$ cells) were purified by FACS using the gating strategy shown in Fig 5.2.2. EAE was induced in C57BL/6 mice by the s.c. injection of an emulsion of MOG and CFA. In addition, immunized mice were injected i.p. with PT on d 0 and d 2. Macrophages were injected s.c. ($1x10^6$/mouse) on d 0 and d 6 post EAE induction. A separate group of mice were injected with PBS on d 0 and d 6 post EAE induction as a control. Mice were weighed daily and observed for changes in clinical score.

The incidence of disease in the PBS control group was 88%. Clinical symptoms were first observed on d 7 and mice reached the peak of disease at d 15 with an average clinical score of 3.4 (Fig 5.26A). The severity of disease was associated with weight loss; on d 14 control mice had lost an average of 18% of their starting body weight (Fig 5.26A). 89% of macrophages from mice injected with PBS (PBS MΦ) were LPM (Fig 5.26B). The incidence of disease in mice injected with PBS MΦ was 83%. Clinical symptoms were observed on d 8 and peaked at d 15 with an average clinical score of 3 (Fig 5.26A). Injection of PBS MΦ reduced clinical scores on d 9 to d 15, reaching statistical significance on d 10 and 11 (Fig 5.26A; $P < 0.01$ in comparison with PBS-injected controls). The injection of PBS MΦ reduced weight loss, and this reached statistical significance on d 10 to 13 (Fig 5.26A; $P < 0.001$ in comparison with PBS-injected controls). On d 14 mice had lost an average of 5% of their body weight, a threefold reduction in weight loss in comparison with PBS-injected mice.

77% of macrophages from mice injected with TriDAP (TriDAP MΦ) were LPM (Fig 5.26B). The incidence of disease in mice injected with TriDAP MΦ was 83%. Clinical symptoms were first observed on d 8, and mice reached the peak of disease on d 15 with an average clinical score of 3.1 (Fig 5.2A). The injection of TriDAP MΦ reduced the average clinical

score in comparison with PBS-injected controls. In addition, there was no significant difference in clinical score between mice injected with either TriDAP MΦ or PBS MΦ. Mice injected with TriDAP MΦ had lost 12% of their starting body weight by d 14, a reduction of 6% in comparison with PBS-injected controls (Fig 5.26A).

25% of macrophages from mice injected with LPS (LPS MΦ) were LPM and 57% were SPM (Fig 5.26B). The incidence of disease in mice injected with LPS MΦ was 100%. Clinical symptoms were first observed on d 9 and peaked on d 15 with an average clinical score of 4 (Fig 5.26A). LPS MΦ initially reduced the average clinical score in comparison with PBS-injected controls, however, by d 10 mice injected with LPS MΦ had developed more severe symptoms, as indicated by an increased average clinical score (Fig 5.26A). A similar trend was observed in weight loss; initially LPS MΦ caused a reduction in weight loss, however, by d 13 mice injected with LPS MΦ had increased weight loss in comparison with PBS-injected controls (Fig 5.26A). Mice injected with LPS MΦ had lost 22% of their starting body weight by d 14; an increase of 4% in comparison with PBS-injected controls, an increase of 10% in comparison with TriDAP MΦ and an increase of 16% in comparison with PBS MΦ (Fig 5.26A).

71% of macrophages from mice injected with IL-4c (IL-4c MΦ) were LPM (Fig 5.26B). The incidence of disease in mice injected with IL-4c MΦ was 60%. The clinical symptoms of EAE were first observed on d 8 and peaked on d 15 with an average clinical score of 2.2 (Fig 5.26A). IL-4c MΦ attenuated disease; mice injected with IL-4c MΦ had reduced clinical scores in comparison with PBS-injected controls (Fig 5.26A). Similarly, mice injected with IL-4c MΦ had reduced weight loss in comparison with PBS-injected controls; mice had lost 7% of their starting body weight by d 14, a reduction of 9% in comparison with PBS-injected controls (Fig 5.26A).

IL-4c MΦ were most effective at reducing the average disease score in comparison with all other treatments. However, due to large variability only the changes elicited by PBS MΦ were statistically significant. LPS MΦ significantly increased the clinical scores in comparison with IL-4c MΦ ($P < 0.05$) and PBS MΦ ($P < 0.05$), indicating a significant difference in phenotype of the respective macrophages. The differences in clinical score between mice injected with PBS MΦ, IL-4c MΦ, or TriDAP MΦ were not significant, suggesting that the macrophages are of a similar phenotype. In summary, PBS MΦ, which

are predominantly LPM, significantly attenuated the clinical symptoms of EAE in terms of weight loss and clinical score. While TriDAP MΦ and IL-4c MΦ also ameliorated disease, the variability was too high to achieve statistical significance. In contrast, LPS MΦ delayed the onset of disease but exacerbated clinical symptoms by d 12.

5.2.13 TriDAP-mediated M2 activation suppresses the development of pathogenic T-cells

The results from Chapter 1 demonstrated that the administration of TriDAP attenuated the clinical symptoms of actively induced EAE, however the mechanism was unclear. EAE can also be induced via the transfer of pathogenic MOG-specific T-cells from immunized mice to naive mice. In this model LN and spleen cells from mice immunized with MOG and CFA are restimulated in vitro with Th17 polarising cytokines, IL-1β and IL-23, in the presence of the autoantigen MOG. This method is known as passively induced EAE. This provided a useful means of assessing the effect of TriDAP on the activation of pathogenic T-cell that induce EAE.

M2 macrophages have been shown to suppress T-cell activation and proliferation via the production of arginase, relm-α and IL-10. The findings of the present study have demonstrated that TriDAP enhanced the expression of arginase and induced the production of IL-10 by peritoneal macrophages (Fig 4.9, Fig 5,15). In addition, TriDAP inhibited the ability of macrophages to present antigen to antigen-specific T-cells (Fig 5.25). Therefore it was hypothesised that TriDAP may inhibit the activation of MOG-specific cells, thus inhibiting the clinical symptoms of EAE following the transfer of these cells into naive mice.C57BL/6 mice were immunized with MOG emulsified in CFA. The mice were sacrificed on d 10 post immunisation. Brachial, auxiliary and inguinal lymph node and spleen cells were cultured with MOG, IL-1β and IL-23 in the presence or absence of TriDAP. After 72 h the cells were washed and injected i.p. into naive C57BL/6 mice. The mice were checked daily for signs of clinical symptoms or weight loss.

Stimulation of LN and spleen cells from MOG-immunized mice with MOG, IL-1β and IL-23 resulted in the production of large concentrations of IL-17, IFN-γ and IL-10 after 72 h (Fig 5.27). The addition of TriDAP did not alter IL-10 or IL-17 production but significantly reduced the production of IFN-γ (Fig 5.27; $P < 0.001$), suggesting that TriDAP inhibits the activation of IFN-γ-producing cells. Mice injected with cells reactivated in vitro in the

absence of TriDAP exhibited symptoms of disease on d 9 and reached the peak of disease at d 16 with an average clinical score of 3 (Fig 5.28). These mice lost up to 14% of their starting body weight by d 14. Mice injected with TriDAP-treated cells exhibited symptoms of disease on d 10 and reached the peak of disease at d 16 with an average clinical score of 1.2 (Fig 5.28). These mice lost up to 7% of their body weight, a reduction of 7% in comparison with control mice. This result demonstrated that administration of TriDAP in vitro during the activation of cells from MOG-immunized mice reduced the ability of these cells to induce EAE, resulting in a significant reduction of clinical scores from d 11 until sacrifice on d 17 (Fig 5.28; $P < 0.01$).

In addition, the spleens of mice with passively induced EAE were processed and incubated with increasing concentrations of MOG to investigate peripheral MOG-specific cytokine production. The production of MOG-specific IL-17 and IFN-γ was not detected in the spleens of mice injected with cells incubated with or without TriDAP. Mice injected with cells incubated with TriDAP produced high concentrations of IL-4 and IL-10 when compared with mice injected with cells incubated without TriDAP (Fig 5.29; $P < 0.001$). However, the production of IL-10 and IL-4 was not antigen-specific; the addition of increasing concentrations of MOG did not significantly increase the production of IL-10 or IL-4 (Fig 5.29).

These results suggest that TriDAP modulates the activation of cells in response to IL-1β and IL-23, leading to an increase in IL-4 and IL-10 production in vivo after the transfer of cells. TriDAP can increase the expression of arginase, relm-α and IL-10 by innate immune cells. Both IL-10 and arginase have been shown to inhibit or alter T-cell activation and may explain why TriDAP modulates the activation of pathogenic cells. To investigate this further, spleen cells were stimulated with IL-1β and IL-23 in the presence or absence of TriDAP. RNA was isolated from the cells after 24 h and real-time PCR was used to quantify the expression of arginase, relm-α and IL-10. NOS2 expression was also assessed as a measure of M1 activation.

IL-1β and IL-23 did not have an effect on the expression of IL-10, relm-α or NOS2 mRNA by spleen cells. Interestingly, incubation of spleen cells with IL-1β and IL-23 induced the expression of arginase (Fig 5.30; $P < 0.001$). Treatment of the cells with TriDAP, in combination with IL-1β and IL-23, increased the expression of arginase by a factor of 20 in

comparison with untreated spleen cells (Fig 5.30; $P < 0.001$). Similarly, TriDAP induced the expression of IL-10 by spleen cells stimulated with IL-1β and IL-23 (Fig 5.30; $P < 0.001$). The addition of TriDAP had no significant effect on the expression of NOS2 or relm-α.

Taken together, these results suggest that NOD1 activation can inhibit the ability of MOG-specific cells to produce IFN-γ and induce EAE. TriDAP-treated cells also induced increased IL-10 and IL-4 production in the periphery. Interestingly, TriDAP enhanced the expression of IL-10 and arginase by spleen cells in response to IL-1β and IL-23, which may contribute to the modulation of pathogenic immune cells.

5.2.14 Gating strategies for sorting macrophages by FACS

Fig 5.2.1 Gating strategy for sorting LPM by FACS

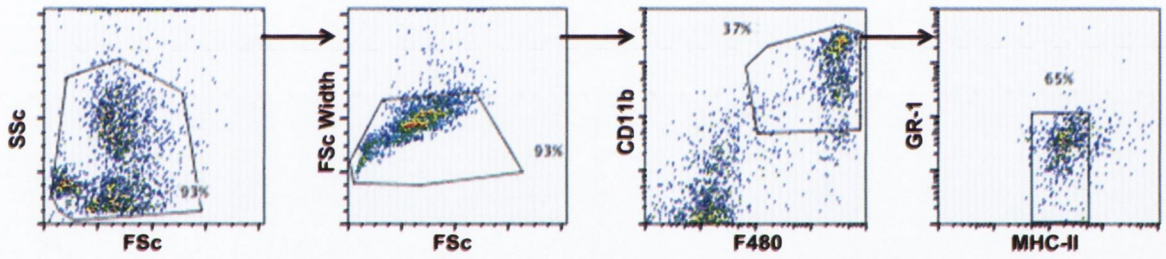

Fig 5.2.2 Gating strategy for sorting total macrophages by FACS

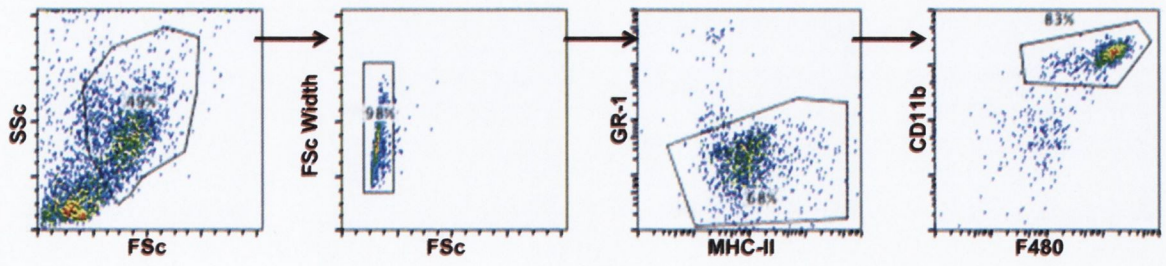

5.3 Discussion

The present study showed that i.p. injection of TriDAP induced changes in cell populations within the peritoneal cavity. While early responses to TriDAP were pro-inflammatory in nature, characterised by the influx of monocytes, TriDAP induced the proliferation of immunosuppressive LPM after 4 days. This was in contrast with the response elicited by LPS, which expanded the population of the pro-inflammatory SPM population. The TriDAP-induced expansion of LPM was dependent on IL-10, which is produced by peritoneal macrophages in response to NOD1 activation. TriDAP also induced LPM to increase the expression of relm-α, IL-10 and arginase, which are indicative of M2 activation. The increase in M2-related gene expression was dependent on IL-4, which was produced by LPM in response to TriDAP. The macrophages expanded by TriDAP were immunosuppressive, less capable of driving antigen specific T-cell responses and inhibited the symptoms of EAE when transferred into mice with disease. In contrast, macrophages transferred from LPS-treated mice exacerbated the clinical score and weight loss of mice with EAE. These results indicate that TriDAP induces the expansion of an immunosuppressive macrophage population by creating a M2 polarising environment via the production of IL-4 and IL-10. Similarly, TriDAP inhibited the activation of pathogenic IFN-γ producing immune cells and induced the production of IL-10 in the spleens of mice with EAE. This was associated with increased IL-10 and arginase expression during the activation immune cells from mice with EAE, suggesting that TriDAP may inhibit pathogenic cell activation during restimulation in vitro by inducing M2-like activation.

It has been reported that sterile inflammation can be generated upon the injection of thioglycollate [335]. The resulting inflammatory response is characterised by the depletion of resident macrophages and the influx of inflammatory monocytes and neutrophils after 16 h. In the present study, LPS injection resulted in a similar inflammatory response, characterised by the influx of neutrophils and monocytes, and the depletion of LPM. TriDAP induced a similar response by recruiting monocytes and neutrophils to the site of injection after 16 h. These findings are in agreement with studies that have shown that NOD1 agonists have a tropic effect on neutrophils by inducing the secretion of chemokines [208]. Moreover, studies show that chemokine production and inflammatory cell recruitment is compromised in NOD1-deficient mice [298, 336]. The present study also showed that TriDAP decreased the frequency of LPM in

the peritoneal cavity after 16 h. Although the mechanism behind this phenomenon is unclear, it is characteristic of the early stages of a thioglycolate-mediated inflammatory response in the peritoneal cavity [100]. While TriDAP induced classical inflammatory responses, the changes in the peritoneal cavity were significantly weaker when compared with LPS. This is consistent with the fact that NOD1 agonists are capable of inducing inflammatory responses but are weak stimulators in comparison with other PAMPs [188, 206, 278].

After the initial influx of innate immune cells, recruited monocytes differentiate into macrophages, which enhance or suppress inflammation depending on the circumstances. The characteristics of these macrophages are dictated by the stimulant, for example thioglycollate induces an expansion of pro-inflammatory SPM within the peritoneal cavity after 4 days [100, 335]. An inflammatory micro-environment can also be induced by PAMPs, such as LPS. The present study showed that LPS expanded the population of SPM within the peritoneal cavity after 4 days. This has been shown to be dependent on the presence of inflammatory monocytes, which infiltrate the peritoneal cavity during the early stages of the inflammatory response and differentiate into mature SPM [100, 337]. The administration of TriDAP also induced the expansion of SPM, although not to the same extent as LPS. LPS has been shown to promote the differentiation of monocytes into M1 macrophages and therefore may directly induce the differentiation of monocytes into SPM. In contrast, this study showed that TriDAP was unable to induce M1 activation, measured by the failure to upregulate the expression of NOS2 or IL-12. The present study also established that LPS induced stronger pro-inflammatory cytokine production in comparison with TriDAP. For example, GM-CSF has been shown to drive the differentiation of M1 macrophages from monocyte progenitors [149] and was produced in response to LPS but not in response to TriDAP. This might explain the difference in LPS- and TriDAP-mediated macrophage activation.

SPM produce pro-inflammatory mediators and function as a bridge between the innate and adaptive immune response by presenting antigen to T-cells [100, 109, 326]. The present study confirmed that SPM have a high level of MHC-II on their surface, indicative of their more potent capability to present antigen [100, 109]. TriDAP increased the expression of MHC-II, indicating that NOD1 activation is playing a part in priming the innate immune system to propagate adaptive immune responses. Similarly, a number of

studies have shown that NOD1 plays a role in the adjuvanticity of CFA and in the efficient clearance of bacterial infections [279, 280, 295, 336].

The present study showed that LPS reduced the frequency and absolute numbers of LPM by d 4 post injection, leaving SPM as the dominant macrophage population in the peritoneal cavity. In contrast, TriDAP significantly increased the numbers of LPM in the peritoneal cavity. LPM are thought to fulfil a homeostatic role and there is evidence that they express markers characteristic of immunosuppressive M2 macrophages, including arginase and relm-α [326]. The present study confirmed that LPM express less MHC-II on their surface in comparison to SPM. Published reports suggest that the expression of MHC-II reflects the function of SPM as key presenters of antigen, while LPM clear apoptotic debris and maintain immune homeostasis [100, 109]. However, the present study established that LPM were capable of inducing antigen specific T-cell activation. In contrast to SPM, LPM constitutively expressed the co-stimulatory molecules CD80 and CD86, suggesting that LPM are primed to activate T-cells, while SPM must be activated.

PD-L2 is a co-inhibitory molecule found on the surface of M2 macrophages and can actively suppress T-cell activation via the ligation of the programmed death receptor (PD-1) [327]. This study established that LPM express PD-L2 constitutively and at a higher level than SPM. LPM can activate T-cells via antigen presentation, however, the presence of PD-L2 suggests that LPM are constrained in their ability to activate T-cells. Interestingly, TriDAP reduced the expression of CD80 and CD86 but not the expression of MHC-II or PD-L2. Further investigation established that TriDAP could inhibit the capability of LPM to induce antigen specific T-cell proliferation, possibly by suppressing the expression of co-stimulatory molecules. This suggests NOD1 activation reinforces the homeostatic function of LPM. This contrasts with the effect of TriDAP on SPM, and indicates that NOD1 activation results in both pro-inflammatory and homeostatic responses. However, the high ratio of LPM:SPM generated in response to TriDAP suggests that immunosuppressive LPM are the dominant immune cell active in response to NOD1 activation.

Dectin-1 is a c-type lectin which functions as a PRR and recognises fungal PAMPs [338]. Dectin-1 is upregulated in response to IL-4 and IL-13 and therefore is a common marker of M2 activation [328]. The present study established that LPM expressed higher levels of dectin-1 than SPM. In addition, the present study established that LPM constitutively

express relm-α and YM1, both characteristic of M2 macrophages. Taken collectively with other published reports that LPM express relm-α and YM1 [325, 326], these results strongly suggest that LPM have many of the characteristics of M2 macrophages, including the expression of the co-inhibitory molecule PD-L2, expression of the immunosuppressive protein relm-α, as well as a weaker capability to induce antigen specific responses in comparison with SPM.

SPM also expressed relm-α at rest, although at much smaller levels compared with LPM. In addition, LPS inhibited the expression of relm-α by SPM and induced an increase in the expression of NOS2, IL-1β and TNF-α by PEC. The increased expression of these M1 markers could be associated with the expansion of SPM in response to LPS or direct activation of the SPM via TLR4 [326]. Taken together, these results suggest that LPS inhibits immunosuppression within the PEC, and creates a pro-inflammatory environment. In contrast, NOD1 activation had no effect on the expression of NOS2, TNF-α and IL-1β but increased the expression of arginase and relm-α in the peritoneal cavity. Although this increase in M2 associated markers may be a result of the increase in numbers of M2-like LPM, which constitutively produce arginase and relm-α [326], the present study established that LPM themselves expressed more arginase and relm-α in response to TriDAP.

Consistent with the findings of chapter 4, IL-10 was also expressed by LPM in response to TriDAP. This suggests that TriDAP not only induces the expansion of LPM but also activates their M2-like immunosuppressive function by increasing the expression of IL-10, arginase and relm-α. In addition, TriDAP administration increased the expression of relm-α and IL-10 in the spleen, suggesting that the M2 polarisation occurs systemically and is not restricted to the site of injection. By expanding a population of M2-like LPM, NOD1 activation is inducing an environment that suppresses inflammation and inhibits the activation of adaptive immune responses. Conversely, LPS expands a population of M1-like SPM which are known to efficiently activate adaptive immune responses and produce pro-inflammatory mediators. This implies that NOD1 agonists can function as inhibitors of excessive inflammation. This may have implications during infection as certain bacteria have been shown to subvert the immune response by inducing the production of IL-10 and the activation of M2 macrophages [339].

IL-4 is a classic inducer of M2 activation and has been shown to induce the expression of relm-α and arginase by macrophages, including LPM [325]. The present study established that the TriDAP–mediated expression of relm-α and arginase by LPM was abrogated in the presence of an IL-4 neutralising antibody. This indicates that physiologically significant concentrations of IL-4 are produced, directly or indirectly, in response to NOD1 activation and that IL-4 induces the alternative activation of LPM in response to TriDAP. TriDAP increased the expression of IL-4 mRNA by LPM in an IL-4-dependent manner, suggesting that IL-4 production, and consequently M2 activation, may be dependent on a positive feedback loop created by the LPM.

Recent studies have shown that NOD1 activation can induce Th2-type responses and enhance the production of IL-4 [214, 215], moreover, results from chapter 4 of the present study indicate that PEC can produce soluble mediators in response to TriDAP that enhance the production of IL-4 by $CD4^+$ T-cells. However, no increase in IL-4 mRNA or IL-4 protein could be detected in vitro, thus, the production of IL-4 by LPM must be mediated by an in vivo mechanism. Magalhaes et al established that NOD1 mediated Th2 responses are dependent on the production of TSLP by stromal cells [215]. This suggests that IL-4 production may only be induced in the presence of stromal cells, which are absent from the in vitro PEC culture. In addition, TriDAP did not increase the expression of relm-α in vitro, possibly because of the absence of IL-4. However, TriDAP increased the expression of arginase by PEC in a p38-dependent manner in vitro, suggesting that TriDAP-mediated expression of arginase is not dependent on IL-4.

IL-10 has also been implicated in inducing the activation of M2 macrophages [143]. A number of studies have shown that M2 macrophage responses elicited by bacterial infections are dependent on the presence of IL-10. Furthermore, macrophages can be alternatively activated in vitro via IL-10 administration [129, 332, 340]. The present study established that both LPS-mediated M1 activation and TriDAP-mediated M2 activation was enhanced in $IL\text{-}10^{-/-}$ mice, indicating that IL-10 suppresses both forms of macrophage activation. However, the injection of recombinant IL-10 increased relm-α expression, indicating that IL-10 may play a role in TriDAP-mediated M2 activation.

Jenkins et al established that IL-4 can induce the proliferation of resident LPM, expanding the resident population of macrophages rather than relying on the differentiation of

monocytes. The present study showed that IL-4c enhanced the expression of the proliferation marker, Ki67, by LPM and this was associated with an expansion of their numbers. Similarly, TriDAP increased the expression of Ki67 by LPM, however, the expansion of the LPM population was only partially dependent on IL-4. This suggests that the main role of IL-4 is to induce the M2 polarisation of LPM (Fig 5.3.1).

The present study established that the TriDAP-mediated expansion of LPM was dependent on IL-10. This data is consistent with the work of Nguyen et al who established that IL-10 was responsible for the expansion of LPM during peritonitis [109]. They concluded that LPM are generated by the differentiation of infiltrating monocytes and not by proliferation of the resident cells. The results of the present study show that TriDAP recruited large numbers of monocytes to the peritoneal cavity, therefore, IL-10 produced in response to NOD1 activation may be converting monocytes into LPM. Injection of IL-10 alone was unable to expand the population of either SPM or LPM, indicating that these cells cannot proliferate in situ in response to IL-10. However, TriDAP increased the proliferation of LPM in situ. In addition, the TriDAP-mediated expansion of LPM was partially dependent on IL-4. Taken together, these results suggest that IL-4 induces the proliferation of resident LPM, whereas IL-10 promotes the differentiation of recruited monocytes into LPM.

LPS also induced the production of IL-10 by PEC in vitro and in vivo, however, LPS reduced the population of LPM and increased the population of SPM (Fig 5.3.1). LPS has been shown to directly induce the differentiation of monocytes into M1 macrophages, therefore, LPS may be directly inducing the differentiation of monocytes into M1-like SPM, even in the presence of IL-10. In addition, LPS induced the production of GM-CSF by PEC, a cytokine which has been implicated in the activation of M1 macrophages [149]. In contrast, TriDAP did not induce the production of GM-CSF. This suggests that the presence of GM-CSF may be responsible for the preferential differentiation of the M1-like SPM in response to LPS.

These results also highlighted an interesting contrast between the role of IL-10 during TriDAP-induced and LPS-induced inflammation. The injection of LPS resulted in recruitment of larger numbers of neutrophils, eosinophils, LPM and SPM in the peritoneal cavity of IL-$10^{-/-}$ mice than in WT mice. Consistent with published reports [290, 341, 342],

these results suggest that IL-10 restricts excessive inflammation and innate immune cell recruitment during TLR4 activation. In contrast, TriDAP did not increase the numbers of LPM in IL-$10^{-/-}$ mice. Furthermore, there was no significant difference between the numbers of SPM or neutrophils in the peritoneal cavity of IL-$10^{-/-}$ mice compared with WT mice after the administration of TriDAP. This suggests that TriDAP does not induce a pro-inflammatory response sufficient for the recruitment of innate immune cells, even in the absence of IL-10. The lack of inflammation then allows the TriDAP-induced IL-10 to promote the expansion of LPM, creating an immunosuppressive environment. In contrast, LPS induces a strong inflammatory response that drives the expansion of SPM, which is exacerbated in the absence of IL-10. LPS induced the production of IL-1β, TNF-α and NOS2, all of which have been implicated in pro-inflammatory cell recruitment. These pro-inflammatory mediators may elicit the differential inflammatory response induced by LPS and TriDAP.

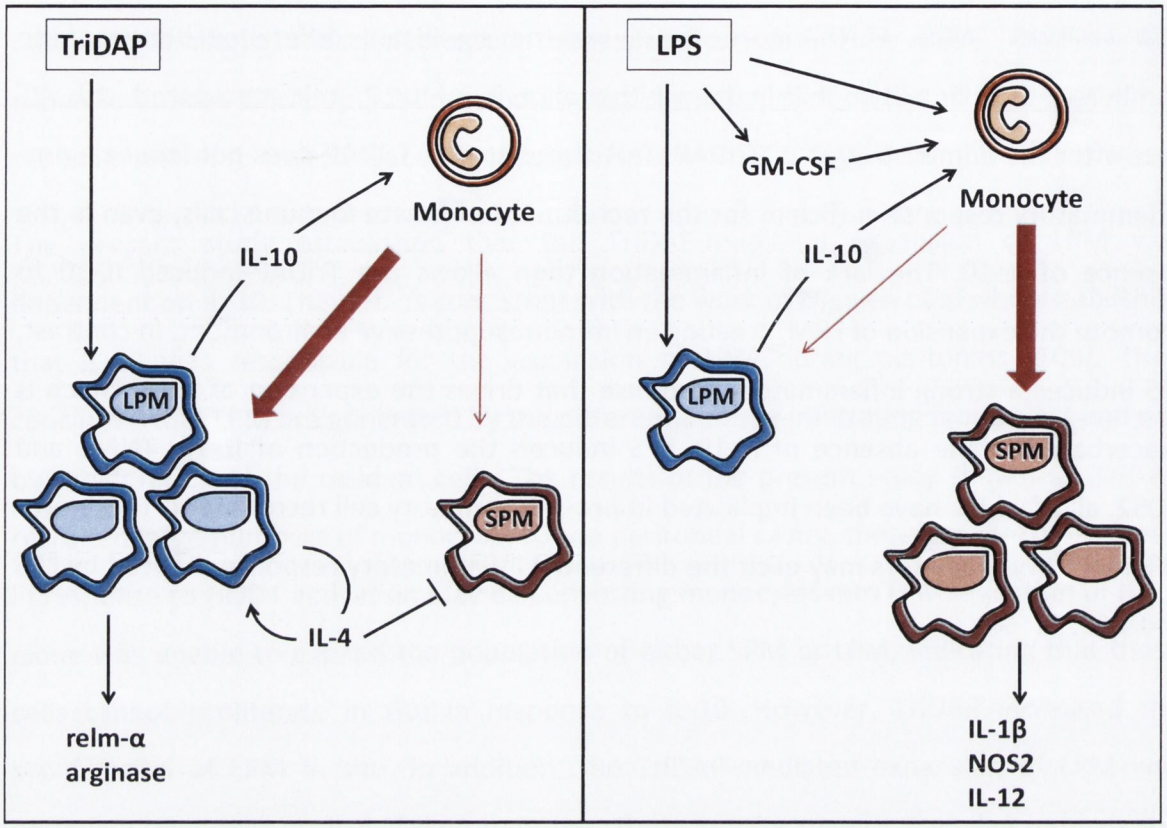

Fig 5.3.1 The possible mechanism for the TriDAP and LPS-mediated expansion of LPM and SPM. TriDAP induces the production of IL-10 by LPM, which mediates the preferential differentiation of monocytes into LPM. TriDAP also induces the production of IL-4 by LPM, which induces the proliferation of LPM. In addition, IL-4 induces the expression of M2-markers relm-α and arginase and inhibits the production of M1 markers by SPM. LPS induces the production of IL-10 and GM-CSF by PEC. GM-CSF and LPS induce the preferential differentiation of monocytes into SPM, even in the presence of IL-10. In addition, LPS induces the expression of M1 markers IL-1β, NOS2 and IL-12 by SPM.

Macrophages from mice injected with PBS, TriDAP or IL-4c ameliorated the clinical symptoms of EAE, suggesting that macrophages from these mice are immunosuppressive in nature. In contrast, macrophages from LPS-treated mice exacerbated the disease. PBS, TriDAP and IL-4c treated mice contain large numbers of M2-like LPM and it has been shown that M2 macrophages play an important role in remission of EAE. Mikita et al showed that high ratios of M2:M1 were present during remission of disease and that the transfer of M2 macrophages could induce remission [182]. The mechanisms by which M2 macrophages attenuate the symptoms of EAE are unclear, but Jiang et al reported that a decrease in pathogenic IL-17 and IFN-γ producing T-cells were associated with M2 activation [183]. M2 macrophages have been shown to mediate immunosuppression in a number of ways; arginase converts arginine to ornithine, depleting the environment of the amino acid and restricting cellular proliferation by nutrient starvation, whereas both relm-α and PD-L2 have been shown to actively suppress the proliferation of T-cells [157-159, 171, 323, 327].

It is possible that any or all of these mechanisms may be actively suppressing pathogenic T-cells in response to macrophage transfer, however, macrophages from TriDAP-treated mice do not suppress to a greater extent than the PBS-treated macrophages. This suggests that TriDAP does not enhance the function of LPM, but importantly, NOD1 activation expands the population of the immunosuppressive LPM population without compromising their function. This suggests that TriDAP induces an immunosuppressive environment by increasing the numbers of immunosuppressive macrophages. This effect was lost when the numbers of macrophages were equalised during the transfer of cells. Importantly, macrophages from LPS-treated mice exacerbated disease. The ratio of SPM: LPM was higher in LPS-treated mice, suggesting that activated SPM may mediate the increase in clinical symptoms of EAE in mice injected with macrophages from LPS-treated mice. This agrees with a report that showed increased disease severity was associated with increased NOS2 expression and M1 macrophage infiltration in the brain [182]. This also highlights the difference in function between LPS and TriDAP in terms of pro- and anti-inflammatory responses.

Cells from MOG-immunized mice restimulated in vitro in the presence of TriDAP were less pathogenic than cells stimulated in the absence of TriDAP. This suggests that NOD1 activation has an immunosuppressive role during the stimulation of immune cells. The

data from this study also established that NOD1 activation induces the expression of IL-10 and arginase in spleen cells. Both arginase and IL-10 have been shown to modulate T-cell responses [74, 157, 158, 171, 273, 323], suggesting that this may be the mechanism by which TriDAP mediates the inhibition of pathogenic immune cells. Furthermore, the present study established that TriDAP treated cells induced IL-10 and IL-4 production in vivo when transferred into naive mice, suggesting that NOD1 activation not only induces IL-10 directly, but also alters the immune response to produce IL-10 and IL-4 indirectly. This further supports the findings of the present study which demonstrated that NOD1 plays an important role in inducing IL-10, which can suppress pathogenic T-cells.

The findings of this study suggest that NOD1 activation enhances immunosuppression and inhibits the activation of pathogenic immune cells by inducing the production of IL-10. IL-10 promotes the expansion of a population of macrophages with the ability to suppress T-cell activation and autoimmune disease. NOD1 also promotes the production of IL-4, which can promote the M2 activation of peritoneal macrophages. Although many studies have characterised the role of NOD1 as an immunostimulatory PRR, the present study highlights a novel role for NOD1 as an immunoregulatory PRR.

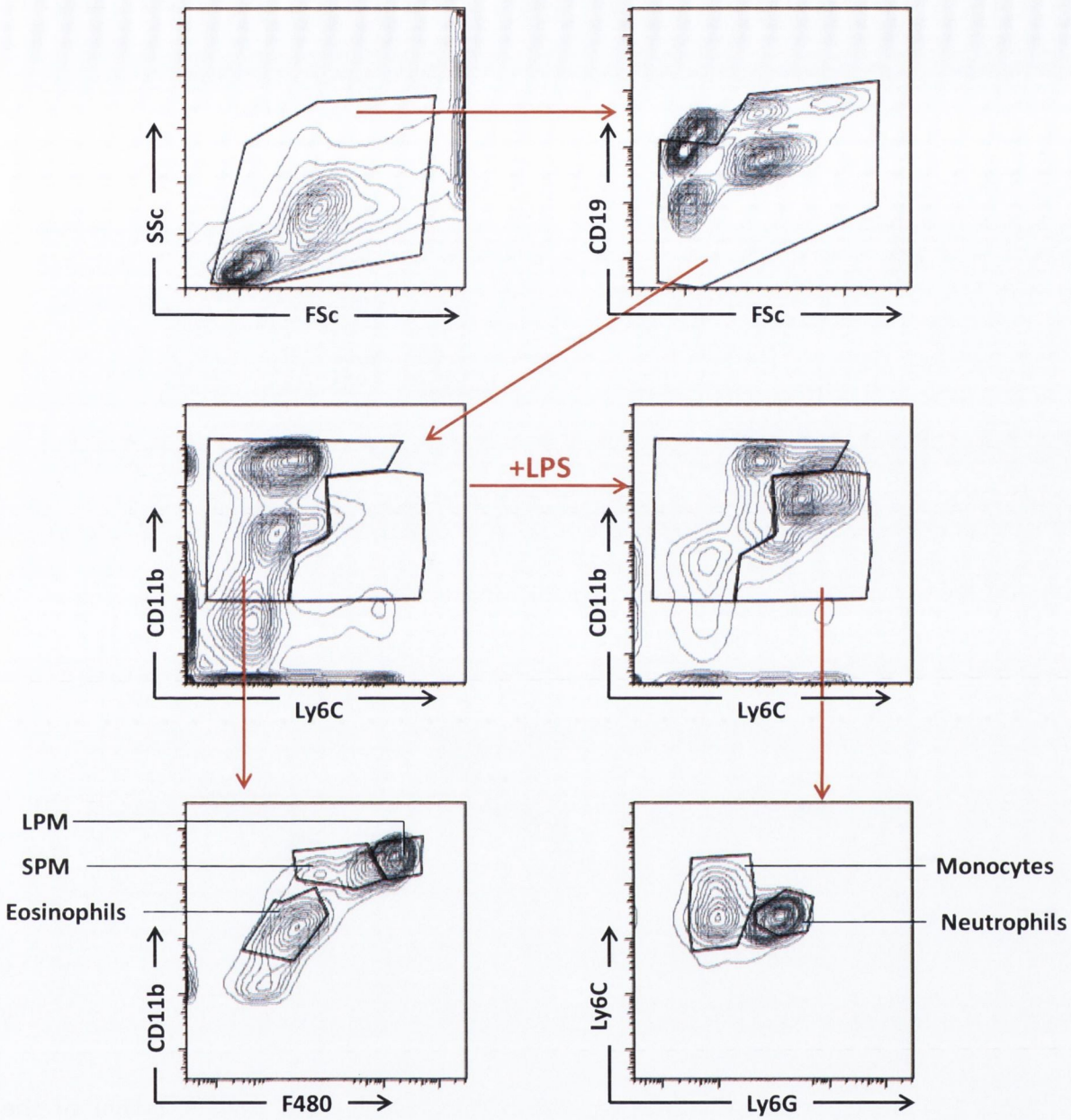

Fig 5.1 Gating strategy for analysing the innate cells of the peritoneal cavity. The peritoneal cavity of C57BL/6 mice were lavaged to obtain PEC. These cells were surface-stained with antibodies specific for CD19, CD11b, F480, Ly6G, Ly6C and MHC-II. The cells were then analysed by flow cytometry. PEC from naive mice contained $CD19^{-}CD11b^{+}Ly6C^{-}$ LPM ($MHC\text{-}II^{o}$), SPM ($MHC\text{-}II^{hi}$) and eosinophils ($SiglecF^{+}$) but did not contain any $Ly6C^{+}$ cells. An injection of LPS i.p. resulted in the influx of $CD19^{-}CD11b^{+}Ly6C^{+}$ monocytes ($MHC\text{-}II^{-}$)and neutrophils ($Ly6G^{+}$) after 16 h. The results shown here represent 5 or more independent experiments.

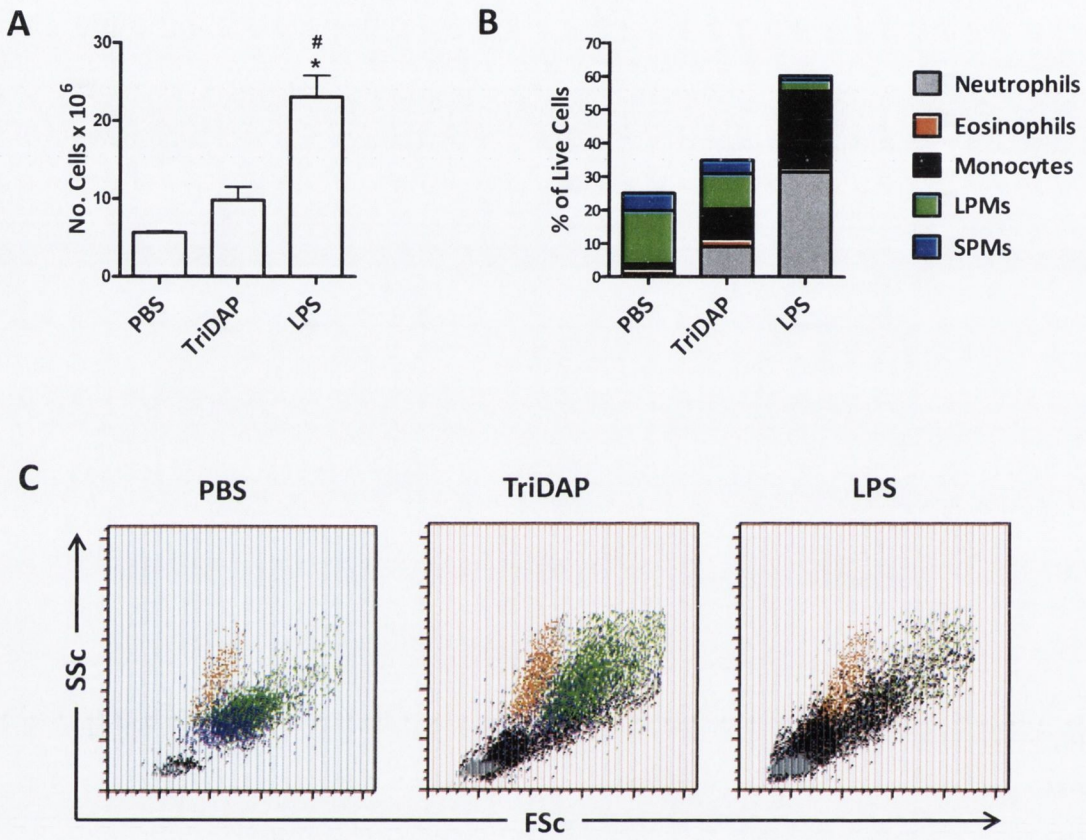

Fig 5.2 Administration of TriDAP or LPS in vivo changes the cellular milieu of the peritoneal cavity after 16 h. C57BL/6 mice were injected i.p. with PBS, TriDAP (100 μg) or LPS (100 ng) (n=3) . After 16 h the mice were sacrificed and the peritoneal cavity was lavaged. The single cell suspension was surface-stained with antibodies specific for CD11b, F480, Ly6G, Ly6C and MHC-II. Cells were counted (A) and analysed by flow cytometry. Different cell types were graphed according to percentage of live cells (B) . Representative FACS plots were gated as described in Fig 5.1 (C) and are representative of n=3. Statistical significance was calculated by one-way ANOVA and a Tukey post test. * = $P < 0.05$ versus PBS, # = $P < 0.05$ versus TriDAP. The results are representative of 3 independent experiments.

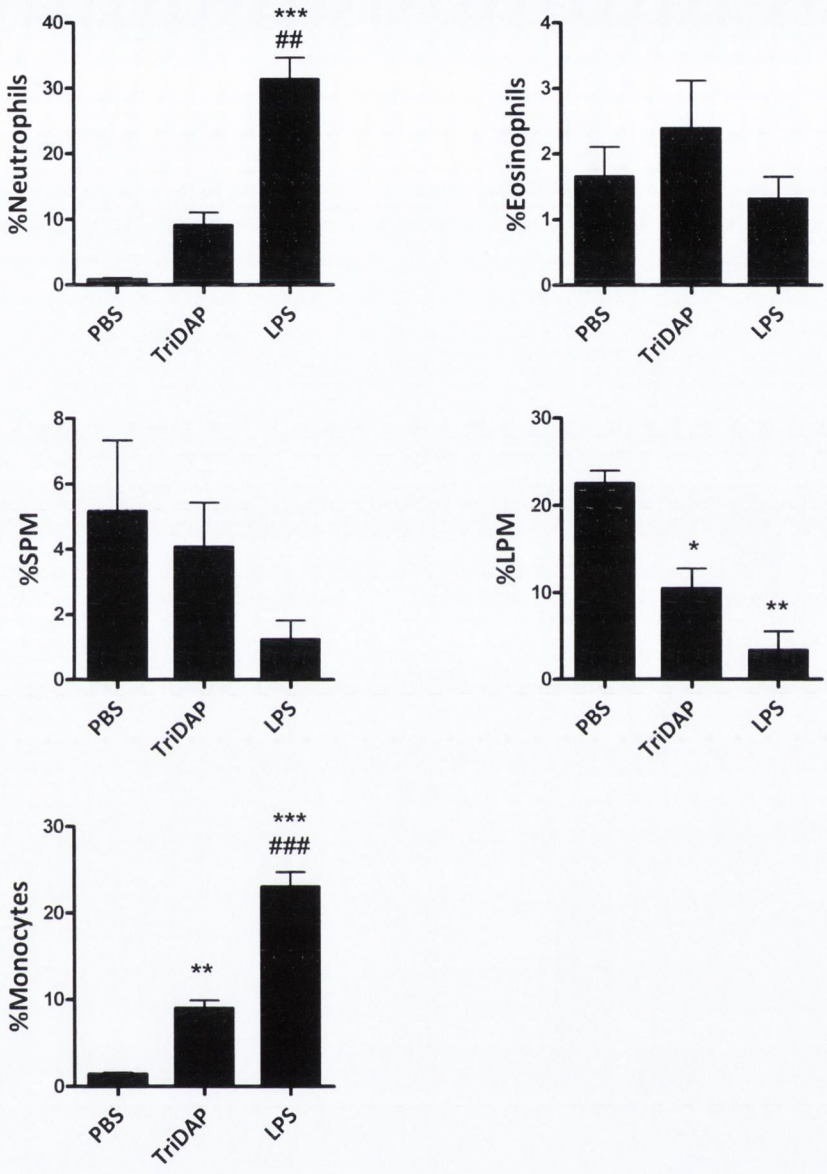

Fig 5.3 Administration of TriDAP or LPS in vivo increases the percentages of inflammatory monocytes and reduces the percentage of LPM in the peritoneal cavity after 16 h. C57BL/6 mice were treated and processed as described in Fig 5.2. The results shown were analysed by flow cytometry using the gating strategy described in Fig 5.1. Different cell types were graphed according to the % of total live cells (n=3). Statistical significance was calculated by one-way ANOVA and a Tukey post test. *= P< 0.05, **= P< 0.01, ***= P< 0.001 in comparison with PBS injected controls. ##= P< 0.01, ###= P< 0.001 in comparison to TriDAP injected mice. The results are representative of 3 independent experiments.

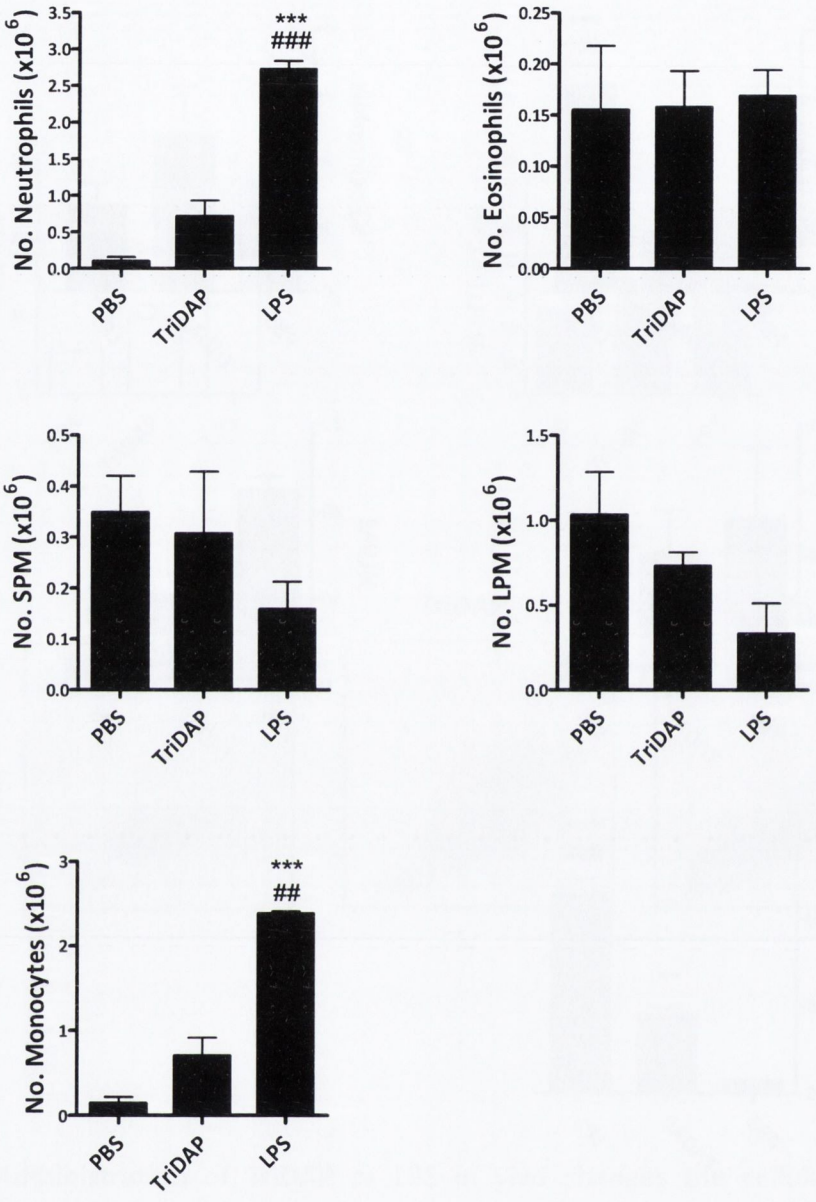

Fig 5.4 Administration of LPS in vivo increases the absolute numbers of inflammatory monocytes and neutrophils in the peritoneal cavity after 16 h. C57BL/6 mice were treated and processed as described in Fig 5.2. The results shown were analysed by flow cytometry using the gating strategy described in Fig 5.1. Different cell types were graphed according to the absolute numbers of live cells (n=3). Statistical significance was calculated by one-way ANOVA and a Tukey post test. ***= $P< 0.001$ in comparison with PBS injected controls. ##= $P< 0.01$, ###= $P< 0.001$ in comparison to TriDAP injected mice. The results are representative of 3 independent experiments.

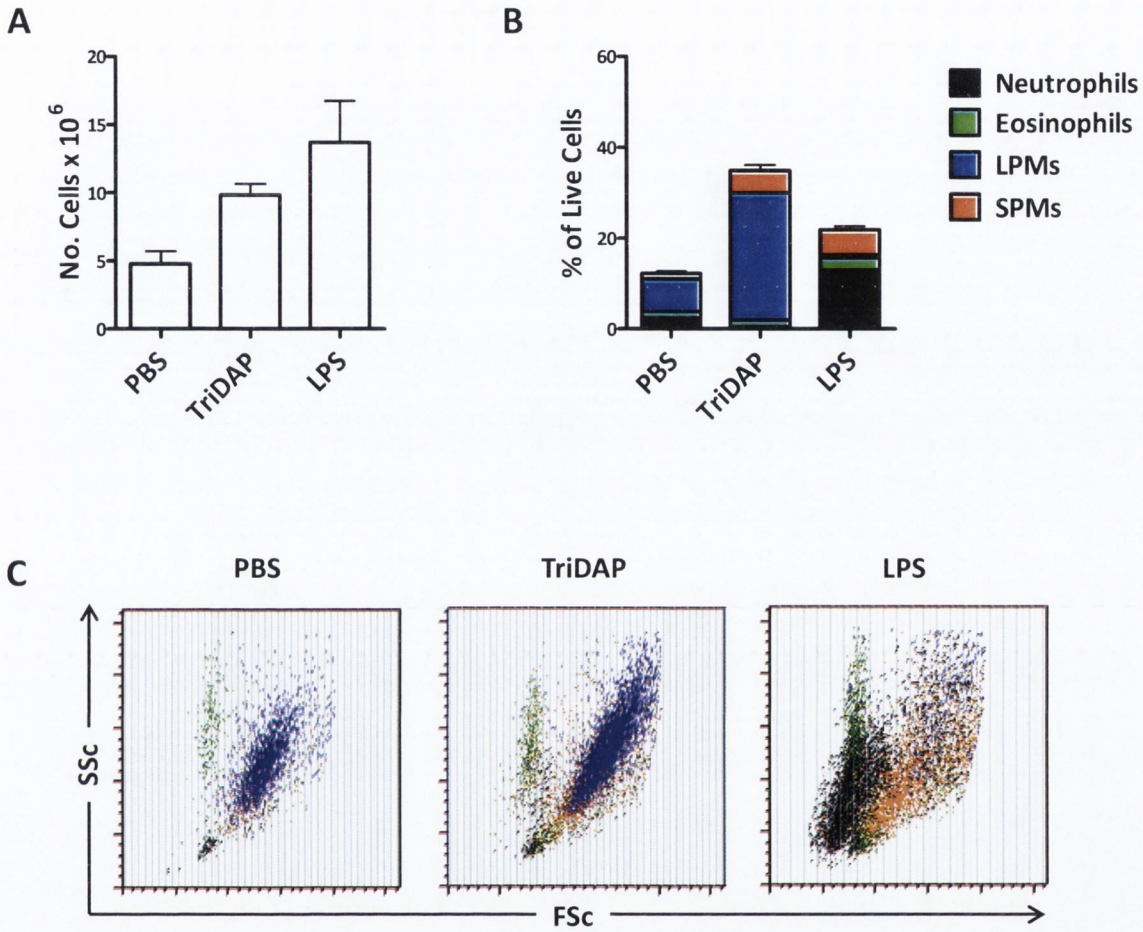

Fig 5.5 The administration of TriDAP or LPS in vivo alters the cellular milieu of the peritoneal cavity. C57BL/6 mice were injected i.p. with PBS, TriDAP (100 μg) or LPS (100 ng) on d 0, 1, 2 and 3 (n=3). The mice were sacrificed on d 4 and the peritoneal cavity was lavaged. The single cell suspension was surface-stained with antibodies specific for CD19, CD11b, F480, Ly6G, Ly6C and MHC-II. Cells were counted (A) and analysed by flow cytometry. Different cell types were graphed according to percentage of live cells (B). Representative FACS plots were gated as described in Fig 5.1 (C) and are representative of n=3. Significance was calculated using a one-way ANOVA with a Tukey post test. The results are representative of 3 or more independent experiments.

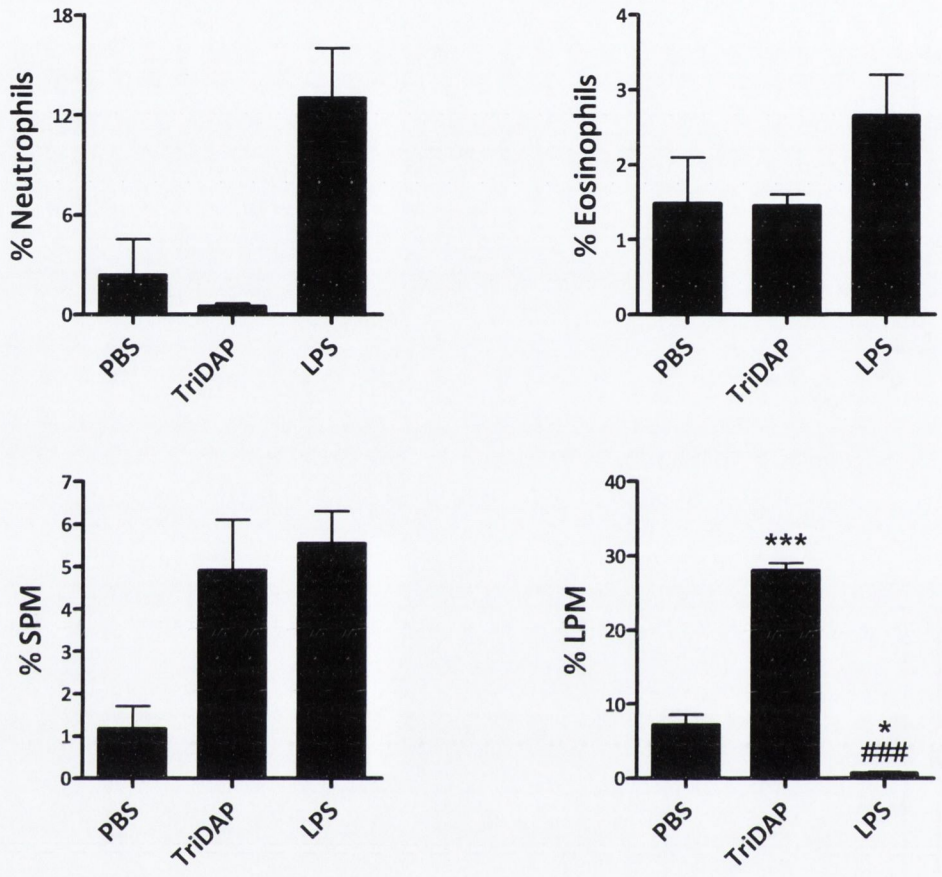

Fig 5.6 The administration of TriDAP in vivo increases the percentage of LPM, whereas LPS decreases the percentage of LPM in the peritoneal cavity. C57BL/6 mice were treated and processed as described in Fig 5.5. Cells were analysed by flow cytometry using the gating strategy descrbed in Fig 5.1. Different cell types were graphed according to % of total live cells (n=3). Statistical significance was calculated using a one-way ANOVA with a Tukey post test. *= P< 0.05, ***= P< 0.001 in comparison with PBS injected controls. ###= P< 0.001 in comparison to TriDAP injected mice. The results shown are representative of 3 or more independent experiments.

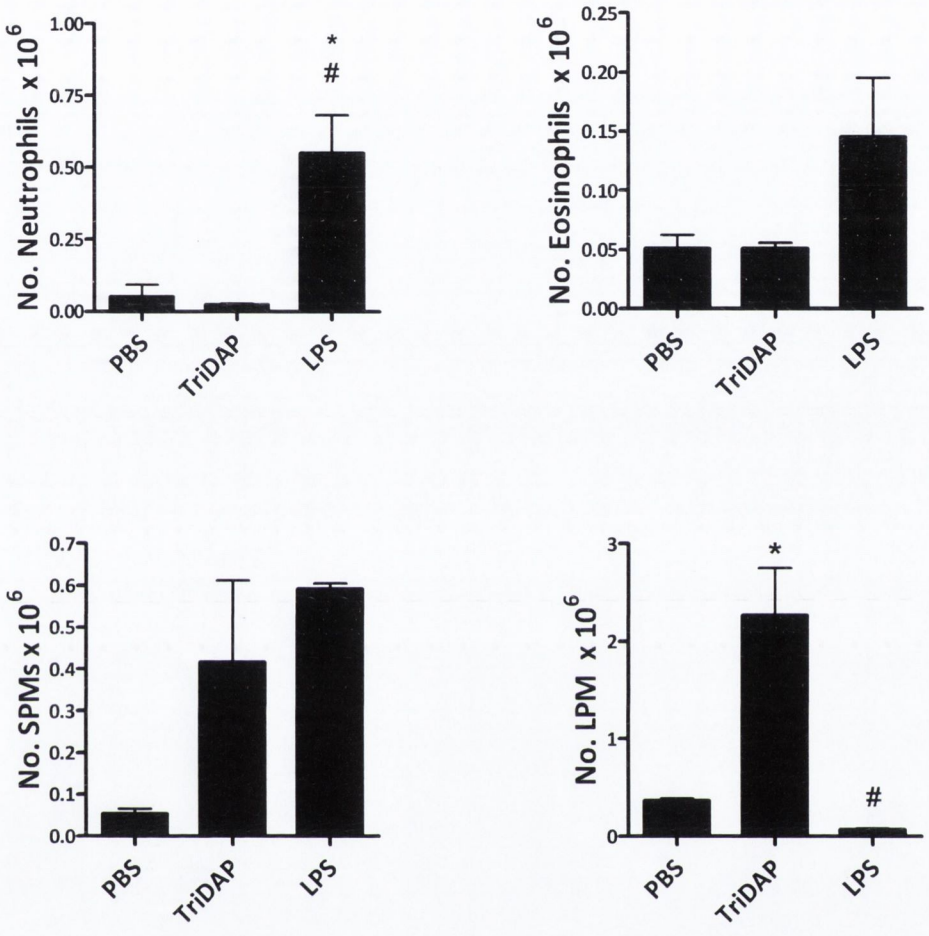

Fig 5.7 The administration of TriDAP in vivo increases the absolute number of LPM in the peritoneal cavity. C57BL/6 mice were treated and processed as described in Fig 5.5. Cells were analysed by flow cytometry using the gating strategy described in Fig 5.1. Different cell types were graphed according to the absolute numbers of cells (n=3). Statistical significance was calculated using a one-way ANOVA with a Tukey post test. *= $P< 0.05$ in comparison with PBS injected controls. #= $P< 0.05$ in comparison to TriDAP injected mice. The results shown are representative of 3 or more independent experiments.

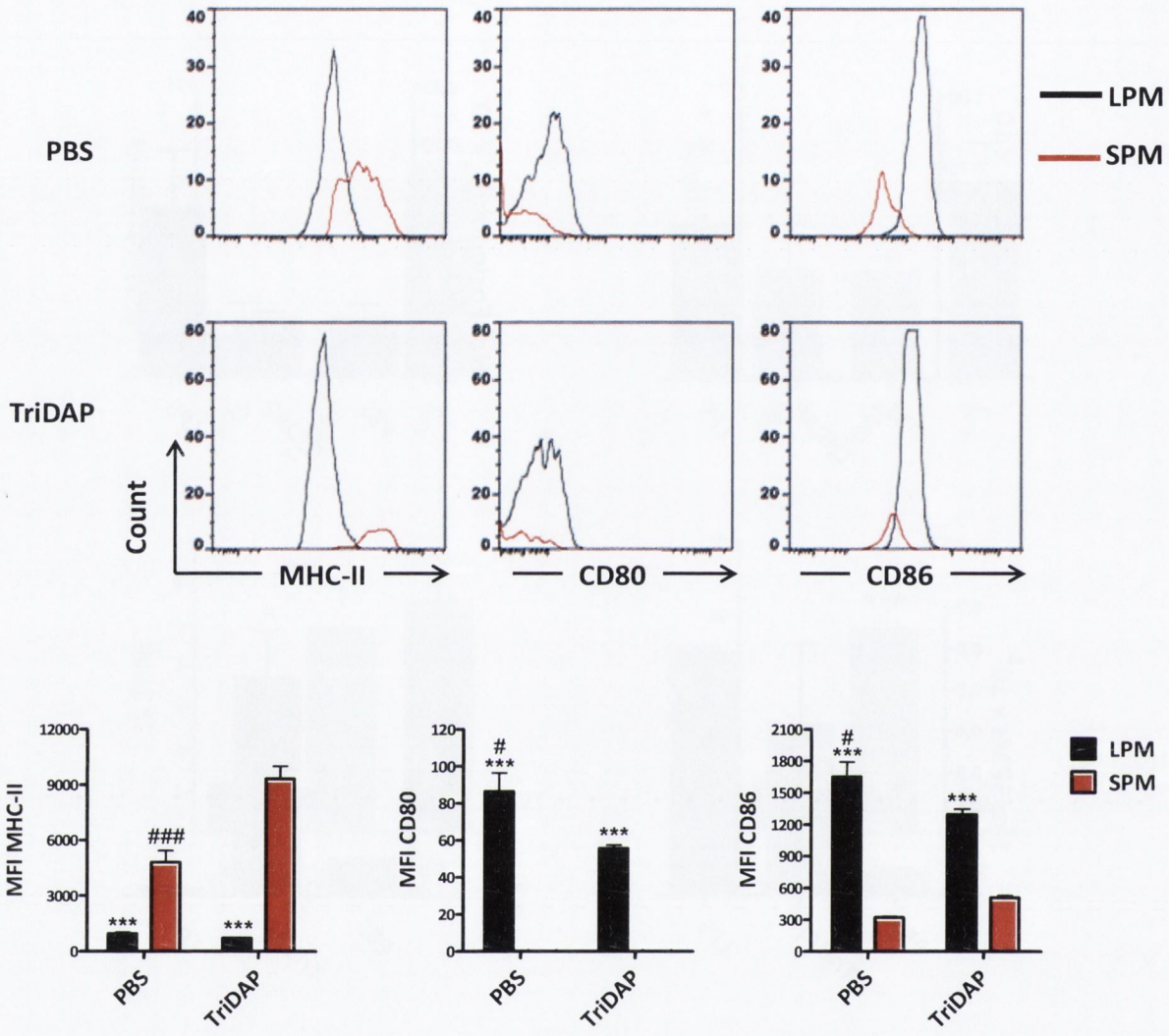

Fig 5.8 LPM express lower levels of MHC-II and higher levels of CD80 and CD86 in comparison with SPM. C57BL/6 mice were injected i.p. with either PBS or TriDAP (100 µg) on d 0, 1, 2 and 3 (n=3). The mice were sacrificed on d 4 and the peritoneal cavity was lavaged. The single cell suspension was surface-stained with antibodies specific for CD11b, F480, Ly6G, Ly6C, CD80, CD86 and MHC-II. The cells were then analysed by flow cytometry. Plots shown were gated on LPM and SPM as described in Fig 5.1 and are representative of n=3. Statistical significance was calculated using a two way ANOVA with Bonferroni post test. ***= $P < 0.001$ versus SPM, #= $P < 0.05$ ### = $P < 0.001$ versus TriDAP injected mice. The results shown are representative of 3 independent experiments.

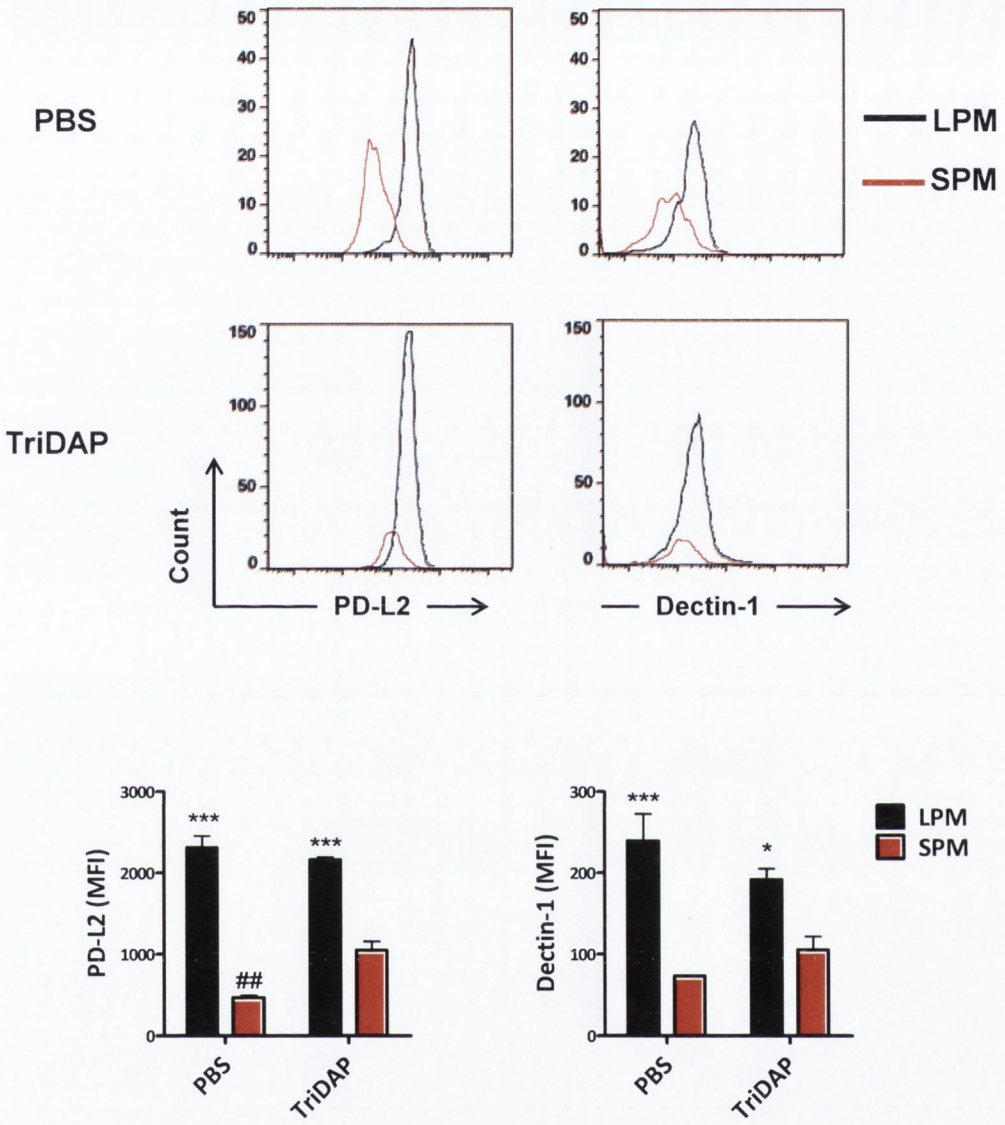

Fig 5.9 LPM express higher levels of PD-L2 and Dectin-1 in comparison with SPM. C57BL/6 mice were injected i.p. with PBS or TriDAP (100 µg) on d 0, 1, 2 and 3 (n=3). The mice were sacrificed on d 4 and the peritoneal cavity was lavaged. The single cell suspension was surface-stained with antibodies specific for CD11b, F480, Ly6G, Ly6C, PD-L2, Dectin-1 and MHC-II. The cells were then analysed by flow cytometry. Plots shown were gated on LPM and SPM as described in Fig 5.1 and are representative of n=3. Statistical significance was calculated using a two way ANOVA with Bonferroni post test. *= $P < 0.05$, ***= $P < 0.001$ versus SPM, ## = $P < 0.01$ versus TriDAP injected mice. The results shown are representative of 3 independent experiments.

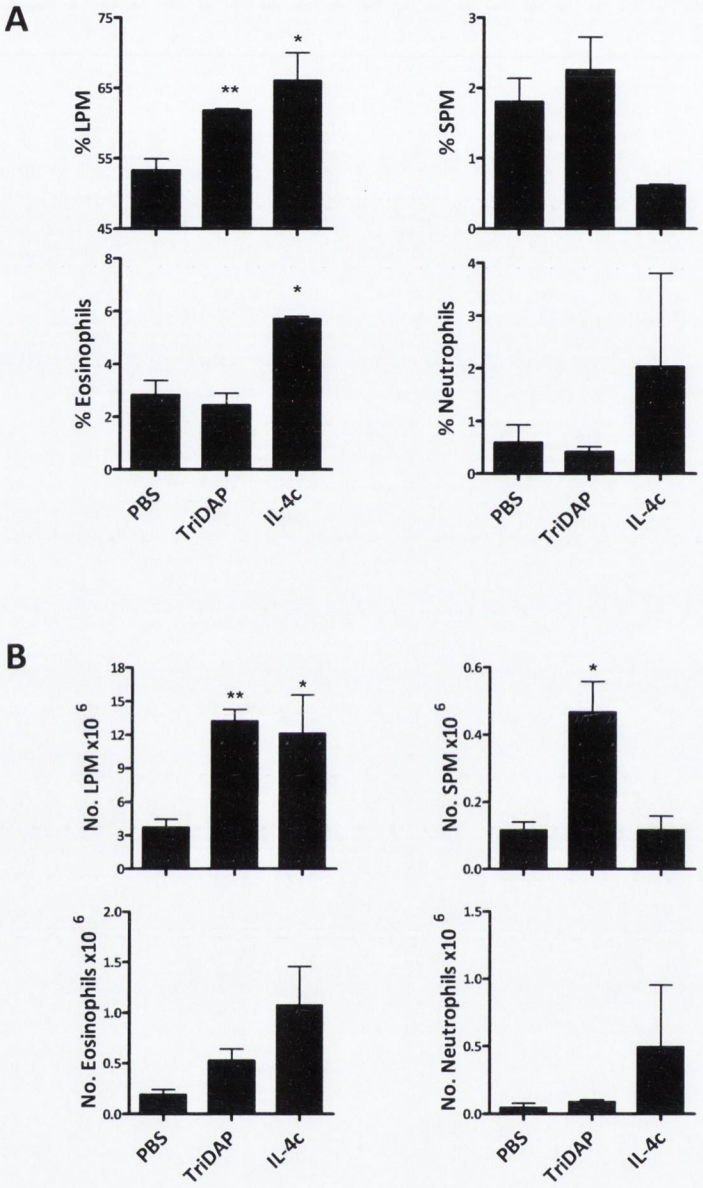

Fig 5.10 Administration of IL-4c i.p. increases the percentage and number of LPMs in the peritoneal cavity. C57BL/6 mice were injected i.p. with PBS, TriDAP (100 μg) on d 0, 1, 2 and 3, or injected with IL-4c (rIL-4, αIL-4; 5 μg, 25 μg) on d 0 and 2 (n=3). The mice were sacrificed on d 4 and the peritoneal cavity was lavaged. The single cell suspension was surface-stained with antibodies specific for CD11b, F480, Ly6G, Ly6C and MHC-II. The cells were then analysed by flow cytometry. Cell populations shown were gated as previously described in Fig 5.1 and are representative of n = 3. Different cell types were graphed according to the percentage of live cells (A) and absolute numbers (B). Statistical significance was calculated using a one-way ANOVA with a Tukey post test. *= $P< 0.05$ **= $P< 0.01$. The results shown are representative of 3 independent experiments.

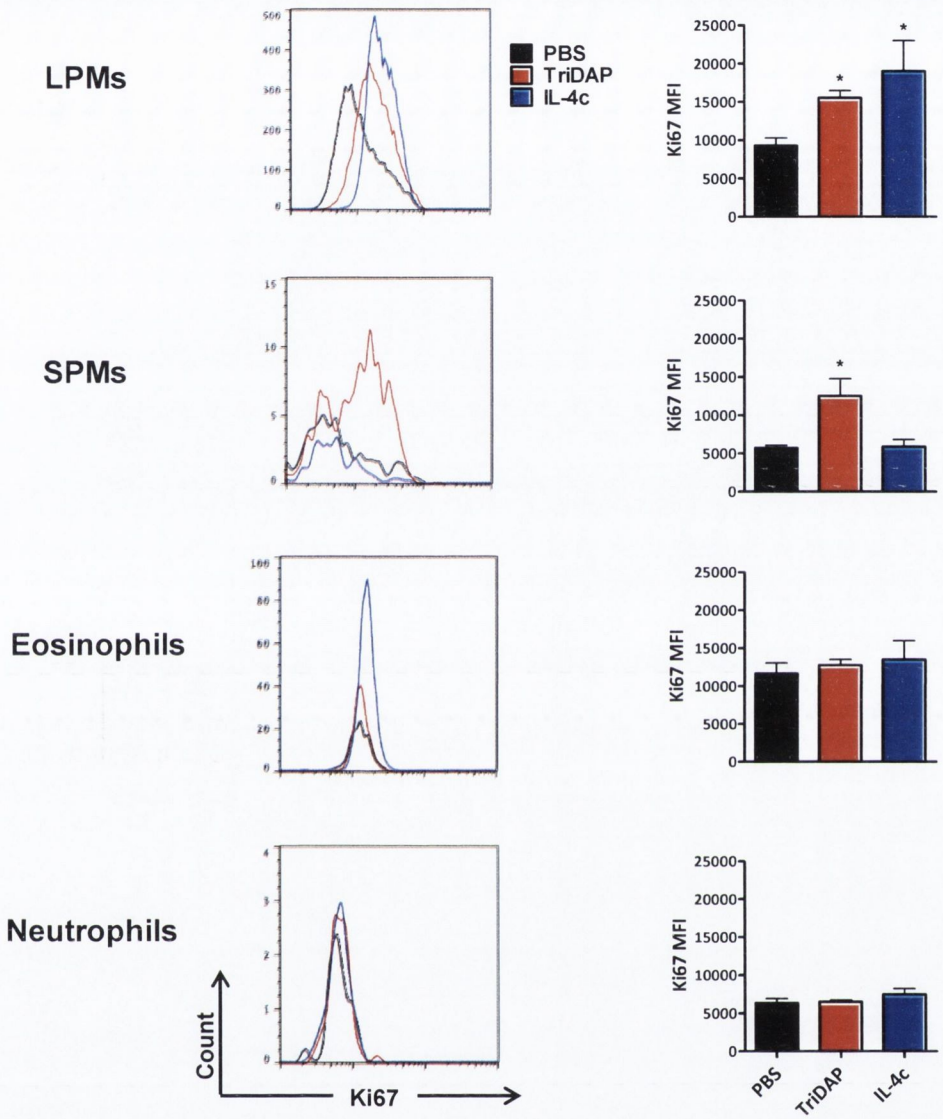

Fig 5.11 Administration of TriDAP in vivo induces the expression of Ki67 in both LPM and SPM. C57BL/6 mice were injected i.p. with either PBS or TriDAP (100 μg) on d 0, 1, 2 and 3, or injected with IL-4c (rIL-4, αIL-4; 5 μg, 25 μg) on d 0 and 2 (n=3). The mice were sacrificed on d 4 and the peritoneal cavity was lavaged. The single cell suspension was surface-stained with antibodies specific for CD11b, F480, Ly6G, Ly6C and MHC-II and stained intranuclearly with antibodies specific for Ki67. The cells were then analysed by flow cytometry. Plots and graphs shown are gated on the labelled cell types using the gating strategy described in Fig 5.1 and are representative of n=3. Statistical significance was calculated using a one way ANOVA with Tukey post test. *=P<0.05 versus PBS controls. The results shown are representative of 3 independent experiments.

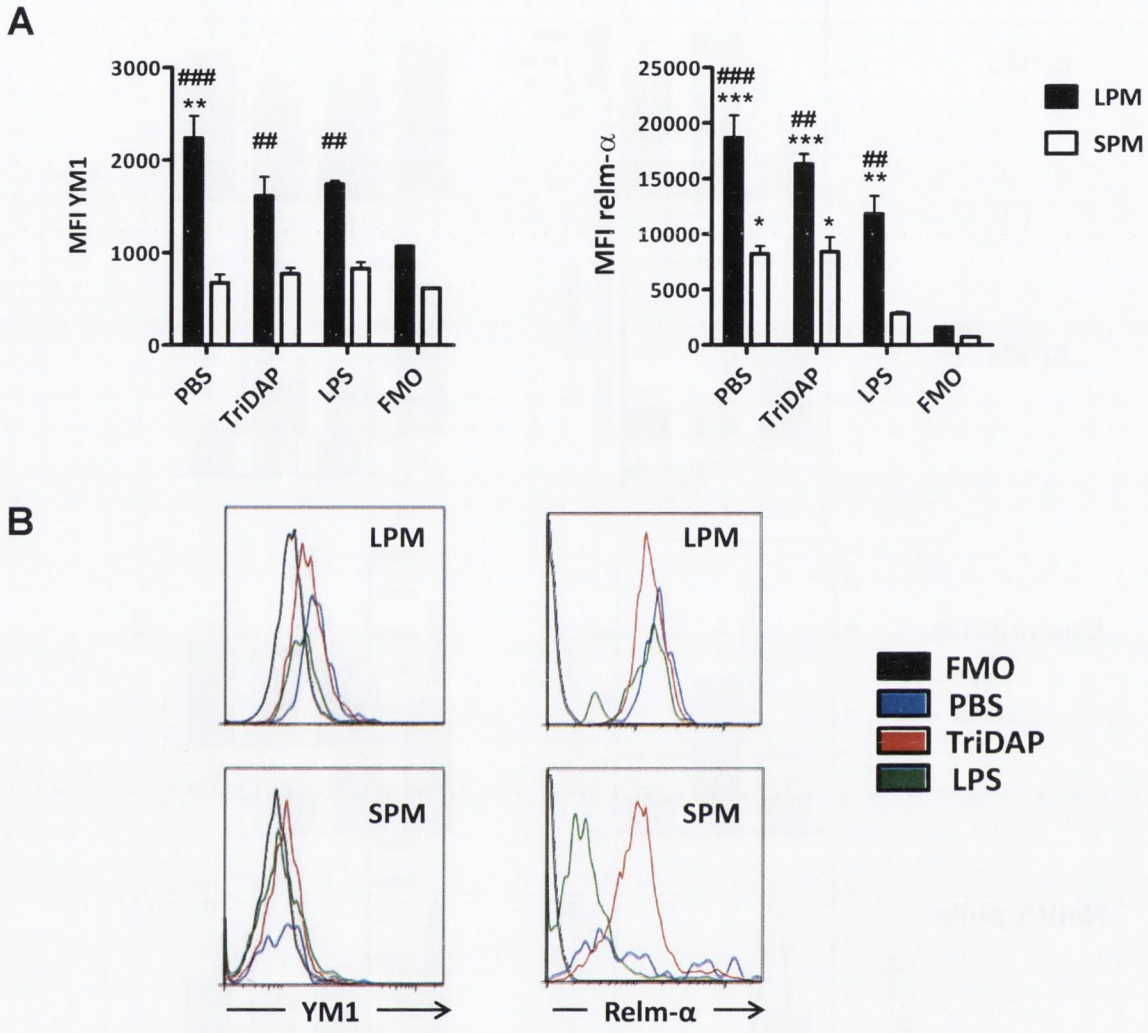

Fig 5.12 LPM express the M2 markers YM1 and Relm-α at higher levels than SPM. C57BL/6 mice were injected i.p. with PBS, TriDAP (100 µg) or LPS (100 ng) on d 0, 1, 2 and 3 (n=3). The mice were sacrificed on d 4 and the peritoneal cavity was lavaged. The single cell suspension was incubated with brefeldin A for 5 h before being surface-stained with antibodies specific for CD11b, F480, Ly6G, Ly6C and MHC-II and stained intracellularly with antibodies specific for YM1 and relm-α. The cells were then analysed by flow cytometry. The MFI of YM1 or relm-α expression in either LPM or SPM was graphed and is representative of n=3 (A). Histograms were gated on LPM or SPM using the gating strategy discussed in Fig 5.1 (B) and are representative of n=3. Statistical significance was calculated using a two-way ANOVA with a Bonferroni post test. ##= P< 0.01, ### = P < 0.001 versus SPM. *= P< 0.05, **= P< 0.01, *** = P < 0.001 versus FMO. The results shown are representative of 3 independent experiments.

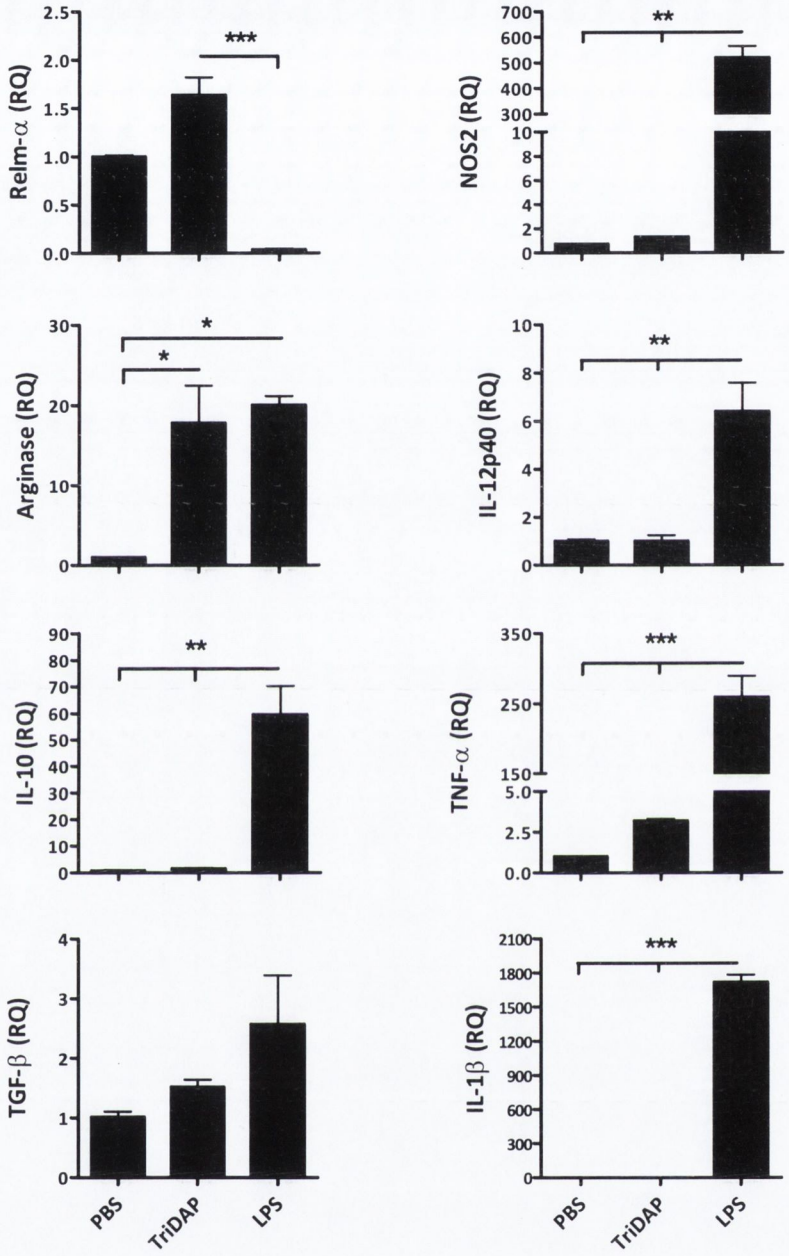

Fig 5.13 Administration of TriDAP in vivo increases the expression of the M2-associated molecules arginase and relm-α mRNA in PEC. C57BL/6 mice were injected i.p. with PBS, TriDAP (100 μg) or LPS (100 ng) on d 0, 1, 2 and 3 (n=3). The mice were sacrificed on d 4 and the peritoneal cavity was lavaged. RNA was isolated from the PEC and converted into cDNA. Real time PCR was used to quantify the expression of mRNA relative to the PBS injected controls. Each combination was examined in triplicate. Statistical significance was calculated by one-way ANOVA with a Tukey post test. *= P< 0.05, **= P< 0.01, ***= P < 0.001. The results shown are representative of 3 independent experiments.

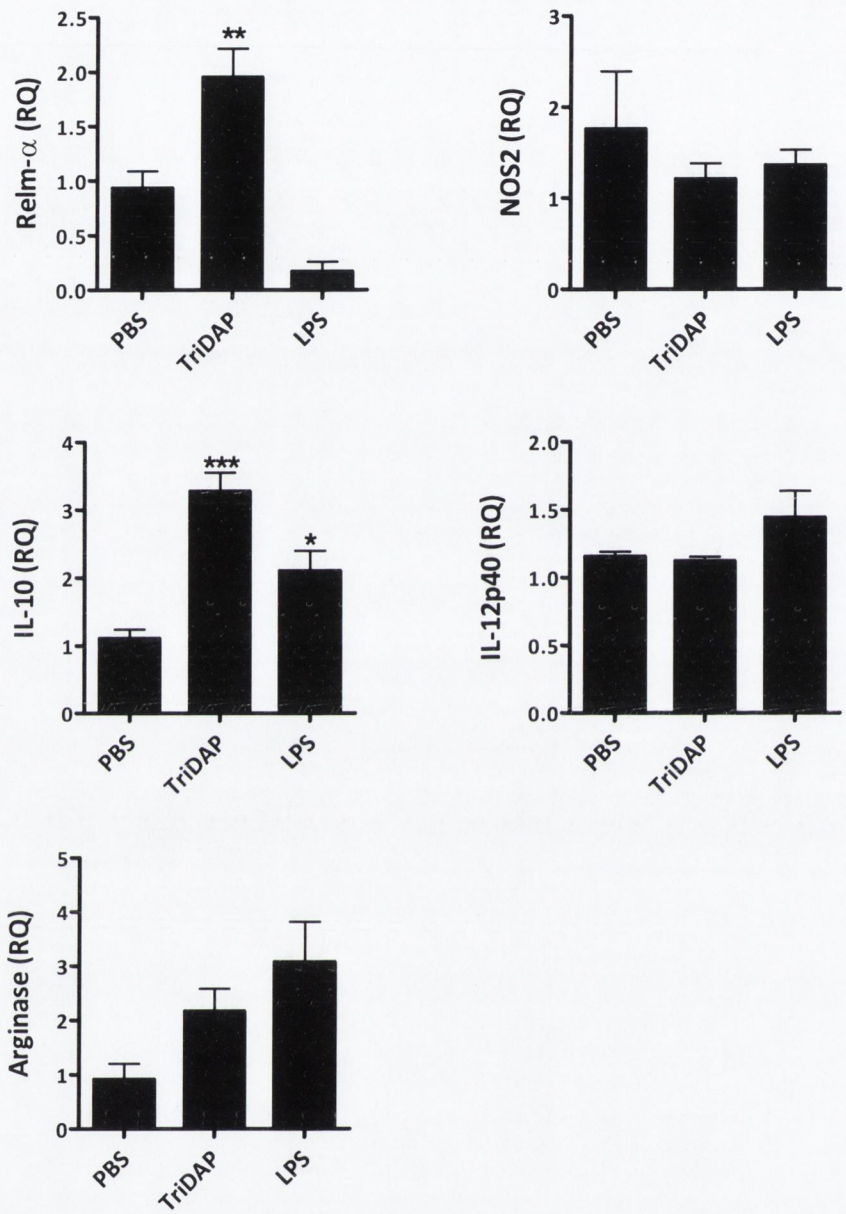

Fig 5.14 Administration of TriDAP in vivo increases the expression of relm-α and IL-10 mRNA in the spleen. C57BL/6 mice were injected i.p. with PBS, TriDAP (100 μg) or LPS (100 ng) on d 0, 1, 2 and 3 (n=3). The mice were sacrificed on d 4 and the spleens were removed and processed. RNA was isolated from splenocytes and converted into cDNA. Real time PCR was used to quantify the expression of mRNA relative to the PBS injected controls. Each combination was examined in triplicate. Statistical significance was calculated by one-way ANOVA with a Tukey post test. *= $P< 0.05$, **= $P< 0.01$, ***= $P < 0.001$ versus PBS injected controls. The results shown are representative of 3 independent experiments.

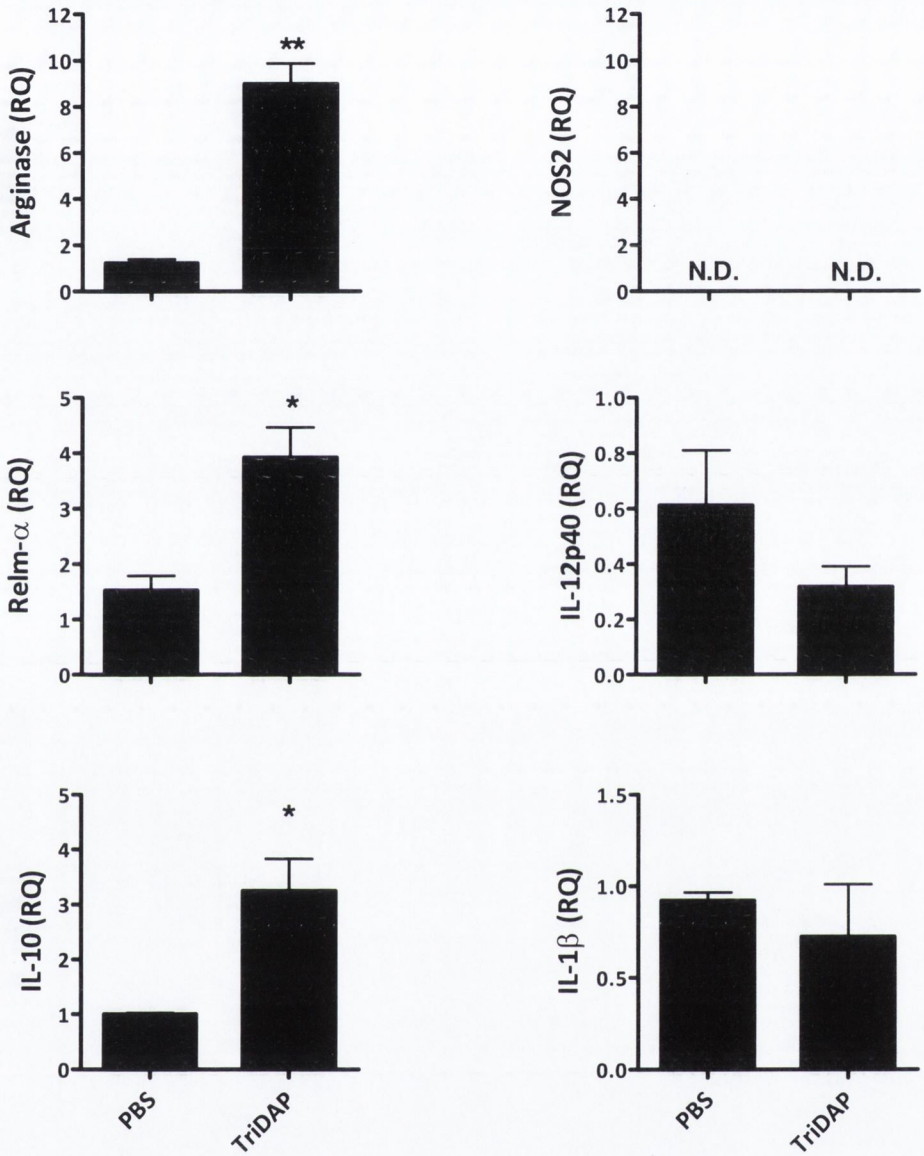

Fig 5.15 Administration of TriDAP in vivo increases the expression of arginase, relmα and IL-10 mRNA in LPM. C57BL/6 mice were injected i.p. with PBS or TriDAP (100 μg) on d 0, 1, 2 and 3 (n=3). The mice were sacrificed on d 4 and the peritoneal cavity was lavaged. The single cell suspension was surface-stained with antibodies specific for CD11b, F480, MHC-II and GR1. $CD11b^{+}F480^{+}GR1^{-}MHC\text{-}II^{-}$ LPM were sorted by FACS (Fig 5.2.1). RNA was isolated from the cells and converted into cDNA. Real time PCR was used to find the expression of mRNA relative to the PBS injected controls. Each combination was examined in triplicate. Statistical significance was calculated using a two-tailed t-test. *= $P< 0.05$ **= $P < 0.01$ versus PBS injected mice. N.D. = not detected. The results shown are representative of 2 independent experiments.

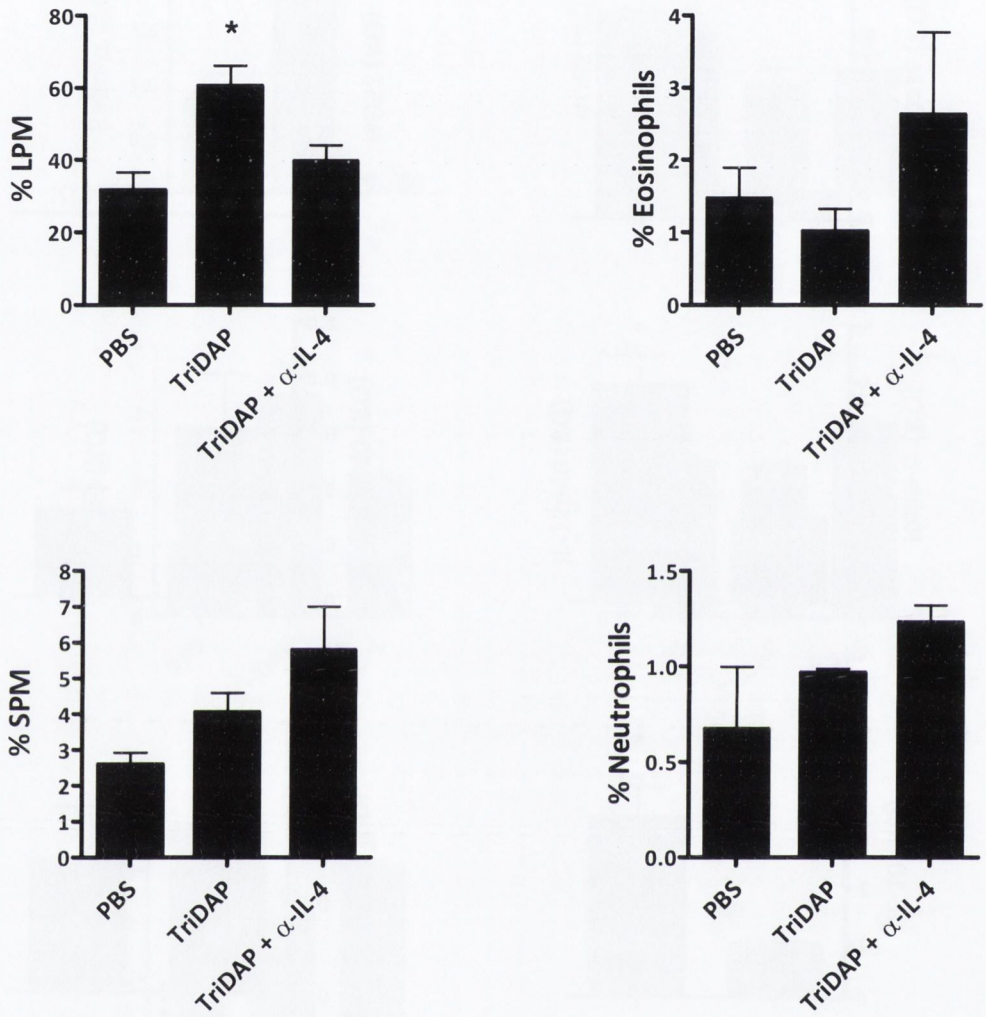

Fig 5.16 The TriDAP-induced increase in percentage of LPM is partially dependent on IL-4 signalling. C57BL/6 mice were injected i.p. with PBS, TriDAP (100 μg) or TriDAP with αIL-4 (660 μg) antibody on d 0, 1, 2 and 3 (n=3). The mice were sacrificed on d 4 and the peritoneal cavity was lavaged. The single cell suspension was surface-stained with antibodies specific for CD11b, F480, Ly6G, Ly6C and MHC-II. The cells were then analysed by flow cytometry using the gating strategy described in Fig 5.1. Different cell types were graphed as % of total live cells and are representative of n=3. Statistical significance was calculated by one-way ANOVA with Tukey post test. *= $P<0.05$ versus PBS treated mice. The results shown are representative of 3 independent experiments.

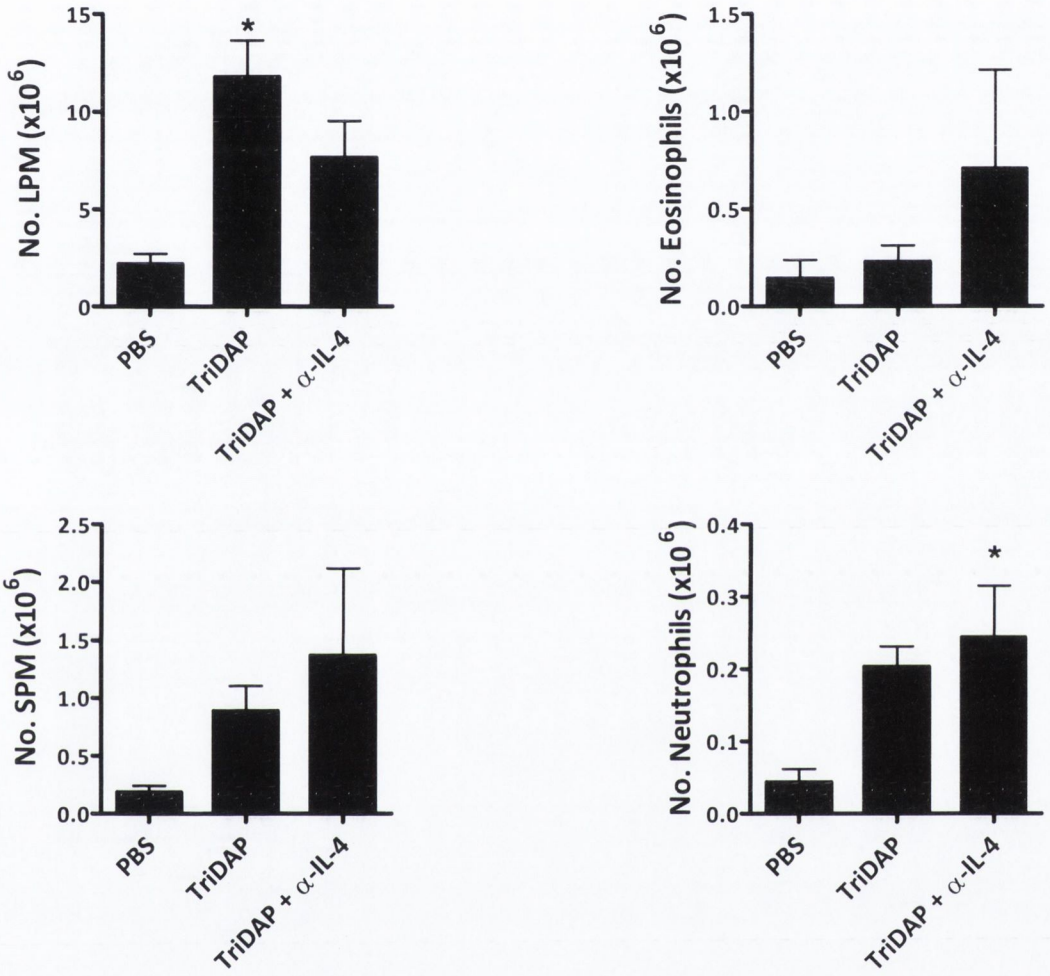

Fig 5.17 The TriDAP-induced increase in absolute number of LPM is partially dependent on IL-4 signalling. C57BL/6 mice were injected i.p. with PBS, TriDAP (100 μg) or TriDAP with αIL-4 (660 μg) antibody on d 0, 1, 2 and 3 (n=3). The mice were sacrificed on d 4 and the peritoneal cavity was lavaged. The single cell suspension was surface-stained with antibodies specific for CD11b, F480, Ly6G, Ly6C and MHC-II. The cells were then analysed by flow cytometry using the gating strategy described in Fig 5.1. Different cell types were graphed as absolute numbers and are representative of n=3. Statistical significance was calculated by one-way ANOVA with Tukey post test. *= $P<0.05$ versus PBS treated mice. The results shown are representative of 3 independent experiments.

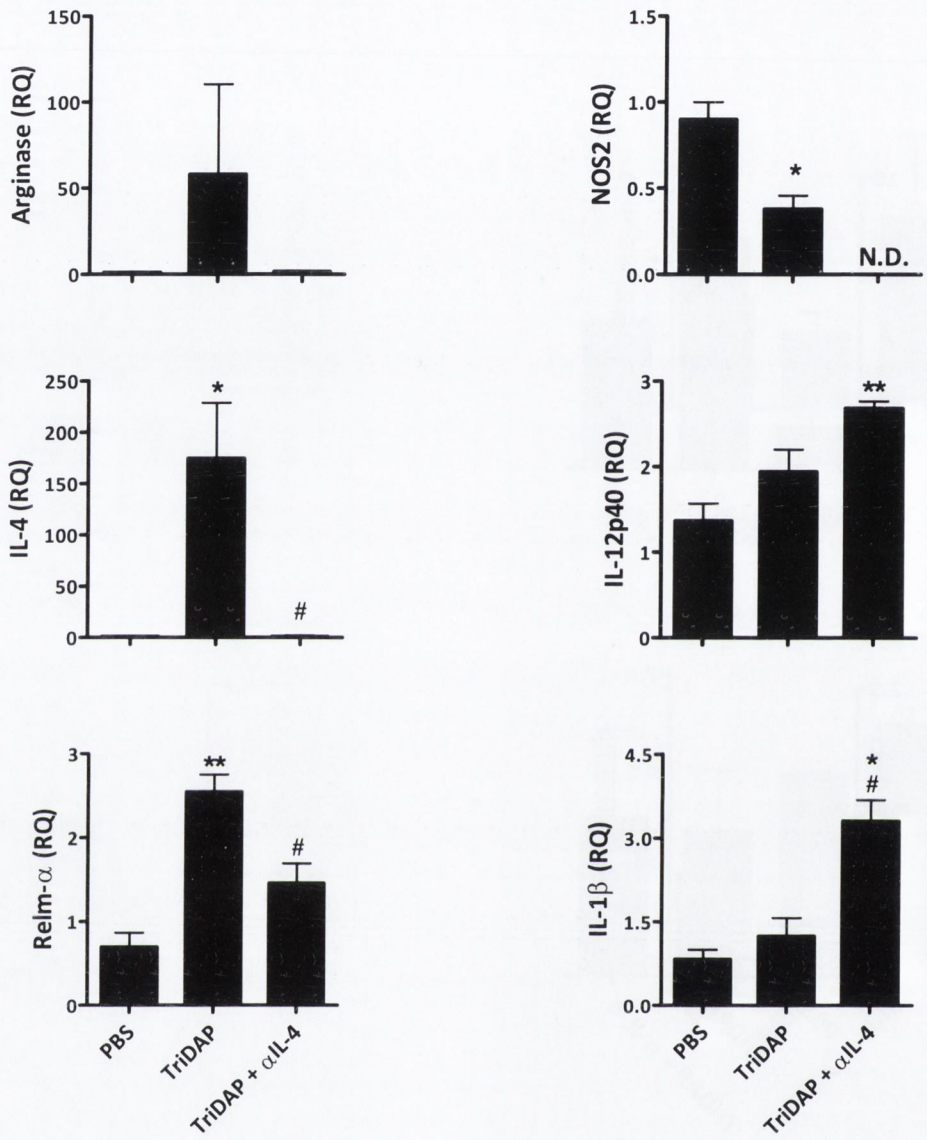

Fig 5.18 Administration of TriDAP in vivo increases the expression of arginase, IL-4 and relm-α by LPM in an IL-4 dependent manner. C57BL/6 mice were injected i.p. with PBS, TriDAP (100 μg) or TriDAP with αIL-4 (660 μg) antibody on d 0, 1, 2 and 3 (n=3). The mice were sacrificed on d 4 and the peritoneal cavity was lavaged. The single cell suspension was surface-stained with antibodies specific for CD11b, F480, MHC-II and GR1. $CD11b^{+}F480^{+}GR1^{-}MHC\text{-}II^{-}$ LPM were sorted by FACS (Fig 5.2.1). RNA was isolated from the cells and converted into cDNA. Real time PCR was used to quantify the expression of mRNA relative to the PBS injected controls. Each combination was examined in triplicate. Statistical significance was calculated using one-way ANOVA with Tukey post test. *= $P< 0.05$, **= $P < 0.01$ versus PBS-injected mice, #= $P <0.05$ versus TriDAP-injected mice. The results shown are representative of 3 independent experiments.

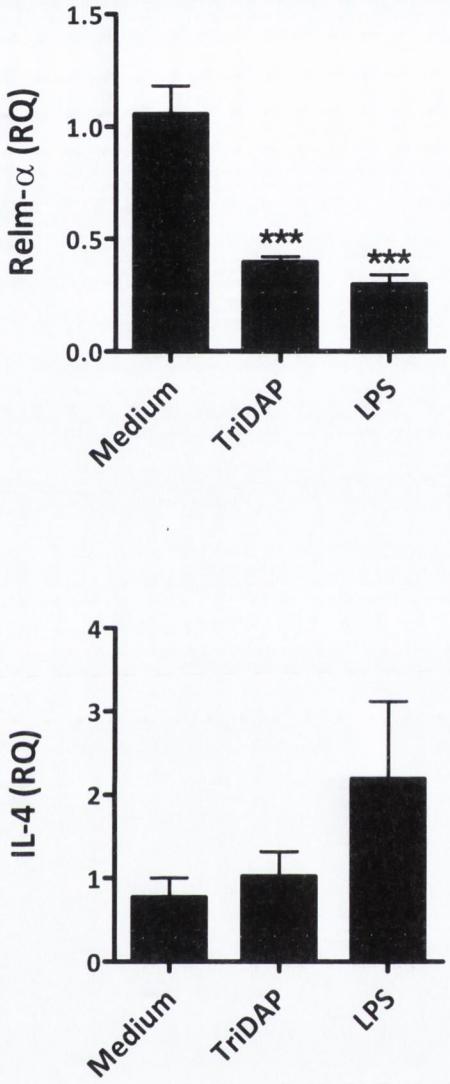

Fig 5.19 Administration of TriDAP in vitro does not induce the expression of IL-4 and reduces the expression of relm-α by PEC. C57BL/6 mice were sacrificed and the peritoneal cavity was lavaged. The single cell suspension was incubated in the presence or absence of either TriDAP (100 μg/ml) or LPS (500 ng/ml). Each combination was set up in triplicate. After 24 h the RNA was isolated from the cells and converted into cDNA by reverse transcription. Real time PCR was used to quantify the expression of mRNA relative to the medium controls. Each sample was examined in triplicate. Statistical significance was calculated using one-way ANOVA with Tukey post test. ***= $P < 0.001$ versus medium. The results shown are representative of 3 independent experiments.

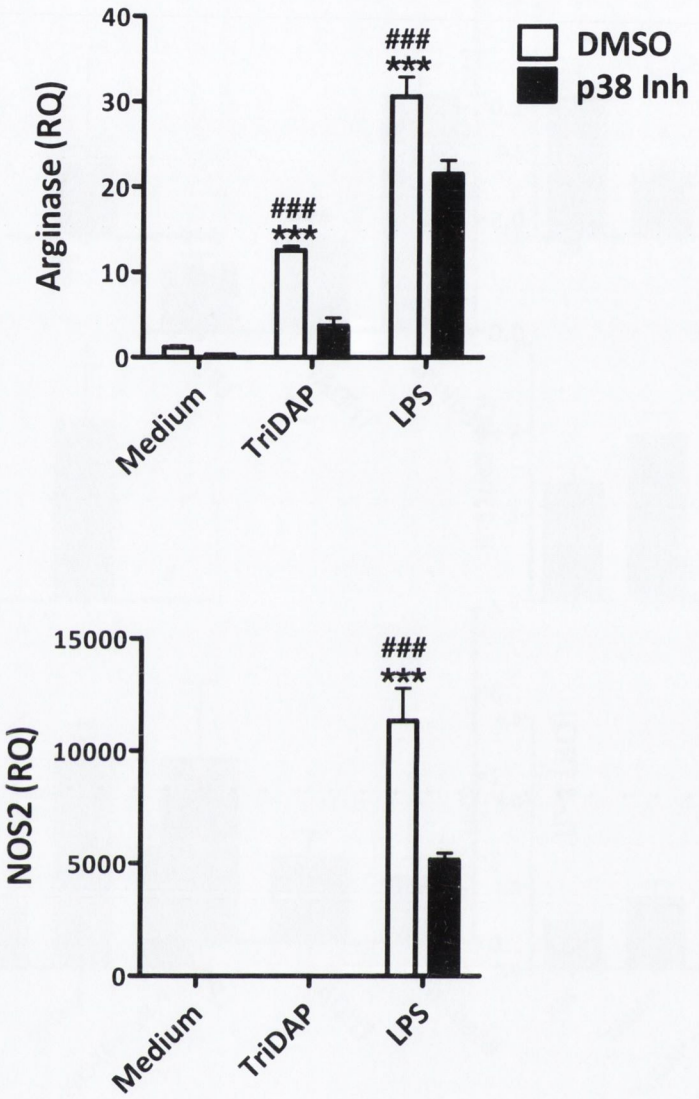

Fig 5.20 Administration of TriDAP in vitro increases the expression of arginase by PEC in a p38 dependent manner. C57BL/6 mice were sacrificed and the peritoneal cavity was lavaged. The single cell suspension incubated in the presence or absence of either TriDAP (100 μg/ml) or LPS (500 ng/ml) with or without a p38 inhibitor (500 nM). DMSO was used as a vehicle control. Each combination was set up in triplicate. After 24 h the RNA was isolated from the cells and converted into cDNA by reverse transcription. Real time PCR was used to quantify the expression of mRNA relative to the medium controls. Each sample was examined in triplicate. Significance was calculated using two-way ANOVA with Bonferroni post test. ***= $P < 0.001$ versus medium, ###= $P < 0.001$ versus p38 inh. The results shown are representative of 3 independent experiments.

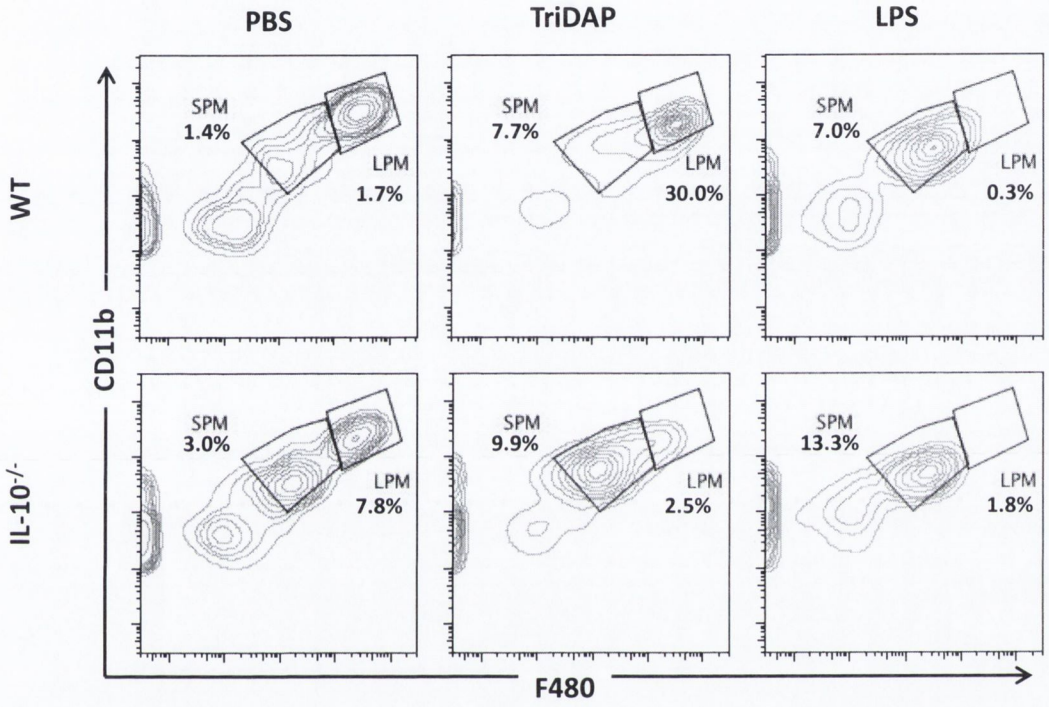

Fig 5.21A The TriDAP-induced expansion of LPM is dependent on IL-10. WT or IL-10$^{-/-}$ C57BL/6 mice were injected i.p. with PBS, TriDAP (100 μg) or LPS (100 ng) on d 0, 1, 2 and 3 (n=3). The mice were sacrificed on d 4 and the peritoneal cavity was lavaged. The single cell suspension was surface-stained with antibodies specific for CD11b, F480, Ly6G, Ly6C and MHC-II. The cells were then analysed by flow cytometry. Plots shown are gated on Ly6C$^-$ Ly6G$^-$CD11b$^+$ and are representative of n=3. The numbers shown are percentages of total live cells. The results shown are representative of 3 independent experiments.

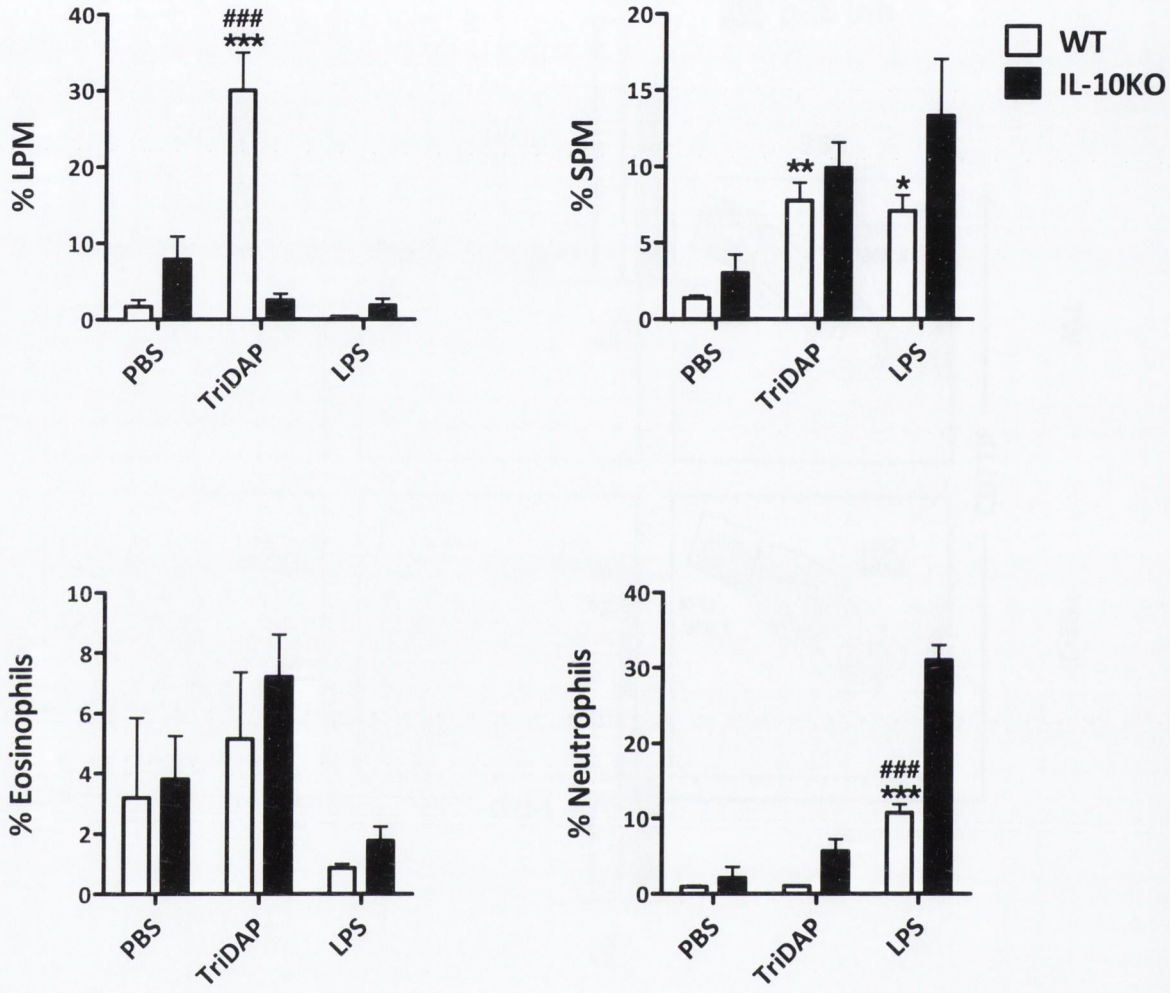

Fig 5.21B The TriDAP-induced increase in the percentage of LPM is dependent on IL-10. WT or IL-$10^{-/-}$ C57BL/6 were treated and processed as described in Fig 5.21A. The cells were analysed by flow cytometry as shown in Fig 5.1. Different cell types were graphed as a % of total live cells and are representative of n=3. Statistical significance was calculated by two-way ANOVA with Bonferroni post test. *=P <0.05, **=P <0.01, ***=P <0.001 versus PBS injected mice, ###= P < 0.001 versus IL-$10^{-/-}$. The results shown are representative of 3 independent experiments.

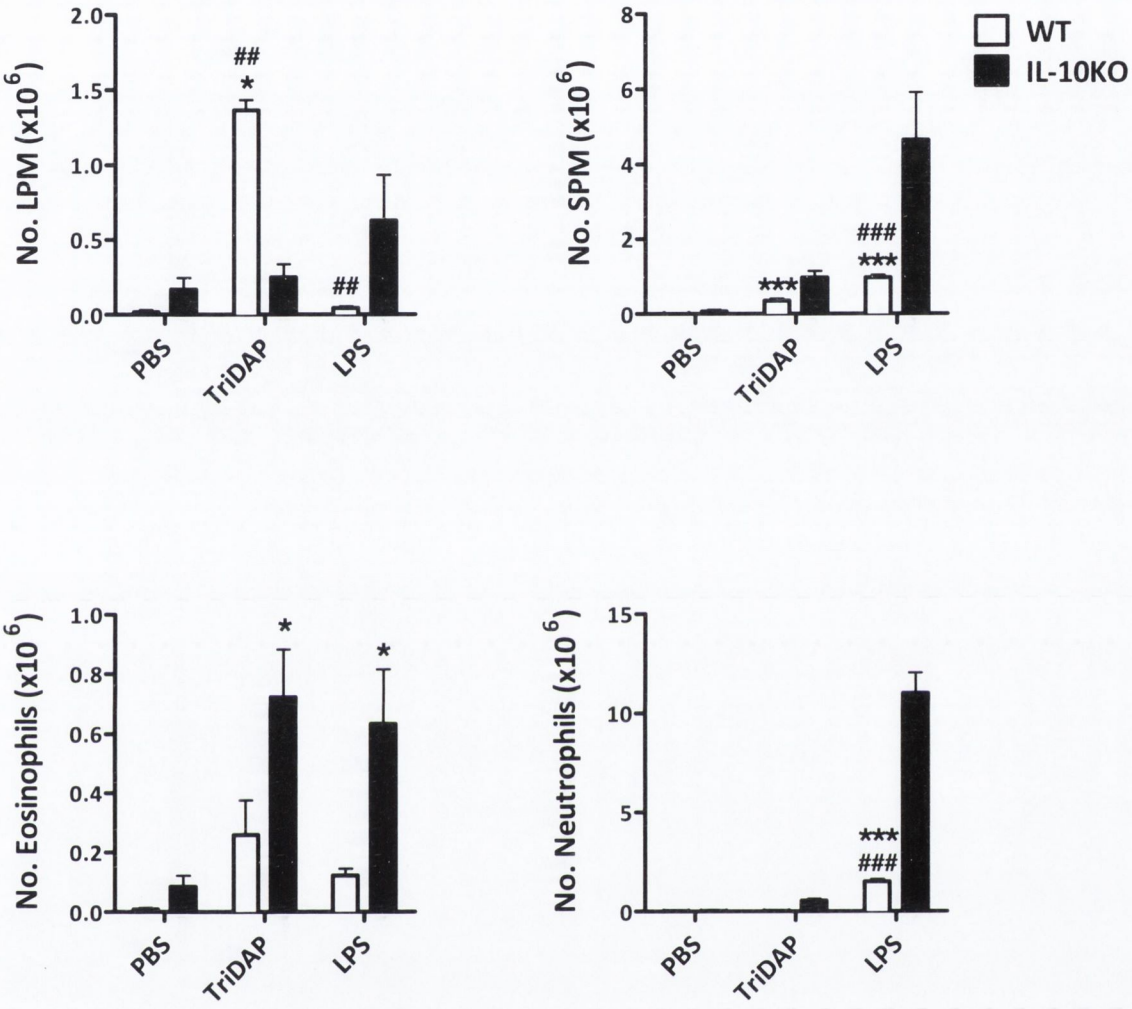

Fig 5.21C The TriDAP-induced increase in absolute number of LPM is dependent on IL-10. WT or IL-$10^{-/-}$ C57BL/6 were treated and processed as described in Fig 5.21A. The cells were analysed by flow cytometry as shown in Fig 5.1. Different cell types were graphed as absolute numbers and are representative of n=3. Statistical significance was calculated by two-way ANOVA with Bonferroni post test. *=P <0.05, **=P <0.01, ***=P <0.001 versus PBS injected mice, ##=P <0.01, ###= P < 0.001 versus IL-$10^{-/-}$. The results shown are representative of 3 independent experiments.

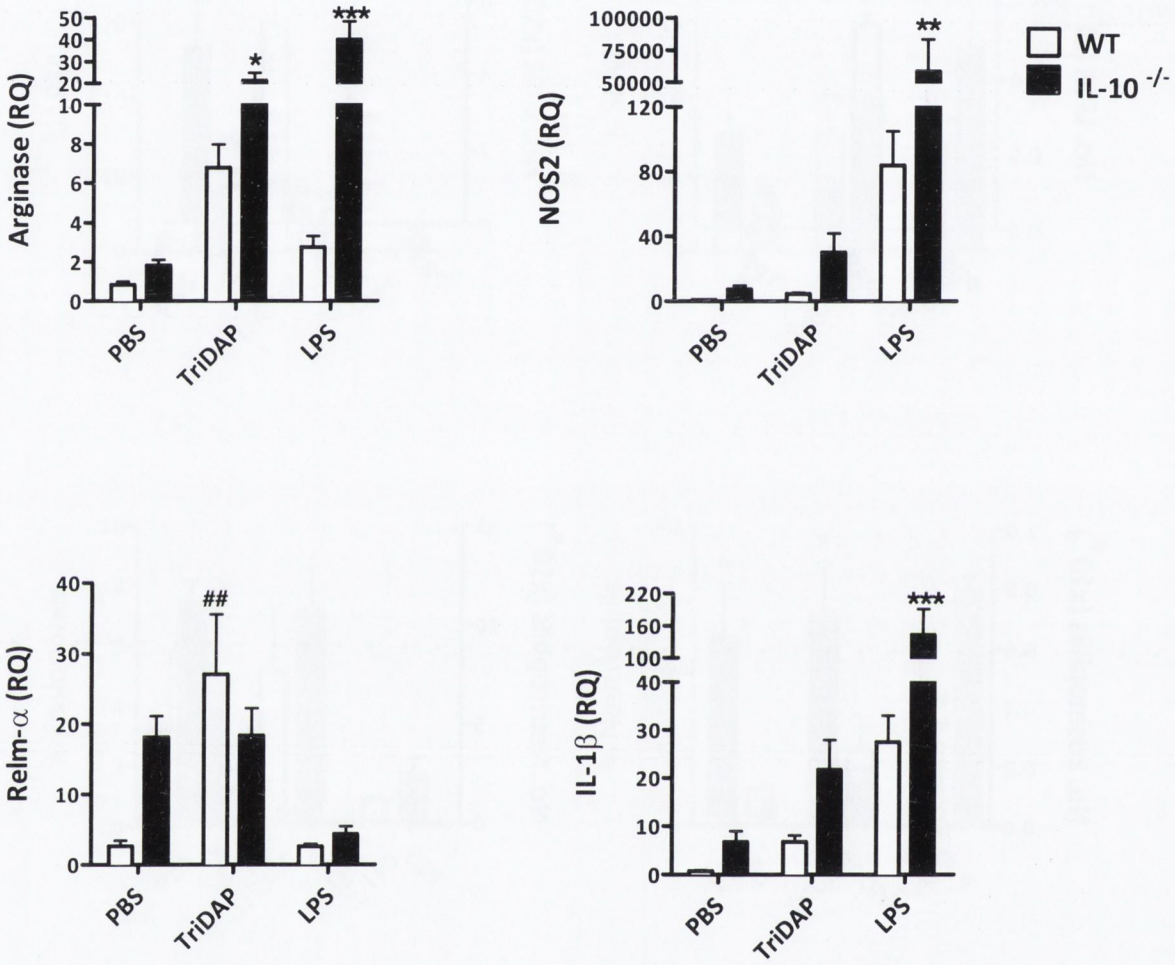

Fig 5.22 IL-10 suppresses both M1 and M2 activation in the peritoneal cavity in response to TriDAP or LPS. WT or IL-$10^{-/-}$ C57BL/6 mice were injected i.p. with PBS, TriDAP (100 µg) or LPS (100 ng) on d 0, 1, 2 and 3 (n=3). The mice were sacrificed on d 4 and the peritoneal cavity was lavaged. RNA was isolated from the PEC and converted into cDNA. Real time PCR was used to quantify the expression of mRNA relative to the PBS injected controls. Each sample was examined in triplicate. Statistical significance was calculated by two-way ANOVA with Bonferroni post test. *=P <0.05, **=P <0.01, ***=P <0.001 versus WT mice, ##= P < 0.01 versus PBS controls. The results shown are representative of 3 independent experiments.

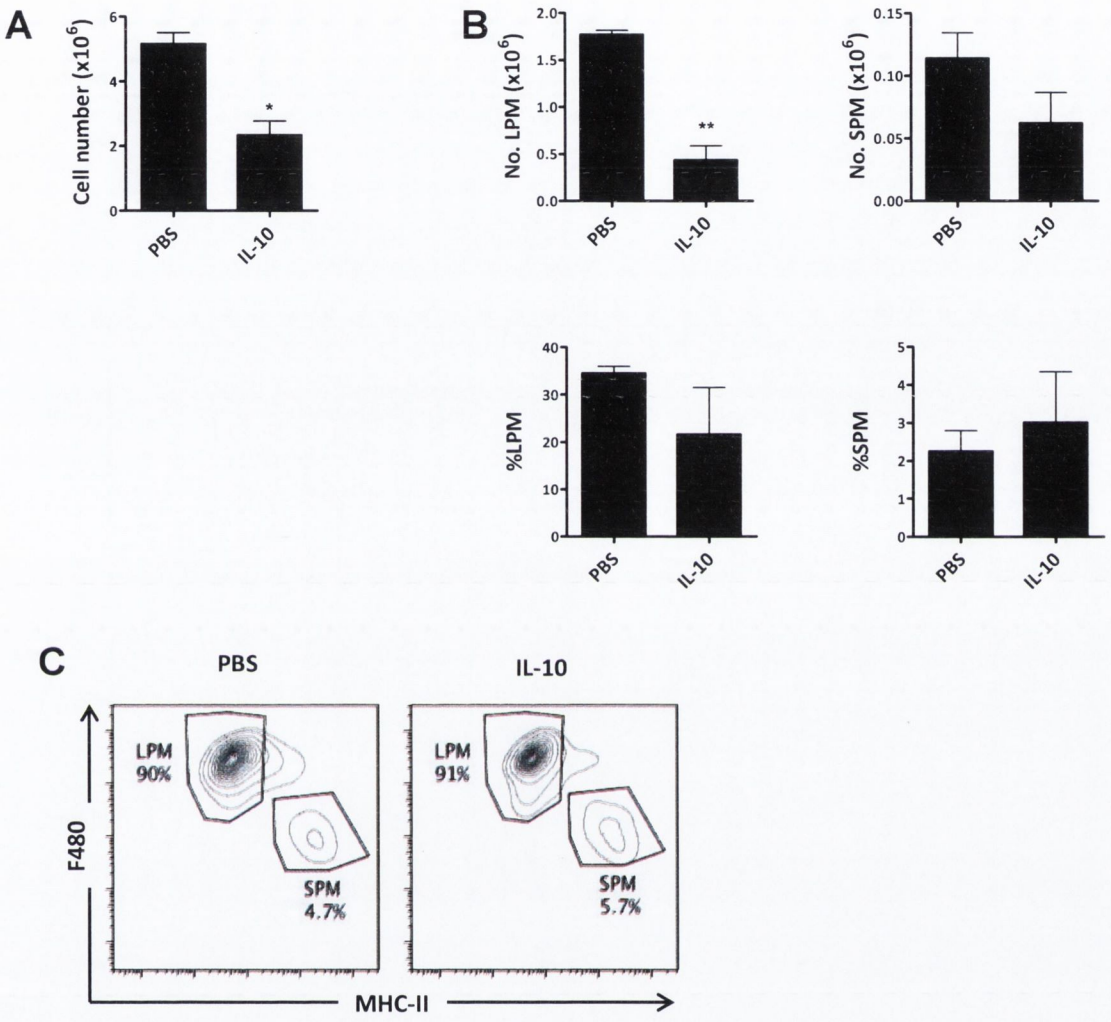

Fig 5.23 The administration of recombinant IL-10 reduces the numbers of LPM in the peritoneal cavity. C57BL/6 mice were injected i.p. with either PBS or IL-10 (200 ng) on d 0 and 2 (n=3). The mice were sacrificed on d 4 and the peritoneal cavity was lavaged. The single cell suspension was counted (A) and surface-stained with antibodies specific for CD11b, F480, Ly6G, Ly6C and MHC-II. The cells were then analysed by flow cytometry. The percentages and absolute numbers of LPM and SPM were analysed using the gating strategy shown in Fig 5.1 (B). Plots shown were gated on CD11b+F480+Ly6G- cells (C) and are representative of n = 3. Statistical significance was calculated by a two tailed t-test. *=P <0.05, **=P <0.001 versus PBS controls.

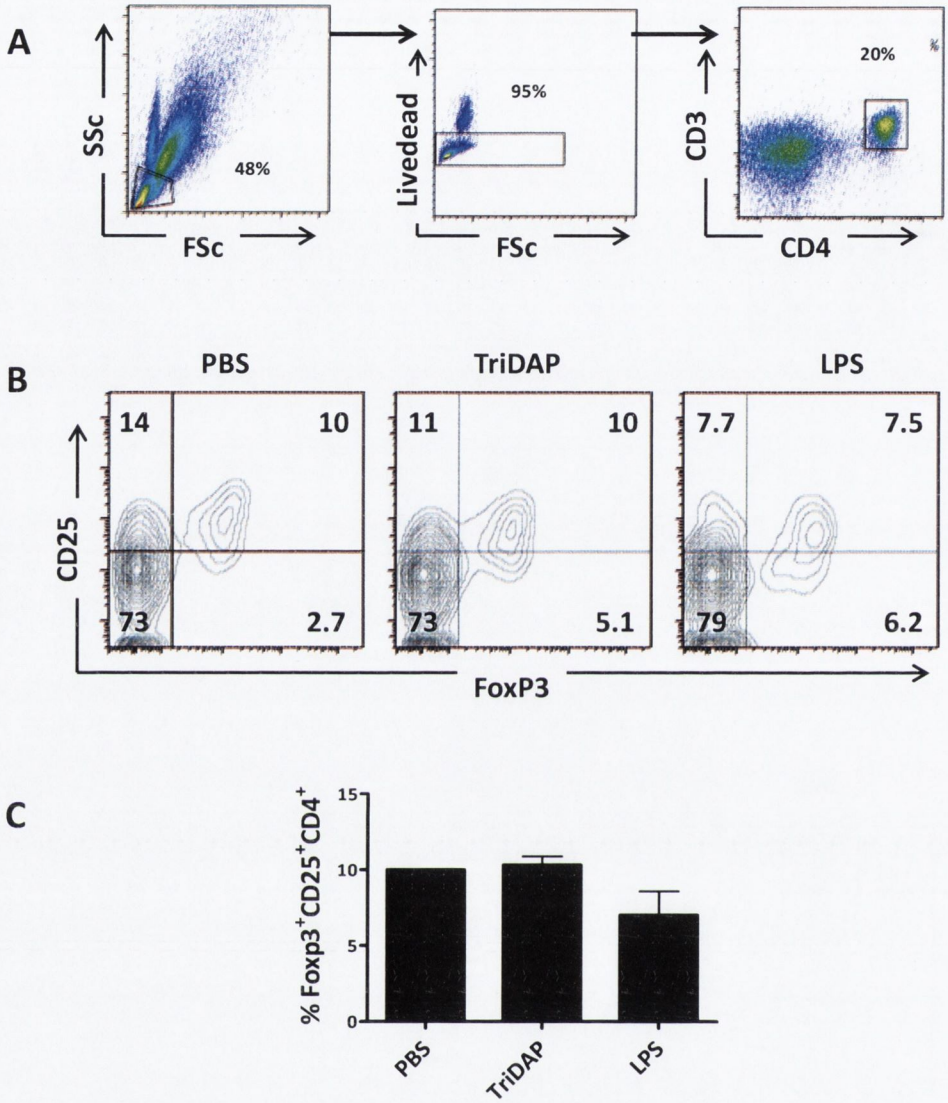

Fig 5.24 Administration of TriDAP in vivo has no effect on the percentage of FoxP3$^+$CD25$^+$CD4$^+$ T-cells in the peritoneal cavity. C57BL/6 mice were injected i.p. with PBS, TriDAP or LPS on d 0, 1, 2 and 3 (n=3). The mice were sacrificed on d 4 and the peritoneal cavity was lavaged. The single cell suspension was surface-stained with antibodies specific for CD4 and CD25. Cells were also stained for intra-nuclear FoxP3. The plots shown are gated on CD4$^+$ lymphocytes (B) using the gating strategy shown (A) and are representative of n=3. The percentages of FoxP3$^+$CD25$^+$CD4$^+$ cells were graphed (C) and are representative of n=3. Statistical significance was calculated using a one-way ANOVA with a Tukey post test. The results shown are representative of 3 independent experiments.

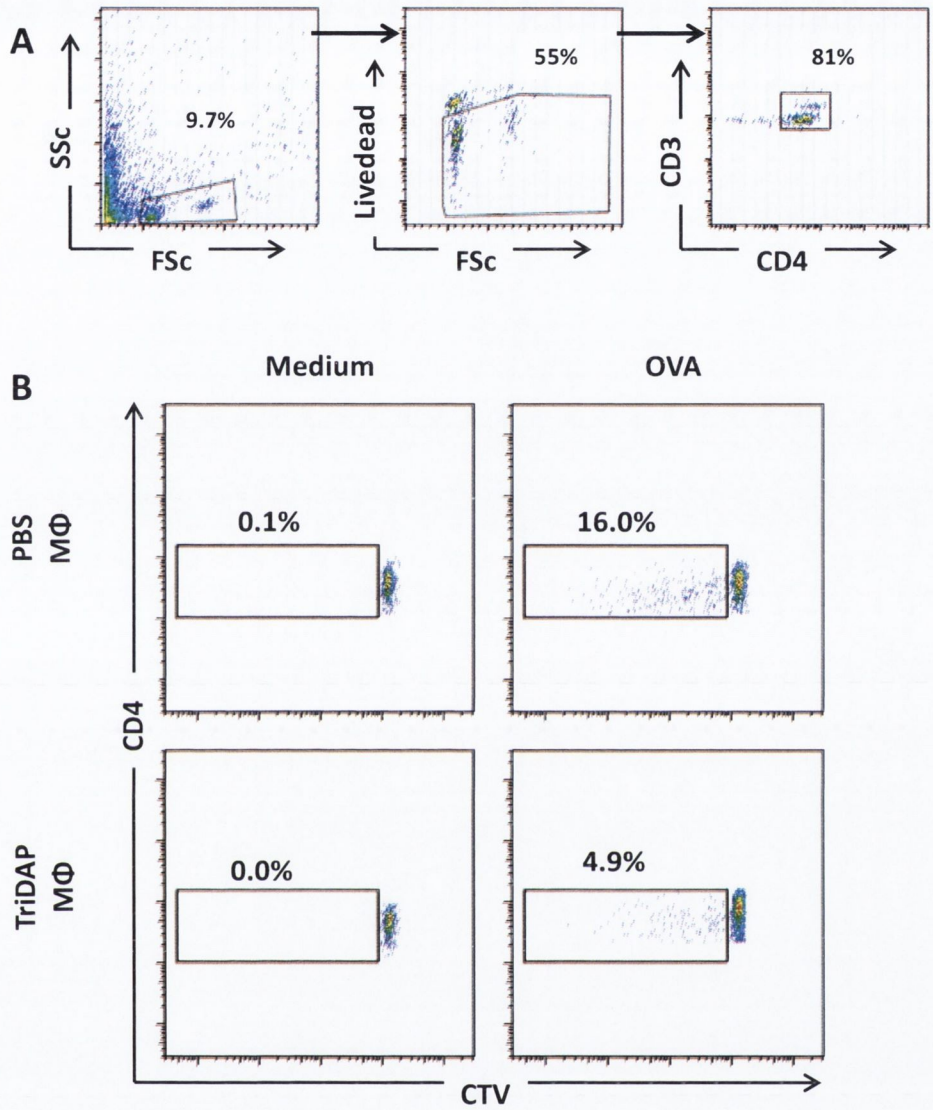

Fig 5.25 LPM from mice injected with TriDAP have a reduced ability to drive antigen-specific CD4⁺ T-cell responses. BALB/c mice were injected with either PBS or TriDAP (100 µg) on d 0, 1, 2 and 3. Mice were sacrificed on d 4 and the peritoneal cavity was lavaged and pooled. The single cell suspension was surface-stained with antibodies specific for CD11b, F480, MHC-II and GR1. LPM were purified by FACS (Fig 5.2.1) and added to a culture containing purified OVA-specific CD4⁺ T-cells labelled with CTV. Each combination was set up in triplicate. The T-cells and macrophages were cultured in the presence or absence of OVA (50 µg/ml). After 72 h the cells were surface stained with antibodies specific for CD4 and CD3. Plots shown (B) were gated using the strategy shown (A) are representative of n=3. The results shown are representative of 3 independent experiments.

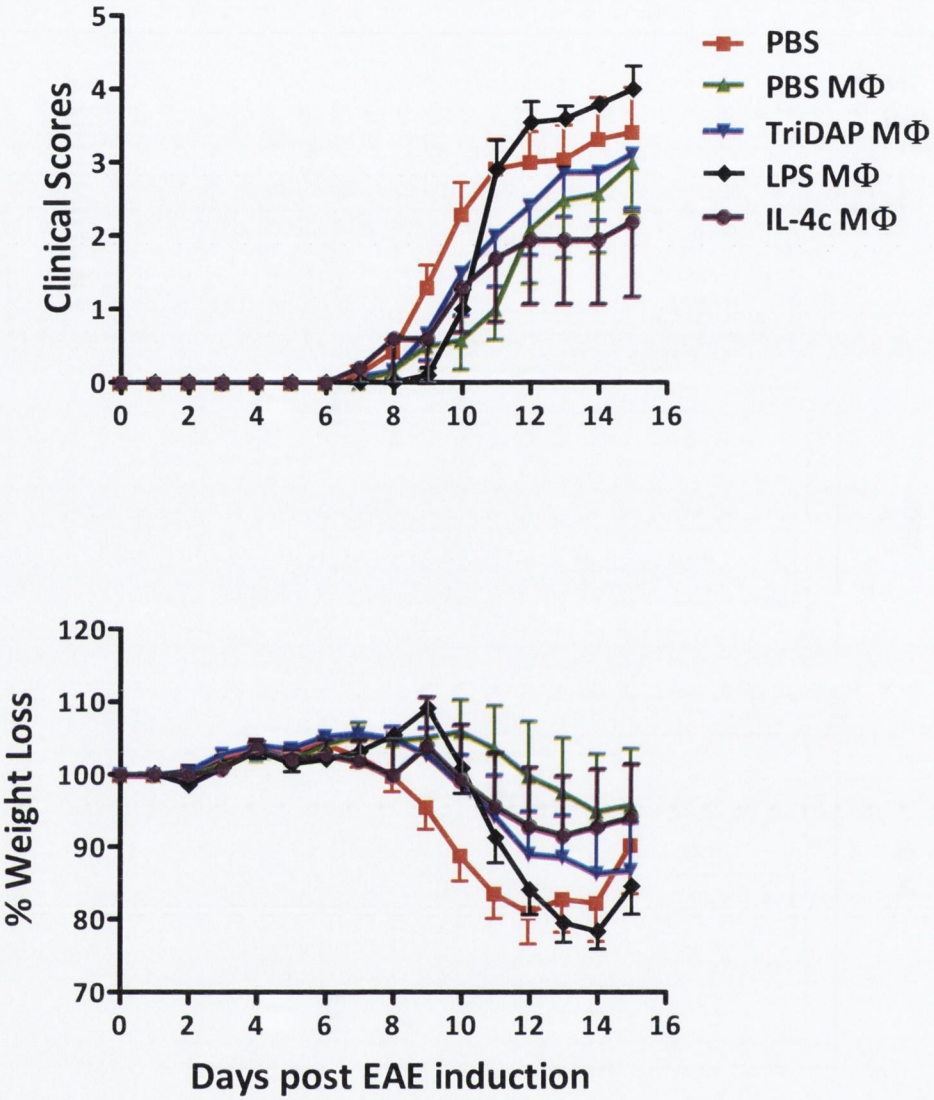

Fig 5.26A The effect of macrophage transfers on the clinical symptoms of EAE. C57BL/6mice were injected with PBS, LPS (100 ng) or TriDAP (100 µg) on d 0, 1, 2 and 3 (n=5). Another group of mice were injected with IL-4c (rIL-4, αIL-4; 5 µg, 25 µg) on d 0 and 2. On d 4 the mice were sacrificed and the peritoneal cavity was lavaged. Cells were stained with antibodies specific for F480, CD11b, GR1 and MHC-II. Macrophages ($CD11b^+F480^+Gr1^-$) were purified from each group using FACS (Fig 5.2.2) and injected s.c. into mice ($1x10^6$ cells/mouse) with EAE on d 0 and d 6 post EAE induction (n=5). EAE was induced in C57BL/6 mice by s.c. injection of MOG (100 µg) emulsified in CFA, followed by an i.p. injection of PT (500 ng) on d 0 and 2. Clinical scores and weights were checked daily. Statistical significance was calculated using a repeated measures two-way ANOVA with a Bonferroni post test.

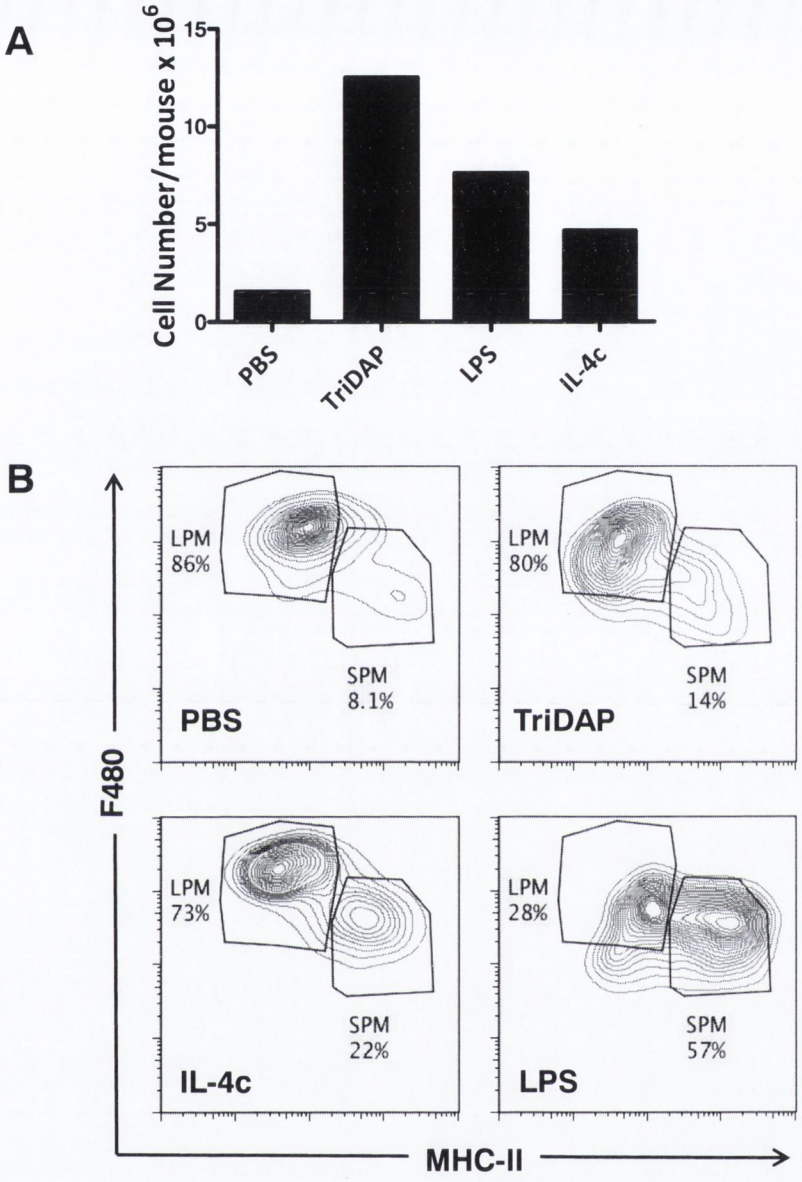

Fig 5.26B Phenotypes of sorted macrophages transferred into mice with EAE. C57BL/6mice were injected with PBS, LPS (100 ng) or TriDAP (100 μg) on d 0, 1, 2 and 3. Another group of mice were injected with IL-4c (rIL-4, αIL-4; 5 μg, 25 μg) on d 0 and 2. On d 4 the mice were sacrificed and the peritoneal cavity was lavaged. Cells were pooled, counted (A) and stained with antibodies specific for F480, CD11b, GR1 and MHC-II. Macrophages ($CD11b^+F480^+Gr1^-$) from each group were purified using FACS (Fig 5.2.2) and injected s.c. into mice ($1x10^6$ cells/mouse) with EAE on d 0 and d 6 post EAE induction. The plots shown are representative of the populations of macrophages (B; $CD11b^+F480^+GR1^-$) injected on both D0 and D6.

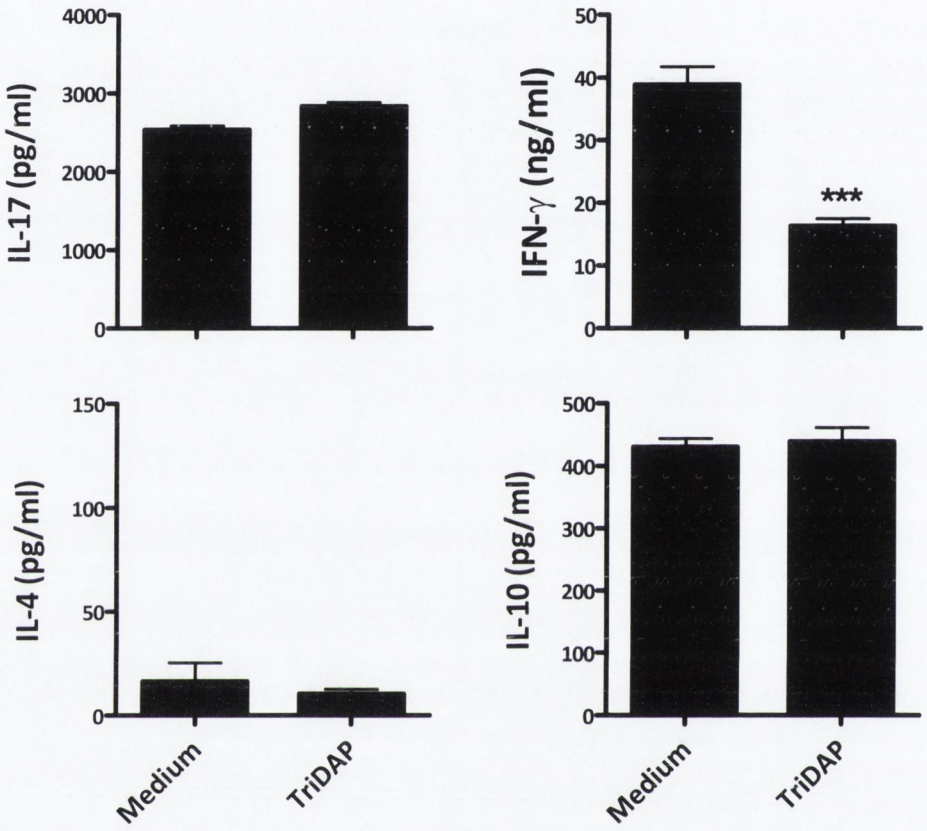

Fig 5.27 TriDAP suppresses IFN-γ production by lymph node and spleen cells from MOG-immunized mice stimulated in vitro with MOG, IL-1β and IL-23. C57BL/6 mice were immunized with s.c. injection of MOG (100 μg) emulsified in CFA. The mice were sacrificed on d 10 and cells from the spleens and lymph nodes were incubated with MOG (100 μg/ml), IL-1β (10 ng/ml) and IL-23 (10 ng/ml), in the presence or absence of TriDAP (100 μg/ml). Each combination was set-up in triplicate. After 72 h the supernatants were removed and the concentrations of cytokines were quantified by ELISA. Statistical significance was calculated using a two-tailed t-test. ***= $P < 0.001$ versus medium.

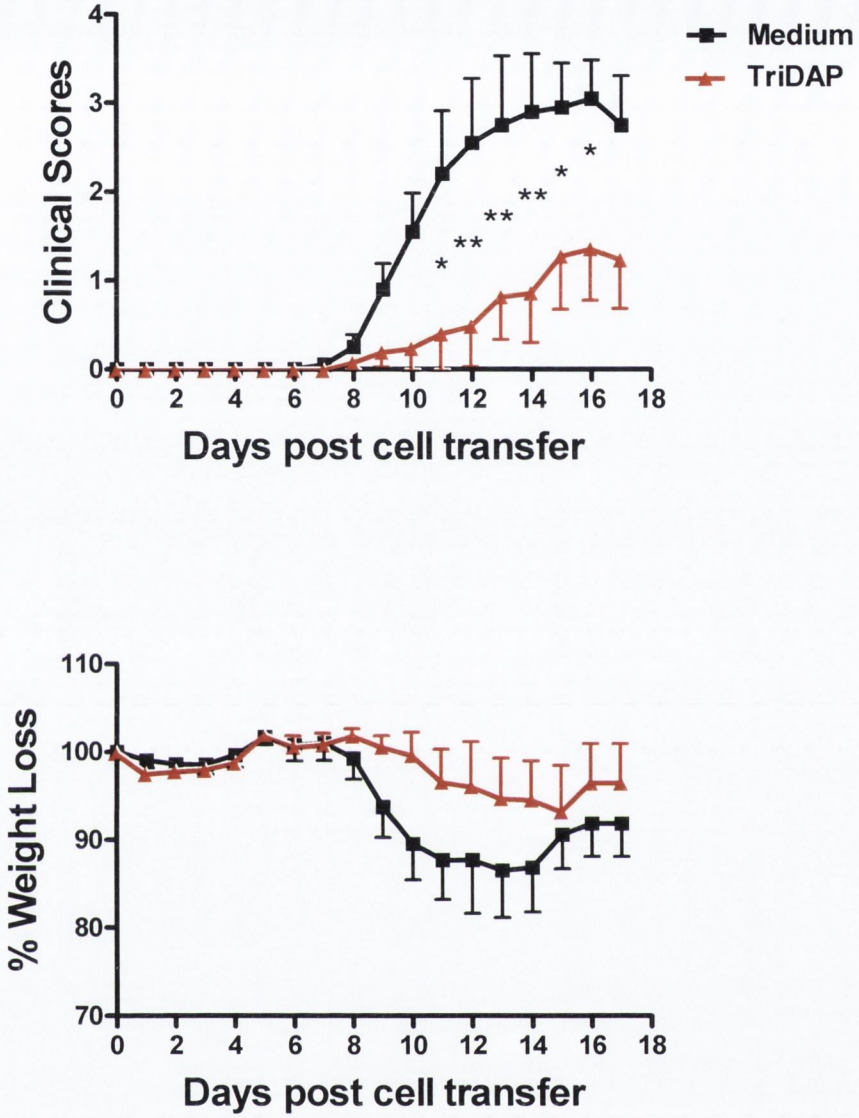

Fig 5.28 TriDAP reduces the pathogenic effect of immune cells from MOG-immunized mice. C57BL/6 mice were immunized with MOG (100 µg) emulsified in CFA. The mice were sacrificed on d 10 and cells from the spleens and lymph nodes were incubated with MOG (100 µg/ml), IL-1β (10ng/ml) and IL-23 (10 ng/ml) in the presence or absence of TriDAP (100 µg/ml). After 72 h the cells were washed and injected i.p. into naive C57BL/6 mice ($15x10^6$ cells/mice; n=5). Clinical scores and weights were checked daily. Statistical significance was calculated using a repeated measures two-way ANOVA with a Bonferroni post test. **= $P < 0.01$ versus medium.

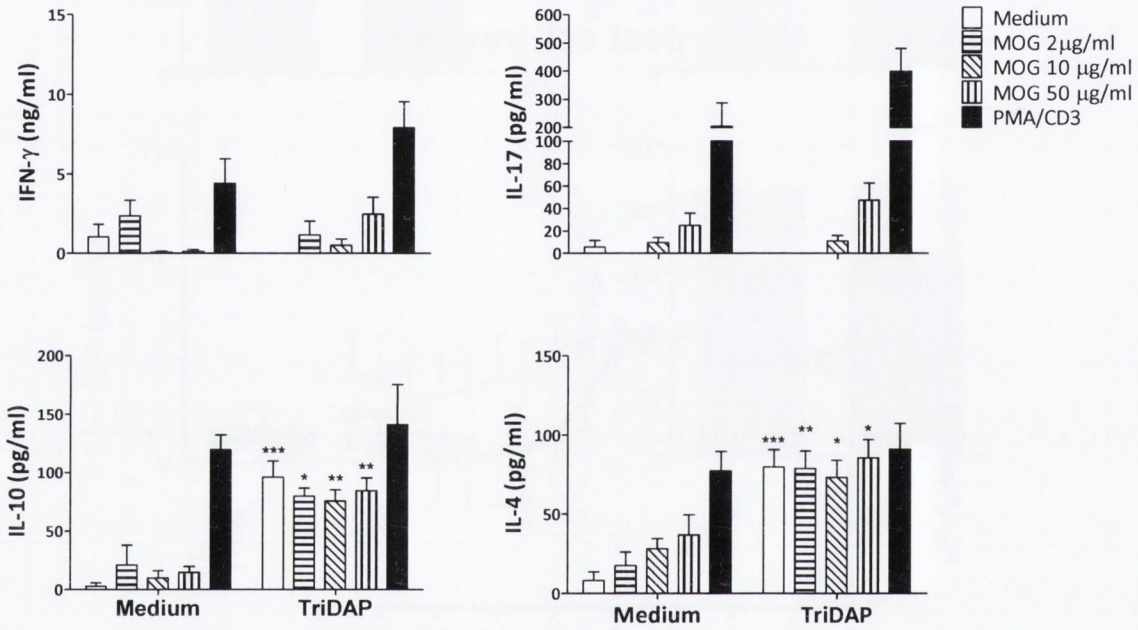

Fig 5.29 IL-10 and IL-4 production is enhanced in mice that recieved TriDAP-treated immune cells from MOG-immunized mice. EAE was induced as described in Fig 5.28. Mice were sacrificed on d 17 and the spleen cells were incubated with increasing concentrations of MOG (2, 10 and 50 μg/ml) or PMA (10 ng/ml) and αCD3 (1 μg/ml). Each combination was set-up in triplicate giving a total of n=15. Supernatants were removed after 72 h and the concentrations of cytokines were quantified by ELISA. Statistical significance was calculated using a two-way ANOVA with Bonferroni post test. *** = $P < 0.001$ vs medium.

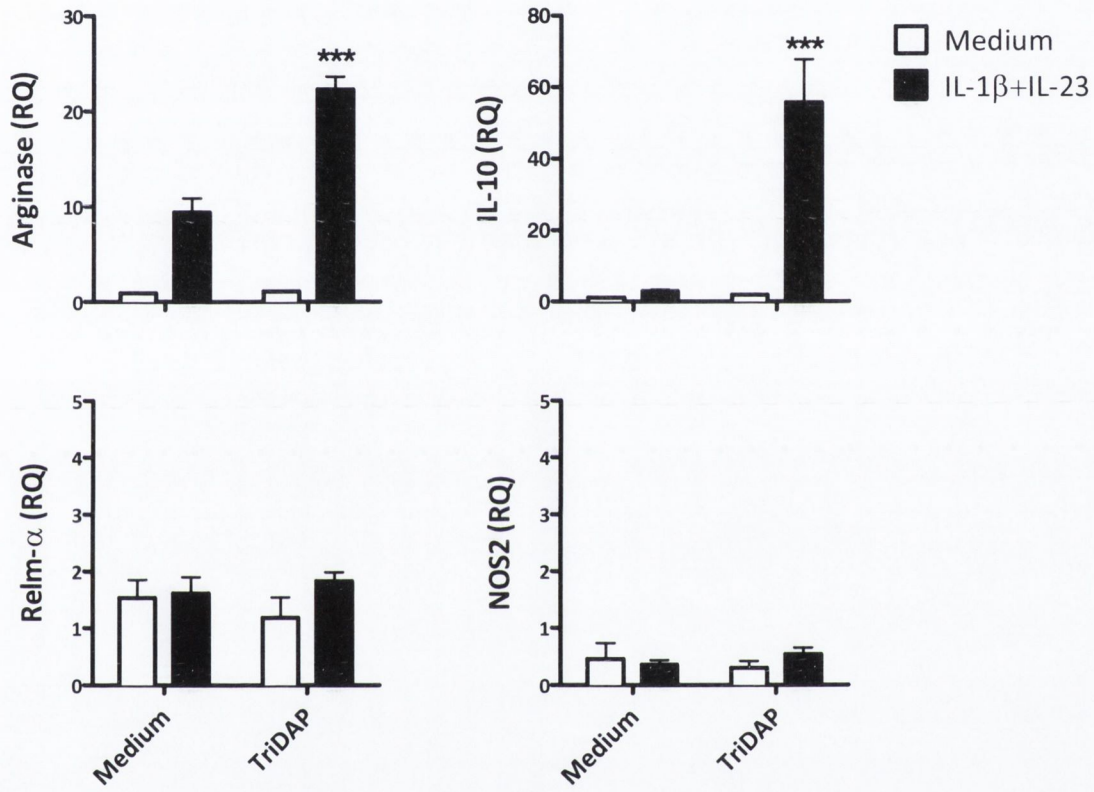

Fig 5.30 TriDAP synergises with IL-1β and IL-23 to increase the expression of arginase and IL-10 by splenocytes. The spleens of C57BL/6 mice were removed and a single cell suspension was obtained. Splenocytes were incubated with IL-1β (10 ng/ml) and IL-23 (10 ng/ml) in the absence or presence of TriDAP (100 μg/ml). Each combination was set-up in triplicate. After 24 h the RNA was isolated from the cells and converted into cDNA. Real time PCR was used to quantify the expression of mRNA relative to the untreated cells. Each sample was examined in triplicate. Statistical significance was calculated by two-way ANOVA with Bonferroni post test. *** = $P < 0.001$ versus medium.

Chapter 6

General discussion

CHAPTER 6 General discussion

This study demonstrated that in vivo administration of the NOD1 agonist TriDAP attenuated the clinical symptoms of actively induced EAE. This was associated with a reduction of IL-17 and IFN-γ responses in the central nervous system and peripheral lymph nodes. In addition, in vitro treatment of MOG-activated cells with TriDAP attenuated the development of passively induced EAE, which was associated with a decrease in clinical score and an increase in IL-10 and IL-4 production in the periphery. It was also demonstrated that NOD1 activation in primary peritoneal macrophages in vitro promoted IL-10 production in a p38-dependent manner. In addition, i.p. administration of TriDAP promoted the expansion of LPM in an IL-10-dependent manner. This was associated with an increase in the expression of the M2 activation markers arginase, relm-α, and IL-4 by LPM. Furthermore, the expression of these markers was abrogated in the presence of an IL-4 neutralising antibody, suggesting that NOD1 activation promotes the expansion of M2 macrophages via the production of IL-10 and IL-4. These results provide substantial insight into the role of NOD1 activation. Collectively, these findings have the potential to change the way NOD1 activation is viewed during autoimmunity, inflammatory disorders and bacterial infection.

There is strong evidence that NOD2 signalling has a protective effect against the intestinal inflammation associated with Crohn's disease. Genetic screenings have shown that loss of function mutations in the CARD15 domain of the NOD2 gene increase the risk of developing Crohn's disease [225, 226]. Genetic studies aimed at finding a similar link between NOD1 polymorphisms and inflammatory bowel disease have resulted in mixed conclusions [240, 243], however, the fact that NOD1 and NOD2 share the same signalling pathways suggests that NOD1 may play a similar anti-inflammatory role during inflammation. In light of this hypothesis, this thesis examined the effect of NOD1 activation on the induction of EAE and the associated pathogenic immune responses.

The results presented in chapter 3 of this thesis demonstrated that administration of TriDAP at the induction and throughout the course of disease attenuated the clinical symptoms of EAE. The attenuation of EAE was associated with reduced IL-17 and IFN-γ production by $CD4^+$ T-cells in the brain and peripheral lymph nodes of sick mice. These findings suggest a protective role for NOD1 activation during autoimmunity. The mechanism behind the TriDAP-mediated attenuation of EAE is unclear. NOD2 activation

has been shown to inhibit TLR-induced pro-inflammatory cytokine production by DC and thereby inhibit the adaptive immune response [125]. It is possible that NOD1 activation may inhibit the induction of EAE via a similar mechanism. However, the findings of the present study suggest NOD1 activation has no effect on the ability of DC to produce pro-inflammatory cytokines in response to heat-killed *M. tuberculosis*, which is the main component of the adjuvant used to induce EAE. This suggests that NOD1 activation does not attenuate EAE by interacting with DC, however, NOD1 activation did induce IL-10 production by primary peritoneal macrophages. IL-10 is an immunosuppressive cytokine and IL-10-deficient mice have a significantly exacerbated clinical course of EAE [273]. Furthermore, administration of IL-10 at the induction of EAE attenuates clinical scores [274, 343, 344]. The present study also demonstrated that TriDAP could reduce the pathogenicity of MOG-specific T-cells when added to cultures of lymph node and spleen cells prior to transfer into naive mice. Mice that received TriDAP-treated cells had lower clinical scores than mice injected with cells that had been cultured with MOG, IL-1β and IL-23 in the absence of TriDAP. The attenuated symptoms of passively induced EAE were associated with increased production of IL-10 and IL-4 in the periphery of mice. It is possible that NOD1-mediated IL-10 production may explain the protective effect of TriDAP in both the actively induced and passively induced EAE model, however, further investigation is required before this hypothesis can be confirmed.

The present study demonstrated that administration of TriDAP i.p. induced the expansion of M2 macrophages. The activation of M2 macrophages has also been shown to have a protective role against EAE. There are increased numbers of M2 macrophages in the brains of mice in the remission phase of relapsing-remitting EAE, moreover, the transfer of M2 macrophages into mice with EAE can attenuate the clinical symptoms of disease [182, 184]. The present study showed that macrophages transferred from TriDAP-treated mice suppressed EAE, but not to a greater extent than macrophages from PBS-treated mice. However, this experiment was complicated by the fact that the macrophages from naive mice are inherently immunosuppressive. In contrast, pro-inflammatory macrophages from LPS-treated mice exacerbated EAE. This finding is consistent with the fact that higher numbers of M1 macrophages are associated with relapses during EAE [182]. Direct administration of TriDAP increased the numbers of immunosuppressive macrophages in vivo, therefore, the TriDAP-mediated attenuation of EAE may be

dependent on increasing the numbers of immunosuppressive macrophages rather than enhancing their function. However, the present study also demonstrated that TriDAP enhanced the expression of M2 markers, arginase and IL-10, during the culture of lymph node and spleen cells with autoantigen, IL-1β and IL-23 prior to transfer in vivo for passive induction of EAE in naive mice. The reduced clinical scores in recipients of TriDAP-treated cells suggests that, under the right circumstances, TriDAP-induced M2 activation can inhibit the generation of a pathogenic T cells that mediate autoimmune disease. In fact, the production of IL-10 and IL-4 was increased in mice who received TriDAP-treated cells, suggesting that NOD1 activation can influence the activation of pathogenic T-cells by indirectly inducing the production of anti-inflammatory cytokines. Importantly, these results provide a link between TriDAP-induced M2 macrophage activation and the attenuation of autoimmune disease.

Although NOD1 is considered to be a promoter of innate and adaptive immune responses [214], the findings of the present study suggest that NOD1 plays a role in anti-inflammatory responses as well as pro-inflammatory responses. In addition, this study demonstrated that TriDAP administration inhibited Th17 and Th1 responses during autoimmunity. This finding is inconsistent with the dogma that PAMPs promote immune responses, however certain PAMPs, such as CpG, have been shown to alter the course of autoimmune, allergy and other inflammatory disorders by shifting the balance away from pathogenic inflammatory immune responses towards therapeutic anti-inflammatory immune responses. For example, CpG is thought to alleviate the pathogenic Th2 inflammation associated with asthma by inducing a Th1 response and is currently in clinical trials as a treatment for asthmatic patients [292]. Another group of PRR, the RIG-I like helicases (RLH), have been shown to restrain autoimmune responses in the CNS. Generally, RLH detect viral RNA and mediate anti-viral immune responses. Similar to the effect of TriDAP administration, administration of viral RNA attenuated EAE and suppressed MOG-specific IL-17 and IFN-γ production by $CD4^+$ T-cells [345]. Viral RNA mediated the suppression of EAE by inducing the production of type I interferons. It is possible that a similar mechanism is involved in the NOD1-mediated attenuation of EAE as studies have shown that NOD1 is involved in the production of type I interferons during bacterial infection [205]. However, preliminary experiments using mice deficient in the type I interferon receptor (IFNAR) were inconclusive.

EAE, a mouse model for MS, has been used to develop novel therapeutics such as fingolimod and tysabri/natalizumab. MS is the leading cause of non-traumatic neurological impairment in young men and women between the ages of 20-40 [246, 249] and although first-line treatments, such as IFN-β, are available, these drugs are not efficacious in all patients. For example, some patients produce anti-IFN-β antibodies, which bind the drug and neutralise its therapeutic effect [124]. Thus, some studies are attempting to induce the production of endogenous anti-inflammatory molecules by the administration of an exogenous immunostimulator, such as viral RNA [345]. In light of the findings of the present study, it is possible that NOD1 agonists could be used in similar fashion as a therapy for autoimmune disease, but first the mechanism behind the NOD1-mediated attenuation of EAE must be investigated further.

The present study demonstrated that the NOD1 agonist TriDAP promoted the production of IL-10 by primary peritoneal macrophages. Both NFkB and MAPK are involved in the NOD1 signalling pathway [190, 295], however, the findings of the present study demonstrated that the production of IL-10 in response to TriDAP was completely dependent on p38 signalling. This is the first report of innate IL-10 production in response to a NOD1 agonist. However, there is evidence to suggest that NOD2, in conjunction with TLR2, mediates the expression of IL-10 in the gut in response to commensal bacteria [95, 234, 346]. Furthermore, NOD2 activation in the absence of IL-10 signalling causes macrophages to become hyperresponsive and promote colitis [235]. These reports and the findings of the present study suggest that NOD receptors have a role in promoting IL-10 production to restrain pro-inflammatory responses. IL-10 is important for gut homeostasis during the steady state as IL-10-deficent mice spontaneously develop colitis in response to commensal bacteria [80]. Therefore the production of IL-10 has been suggested as one of the possible mechanisms of NOD2-mediated protection against Crohn's disease. Taken together these findings highlight the need for further investigation into NOD1-mediated IL-10 production and its implications for immune homeostasis in the gut. Watanabe et al have shown that administration of a NOD2 agonist can attenuate experimental colitis [281] and the findings of the present study demonstrated that a NOD1 agonist had a protective effect during EAE. Therefore the next step may be to investigate the potential protective effect of TriDAP administration in experimental colitis.

One of the main roles of IL-10 is to restrict excess inflammation during infection, which prevents collateral damage in the surrounding tissue. Therefore, it is important that IL-10 is produced at the same time as pro-inflammatory mediators during infection. For example, LPS induces the production of IL-10 in addition to inducing the production of pro-inflammatory cytokines, such as TNF-α [94]. The importance of the production of IL-10 during infection is highlighted by the fact that IL-10-deficient mice have a higher mortality rate from *E. coli* peritonitis than WT mice [81]. The present study demonstrated that the NOD1 agonist TriDAP can contribute to pro-inflammatory responses by inducing the production of IL-6 and enhancing TLR-mediated pro-inflammatory cytokine production, however, TriDAP also promoted IL-10 production by peritoneal macrophages. These findings suggest that NOD1 agonists, similar to other PAMPs, also restrict excessive inflammation during bacterial infection by inducing the production of IL-10.

IL-10 plays a role in maintaining tolerance to commensal bacteria in the gut and has been assessed as a therapeutic for Crohn's disease [347-349]. Some studies even suggest that altering the commensal bacteria of the gut to induce the production of IL-10 may be used as a therapeutic for IBD [350, 351]. The findings of the present study suggest that NOD1-activating bacteria may promote IL-10 production and represents a new subject for potential investigation. In fact, *H. pylori* activates NOD1 efficiently, promotes the production of IL-10 [352, 353] and a number of reports have described a correlation between the onset of Crohn's disease and the eradication of *H. pylori* infection in the intestine [354, 355]. While H. pylori has been strongly linked with pathogenic gastritis, a clinical review by Luther et al came to the conclusion that *H. pylori* colonisation of the intestine has a protective effect against the development of Crohn's disease [356]. While other studies have investigated the role of NOD1 in mediating the pro-inflammatory responses to *H. pylori* infection, no reports have shown a role for NOD1 in *H. pylori*-induced IL-10 production. Hence, the role of NOD1 in responding to bacterial infection and the possible effects it has on gut homeostasis represents an interesting topic for further investigation.

The findings presented in chapter 5 of this thesis established that administration of the NOD1 agonist TriDAP increased the numbers of LPM in the peritoneal cavity. This was associated with an increased expression of arginase, relm-α and IL-10 by LPM, which indicated that NOD1 activation also promoted the alternative activation of these

macrophages. The expansion of LPM in response to TriDAP was dependent on IL-10, therefore confirming that significant amounts of IL-10 are produced in vivo in response to TriDAP. This study also demonstrated that NOD1-induced M2 activation of LPM was dependent on IL-4 signalling. These findings are novel and suggest a previously unknown role for NOD1 in M2 macrophage activation.

LPM play a homeostatic role in the peritoneal cavity and are immunosuppressive during the steady state. Similar to other resident macrophages they are classified as M2-like due to their immunosuppressive characteristics [147]. In addition, LPM are thought to play a major role in restoring homeostasis after a bacterial challenge or tissue injury [109]. The expansion of LPM in response to TriDAP indicates that NOD1 activation in vivo elicits an immune response that is pre-dominantly immunosuppressive, as other studies have shown that LPM numbers are depleted rather than expanded in the presence of an inflammatory environment [100]. These results are at variance with most studies that focus on NOD1 activation as a mediator of inflammation. However, the IL-10-mediated expansion of LPM in response to TriDAP is consistent with the previous observation that TriDAP promotes IL-10 production by peritoneal macrophages in vitro. Furthermore, the results of the present study are consistent with those of Nguyen et al who showed that IL-10 production in the peritoneal cavity preferentially expands the numbers of LPM in response to peritonitis.

The expansion of M2-like LPM in response to TriDAP suggests that NOD1 activation plays a role in the resolution of inflammation and tissue repair. M2 macrophages have evolved in conjunction with parasitic infections, which cause significant collateral damage to surrounding tissues. In addition to parasitic infection, M2-like macrophages are activated during bacterial infections in response to IL-10/IL-4-signalling. M2 macrophages produce arginase, relm-α and IL-10, which promote tissue repair and restrict pathogenic inflammation [134, 156]. NOD1-mediated IL-10 and IL-4 production, and hence M2 macrophage activation, may play a vital role in mediating a return to steady state immune homeostasis after a bacterial challenge. This highlights the importance of further research into the role of NOD1 during the resolution of bacterial infection.

In addition to preventing pathogenic inflammation, there is evidence that immunosuppressive M2 macrophages are induced by bacteria to promote chronic

infection [357]. *Mycobacterium tuberculosis, Mycobacterium ulcerans, Brucella abortus, Coxiella burnetti* all promote M2-like macrophage responses during chronic infection by inducing the production of IL-4, IL-10 or a combination of both IL-4 and IL-10 [143, 177, 178, 340, 358, 359]. In some cases the inhibition of these M2 polarising cytokines can resolve chronic infection [178]. The present study showed that NOD1 activation in vivo expanded the numbers of immunosuppressive LPM by inducing the production of IL-10 and IL-4. In addition, LPM from TriDAP treated-mice were less able to activate antigen specific T-cell responses and suppressed autoimmune disease when transferred into mice with EAE. These findings suggest that NOD1-activated macrophages may inhibit the efficient clearance of bacteria during infection.

M. tuberculosis is an example of a chronic bacterial infection that represents a significant health problem. Tuberculosis results in approximately 1.7 million deaths each year and the rates of drug resistant tuberculosis are increasing [360]. Therefore, novel ways of inhibiting chronic *M. tuberculosis* infections are in great demand. *M. tuberculosis* induces IL-10 production, which has been shown to inhibit anti-bacterial immune responses in a variety of ways, including inhibiting Th1 and CTL responses and inhibiting phagocytic killing [359]. In addition, IL-10 has been shown to promote the activation of immunosuppressive M2 macrophages during *M. tuberculosis* infection [143]. The production of IL-10 in response to NOD1 activation highlights a novel signalling pathway that bacteria, such as *M. tuberculosis*, may use to suppress immune responses. Although the production of IL-10 in response to *M. tuberculosis* infection was unchanged in NOD2-deficient mice [361], the role of NOD1 in mediating IL-10 production in response to *M. tuberculosis* has not yet been investigated. In light of the findings of this thesis, the NOD1-mediated, IL-10-dependent expansion of M2 macrophages warrants investigation in the context of chronic bacterial infection.

The findings of this thesis provide solid evidence for a role for NOD1 in immune homeostasis and immune regulation. The production of IL-10 and M2 macrophage activation are two characteristic mechanisms of immune homeostasis that are mediated by NOD1 activation. In addition, it was found that a NOD1 agonist could attenuate the clinical symptoms of EAE, a murine model for MS, and prevent the generation of pathogenic immune cells. These results provide evidence of a role for TriDAP-induced IL-10 production and M2 activation in the NOD1-mediated attenuation of autoimmunity. In

conjunction with reports that NOD receptors play an essential role in gut homeostasis, the present thesis highlights the need for scientific investigation into the role of NOD1 in the resolution of inflammation during inflammatory disorders, autoimmune disease and bacterial infection. Furthermore, this opens the possibility of exploiting NOD1 as a therapy for autoimmune disease.

Chapter 7

Bibliography

CHAPTER 7: Bibliography

1. Janeway, C., *Immunobiology, 5th edition, The Immune System in Health and Disease.* New York: Garland Science, 2001.

2. Ganz, T., *Defensins: antimicrobial peptides of innate immunity.* Nat Rev Immunol, 2003. **3**(9): p. 710-20.

3. Janeway, C.A., Jr. and R. Medzhitov, *Innate immune recognition.* Annu Rev Immunol, 2002. **20**: p. 197-216.

4. Medzhitov, R., *Toll-like receptors and innate immunity.* Nat Rev Immunol, 2001. **1**(2): p. 135-45.

5. Janeway, C., *Immunogenicity signals 1,2,3 ... and 0.* Immunol Today, 1989. **10**(9): p. 283-6.

6. O'Neill, L.A., D. Golenbock, and A.G. Bowie, *The history of Toll-like receptors - redefining innate immunity.* Nat Rev Immunol, 2013. **13**(6): p. 453-60.

7. Nishiya, T. and A.L. DeFranco, *Ligand-regulated chimeric receptor approach reveals distinctive subcellular localization and signaling properties of the Toll-like receptors.* J Biol Chem, 2004. **279**(18): p. 19008-17.

8. Lemaitre, B., et al., *The dorsoventral regulatory gene cassette spatzle/Toll/cactus controls the potent antifungal response in Drosophila adults.* Cell, 1996. **86**(6): p. 973-83.

9. Poltorak, A., et al., *Defective LPS signaling in C3H/HeJ and C57BL/10ScCr mice: mutations in Tlr4 gene.* Science, 1998. **282**(5396): p. 2085-8.

10. Adachi, O., et al., *Targeted disruption of the MyD88 gene results in loss of IL-1- and IL-18-mediated function.* Immunity, 1998. **9**(1): p. 143-50.

11. Akira, S., S. Uematsu, and O. Takeuchi, *Pathogen recognition and innate immunity.* Cell, 2006. **124**(4): p. 783-801.

12. Jarnicki, A.G., et al., *Attenuating regulatory T cell induction by TLR agonists through inhibition of p38 MAPK signaling in dendritic cells enhances their efficacy as vaccine adjuvants and cancer immunotherapeutics.* J Immunol, 2008. **180**(6): p. 3797-806.

13. Brereton, C.F., et al., *Inhibition of ERK MAPK suppresses IL-23- and IL-1-driven IL-17 production and attenuates autoimmune disease.* J Immunol, 2009. **183**(3): p. 1715-23.

14. Doyle, S., et al., *IRF3 mediates a TLR3/TLR4-specific antiviral gene program.* Immunity, 2002. **17**(3): p. 251-63.

15. Yamamoto, M., et al., *TRAM is specifically involved in the Toll-like receptor 4-mediated MyD88-independent signaling pathway.* Nat Immunol, 2003. **4**(11): p. 1144-50.

16. Janeway, C.A., Jr., *How the immune system protects the host from infection.* Microbes Infect, 2001. **3**(13): p. 1167-71.

17. Chen, L., *Co-inhibitory molecules of the B7-CD28 family in the control of T-cell immunity.* Nat Rev Immunol, 2004. **4**(5): p. 336-47.

18. Mosmann, T.R., et al., *Two types of murine helper T cell clone. I. Definition according to profiles of lymphokine activities and secreted proteins.* J Immunol, 1986. **136**(7): p. 2348-57.

19. Sica, A. and A. Mantovani, *Macrophage plasticity and polarization: in vivo veritas.* J Clin Invest, 2012. **122**(3): p. 787-95.

20. Trinchieri, G., S. Pflanz, and R.A. Kastelein, *The IL-12 family of heterodimeric cytokines: new players in the regulation of T cell responses.* Immunity, 2003. **19**(5): p. 641-4.

21. Pflanz, S., et al., *IL-27, a heterodimeric cytokine composed of EBI3 and p28 protein, induces proliferation of naive CD4(+) T cells.* Immunity, 2002. **16**(6): p. 779-90.

22. Takeda, A., et al., *Cutting edge: role of IL-27/WSX-1 signaling for induction of T-bet through activation of STAT1 during initial Th1 commitment.* J Immunol, 2003. **170**(10): p. 4886-90.

23. Flavell, R.A., et al., *Molecular basis of T-cell differentiation.* Cold Spring Harb Symp Quant Biol, 1999. **64**: p. 563-71.

24. Finotto, S., et al., *Development of spontaneous airway changes consistent with human asthma in mice lacking T-bet.* Science, 2002. **295**(5553): p. 336-8.

25. Le Gros, G., et al., *Generation of interleukin 4 (IL-4)-producing cells in vivo and in vitro: IL-2 and IL-4 are required for in vitro generation of IL-4-producing cells.* J Exp Med, 1990. **172**(3): p. 921-9.

26. Zhu, J., et al., *Conditional deletion of Gata3 shows its essential function in T(H)1-T(H)2 responses.* Nat Immunol, 2004. **5**(11): p. 1157-65.

27. Neill, D.R., et al., *Nuocytes represent a new innate effector leukocyte that mediates type-2 immunity.* Nature, 2010. **464**(7293): p. 1367-70.

28. Liu, Y.J., et al., *TSLP: an epithelial cell cytokine that regulates T cell differentiation by conditioning dendritic cell maturation.* Annu Rev Immunol, 2007. **25**: p. 193-219.

29. Eiwegger, T. and C.A. Akdis, *IL-33 links tissue cells, dendritic cells and Th2 cell development in a mouse model of asthma.* Eur J Immunol, 2011. **41**(6): p. 1535-8.

30. Ito, T., et al., *TSLP-activated dendritic cells induce an inflammatory T helper type 2 cell response through OX40 ligand.* J Exp Med, 2005. **202**(9): p. 1213-23.

31. Kapsenberg, M.L., *Dendritic-cell control of pathogen-driven T-cell polarization.* Nat Rev Immunol, 2003. **3**(12): p. 984-93.

32. Zhu, J. and W.E. Paul, *Peripheral CD4+ T-cell differentiation regulated by networks of cytokines and transcription factors.* Immunol Rev, 2010. **238**(1): p. 247-62.

33. Aggarwal, S., et al., *Interleukin-23 promotes a distinct CD4 T cell activation state characterized by the production of interleukin-17.* J Biol Chem, 2003. **278**(3): p. 1910-4.

34. Weaver, C.T., et al., *IL-17 family cytokines and the expanding diversity of effector T cell lineages.* Annu Rev Immunol, 2007. **25**: p. 821-52.

35. Ye, P., et al., *Requirement of interleukin 17 receptor signaling for lung CXC chemokine and granulocyte colony-stimulating factor expression, neutrophil recruitment, and host defense.* J Exp Med, 2001. **194**(4): p. 519-27.

36. Langrish, C.L., et al., *IL-23 drives a pathogenic T cell population that induces autoimmune inflammation.* J Exp Med, 2005. **201**(2): p. 233-40.

37. Raychaudhuri, S.P., *Role of IL-17 in psoriasis and psoriatic arthritis.* Clin Rev Allergy Immunol, 2013. **44**(2): p. 183-93.

38. Chiricozzi, A. and J.G. Krueger, *IL-17 targeted therapies for psoriasis.* Expert Opin Investig Drugs, 2013. **22**(8): p. 993-1005.

39. Cua, D.J., et al., *Interleukin-23 rather than interleukin-12 is the critical cytokine for autoimmune inflammation of the brain.* Nature, 2003. **421**(6924): p. 744-8.

40. McGeachy, M.J., et al., *The interleukin 23 receptor is essential for the terminal differentiation of interleukin 17-producing effector T helper cells in vivo.* Nat Immunol, 2009. **10**(3): p. 314-24.

41. Sutton, C., et al., *A crucial role for interleukin (IL)-1 in the induction of IL-17-producing T cells that mediate autoimmune encephalomyelitis.* J Exp Med, 2006. **203**(7): p. 1685-91.

42. Mangan, P.R., et al., *Transforming growth factor-beta induces development of the T(H)17 lineage.* Nature, 2006. **441**(7090): p. 231-4.

43. Nurieva, R., et al., *Essential autocrine regulation by IL-21 in the generation of inflammatory T cells.* Nature, 2007. **448**(7152): p. 480-3.

44. Zhou, L., et al., *IL-6 programs T(H)-17 cell differentiation by promoting sequential engagement of the IL-21 and IL-23 pathways.* Nat Immunol, 2007. **8**(9): p. 967-74.

45. Das, J., et al., *Transforming growth factor beta is dispensable for the molecular orchestration of Th17 cell differentiation.* J Exp Med, 2009. **206**(11): p. 2407-16.

46. Harrington, L.E., et al., *Interleukin 17-producing CD4+ effector T cells develop via a lineage distinct from the T helper type 1 and 2 lineages.* Nat Immunol, 2005. **6**(11): p. 1123-32.

47. Cooney, L.A., et al., *Sensitivity and resistance to regulation by IL-4 during Th17 maturation.* J Immunol, 2011. **187**(9): p. 4440-50.

48. Park, H., et al., *A distinct lineage of CD4 T cells regulates tissue inflammation by producing interleukin 17.* Nat Immunol, 2005. **6**(11): p. 1133-41.

49. Cobb, D., D. Hambright, and R.B. Smeltz, *T-bet-independent effects of IL-12 family cytokines on regulation of Th17 responses to experimental T. cruzi infection.* J Leukoc Biol, 2010. **88**(5): p. 965-71.

50. Diveu, C., et al., *IL-27 blocks RORc expression to inhibit lineage commitment of Th17 cells.* J Immunol, 2009. **182**(9): p. 5748-56.

51. Hirota, K., et al., *Fate mapping of IL-17-producing T cells in inflammatory responses.* Nat Immunol, 2011. **12**(3): p. 255-63.

52. Shimizu, J., et al., *Excessive CD4+ T cells co-expressing interleukin-17 and interferon-gamma in patients with Behcet's disease.* Clin Exp Immunol, 2012. **168**(1): p. 68-74.

53. Sujino, T., et al., *Regulatory T cells suppress development of colitis, blocking differentiation of T-helper 17 into alternative T-helper 1 cells.* Gastroenterology, 2011. **141**(3): p. 1014-23.

54. Steele, C.R., D.E. Oppenheim, and A.C. Hayday, *Gamma(delta) T cells: non-classical ligands for non-classical cells.* Curr Biol, 2000. **10**(7): p. R282-5.

55. Sutton, C.E., et al., *Interleukin-1 and IL-23 induce innate IL-17 production from gammadelta T cells, amplifying Th17 responses and autoimmunity.* Immunity, 2009. **31**(2): p. 331-41.

56. Martin, B., et al., *Interleukin-17-producing gammadelta T cells selectively expand in response to pathogen products and environmental signals.* Immunity, 2009. **31**(2): p. 321-30.

57. Holtmeier, W., *Compartmentalization gamma/delta T cells and their putative role in mucosal immunity.* Crit Rev Immunol, 2003. **23**(5-6): p. 473-88.

58. Bonneville, M., R.L. O'Brien, and W.K. Born, *Gammadelta T cell effector functions: a blend of innate programming and acquired plasticity.* Nat Rev Immunol, 2010. **10**(7): p. 467-78.

59. Sutton, C.E., L.A. Mielke, and K.H. Mills, *IL-17-producing gammadelta T cells and innate lymphoid cells.* Eur J Immunol, 2012. **42**(9): p. 2221-31.

60. Shibata, K., et al., *Resident Vdelta1+ gammadelta T cells control early infiltration of neutrophils after Escherichia coli infection via IL-17 production.* J Immunol, 2007. **178**(7): p. 4466-72.

61. Dejima, T., et al., *Protective role of naturally occurring interleukin-17A-producing gammadelta T cells in the lung at the early stage of systemic candidiasis in mice.* Infect Immun, 2011. **79**(11): p. 4503-10.

62. King, D.P., et al., *Cutting edge: protective response to pulmonary injury requires gamma delta T lymphocytes.* J Immunol, 1999. **162**(9): p. 5033-6.

63. Moore, T.A., et al., *Gamma delta-T cells are critical for survival and early proinflammatory cytokine gene expression during murine Klebsiella pneumonia.* J Immunol, 2000. **165**(5): p. 2643-50.

64. Sakaguchi, S., et al., *Immunologic self-tolerance maintained by activated T cells expressing IL-2 receptor alpha-chains (CD25). Breakdown of a single mechanism of self-tolerance causes various autoimmune diseases.* J Immunol, 1995. **155**(3): p. 1151-64.

65. Sakaguchi, S., *Naturally arising CD4+ regulatory t cells for immunologic self-tolerance and negative control of immune responses.* Annu Rev Immunol, 2004. **22**: p. 531-62.

66. Bettelli, E., M. Dastrange, and M. Oukka, *Foxp3 interacts with nuclear factor of activated T cells and NF-kappa B to repress cytokine gene expression and effector functions of T helper cells.* Proc Natl Acad Sci U S A, 2005. **102**(14): p. 5138-43.

67. Zheng, Y. and A.Y. Rudensky, *Foxp3 in control of the regulatory T cell lineage.* Nat Immunol, 2007. **8**(5): p. 457-62.

68. Chen, W., et al., *Conversion of peripheral CD4+CD25- naive T cells to CD4+CD25+ regulatory T cells by TGF-beta induction of transcription factor Foxp3.* J Exp Med, 2003. **198**(12): p. 1875-86.

69. Feuerer, M., et al., *Foxp3+ regulatory T cells: differentiation, specification, subphenotypes.* Nat Immunol, 2009. **10**(7): p. 689-95.

70. Fu, S., et al., *TGF-beta induces Foxp3 + T-regulatory cells from CD4 + CD25 - precursors.* Am J Transplant, 2004. **4**(10): p. 1614-27.

71. Groux, H., et al., *A CD4+ T-cell subset inhibits antigen-specific T-cell responses and prevents colitis.* Nature, 1997. **389**(6652): p. 737-42.

72. O'Garra, A. and F.J. Barrat, *In vitro generation of IL-10-producing regulatory CD4+ T cells is induced by immunosuppressive drugs and inhibited by Th1- and Th2-inducing cytokines.* Immunol Lett, 2003. **85**(2): p. 135-9.

73. Barrat, F.J., et al., *In vitro generation of interleukin 10-producing regulatory CD4(+) T cells is induced by immunosuppressive drugs and inhibited by T helper type 1 (Th1)- and Th2-inducing cytokines.* J Exp Med, 2002. **195**(5): p. 603-16.

74. Fiorentino, D.F., M.W. Bond, and T.R. Mosmann, *Two types of mouse T helper cell. IV. Th2 clones secrete a factor that inhibits cytokine production by Th1 clones.* J Exp Med, 1989. **170**(6): p. 2081-95.

75. Liu, Y., et al., *Expression cloning and characterization of a human IL-10 receptor.* J Immunol, 1994. **152**(4): p. 1821-9.

76. Spencer, S.D., et al., *The orphan receptor CRF2-4 is an essential subunit of the interleukin 10 receptor.* J Exp Med, 1998. **187**(4): p. 571-8.

77. Moore, K.W., et al., *Interleukin-10 and the interleukin-10 receptor.* Annu Rev Immunol, 2001. **19**: p. 683-765.

78. Pestka, S., et al., *Interleukin-10 and related cytokines and receptors.* Annu Rev Immunol, 2004. **22**: p. 929-79.

79. Ouyang, W., et al., *Regulation and functions of the IL-10 family of cytokines in inflammation and disease.* Annu Rev Immunol, 2011. **29**: p. 71-109.

80. Kuhn, R., et al., *Interleukin-10-deficient mice develop chronic enterocolitis.* Cell, 1993. **75**(2): p. 263-74.

81. Sewnath, M.E., et al., *IL-10-deficient mice demonstrate multiple organ failure and increased mortality during Escherichia coli peritonitis despite an accelerated bacterial clearance.* J Immunol, 2001. **166**(10): p. 6323-31.

82. Gazzinelli, R.T., et al., *In the absence of endogenous IL-10, mice acutely infected with Toxoplasma gondii succumb to a lethal immune response dependent on CD4+ T cells and accompanied by overproduction of IL-12, IFN-gamma and TNF-alpha.* J Immunol, 1996. **157**(2): p. 798-805.

83. Vazquez-Torres, A., et al., *Early resistance of interleukin-10 knockout mice to acute systemic candidiasis.* Infect Immun, 1999. **67**(2): p. 670-4.

84. Murray, P.J. and R.A. Young, *Increased antimycobacterial immunity in interleukin-10-deficient mice.* Infect Immun, 1999. **67**(6): p. 3087-95.

85. Anderson, C.F. and D.M. Mosser, *Cutting edge: biasing immune responses by directing antigen to macrophage Fc gamma receptors.* J Immunol, 2002. **168**(8): p. 3697-701.

86. Tournoy, K.G., J.C. Kips, and R.A. Pauwels, *Endogenous interleukin-10 suppresses allergen-induced airway inflammation and nonspecific airway responsiveness.* Clin Exp Allergy, 2000. **30**(6): p. 775-83.

87. Murai, M., et al., *Interleukin 10 acts on regulatory T cells to maintain expression of the transcription factor Foxp3 and suppressive function in mice with colitis.* Nat Immunol, 2009. **10**(11): p. 1178-84.

88. Finbloom, D.S. and K.D. Winestock, *IL-10 induces the tyrosine phosphorylation of tyk2 and Jak1 and the differential assembly of STAT1 alpha and STAT3 complexes in human T cells and monocytes.* J Immunol, 1995. **155**(3): p. 1079-90.

89. Takeda, K., et al., *Enhanced Th1 activity and development of chronic enterocolitis in mice devoid of Stat3 in macrophages and neutrophils.* Immunity, 1999. **10**(1): p. 39-49.

90. Ding, Y., et al., *Suppressor of cytokine signaling 1 inhibits IL-10-mediated immune responses.* J Immunol, 2003. **170**(3): p. 1383-91.

91. Alexander, W.S., et al., *SOCS1 is a critical inhibitor of interferon gamma signaling and prevents the potentially fatal neonatal actions of this cytokine.* Cell, 1999. **98**(5): p. 597-608.

92. Naka, T., et al., *SOCS-1/SSI-1-deficient NKT cells participate in severe hepatitis through dysregulated cross-talk inhibition of IFN-gamma and IL-4 signaling in vivo.* Immunity, 2001. **14**(5): p. 535-45.

93. Shames, B.D., et al., *Interleukin-10 stabilizes inhibitory kappaB-alpha in human monocytes.* Shock, 1998. **10**(6): p. 389-94.

94. Saraiva, M. and A. O'Garra, *The regulation of IL-10 production by immune cells.* Nat Rev Immunol, 2010. **10**(3): p. 170-81.

95. Moreira, L.O., et al., *The TLR2-MyD88-NOD2-RIPK2 signalling axis regulates a balanced pro-inflammatory and IL-10-mediated anti-inflammatory cytokine response to Gram-positive cell walls.* Cell Microbiol, 2008. **10**(10): p. 2067-77.

96. Saraiva, M., et al., *Interleukin-10 production by Th1 cells requires interleukin-12-induced STAT4 transcription factor and ERK MAP kinase activation by high antigen dose.* Immunity, 2009. **31**(2): p. 209-19.

97. Owaki, T., et al., *IL-27 induces Th1 differentiation via p38 MAPK/T-bet- and intercellular adhesion molecule-1/LFA-1/ERK1/2-dependent pathways.* J Immunol, 2006. **177**(11): p. 7579-87.

98. Hu, X., et al., *IFN-gamma suppresses IL-10 production and synergizes with TLR2 by regulating GSK3 and CREB/AP-1 proteins.* Immunity, 2006. **24**(5): p. 563-74.

99. Geissmann, F., S. Jung, and D.R. Littman, *Blood monocytes consist of two principal subsets with distinct migratory properties.* Immunity, 2003. **19**(1): p. 71-82.

100. Ghosn, E.E., et al., *Two physically, functionally, and developmentally distinct peritoneal macrophage subsets.* Proc Natl Acad Sci U S A, 2010. **107**(6): p. 2568-73.

101. Steinman, R.M. and Z.A. Cohn, *Identification of a novel cell type in peripheral lymphoid organs of mice. I. Morphology, quantitation, tissue distribution.* J Exp Med, 1973. **137**(5): p. 1142-62.

102. Gordon, S. and P.R. Taylor, *Monocyte and macrophage heterogeneity.* Nat Rev Immunol, 2005. **5**(12): p. 953-64.

103. Yona, S., et al., *Fate mapping reveals origins and dynamics of monocytes and tissue macrophages under homeostasis.* Immunity, 2013. **38**(1): p. 79-91.

104. Hashimoto, D., et al., *Tissue-resident macrophages self-maintain locally throughout adult life with minimal contribution from circulating monocytes.* Immunity, 2013. **38**(4): p. 792-804.

105. van Furth, R., *Macrophage activity and clinical immunology. Origin and kinetics of mononuclear phagocytes.* Ann N Y Acad Sci, 1976. **278**: p. 161-75.

106. van Furth, R. and Z.A. Cohn, *The origin and kinetics of mononuclear phagocytes.* J Exp Med, 1968. **128**(3): p. 415-35.

107. Carlin, L.M., et al., *Nr4a1-dependent Ly6C(low) monocytes monitor endothelial cells and orchestrate their disposal.* Cell, 2013. **153**(2): p. 362-75.

108. Jakubzick, C., et al., *Minimal Differentiation of Classical Monocytes as They Survey Steady-State Tissues and Transport Antigen to Lymph Nodes.* Immunity, 2013.

109. Nguyen, H.H., et al., *IL-10 acts as a developmental switch guiding monocyte differentiation to macrophages during a murine peritoneal infection.* J Immunol, 2012. **189**(6): p. 3112-20.

110. Steinman, R.M., et al., *Identification of a novel cell type in peripheral lymphoid organs of mice. V. Purification of spleen dendritic cells, new surface markers, and maintenance in vitro.* J Exp Med, 1979. **149**(1): p. 1-16.

111. Steinman, R.M., J.C. Adams, and Z.A. Cohn, *Identification of a novel cell type in peripheral lymphoid organs of mice. IV. Identification and distribution in mouse spleen.* J Exp Med, 1975. **141**(4): p. 804-20.

112. Steinman, R.M., D.S. Lustig, and Z.A. Cohn, *Identification of a novel cell type in peripheral lymphoid organs of mice. 3. Functional properties in vivo.* J Exp Med, 1974. **139**(6): p. 1431-45.

113. Steinman, R.M. and Z.A. Cohn, *Identification of a novel cell type in peripheral lymphoid organs of mice. II. Functional properties in vitro.* J Exp Med, 1974. **139**(2): p. 380-97.

114. Murray, P.J. and T.A. Wynn, *Protective and pathogenic functions of macrophage subsets.* Nat Rev Immunol, 2011. **11**(11): p. 723-37.

115. Trinchieri, G., D. Santoli, and H. Koprowski, *Spontaneous cell-mediated cytotoxicity in humans: role of interferon and immunoglobulins.* J Immunol, 1978. **120**(6): p. 1849-55.

116. Yoneyama, H., et al., *Plasmacytoid DCs help lymph node DCs to induce anti-HSV CTLs.* J Exp Med, 2005. **202**(3): p. 425-35.

117. Edwards, A.D., et al., *Toll-like receptor expression in murine DC subsets: lack of TLR7 expression by CD8 alpha+ DC correlates with unresponsiveness to imidazoquinolines.* Eur J Immunol, 2003. **33**(4): p. 827-33.

118. Maraskovsky, E., et al., *Dramatic increase in the numbers of functionally mature dendritic cells in Flt3 ligand-treated mice: multiple dendritic cell subpopulations identified.* J Exp Med, 1996. **184**(5): p. 1953-62.

119. Karsunky, H., et al., *Flt3 ligand regulates dendritic cell development from Flt3+ lymphoid and myeloid-committed progenitors to Flt3+ dendritic cells in vivo.* J Exp Med, 2003. **198**(2): p. 305-13.

120. Cheong, C., et al., *Microbial stimulation fully differentiates monocytes to DC-SIGN/CD209(+) dendritic cells for immune T cell areas.* Cell, 2010. **143**(3): p. 416-29.

121. Inaba, K., et al., *Dendritic cell progenitors phagocytose particulates, including bacillus Calmette-Guerin organisms, and sensitize mice to mycobacterial antigens in vivo.* J Exp Med, 1993. **178**(2): p. 479-88.

122. Young, J.W., et al., *The B7/BB1 antigen provides one of several costimulatory signals for the activation of CD4+ T lymphocytes by human blood dendritic cells in vitro.* J Clin Invest, 1992. **90**(1): p. 229-37.

123. Banchereau, J. and R.M. Steinman, *Dendritic cells and the control of immunity.* Nature, 1998. **392**(6673): p. 245-52.

124. Sweeney, C.M., et al., *IL-27 mediates the response to IFN-beta therapy in multiple sclerosis patients by inhibiting Th17 cells.* Brain Behav Immun, 2011. **25**(6): p. 1170-81.

125. Watanabe, T., et al., *NOD2 is a negative regulator of Toll-like receptor 2-mediated T helper type 1 responses.* Nat Immunol, 2004. **5**(8): p. 800-8.

126. Hayashi, A., et al., *A single strain of Clostridium butyricum induces intestinal IL-10-producing macrophages to suppress acute experimental colitis in mice.* Cell Host Microbe, 2013. **13**(6): p. 711-22.

127. Watanabe, N., et al., *Elimination of local macrophages in intestine prevents chronic colitis in interleukin-10-deficient mice.* Dig Dis Sci, 2003. **48**(2): p. 408-14.

128. Hibbs, J.B., Jr., *Infection and nitric oxide.* J Infect Dis, 2002. **185 Suppl 1**: p. S9-17.

129. Mantovani, A., et al., *The chemokine system in diverse forms of macrophage activation and polarization.* Trends Immunol, 2004. **25**(12): p. 677-86.

130. Mosser, D.M., *The many faces of macrophage activation.* J Leukoc Biol, 2003. **73**(2): p. 209-12.

131. Ehrt, S., et al., *Reprogramming of the macrophage transcriptome in response to interferon-gamma and Mycobacterium tuberculosis: signaling roles of nitric oxide synthase-2 and phagocyte oxidase.* J Exp Med, 2001. **194**(8): p. 1123-40.

132. Abramson, S.L. and J.I. Gallin, *IL-4 inhibits superoxide production by human mononuclear phagocytes.* J Immunol, 1990. **144**(2): p. 625-30.

133. Cao, H., et al., *Differential regulation of class II MHC determinants on macrophages by IFN-gamma and IL-4.* J Immunol, 1989. **143**(11): p. 3524-31.

134. Gordon, S., *Alternative activation of macrophages.* Nat Rev Immunol, 2003. **3**(1): p. 23-35.

135. Wirth, J.J., F. Kierszenbaum, and A. Zlotnik, *Effects of IL-4 on macrophage functions: increased uptake and killing of a protozoan parasite (Trypanosoma cruzi).* Immunology, 1989. **66**(2): p. 296-301.

136. Smith, P., et al., *Infection with a helminth parasite prevents experimental colitis via a macrophage-mediated mechanism.* J Immunol, 2007. **178**(7): p. 4557-66.

137. Montaner, L.J., et al., *Type 1 and type 2 cytokine regulation of macrophage endocytosis: differential activation by IL-4/IL-13 as opposed to IFN-gamma or IL-10.* J Immunol, 1999. **162**(8): p. 4606-13.

138. Mukherjee, S., et al., *Lipopolysaccharide-driven Th2 cytokine production in macrophages is regulated by both MyD88 and TRAM.* J Biol Chem, 2009. **284**(43): p. 29391-8.

139. La Flamme, A.C., et al., *Type II-activated murine macrophages produce IL-4.* PLoS One, 2012. **7**(10): p. e46989.

140. Gerber, J.S. and D.M. Mosser, *Reversing lipopolysaccharide toxicity by ligating the macrophage Fc gamma receptors.* J Immunol, 2001. **166**(11): p. 6861-8.

141. Sutterwala, F.S., et al., *Selective suppression of interleukin-12 induction after macrophage receptor ligation.* J Exp Med, 1997. **185**(11): p. 1977-85.

142. Pils, M.C., et al., *Monocytes/macrophages and/or neutrophils are the target of IL-10 in the LPS endotoxemia model.* Eur J Immunol, 2010. **40**(2): p. 443-8.

143. Schreiber, T., et al., *Autocrine IL-10 induces hallmarks of alternative activation in macrophages and suppresses antituberculosis effector mechanisms without compromising T cell immunity.* J Immunol, 2009. **183**(2): p. 1301-12.

144. Avni, D., Y. Glucksam, and T. Zor, *The phosphatidylinositol 3-kinase (PI3K) inhibitor LY294002 modulates cytokine expression in macrophages via p50 nuclear factor kappaB inhibition, in a PI3K-independent mechanism.* Biochem Pharmacol, 2012. **83**(1): p. 106-14.

145. Burgess, A.W. and D. Metcalf, *The nature and action of granulocyte-macrophage colony stimulating factors.* Blood, 1980. **56**(6): p. 947-58.

146. Hamilton, J.A., et al., *Stimulation of macrophage plasminogen activator activity by colony-stimulating factors.* J Cell Physiol, 1980. **103**(3): p. 435-45.

147. Hamilton, J.A., *Colony-stimulating factors in inflammation and autoimmunity.* Nat Rev Immunol, 2008. **8**(7): p. 533-44.

148. Falk, L.A. and S.N. Vogel, *Comparison of bone marrow progenitors responsive to granulocyte-macrophage colony stimulating factor and macrophage colony stimulating factor-1.* J Leukoc Biol, 1988. **43**(2): p. 148-57.

149. Fleetwood, A.J., et al., *Granulocyte-macrophage colony-stimulating factor (CSF) and macrophage CSF-dependent macrophage phenotypes display differences in cytokine profiles and transcription factor activities: implications for CSF blockade in inflammation.* J Immunol, 2007. **178**(8): p. 5245-52.

150. Wiktor-Jedrzejczak, W., et al., *Total absence of colony-stimulating factor 1 in the macrophage-deficient osteopetrotic (op/op) mouse.* Proc Natl Acad Sci U S A, 1990. **87**(12): p. 4828-32.

151. Cecchini, M.G., et al., *Role of colony stimulating factor-1 in the establishment and regulation of tissue macrophages during postnatal development of the mouse.* Development, 1994. **120**(6): p. 1357-72.

152. Stanley, E., et al., *Granulocyte/macrophage colony-stimulating factor-deficient mice show no major perturbation of hematopoiesis but develop a characteristic pulmonary pathology.* Proc Natl Acad Sci U S A, 1994. **91**(12): p. 5592-6.

153. Sindrilaru, A., et al., *An unrestrained proinflammatory M1 macrophage population induced by iron impairs wound healing in humans and mice.* J Clin Invest, 2011. **121**(3): p. 985-97.

154. Wynn, T.A. and L. Barron, *Macrophages: master regulators of inflammation and fibrosis.* Semin Liver Dis, 2010. **30**(3): p. 245-57.

155. Arnold, L., et al., *Inflammatory monocytes recruited after skeletal muscle injury switch into antiinflammatory macrophages to support myogenesis.* J Exp Med, 2007. **204**(5): p. 1057-69.

156. Allen, J.E. and T.A. Wynn, *Evolution of Th2 immunity: a rapid repair response to tissue destructive pathogens.* PLoS Pathog, 2011. **7**(5): p. e1002003.

157. Pesce, J.T., et al., *Arginase-1-expressing macrophages suppress Th2 cytokine-driven inflammation and fibrosis.* PLoS Pathog, 2009. **5**(4): p. e1000371.

158. Herbert, D.R., et al., *Arginase I suppresses IL-12/IL-23p40-driven intestinal inflammation during acute schistosomiasis.* J Immunol, 2010. **184**(11): p. 6438-46.

159. Pesce, J.T., et al., *Retnla (relmalpha/fizz1) suppresses helminth-induced Th2-type immunity.* PLoS Pathog, 2009. **5**(4): p. e1000393.

160. London, A., et al., *Neuroprotection and progenitor cell renewal in the injured adult murine retina requires healing monocyte-derived macrophages.* J Exp Med, 2011. **208**(1): p. 23-39.

161. Barron, L. and T.A. Wynn, *Fibrosis is regulated by Th2 and Th17 responses and by dynamic interactions between fibroblasts and macrophages.* Am J Physiol Gastrointest Liver Physiol, 2011. **300**(5): p. G723-8.

162. Wilson, M.S., et al., *IL-13Ralpha2 and IL-10 coordinately suppress airway inflammation, airway-hyperreactivity, and fibrosis in mice.* J Clin Invest, 2007. **117**(10): p. 2941-51.

163. Biswas, S.K. and A. Mantovani, *Macrophage plasticity and interaction with lymphocyte subsets: cancer as a paradigm.* Nat Immunol, 2010. **11**(10): p. 889-96.

164. Ahn, G.O., et al., *Inhibition of Mac-1 (CD11b/CD18) enhances tumor response to radiation by reducing myeloid cell recruitment.* Proc Natl Acad Sci U S A, 2010. **107**(18): p. 8363-8.

165. Steidl, C., et al., *Tumor-associated macrophages and survival in classic Hodgkin's lymphoma.* N Engl J Med, 2010. **362**(10): p. 875-85.

166. Qin, F.X., *Dynamic behavior and function of Foxp3+ regulatory T cells in tumor bearing host.* Cell Mol Immunol, 2009. **6**(1): p. 3-13.

167. Stout, R.D., S.K. Watkins, and J. Suttles, *Functional plasticity of macrophages: in situ reprogramming of tumor-associated macrophages.* J Leukoc Biol, 2009. **86**(5): p. 1105-9.

168. Duluc, D., et al., *Interferon-gamma reverses the immunosuppressive and protumoral properties and prevents the generation of human tumor-associated macrophages.* Int J Cancer, 2009. **125**(2): p. 367-73.

169. Sinha, P., V.K. Clements, and S. Ostrand-Rosenberg, *Interleukin-13-regulated M2 macrophages in combination with myeloid suppressor cells block immune surveillance against metastasis.* Cancer Res, 2005. **65**(24): p. 11743-51.

170. Brower, V., *Macrophages: cancer therapy's double-edged sword.* J Natl Cancer Inst, 2012. **104**(9): p. 649-52.

171. El Kasmi, K.C., et al., *Toll-like receptor-induced arginase 1 in macrophages thwarts effective immunity against intracellular pathogens.* Nat Immunol, 2008. **9**(12): p. 1399-406.

172. Hesse, M., et al., *Differential regulation of nitric oxide synthase-2 and arginase-1 by type 1/type 2 cytokines in vivo: granulomatous pathology is shaped by the pattern of L-arginine metabolism.* J Immunol, 2001. **167**(11): p. 6533-44.

173. Cao, Q., et al., *IL-10/TGF-beta-modified macrophages induce regulatory T cells and protect against adriamycin nephrosis.* J Am Soc Nephrol, 2010. **21**(6): p. 933-42.

174. Tumitan, A.R., et al., *Pattern of macrophage activation in yersinia-resistant and yersinia-susceptible strains of mice.* Microbiol Immunol, 2007. **51**(10): p. 1021-8.

175. Tansini, A. and B.M. de Medeiros, *Susceptibility to Yersinia pseudotuberculosis infection is linked to the pattern of macrophage activation.* Scand J Immunol, 2009. **69**(4): p. 310-8.

176. Ghigo, E., et al., *Link between impaired maturation of phagosomes and defective Coxiella burnetii killing in patients with chronic Q fever.* J Infect Dis, 2004. **190**(10): p. 1767-72.

177. Meghari, S., et al., *Persistent Coxiella burnetii infection in mice overexpressing IL-10: an efficient model for chronic Q fever pathogenesis.* PLoS Pathog, 2008. **4**(2): p. e23.

178. Fernandes, D.M., et al., *Comparison of T cell cytokines in resistant and susceptible mice infected with virulent Brucella abortus strain 2308.* FEMS Immunol Med Microbiol, 1996. **16**(3-4): p. 193-203.

179. Strober, W., et al., *Proinflammatory cytokines underlying the inflammation of Crohn's disease.* Curr Opin Gastroenterol, 2010. **26**(4): p. 310-7.

180. Kamada, N., et al., *Unique CD14 intestinal macrophages contribute to the pathogenesis of Crohn disease via IL-23/IFN-gamma axis.* J Clin Invest, 2008. **118**(6): p. 2269-80.

181. Smith, A.M., et al., *Disordered macrophage cytokine secretion underlies impaired acute inflammation and bacterial clearance in Crohn's disease.* J Exp Med, 2009. **206**(9): p. 1883-97.

182. Mikita, J., et al., *Altered M1/M2 activation patterns of monocytes in severe relapsing experimental rat model of multiple sclerosis. Amelioration of clinical status by M2 activated monocyte administration.* Mult Scler, 2011. **17**(1): p. 2-15.

183. Jiang, H.R., et al., *IL-33 attenuates EAE by suppressing IL-17 and IFN-gamma production and inducing alternatively activated macrophages.* Eur J Immunol, 2012. **42**(7): p. 1804-14.

184. Liu, C., et al., *Targeting the shift from M1 to M2 macrophages in experimental autoimmune encephalomyelitis mice treated with fasudil.* PLoS One, 2013. **8**(2): p. e54841.

185. Martinon, F., K. Burns, and J. Tschopp, *The inflammasome: a molecular platform triggering activation of inflammatory caspases and processing of proIL-beta.* Mol Cell, 2002. **10**(2): p. 417-26.

186. Girardin, S.E., et al., *Peptidoglycan molecular requirements allowing detection by Nod1 and Nod2.* J Biol Chem, 2003. **278**(43): p. 41702-8.

187. Laroui, H., et al., *L-Ala-gamma-D-Glu-meso-diaminopimelic acid (DAP) interacts directly with leucine-rich region domain of nucleotide-binding oligomerization domain 1, increasing phosphorylation activity of receptor-interacting serine/threonine-protein kinase 2 and its interaction with nucleotide-binding oligomerization domain 1.* J Biol Chem, 2011. **286**(35): p. 31003-13.

188. Girardin, S.E., et al., *Nod1 detects a unique muropeptide from gram-negative bacterial peptidoglycan.* Science, 2003. **300**(5625): p. 1584-7.

189. Girardin, S.E., et al., *Nod2 is a general sensor of peptidoglycan through muramyl dipeptide (MDP) detection.* J Biol Chem, 2003. **278**(11): p. 8869-72.

190. Inohara, N., et al., *Nod1, an Apaf-1-like activator of caspase-9 and nuclear factor-kappaB.* J Biol Chem, 1999. **274**(21): p. 14560-7.

191. Ogura, Y., et al., *Nod2, a Nod1/Apaf-1 family member that is restricted to monocytes and activates NF-kappaB.* J Biol Chem, 2001. **276**(7): p. 4812-8.

192. Gutierrez, O., et al., *Induction of Nod2 in myelomonocytic and intestinal epithelial cells via nuclear factor-kappa B activation.* J Biol Chem, 2002. **277**(44): p. 41701-5.

193. Voss, E., et al., *NOD2/CARD15 mediates induction of the antimicrobial peptide human beta-defensin-2.* J Biol Chem, 2006. **281**(4): p. 2005-11.

194. Vavricka, S.R., et al., *hPepT1 transports muramyl dipeptide, activating NF-kappaB and stimulating IL-8 secretion in human colonic Caco2/bbe cells.* Gastroenterology, 2004. **127**(5): p. 1401-9.

195. Marina-Garcia, N., et al., *Clathrin- and dynamin-dependent endocytic pathway regulates muramyl dipeptide internalization and NOD2 activation.* J Immunol, 2009. **182**(7): p. 4321-7.

196. Lee, J., et al., *pH-dependent internalization of muramyl peptides from early endosomes enables Nod1 and Nod2 signaling.* J Biol Chem, 2009. **284**(35): p. 23818-29.

197. Kufer, T.A., et al., *The pattern-recognition molecule Nod1 is localized at the plasma membrane at sites of bacterial interaction.* Cell Microbiol, 2008. **10**(2): p. 477-86.

198. Lecine, P., et al., *The NOD2-RICK complex signals from the plasma membrane.* J Biol Chem, 2007. **282**(20): p. 15197-207.

199. Mo, J., et al., *Pathogen sensing by nucleotide-binding oligomerization domain-containing protein 2 (NOD2) is mediated by direct binding to muramyl dipeptide and ATP.* J Biol Chem, 2012. **287**(27): p. 23057-67.

200. Hasegawa, M., et al., *A critical role of RICK/RIP2 polyubiquitination in Nod-induced NF-kappaB activation.* EMBO J, 2008. **27**(2): p. 373-83.

201. Kobayashi, K., et al., *RICK/Rip2/CARDIAK mediates signalling for receptors of the innate and adaptive immune systems.* Nature, 2002. **416**(6877): p. 194-9.

202. Yang, S., et al., *Pellino3 ubiquitinates RIP2 and mediates Nod2-induced signaling and protective effects in colitis.* Nat Immunol, 2013. **14**(9): p. 927-36.

203. Kim, Y.G., et al., *Cross-tolerization between Nod1 and Nod2 signaling results in reduced refractoriness to bacterial infection in Nod2-deficient macrophages.* J Immunol, 2008. **181**(6): p. 4340-6.

204. Allison, C.C., et al., *Helicobacter pylori induces MAPK phosphorylation and AP-1 activation via a NOD1-dependent mechanism.* J Immunol, 2009. **183**(12): p. 8099-109.

205. Watanabe, T., et al., *NOD1 contributes to mouse host defense against Helicobacter pylori via induction of type I IFN and activation of the ISGF3 signaling pathway.* J Clin Invest.

206. Fritz, J.H., et al., *Synergistic stimulation of human monocytes and dendritic cells by Toll-like receptor 4 and NOD1- and NOD2-activating agonists.* Eur J Immunol, 2005. **35**(8): p. 2459-70.

207. Chamaillard, M., et al., *An essential role for NOD1 in host recognition of bacterial peptidoglycan containing diaminopimelic acid.* Nat Immunol, 2003. **4**(7): p. 702-7.

208. Werts, C., et al., *Nod1 and Nod2 induce CCL5/RANTES through the NF-kappaB pathway.* Eur J Immunol, 2007. **37**(9): p. 2499-508.

209. Hruz, P., et al., *NOD2 contributes to cutaneous defense against Staphylococcus aureus through alpha-toxin-dependent innate immune activation.* Proc Natl Acad Sci U S A, 2009. **106**(31): p. 12873-8.

210. Uehara, A., et al., *Various human epithelial cells express functional Toll-like receptors, NOD1 and NOD2 to produce anti-microbial peptides, but not proinflammatory cytokines.* Mol Immunol, 2007. **44**(12): p. 3100-11.

211. Tada, H., et al., *Synergistic effect of Nod1 and Nod2 agonists with toll-like receptor agonists on human dendritic cells to generate interleukin-12 and T helper type 1 cells.* Infect Immun, 2005. **73**(12): p. 7967-76.

212. Adam, A., et al., *Adjuvant activity of monomeric bacterial cell wall peptidoglycans.* Biochem Biophys Res Commun, 1974. **56**(3): p. 561-7.

213. Kotani, S., et al., *Immunoadjuvant activities of cell walls, their water-soluble fractions and peptidoglycan subunits, prepared from various gram-positive bacteria, and of synthetic n-acetylmuramyl peptides.* Z Immunitatsforsch Exp Klin Immunol, 1975. **149**(2-4): p. 302-19.

214. Magalhaes, J.G., et al., *Essential role of Rip2 in the modulation of innate and adaptive immunity triggered by Nod1 and Nod2 ligands.* Eur J Immunol, 2011. **41**(5): p. 1445-55.

215. Magalhaes, J.G., et al., *Nucleotide oligomerization domain-containing proteins instruct T cell helper type 2 immunity through stromal activation.* Proc Natl Acad Sci U S A, 2011. **108**(36): p. 14896-901.

216. Shaw, M.H., et al., *T cell-intrinsic role of Nod2 in promoting type 1 immunity to Toxoplasma gondii.* Nat Immunol, 2009. **10**(12): p. 1267-74.

217. Geddes, K., et al., *Identification of an innate T helper type 17 response to intestinal bacterial pathogens.* Nat Med, 2011. **17**(7): p. 837-44.

218. Viala, J., et al., *Nod1 responds to peptidoglycan delivered by the Helicobacter pylori cag pathogenicity island.* Nat Immunol, 2004. **5**(11): p. 1166-74.

219. Travassos, L.H., et al., *Nod1 participates in the innate immune response to Pseudomonas aeruginosa.* J Biol Chem, 2005. **280**(44): p. 36714-8.

220. Theivanthiran, B., et al., *NOD2 signaling contributes to host defense in the lungs against Escherichia coli infection.* Infect Immun, 2012. **80**(7): p. 2558-69.

221. Kobayashi, K.S., et al., *Nod2-dependent regulation of innate and adaptive immunity in the intestinal tract.* Science, 2005. **307**(5710): p. 731-4.

222. Silva, G.K., et al., *Cutting edge: nucleotide-binding oligomerization domain 1-dependent responses account for murine resistance against Trypanosoma cruzi infection.* J Immunol, 2010. **184**(3): p. 1148-52.

223. Kim, J.G., S.J. Lee, and M.F. Kagnoff, *Nod1 is an essential signal transducer in intestinal epithelial cells infected with bacteria that avoid recognition by toll-like receptors.* Infect Immun, 2004. **72**(3): p. 1487-95.

224. Zilbauer, M., et al., *A major role for intestinal epithelial nucleotide oligomerization domain 1 (NOD1) in eliciting host bactericidal immune responses to Campylobacter jejuni.* Cell Microbiol, 2007. **9**(10): p. 2404-16.

225. Ogura, Y., et al., *A frameshift mutation in NOD2 associated with susceptibility to Crohn's disease.* Nature, 2001. **411**(6837): p. 603-6.

226. Hugot, J.P., et al., *Association of NOD2 leucine-rich repeat variants with susceptibility to Crohn's disease.* Nature, 2001. **411**(6837): p. 599-603.

227. Inohara, N., et al., *Host recognition of bacterial muramyl dipeptide mediated through NOD2. Implications for Crohn's disease.* J Biol Chem, 2003. **278**(8): p. 5509-12.

228. Kim, Y.G., et al., *Cutting edge: Crohn's disease-associated Nod2 mutation limits production of proinflammatory cytokines to protect the host from Enterococcus faecalis-induced lethality.* J Immunol, 2011. **187**(6): p. 2849-52.

229. van Heel, D.A., et al., *Muramyl dipeptide and toll-like receptor sensitivity in NOD2-associated Crohn's disease.* Lancet, 2005. **365**(9473): p. 1794-6.

230. Chen, G., et al., *NOD-like receptors: role in innate immunity and inflammatory disease.* Annu Rev Pathol, 2009. **4**: p. 365-98.

231. Wehkamp, J., et al., *NOD2 (CARD15) mutations in Crohn's disease are associated with diminished mucosal alpha-defensin expression.* Gut, 2004. **53**(11): p. 1658-64.

232. Ogura, Y., et al., *Expression of NOD2 in Paneth cells: a possible link to Crohn's ileitis.* Gut, 2003. **52**(11): p. 1591-7.

233. Maeda, S., et al., *Nod2 mutation in Crohn's disease potentiates NF-kappaB activity and IL-1beta processing.* Science, 2005. **307**(5710): p. 734-8.

234. Netea, M.G., et al., *NOD2 mediates anti-inflammatory signals induced by TLR2 ligands: implications for Crohn's disease.* Eur J Immunol, 2004. **34**(7): p. 2052-9.

235. Jamontt, J., et al., *Nucleotide-binding oligomerization domain 2 signaling promotes hyperresponsive macrophages and colitis in IL-10-deficient mice.* J Immunol, 2013. **190**(6): p. 2948-58.

236. Mannon, P.J., et al., *Anti-interleukin-12 antibody for active Crohn's disease.* N Engl J Med, 2004. **351**(20): p. 2069-79.

237. Weidinger, S., et al., *Association of NOD1 polymorphisms with atopic eczema and related phenotypes.* J Allergy Clin Immunol, 2005. **116**(1): p. 177-84.

238. Hysi, P., et al., *NOD1 variation, immunoglobulin E and asthma.* Hum Mol Genet, 2005. **14**(7): p. 935-41.

239. Wong, C.K., et al., *NOD-like receptors mediated activation of eosinophils interacting with bronchial epithelial cells: a link between innate immunity and allergic asthma.* Cell Mol Immunol, 2013. **10**(4): p. 317-29.

240. Molnar, T., et al., *NOD1 gene E266K polymorphism is associated with disease susceptibility but not with disease phenotype or NOD2/CARD15 in Hungarian patients with Crohn's disease.* Dig Liver Dis, 2007. **39**(12): p. 1064-70.

241. McGovern, D.P., et al., *Association between a complex insertion/deletion polymorphism in NOD1 (CARD4) and susceptibility to inflammatory bowel disease.* Hum Mol Genet, 2005. **14**(10): p. 1245-50.

242. Franke, A., et al., *No association between the functional CARD4 insertion/deletion polymorphism and inflammatory bowel diseases in the German population.* Gut, 2006. **55**(11): p. 1679-80.

243. Van Limbergen, J., et al., *Contribution of the NOD1/CARD4 insertion/deletion polymorphism +32656 to inflammatory bowel disease in Northern Europe.* Inflamm Bowel Dis, 2007. **13**(7): p. 882-9.

244. Sospedra, M. and R. Martin, *Immunology of multiple sclerosis.* Annu Rev Immunol, 2005. **23**: p. 683-747.

245. Trapp, B.D., et al., *Axonal transection in the lesions of multiple sclerosis.* N Engl J Med, 1998. **338**(5): p. 278-85.

246. Hafler, D.A., *Multiple sclerosis.* J Clin Invest, 2004. **113**(6): p. 788-94.

247. Confavreux, C., et al., *Relapses and progression of disability in multiple sclerosis.* N Engl J Med, 2000. **343**(20): p. 1430-8.

248. Hohol, M.J., et al., *Treatment of progressive multiple sclerosis with pulse cyclophosphamide/methylprednisolone: response to therapy is linked to the duration of progressive disease.* Mult Scler, 1999. **5**(6): p. 403-9.

249. Keegan, B.M. and J.H. Noseworthy, *Multiple sclerosis.* Annu Rev Med, 2002. **53**: p. 285-302.

250. Cook, S.D., *Multiple sclerosis and viruses.* Mult Scler, 1997. **3**(6): p. 388-9.

251. Dalgleish, A.G., *Viruses and multiple sclerosis.* Acta Neurol Scand Suppl, 1997. **169**: p. 8-15.

252. Wandinger, K., et al., *Association between clinical disease activity and Epstein-Barr virus reactivation in MS.* Neurology, 2000. **55**(2): p. 178-84.

253. Panitch, H.S. and C.T. Bever, Jr., *Clinical trials of interferons in multiple sclerosis. What have we learned?* J Neuroimmunol, 1993. **46**(1-2): p. 155-64.

254. Johnson, K.P., et al., *Sustained clinical benefits of glatiramer acetate in relapsing multiple sclerosis patients observed for 6 years. Copolymer 1 Multiple Sclerosis Study Group.* Mult Scler, 2000. **6**(4): p. 255-66.

255. Jacobs, L.D., et al., *Intramuscular interferon beta-1a therapy initiated during a first demyelinating event in multiple sclerosis. CHAMPS Study Group.* N Engl J Med, 2000. **343**(13): p. 898-904.

256. Cohen, J.A., et al., *Oral fingolimod or intramuscular interferon for relapsing multiple sclerosis.* N Engl J Med, 2010. **362**(5): p. 402-15.

257. Hughes, J., *ACP Journal Club. Oral fingolimod was more effective than intramuscular interferon for relapsing-remitting multiple sclerosis.* Ann Intern Med, 2010. **152**(10): p. JC5-6, JC5-7, JC5-8.

258. Brinkmann, V., et al., *The immune modulator FTY720 targets sphingosine 1-phosphate receptors.* J Biol Chem, 2002. **277**(24): p. 21453-7.

259. Kawamoto, E., et al., *Anti-integrin therapy for multiple sclerosis.* Autoimmune Dis, 2012. **2012**: p. 357101.

260. Rice, G.P., H.P. Hartung, and P.A. Calabresi, *Anti-alpha4 integrin therapy for multiple sclerosis: mechanisms and rationale.* Neurology, 2005. **64**(8): p. 1336-42.

261. Saidha, S., C. Eckstein, and P.A. Calabresi, *New and emerging disease modifying therapies for multiple sclerosis.* Ann N Y Acad Sci, 2012. **1247**: p. 117-37.

262. Ryschkewitsch, C.F., et al., *JC virus persistence following progressive multifocal leukoencephalopathy in multiple sclerosis patients treated with natalizumab.* Ann Neurol, 2010. **68**(3): p. 384-91.

263. Linda, H., et al., *Progressive multifocal leukoencephalopathy after natalizumab monotherapy.* N Engl J Med, 2009. **361**(11): p. 1081-7.

264. Baxter, A.G., *The origin and application of experimental autoimmune encephalomyelitis.* Nat Rev Immunol, 2007. **7**(11): p. 904-12.

265. Miller, S.D. and W.J. Karpus, *Experimental autoimmune encephalomyelitis in the mouse.* Curr Protoc Immunol, 2007. **Chapter 15**: p. Unit 15 1.

266. Stromnes, I.M. and J.M. Goverman, *Passive induction of experimental allergic encephalomyelitis.* Nat Protoc, 2006. **1**(4): p. 1952-60.

267. Zamvil, S.S., et al., *T-cell epitope of the autoantigen myelin basic protein that induces encephalomyelitis.* Nature, 1986. **324**(6094): p. 258-60.

268. Pettinelli, C.B. and D.E. McFarlin, *Adoptive transfer of experimental allergic encephalomyelitis in SJL/J mice after in vitro activation of lymph node cells by myelin basic protein: requirement for Lyt 1+ 2- T lymphocytes.* J Immunol, 1981. **127**(4): p. 1420-3.

269. Horwitz, M.S., et al., *Primary demyelination in transgenic mice expressing interferon-gamma.* Nat Med, 1997. **3**(9): p. 1037-41.

270. Segal, B.M., B.K. Dwyer, and E.M. Shevach, *An interleukin (IL)-10/IL-12 immunoregulatory circuit controls susceptibility to autoimmune disease.* J Exp Med, 1998. **187**(4): p. 537-46.

271. Gran, B., et al., *IL-12p35-deficient mice are susceptible to experimental autoimmune encephalomyelitis: evidence for redundancy in the IL-12 system in the induction of central nervous system autoimmune demyelination.* J Immunol, 2002. **169**(12): p. 7104-10.

272. Kroenke, M.A., S.W. Chensue, and B.M. Segal, *EAE mediated by a non-IFN-gamma/non-IL-17 pathway.* Eur J Immunol. **40**(8): p. 2340-8.

273. Bettelli, E., et al., *IL-10 is critical in the regulation of autoimmune encephalomyelitis as demonstrated by studies of IL-10- and IL-4-deficient and transgenic mice.* J Immunol, 1998. **161**(7): p. 3299-306.

274. Cua, D.J., et al., *Central nervous system expression of IL-10 inhibits autoimmune encephalomyelitis.* J Immunol, 2001. **166**(1): p. 602-8.

275. Fitzgerald, D.C., et al., *Suppressive effect of IL-27 on encephalitogenic Th17 cells and the effector phase of experimental autoimmune encephalomyelitis.* J Immunol, 2007. **179**(5): p. 3268-75.

276. Batten, M., et al., *Interleukin 27 limits autoimmune encephalomyelitis by suppressing the development of interleukin 17-producing T cells.* Nat Immunol, 2006. **7**(9): p. 929-36.

277. Inohara, N., Y. Ogura, and G. Nunez, *Nods: a family of cytosolic proteins that regulate the host response to pathogens.* Curr Opin Microbiol, 2002. **5**(1): p. 76-80.

278. van Heel, D.A., et al., *Synergistic enhancement of Toll-like receptor responses by NOD1 activation.* Eur J Immunol, 2005. **35**(8): p. 2471-6.

279. Fritz, J.H., et al., *Nod1-mediated innate immune recognition of peptidoglycan contributes to the onset of adaptive immunity.* Immunity, 2007. **26**(4): p. 445-59.

280. Shaw, P.J., et al., *Signaling via the RIP2 adaptor protein in central nervous system-infiltrating dendritic cells promotes inflammation and autoimmunity.* Immunity, 2011. **34**(1): p. 75-84.

281. Watanabe, T., et al., *Muramyl dipeptide activation of nucleotide-binding oligomerization domain 2 protects mice from experimental colitis.* J Clin Invest, 2008. **118**(2): p. 545-59.

282. Liu, Z., et al., *Role of interleukin-12 in the induction of mucosal inflammation and abrogation of regulatory T cell function in chronic experimental colitis.* Eur J Immunol, 2001. **31**(5): p. 1550-60.

283. Kroenke, M.A. and B.M. Segal, *IL-23 modulated myelin-specific T cells induce EAE via an IFNgamma driven, IL-17 independent pathway.* Brain Behav Immun. **25**(5): p. 932-7.

284. Krakowski, M. and T. Owens, *Interferon-gamma confers resistance to experimental allergic encephalomyelitis.* Eur J Immunol, 1996. **26**(7): p. 1641-6.

285. Bailey, S.L., et al., *CNS myeloid DCs presenting endogenous myelin peptides 'preferentially' polarize CD4+ T(H)-17 cells in relapsing EAE.* Nat Immunol, 2007. **8**(2): p. 172-80.

286. Dittel, B.N., et al., *Presentation of the self antigen myelin basic protein by dendritic cells leads to experimental autoimmune encephalomyelitis.* J Immunol, 1999. **163**(1): p. 32-9.

287. Lalor, S.J., et al., *Caspase-1-processed cytokines IL-1beta and IL-18 promote IL-17 production by gammadelta and CD4 T cells that mediate autoimmunity.* J Immunol. **186**(10): p. 5738-48.

288. Medvedev, A.E., K.M. Kopydlowski, and S.N. Vogel, *Inhibition of lipopolysaccharide-induced signal transduction in endotoxin-tolerized mouse macrophages: dysregulation of cytokine, chemokine, and toll-like receptor 2 and 4 gene expression.* J Immunol, 2000. **164**(11): p. 5564-74.

289. Weir, C.R., K. Nicolson, and B.T. Backstrom, *Experimental autoimmune encephalomyelitis induction in naive mice by dendritic cells presenting a self-peptide.* Immunol Cell Biol, 2002. **80**(1): p. 14-20.

290. Leon, L.R., W. Kozak, and M.J. Kluger, *Role of IL-10 in inflammation. Studies using cytokine knockout mice.* Ann N Y Acad Sci, 1998. **856**: p. 69-75.

291. Doggrell, S.A., *Oral fingolimod for relapsing-remitting multiple sclerosis Evaluation of: Kappos L, Radue E-M, O'Connor P, et al. A placebo-controlled trial of oral fingolimod in relapsing multiple sclerosis. N Engl J Med 2010;362:387-401; and Cohen JA, Barkhof F, Comi G, et al. Oral fingolimod or intramuscular interferon for relapsing multiple sclerosis. N Engl J Med 2010;362:402-15.* Expert Opin Pharmacother, 2010. **11**(10): p. 1777-81.

292. Fonseca, D.E. and J.N. Kline, *Use of CpG oligonucleotides in treatment of asthma and allergic disease.* Adv Drug Deliv Rev, 2009. **61**(3): p. 256-62.

293. Nembrini, C., et al., *The kinase activity of Rip2 determines its stability and consequently Nod1- and Nod2-mediated immune responses.* J Biol Chem, 2009. **284**(29): p. 19183-8.

294. Park, J.H., et al., *RICK/RIP2 mediates innate immune responses induced through Nod1 and Nod2 but not TLRs.* J Immunol, 2007. **178**(4): p. 2380-6.

295. Girardin, S.E., et al., *CARD4/Nod1 mediates NF-kappaB and JNK activation by invasive Shigella flexneri.* EMBO Rep, 2001. **2**(8): p. 736-42.

296. Hsu, Y.M., et al., *The adaptor protein CARD9 is required for innate immune responses to intracellular pathogens.* Nat Immunol, 2007. **8**(2): p. 198-205.

297. Opitz, B., et al., *Listeria monocytogenes activated p38 MAPK and induced IL-8 secretion in a nucleotide-binding oligomerization domain 1-dependent manner in endothelial cells.* J Immunol, 2006. **176**(1): p. 484-90.

298. Shimada, K., et al., *The NOD/RIP2 pathway is essential for host defenses against Chlamydophila pneumoniae lung infection.* PLoS Pathog, 2009. **5**(4): p. e1000379.

299. Kim, Y.G., et al., *The cytosolic sensors Nod1 and Nod2 are critical for bacterial recognition and host defense after exposure to Toll-like receptor ligands.* Immunity, 2008. **28**(2): p. 246-57.

300. Hou, J., et al., *Induction of interleukin-10 is dependent on p38 mitogen-activated protein kinase pathway in macrophages infected with porcine reproductive and respiratory syndrome virus.* Virol J, 2012. **9**: p. 165.

301. Craig, R., et al., *p38 MAPK and NF-kappa B collaborate to induce interleukin-6 gene expression and release. Evidence for a cytoprotective autocrine signaling pathway in a cardiac myocyte model system.* J Biol Chem, 2000. **275**(31): p. 23814-24.

302. Godl, K., et al., *An efficient proteomics method to identify the cellular targets of protein kinase inhibitors.* Proc Natl Acad Sci U S A, 2003. **100**(26): p. 15434-9.

303. Oh, S.J., J.H. Kim, and D.H. Chung, *NOD2-mediated suppression of CD55 on neutrophils enhances C5a generation during polymicrobial sepsis.* PLoS Pathog, 2013. **9**(5): p. e1003351.

304. Murugaiyan, G., et al., *IL-27 is a key regulator of IL-10 and IL-17 production by human CD4+ T cells.* J Immunol, 2009. **183**(4): p. 2435-43.

305. Hsieh, C.S., et al., *Differential regulation of T helper phenotype development by interleukins 4 and 10 in an alpha beta T-cell-receptor transgenic system.* Proc Natl Acad Sci U S A, 1992. **89**(13): p. 6065-9.

306. Anderson, C.F., et al., *IL-27 regulates IL-10 and IL-17 from CD4+ cells in nonhealing Leishmania major infection.* J Immunol, 2009. **183**(7): p. 4619-27.

307. Yoshimura, T., et al., *Two-sided roles of IL-27: induction of Th1 differentiation on naive CD4+ T cells versus suppression of proinflammatory cytokine production including IL-23-induced IL-17 on activated CD4+ T cells partially through STAT3-dependent mechanism.* J Immunol, 2006. **177**(8): p. 5377-85.

308. Molle, C., M. Goldman, and S. Goriely, *Critical Role of the IFN-Stimulated Gene Factor 3 Complex in TLR-Mediated IL-27p28 Gene Expression Revealing a Two-Step Activation Process.* J Immunol.

309. Molle, C., et al., *IL-27 synthesis induced by TLR ligation critically depends on IFN regulatory factor 3.* J Immunol, 2007. **178**(12): p. 7607-15.

310. Noguchi, E., et al., *A Crohn's disease-associated NOD2 mutation suppresses transcription of human IL10 by inhibiting activity of the nuclear ribonucleoprotein hnRNP-A1.* Nat Immunol, 2009. **10**(5): p. 471-9.

311. Loving, C.L., et al., *Nod1/Nod2-mediated recognition plays a critical role in induction of adaptive immunity to anthrax after aerosol exposure.* Infect Immun, 2009. **77**(10): p. 4529-37.

312. Bettelli, E., L.B. Nicholson, and V.K. Kuchroo, *IL-10, a key effector regulatory cytokine in experimental autoimmune encephalomyelitis.* J Autoimmun, 2003. **20**(4): p. 265-7.

313. Burkhart, C., et al., *Peptide-induced T cell regulation of experimental autoimmune encephalomyelitis: a role for IL-10.* Int Immunol, 1999. **11**(10): p. 1625-34.

314. Gunzl, P., et al., *Anti-inflammatory properties of the PI3K pathway are mediated by IL-10/DUSP regulation.* J Leukoc Biol, 2010. **88**(6): p. 1259-69.

315. Wang, Y.H., et al., *IL-25 augments type 2 immune responses by enhancing the expansion and functions of TSLP-DC-activated Th2 memory cells.* J Exp Med, 2007. **204**(8): p. 1837-47.

316. Yang, X.O., et al., *T helper 17 lineage differentiation is programmed by orphan nuclear receptors ROR alpha and ROR gamma.* Immunity, 2008. **28**(1): p. 29-39.

317. Kopf, M., et al., *Impaired immune and acute-phase responses in interleukin-6-deficient mice.* Nature, 1994. **368**(6469): p. 339-42.

318. MacMicking, J., Q.W. Xie, and C. Nathan, *Nitric oxide and macrophage function.* Annu Rev Immunol, 1997. **15**: p. 323-50.

319. Jouanguy, E., et al., *IL-12 and IFN-gamma in host defense against mycobacteria and salmonella in mice and men.* Curr Opin Immunol, 1999. **11**(3): p. 346-51.

320. Schebesch, C., et al., *Alternatively activated macrophages actively inhibit proliferation of peripheral blood lymphocytes and CD4+ T cells in vitro.* Immunology, 1997. **92**(4): p. 478-86.

321. Sutterwala, F.S., et al., *Reversal of proinflammatory responses by ligating the macrophage Fcgamma receptor type I.* J Exp Med, 1998. **188**(1): p. 217-22.

322. Rutschman, R., et al., *Cutting edge: Stat6-dependent substrate depletion regulates nitric oxide production.* J Immunol, 2001. **166**(4): p. 2173-7.

323. Munder, M., et al., *Suppression of T-cell functions by human granulocyte arginase.* Blood, 2006. **108**(5): p. 1627-34.

324. Zhang, X., R. Goncalves, and D.M. Mosser, *The isolation and characterization of murine macrophages.* Curr Protoc Immunol, 2008. **Chapter 14**: p. Unit 14 1.

325. Jenkins, S.J., et al., *Local macrophage proliferation, rather than recruitment from the blood, is a signature of TH2 inflammation.* Science, 2011. **332**(6035): p. 1284-8.

326. Spence, S., et al., *Suppressors of cytokine signaling 2 and 3 diametrically control macrophage polarization.* Immunity, 2013. **38**(1): p. 66-78.

327. Huber, S., et al., *Alternatively activated macrophages inhibit T-cell proliferation by Stat6-dependent expression of PD-L2.* Blood, 2010. **116**(17): p. 3311-20.

328. Willment, J.A., et al., *Dectin-1 expression and function are enhanced on alternatively activated and GM-CSF-treated macrophages and are negatively regulated by IL-10, dexamethasone, and lipopolysaccharide.* J Immunol, 2003. **171**(9): p. 4569-73.

329. Starborg, M., et al., *The murine Ki-67 cell proliferation antigen accumulates in the nucleolar and heterochromatic regions of interphase cells and at the periphery of the mitotic chromosomes in a process essential for cell cycle progression.* J Cell Sci, 1996. **109 (Pt 1)**: p. 143-53.

330. Raes, G., et al., *Differential expression of FIZZ1 and Ym1 in alternatively versus classically activated macrophages.* J Leukoc Biol, 2002. **71**(4): p. 597-602.

331. Wang, W.W., et al., *Co-induction of arginase and nitric oxide synthase in murine macrophages activated by lipopolysaccharide.* Biochem Biophys Res Commun, 1995. **210**(3): p. 1009-16.

332. Deng, B., et al., *IL-10 triggers changes in macrophage phenotype that promote muscle growth and regeneration.* J Immunol, 2012. **189**(7): p. 3669-80.

333. Sakaguchi, S., et al., *Regulatory T cells and immune tolerance.* Cell, 2008. **133**(5): p. 775-87.

334. Savage, N.D., et al., *Human anti-inflammatory macrophages induce Foxp3+ GITR+ CD25+ regulatory T cells, which suppress via membrane-bound TGFbeta-1.* J Immunol, 2008. **181**(3): p. 2220-6.

335. Takahashi, M., et al., *Monocyte chemoattractant protein-1 (MCP-1), not MCP-3, is the primary chemokine required for monocyte recruitment in mouse peritonitis induced with thioglycollate or zymosan A.* J Immunol, 2009. **183**(5): p. 3463-71.

336. Berrington, W.R., et al., *NOD1 and NOD2 regulation of pulmonary innate immunity to Legionella pneumophila.* Eur J Immunol, 2010. **40**(12): p. 3519-27.

337. van Furth, R., *Monocyte production during inflammation.* Comp Immunol Microbiol Infect Dis, 1985. **8**(2): p. 205-11.

338. Brown, G.D. and S. Gordon, *Immune recognition. A new receptor for beta-glucans.* Nature, 2001. **413**(6851): p. 36-7.

339. Benoit, M., B. Desnues, and J.L. Mege, *Macrophage polarization in bacterial infections.* J Immunol, 2008. **181**(6): p. 3733-9.

340. Sieling, P.A. and R.L. Modlin, *Cytokine patterns at the site of mycobacterial infection.* Immunobiology, 1994. **191**(4-5): p. 378-87.

341. Leon, L.R., et al., *An antipyretic role for interleukin-10 in LPS fever in mice.* Am J Physiol, 1999. **276**(1 Pt 2): p. R81-9.

342. Berg, D.J., et al., *Interleukin-10 is a central regulator of the response to LPS in murine models of endotoxic shock and the Shwartzman reaction but not endotoxin tolerance.* J Clin Invest, 1995. **96**(5): p. 2339-47.

343. Nagelkerken, L., B. Blauw, and M. Tielemans, *IL-4 abrogates the inhibitory effect of IL-10 on the development of experimental allergic encephalomyelitis in SJL mice.* Int Immunol, 1997. **9**(9): p. 1243-51.

344. Rott, O., B. Fleischer, and E. Cash, *Interleukin-10 prevents experimental allergic encephalomyelitis in rats.* Eur J Immunol, 1994. **24**(6): p. 1434-40.

345. Dann, A., et al., *Cytosolic RIG-I-like helicases act as negative regulators of sterile inflammation in the CNS.* Nat Neurosci, 2012. **15**(1): p. 98-106.

346. Philpott, D.J. and S.E. Girardin, *Crohn's disease-associated Nod2 mutants reduce IL10 transcription.* Nat Immunol, 2009. **10**(5): p. 455-7.

347. Fedorak, R.N., et al., *Recombinant human interleukin 10 in the treatment of patients with mild to moderately active Crohn's disease. The Interleukin 10 Inflammatory Bowel Disease Cooperative Study Group.* Gastroenterology, 2000. **119**(6): p. 1473-82.

348. Schreiber, S., et al., *Safety and efficacy of recombinant human interleukin 10 in chronic active Crohn's disease. Crohn's Disease IL-10 Cooperative Study Group.* Gastroenterology, 2000. **119**(6): p. 1461-72.

349. Colombel, J.F., et al., *Interleukin 10 (Tenovil) in the prevention of postoperative recurrence of Crohn's disease.* Gut, 2001. **49**(1): p. 42-6.

350. Kanauchi, O., K. Mitsuyama, and A. Andoh, *The therapeutic impact of manipulating microbiota in inflammatory bowel disease.* Curr Pharm Des, 2009. **15**(18): p. 2074-86.

351. Damman, C.J., et al., *The microbiome and inflammatory bowel disease: is there a therapeutic role for fecal microbiota transplantation?* Am J Gastroenterol, 2012. **107**(10): p. 1452-9.

352. Matsumoto, Y., et al., *Eradication of Helicobacter pylori and resolution of gastritis in the gastric mucosa of IL-10-deficient mice.* Helicobacter, 2005. **10**(5): p. 407-15.

353. Bodger, K., J.I. Wyatt, and R.V. Heatley, *Gastric mucosal secretion of interleukin-10: relations to histopathology, Helicobacter pylori status, and tumour necrosis factor-alpha secretion.* Gut, 1997. **40**(6): p. 739-44.

354. Jovanovic, I.R., et al., *Clinical onset of the Crohn's disease after eradication therapy of Helicobacter pylori infection. Does Helicobacter pylori infection interact with natural history of inflammatory bowel diseases?* Med Sci Monit, 2001. **7**(1): p. 137-41.

355. Tursi, A., *Onset of Crohn's disease after Helicobacter pylori eradication.* Inflamm Bowel Dis, 2006. **12**(10): p. 1008-9.

356. Luther, J., et al., *Association between Helicobacter pylori infection and inflammatory bowel disease: a meta-analysis and systematic review of the literature.* Inflamm Bowel Dis, 2010. **16**(6): p. 1077-84.

357. Mege, J.L., V. Mehraj, and C. Capo, *Macrophage polarization and bacterial infections.* Curr Opin Infect Dis, 2011. **24**(3): p. 230-4.

358. Kiszewski, A.E., et al., *The local immune response in ulcerative lesions of Buruli disease.* Clin Exp Immunol, 2006. **143**(3): p. 445-51.

359. Redford, P.S., P.J. Murray, and A. O'Garra, *The role of IL-10 in immune regulation during M. tuberculosis infection.* Mucosal Immunol, 2011. **4**(3): p. 261-70.

360. Lawn, S.D. and A.I. Zumla, *Tuberculosis.* Lancet, 2011. **378**(9785): p. 57-72.

361. Divangahi, M., et al., *NOD2-deficient mice have impaired resistance to Mycobacterium tuberculosis infection through defective innate and adaptive immunity.* J Immunol, 2008. **181**(10): p. 7157-65.